January 2015

Observing, Understanding, and Manipulating Biological Membranes

Ian Mc Cabe
Syracuse University

Abstract

The phospholipid bilayer is one of the hallmarks of eukaryotic life. This complicated two dimensionally fluid surface is composed of a double layer of lipids which have a region that is hydrophobic and a region that is hydrophilic. The lipid bilayer membranes of a cell act as a barrier that distinguishes the cells and the organelles interiors from the outside environment. In order for the cell to be able to effectively communicate across these impermeable barriers they have evolved many intricate systems of lipid and protein interaction that serve to transmit information from one side of the membrane to the other. The abundance of functionality in the membrane has made them incredibly complicated and intricate structures. This complexity makes the study of any one membrane associated signaling pathway or system more often than not very challenging if not impossible. Because of this a simplified analogue of the biological membrane is necessary for controlled and quantitative studies. The amphiphilic nature of phospholipids allows researcher to create lipid bilayer that can be controlled for composition and placed on a surface that is accessible to many investigative systems. These supported lipid bilayer (SLB) systems have been used for decades to figure out the intricate series of actions and reactions that occur in a natural biomembrane. While there is still a lot to be learned from simple lipid bilayer systems there is also now the need to produce bilayers that incorporate more of the functions of a living cell. These will permit the study of signaling systems involving multiple molecules, the direct observation of cellular responses to surface stimuli, and even the control of cellular behavior. Along with providing greater versatility in the study of cells and membrane mediated systems these enhanced lipid bilayers will have major biomedical applications. Given that a lipid bilayer is the exterior presented by cells in nature there can be no more biocompatible

surface than a lipid bilayer, for the surface treatment of medical devices this could have great implications. For instance, if sufficient knowledge is developed about these systems, then all types of medical implants could have a customized lipid bilayer based coating that would help it to integrate perfectly with the tissue to which it is embedded. Joint replacements could have a surface that would promote the growth of osteoblast cells, a cardiac stent could have a coating to prevent clot formation while promoting epithelial cell growth and discouraging smooth muscle cell growth, perhaps even neural implants capable of two way communication for the treatment of paralysis.

It is with this long term vision that we set out to advance the field of lipid bilayer systems to increase the capacity for dynamic control, artificial enhancement, and tissue interface. A series of investigations were undertaken with the goal of promoting each one of these facets.

In the first investigation we studied the dynamic behavior of the PIP_2 phospholipid in varying physiological calcium concentrations. This anionic lipid has been hypothesized to have the capacity to organize itself spatially in response to fluctuations in calcium levels. No investigation has been so far carried out that look at PIP_2s reaction to physiologically relevant changes in the calcium concentration. We used fluorescence correlation spectroscopy (FCS) and photon counting histogram (PCH) analysis to look at changes in the dynamics and the brightness of PIP_2 in polymer supported lipid bilayers. We found that PIP_2 appears to make electrostatic associations with zwitterionic lipids in the bilayer when there is no calcium present which are disrupted with the addition of calcium.

In the second investigation we developed a genetically encoded protein/lipid anchoring system based on an aldehyde. This system allows proteins to be genetically modified to bear a 6 amino

acid consensus sequence at, theoretically any position along its amino acid chain. This consensus sequence targets a cysteine within the sequence to a formylglycine generating enzyme (FGE) that converts the cysteine to a formylglycine. Formylglycine bears an aldehyde on one of its residues. Aldehydes are found very rarely in the mammals and are also highly reactive with certain elements such as aminooxy and hydrazides which are also very rare in mammalian biology. This makes an aldehyde an excellent anchoring method for medical applications. We produced aldehyde tagged enhanced green fluorescent proteins (EGFP) and successfully incorporated them with aminooxy modified lipids in a supported lipid bilayer. This showed that the system is a viable and in fact improved alternative to the lipid/protein anchoring systems currently in use.

The third investigation centered on the capacity to culture cells on a SLB surface. Previous studies have found that SLBs have an anti-adhesion property for both proteins and cells. We investigated whether the inclusion of various quantities of both positively and negatively charged lipid into the bilayer would effect the capacity of fibroblast cells to adhere and proliferate. Our system prototyped a novel high throughput technique for bilayer/cell investigations. We found that cells initially had difficulty in adhering to all bilayer surfaces but the inclusion of greater quantities of negatively charged lipids produced a more favorable environment for cell growth. We also looked at how glycolipids, commonly held to be promoters of cell recognition and adhesion, effected fibroblast cells. Such bilayers with sugar elaborations were as suitable for fibroblast growth as the control subjects on collagenated glass. These findings are a significant advancement in the development of bilayer – cell interfaces.

This body of work has provided exciting advances in the capacity to produce and understand biomimetic surfaces. While there is much work to be done yet before fully interfacial surfaces

are possible, I have developed some novel tools and unearth some interesting findings that can provide some of the next steps towards this goal.

Observing, Understanding, and Manipulating Biological Membranes

By

Ian P. Mc Cabe

M.Sc. Syracuse University, 2011

B.Sc. NUI Galway, 2007

Doctoral Dissertation

Submitted in partial fulfillment of the requirements

for the degree of Doctor of Philosophy,

in Biomedical Engineering,

Syracuse University

August 2015

Acknowledgements

I would like to take this opportunity to thanks some of the people who have made it possible for me to be here today. First and foremost I would like to thank Dr. Forstner, without whom I would never have been given the opportunity I needed to become a scientist. His wisdom and advice have been instrumental in my development and maturation as a researcher and a person. I would also like to thank my colleagues in the Forstner Lab, especially Adolphe and Eleni with whom I started this journey many years ago. I would like to thank Dr. Bader and Dr. Movilueanu for their guidance and aid throughout my almost seven years in graduate school. I would like to thank my parents, Bernard and Mary McCabe either of whom could have earned a PhD in half the time it took me if they had been given a chance. They provided me with the two types of learning (theoretical from my mother, application from my father) that have been essential for all of my research. I would also like to thank both of my grandmothers, Mary B. Mc Cabe and Sadie Prendergast for instilling a great respect for education in me from a young age and for helping me to get that education; I hope they would be proud. I would like to thank my parents in law, Kevin and Carla Bellosa for their constant support and encouragement for the past seven years and for standing in as surrogate parents for me while I've been so far from home. I would like to thanks my two little boys. Tadhg and Oscar (and the one on the way) for thinking that being a scientist is as cool as being a firefighter, an astronaut, or Spiderman. Finally, and most importantly, I would like to thank my wonderful wife Lindsey; she has stood by my side with little complaint, sacrificing your own aspirations so I can pursue mine. Her constant love and support are worth more to me than any degree.

Table of Contents

Abstract i
Observing, Understanding, and Manipulating Biological Membranes v
Acknowledgements vii
Chapter 1: Fundamentals 1
1.1. Introduction 1
1.2. Biomembranes in the Cell 3
1.2.1. Introduction 3
1.2.2. Lipids 4
1.2.3. Proteins 8
1.2.4. Structure and Dynamics 9
1.3. Artificial Biomembranes 12
1.3.1. Biomembranes in the Laboratory 12
1.3.2. Biomembranes as manufactured Biointerfaces 15
1.4. Polymer Supported Phospholipid Bilayers 17
1.4.1. Introduction 17
1.4.2. Polymer Supports for Lipid Bilayers 19
1.4.2.1. Independent polymer support 21
1.4.2.2. Coupled membrane polymer systems 26
1.4.3. Bilayer Deposition on Polymer Support 29
1.4.4. Advantages and Limitations of Polymer Supports 31
1.4.5. What Lies ahead for Polymer Cushioned Bilayers? 33
1.4.6. Conclusions 34
1.5. Optical Techniques for Biological Imaging and Detection 34
1.5.1. Imaging methods 36
1.5.2. Single Particle and Fluorophore Tracking 38
1.5.3. Fluorescence Recovery After Photo-bleaching (FRAP) 40
1.5.4. Total Internal Reflection Fluorescence Microscopy (TIRFM) 41
1.5.5. dSTORM 44
1.5.6. Fluorescence Correlation Spectroscopy (FCS) 45
1.5.7. Photon Counting Histogram Analysis 50

1.6. Dual Color FCS/TIRF machine 54
1.6.1. Design 55
1.6.2. General requirements 60
1.6.3. System Calibration 66
1.7. Scope of proposal 71
1.8. Structure of rest of document 72
Chapter 2: The Effects of Ca^{2+} on the dynamics of PIP_2 Containing Lipid Bilayers 75
Summary 75
2.1. Introduction and motivation 76
2.2. Materials and Methods 81
2.2.2. Preparation of Polymer Supported Lipid Bilayers. 82
2.2.3. Fluorescence Correlation Spectroscopy (FCS) 83
2.2.4). Photon Counting Histogram (PCH) Analysis. 86
2.3) Results and Discussion 87
Section 3: A Biosynthetic Membrane-Anchor/Protein System Based on a Genetically Encoded "Aldehyde Tag" 97
Summary 97
3.1) Introduction 98
3.2. Materials and Methods 106
3.2.1. Materials 106
3.2.2. Protein Modification 106
3.2.3. Chemical Lipid Modification 107
3.2.4. Small Unilamellar Vesicle Preparation 108
3.2.5. Bilayer Formation 109
3.2.5. Protein-Lipid Conjugation 110
3.2.6. Imaging and FCS 111
3.2.7. In Vitro Conversion of Cysteine to Formylglycine 112
3.3. Results and Discussion 113
Section 4: The Effect of Bilayer Charge on the Adhesion and Proliferation of Adherent Cells 120
Summary 120
4.2 Materials and Methods 126

4.2.1 Materials 126
4.2.2 Cell Line 126
4.2.3 Cell Culture 127
4.2.4 Glass Substrate Preparation 127
4.2.5 Supported Lipid Bilayer Preparation 129
4.2.6 Proliferation Experiment 130
4.2.7 Adhesion Experiment 131
4.3 Results and Discussion 133
4.3.1) Control Groups 134
4.3.2 Supported Lipid Bilayers. 136
Chapter 5, Minor Projects 151
5.1 Super-Resolution Imaging of Cellular Spectrin 151
5.1.1 Introduction 151
5.1.2 Materials and Methods 156
5.1.3. Results and Discussion 158
5.2 Hybrid Lipo-Polymer cell substrate 161
5.2.1 Introduction 161
5.2.2 Materials and Methods 163
5.2.3 Results and Discussion 164
Chapter 6: Discussion and Conclusions 169
6.1 General Discussion 169
6.2 PIP_2 Dynamics 169
6.3 Aldehyde Tag 171
6.4 Charged Lipid Bilayers 172
6.5 Outlook 173
6.6 Case Study: Stents 173
6.7 Conclusions 176
References 177
Vita 197

Figure 1.1.: A typical animal cell..... 1

Figure 1.2.: Phospholipid Anatomy..... 4

Figure1.3.: Lipid self-assemblies..... 5

Figure 1.4.: A Green Fluorescent Protein..... 8

Figure 1.5.: A model of a cellular plasma membrane..... 10

Figure 1.6.: Examples of membrane organisation..... 11

Figure 1.7.: A Langmuir film balance. 14

Figure 1.8.: A Conventional solid supported lipid bilayer and its limitations. 19

Figure 1.9.: Schematic of the two major classes of polymer supported lipid bilayers. 21

Figure 1.10.: Chemical structure of commonly used polymers for bilayer support..... 23

Figure 1.11.: Deposition of a lipid bilayer on a polymer cushion. 30

Figure 1.12.: A fluorescence excitation and emission spectra for the Texas-Red fluorophore. ... 35

Figure 1.13.: A typical energy level diagram for fluorescent excitation and emission. 36

Figure 1.14.: An epifluorescence filter cube..... 37

Figure 1.15.: An example of the spectra of the components of a typical filter cube. 38

Figure 1.16.: Fluorescence recovery after photobleaching..... 39

Figure 1.17.: Total internal reflection. 41

Figure 1.18.: Total internal reflection fluorescence microscopy..... 43

Figure 1.19.: Fluorescence Correlation Spectroscopy Illumination 45

Figure 1.21.: The development of an autocorrelation curve..... 47

Figure 1.22.: Auto correlation of a 2-D diffusive sample. 48

Figure 1.23.: Photon arrival times translated into intensity over time graph..... 51

Figure 1.24.: a Xenon spectrum..... 54

Figure 1.25.: A filter cube. 55

Figure 1.26.: A Nikon Eclipse Ti microscope.. 56

Figure 1.27.: The optics table. 57

Figure 1.28.: FCS/TIRF system on the optics table. 59

Figure 1.29.: A typical TIRF ray diagram 61

Figure 1.30.: A conceptual schematic of the dual color FCS/TIRF optics layout. 62

Figure 1.31.: A schematic of a stage micrometer. 66

Figure 1.32.: Correlation traces of varying concentrations of fluorescein 68

Figure 1.33.: FCS curve of a 99.995 mol% DOPC/ 0.005 mol% SLB.. 69

Figure 2.1.: PIP2 and DOPC. 76

Figure 2.2.: Calcium signaling: 77

Figure 2.3.: Our proposed experimental system 80

Figure 2.4.: FCS measurements of EGTA containing system.. 85

Figure 2.5.: A PCH curve 86

Figure 2.7.: A polymer supported bilayer.. 88

Figure 2.6.: The 2-D diffusion of a fluorescently labeled PIP_2 88

Figure 2.8.: Fluorescence recovery after photo-bleaching of a PLLA supported lipid bilayer. 89

Figure 2.9.: Combined FCS/PCH data for fluorescent PIP2. 90

Figure 2.10.: Combined FCS/PCH data for fluorescent PC with PIP2 present. 91

Figure 2.11.: Combined FCS/PCH data for fluorescent PC with PIP2 absent.. 92

Figure 2.12.: PIP2 induced zwitterionic lipids organisation 93

Figure 3.1.: A GPI anchor 100

Figure 3.3.: Biotin + streptavidin membrane anchor 101

Figure 3..: Histidine Tag + Nickel membrane anchoring. 101

Figure 3.4.: The Aldehyde Tag technology 102

Figure 3.5.: An aldehyde used to attach a lipidic anchor to a green fluorescent protein.. 104

Figure 3.6.: EGFP on a supported lipid bilayer via an aldehyde tag s..... 105

Figure 3.7.: Reaction Schematics for the Aminooxy-Modification of a Lipid 107

Figure 3.8.: EGFP integrated onto a supported lipid bilayer. 113

Figure 3.9.: The integrity of the underlying bilayer..... 114

Figure 3.10.: An example of an FCS correlation curve for an EGFP bound to a bilayer..... 114

Figure 3.11.: Lipid phase separation. 117

Figure 4.1.: Enhanced Bilayers.. 121

Figure 4.2.: Cell counting. 132

Figure 4.3.: Change in cell population for fibroblast cells adhered to control substrates 134

Figure 4.4.: Morphology of 3T3 fibroblasts on control substrates. 136

Figure 4.5.: Proliferation percentage of cells adhered to charged bilayers 1. 137

Figure 4.6.: Proliferation percentage of cells adhered to charged bilayers 2. 138

Figure 4.7.: Cells cultured on SLBs containing 5 mol% of a glycolipid. 139

Figure 4.8.: Cells on 10 mol% negatively charged lipid bilayers..... 142

Figure 4.9.:Cells on 0 mol% net charged lipid bilayers..... 143

Figure 4.10.: Cells on 5 mol% negatively charged lipid bilayers 143

Figure 4.11.: Cells on 5 mol% positively charged lipid bilayers 144

Figure 4.12.: Cells on 10 mol% positively charged lipid bilayers 145

Figure 4.13.: 3T3 Cells on a 5 mol% GM1 glycolipid containing SLB. 146

Figure 4.14.: 3T3 Cells on a 5 mol% DOPE-Lactosyl containing SLB 148

Figure 5.1.: murine cardiomyocyte super-resolution image. 158

Figure 5.2.: A 3T3 cell with all spectrin isophorms labeled 159

Figure 5.3.: Cardiomyocyte under high magnification Epifluorescence and under dSTORM super-resolution imaging. 160

Figure 5.4.: A schematic of a polymer supported lipid bilayer 161

Figure 5.5.: Polyacrylamide 163

Figure 5.6.: Langmuir- Schäfer technique to form a bilayer 164

Figure 5.7.: Diffusion rate versus pore size 165

Figure 5.8.: Micelle diameter estimate 166

Figure 5.9.: Floating micelle diffusion rate 166

Figure 6.1: A cardiac stent 174

Chapter 1: Fundamentals

1.1. Introduction

In 1665 Robert Hooke described the microscopic structure of cork as being made up of 'Cells' due to their resemblance to the cells in a honeycomb [10]. Since then cells have been the subject of extensive study and prolonged curiosity. It was not until 174 years after Hooke's observation that Theodor Schwann and Matthias Schleiden determined the basis for modern Cell Theory: namely that 1) the cell is the most basic unit of life, and 2) that all living creatures are made up of one or more cells[11]. Today, 176 years later, we have a vast profundity of knowledge on the structure and functions of cells, however some of the basics still elude us. The

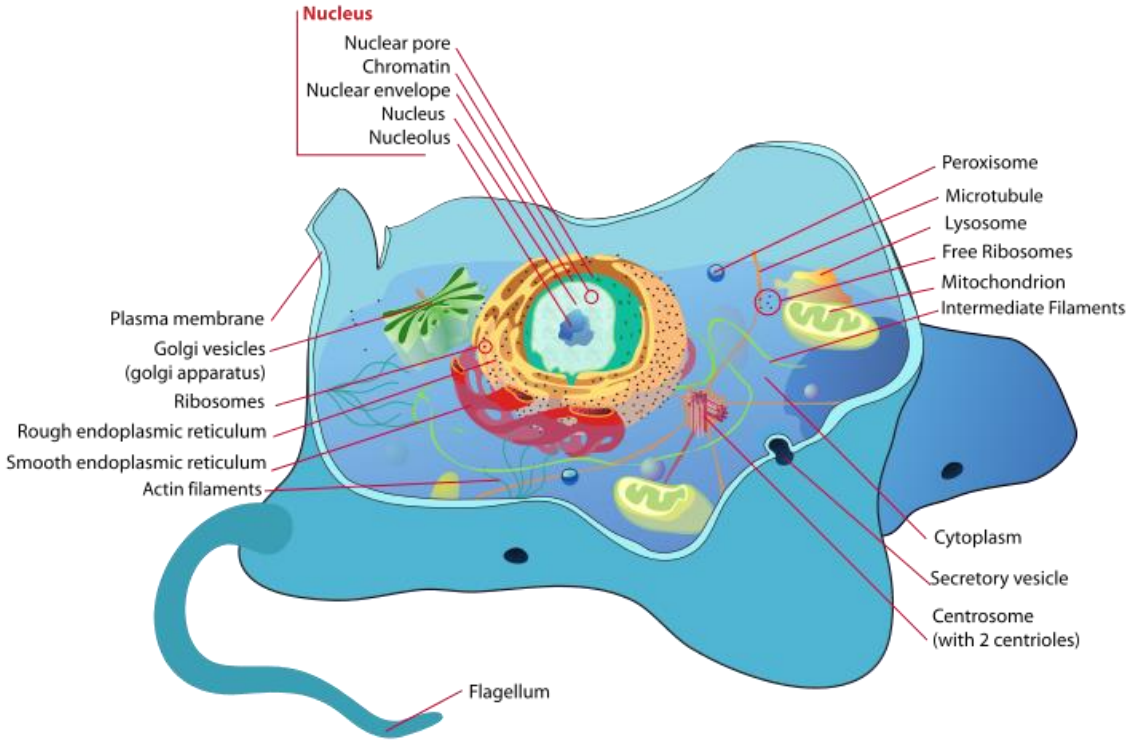

Figure 1.1.: A Typical Animal Cell. A typical animal cell with some common cellular components labeled [5]. Image: Public Domain

eukaryotic cell is a vastly complex and enigmatic structure, it is the building block of all higher life, while also existing as single cell entities. In mammals cells forms the tissue of our organs, coming together to make structures more complicated than is possible for individual cells to achieve. Working in unison, cells are able to digest food, provide locomotion and process stimuli into thought.

With the exception of sponges all animals have bodies differentiated into separate tissues. In mammals these tissues can be organized into organs which perform specific functions in the body. There is typically a skeletal system to aid in locomotion, a nervous system to gather environmental information, and an external protective skin that keeps pathogens out and water in. Cellular structure in eukaryotes broadly reflects the make-up of the mammalian body. Cells have a skin like membrane, the plasma membrane, which encloses the cell as a whole. Internally the cell has organelles which carry out specific functions. There is a rigid cytoskeleton which aids in locomotion. There is also a broad array of sensory molecules to gather information about the cells environment.

All knowledge that a cell has about its environment and any interactions it has with other cells must pass through the plasma membrane via one of the many mechanisms designed to do so. The plasma membrane is selectively permeable and so controls the passage of molecules in and out of the cell, organelles have their own enclosing membranes that regulate the passage of molecules from the organelles into the cytosol. Because of the copious number of functions required of cellular membranes they have evolved to be highly complex and intricate structures.

As a natural part of the extensive investigations into how the biomembrane performs its copious functions, engineers and scientists have been envisioning ways to utilize this knowledge

in new and different capacities. The fact that a phospholipid bilayer is the surface that a eukaryotic cell presents to its environment makes an artificial lipid bilayer the ideal choice to interface between man-made material and organic tissues. Already researchers have discovered how to use spheres of lipids to transport drugs and genetic therapies into the heart of cells[13], other researchers are investigating how to use biomembranes as biosensors [14], cell interfaces [15], and platforms for next generation interactive cell studies[16]. In this work we aim to provide a foundation of knowledge that will enable the next round of advancement in this exciting field.

1.2. Biomembranes in the Cell

1.2.1. Introduction

The primary function of the plasma membrane (indicated in Figure 1.1.) is to protect the cell from its environment. The plasma membrane is a selectively permeable barrier consisting of a double layer of phospholipids with numerous proteins and carbohydrates in, on, and through it. Structurally the lipids provide a quasi-two dimensional fluid surface which permits the dynamic rearrangement of bilayer components. This fluidity facilitates the reorganization of bilayer components for the optimum configuration for each specific task. On the extracellular side of the eukaryotic plasma membrane there is a carbohydrate mat called the Glycocalix. The Glycocalix consists of polysaccharides, glycoproteins and glycolipids. These glycolipids and glycoproteins aid in cell – cell recognition, adhesion and communication[17]. For example glycosphingolipids are crucial for the recognition of human leukocytes by *E-selectin* on the vascular endothelium during inflammation [18]. On the cytosolic side of the plasma membrane there lies an actin based membrane skeleton, this filamentous structure provides support for the plasma membrane and also serves to transmit environmental stresses and forces into the cell via trans membrane

proteins [19, 20]. The actin network is also crucial for the movement of cells; directed actin polymerization stretches a portion of the cell in the desired direction of motion [21].

1.2.2. Lipids

It can be argued that lipids are, structurally, the most important of the membrane constituents. The amphiphilic nature of the membrane lipid is what gives the membrane its two dimensional fluid nature [22]. This fluidity permits the dynamic rearrangement of structures on and in the bilayer which take part in biochemical reactions at the membrane surface[7]. Once thought to be a passive element in the signaling systems, lipids have been recognized as important biochemical messengers and facilitators in their own right [23, 24]. The primary lipids in bio-membranes are the glycerophospholipids[5]. There are five main types of these; Phosphatidylcholine, Phosphatidylethanolamine, Phosphatidylinositol, and Phosphatidylserine, all of which have numerous subtypes [25]. A typical Phospholipid consists of a hydrophobic ‘tail’ region comprising of, typically, two fatty acid chains. Attached to this is a glycerol ‘backbone’, to which a Phosphate group is bound. Finally a simple organic molecule such as a choline, alcohol

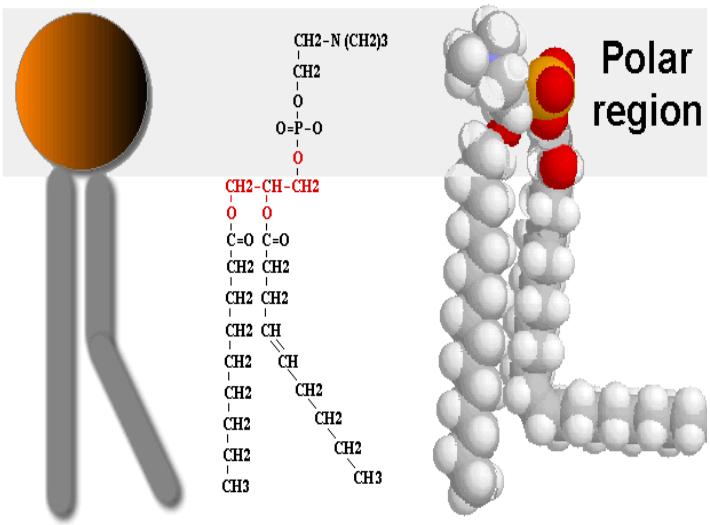

Figure 1.2.: Phospholipid Anatomy. Cell membranes consist mainly of phospholipids. Phospholipids have two parts: a polar phosphate "head" and two nonpolar fatty acid "tails." Note the double bonded hydrocarbons on the right hand ‘tail’ which causes it to kink .image: Public Domain

or an inositol is attached to the phosphate. The glycerol, phosphate and the organic molecule make up the head region that exhibits an asymmetric charge arrangement even for net neutral lipids. This renders the head groups polar and ultimately hydrophilic. The hydrocarbon fatty acid chain is non-polar and therefore hydrophobic [26].While the primary lipids in bio-membranes are the glycerophospholipids (as depicted in Figure 1.2.), there are numerous different types of lipids that differ in their particular chemical makeup including: sphingolipids who have a backbone of sphingoid bases, and the sterol lipids including the highly important Cholesterol to name a few.

Lipids can have one to three hydrophobic tails. These are un-branched chains of carbon atoms. Variation in the saturation of the bonds between the hydrocarbons in the tail contributes to the overall fluidity of the lipid in a bilayer. Less hydrogen saturation leads to more carbon-carbon double bonding. The latter constrains the freedom of movement of the hydrocarbon chain as the double bound does not allow for rotations of the carbons. With fewer structural conformations available the associated lipids require more space to diffuse and therefore have different diffusive and material properties than their unsaturated variants; specifically saturated lipids require a larger diffusive space which results in less dense packing and therefore greater fluidity.

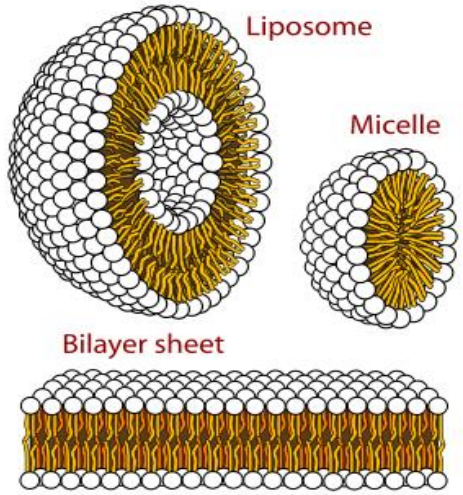

Figure1.3.: Lipid Self Assemblies. Lipids can self-assemble into the above structures when in an aqueous environment.
image: Maria Villarreal –Public domain

Having the dual properties of both a

hydrophobic region in their tails and a hydrophilic region in their heads, lipids have the ability to self-assemble into more energetically favorable structures when in an aqueous environment [27]. The head group contains regions that have greater negative or positive charge that permits the water molecule to interact with it electrostatically. The non-polar tails lack the ionic diversity necessary for water interaction which disrupts the dynamic hydrogen bonds between water molecules. In order to preserve this intermolecular hydrogen bonding the water molecules rearrange themselves around nonpolar surfaces creating an exclusion shell. This exclusion shell results in a decrease in the total entropy of the system which consequently requires an increase in the free energy. In order to minimize this phenomenon and therefore increase the entropy/ decrease the free energy, hydrophobic molecules will aggregate into more ordered structures that minimize their exposure to water molecules. At high water content, the resulting assemblies can be planar lipid bilayers, liposomes or micelles [28, 29]. Bilayers are two dimensional sheets of lipids arranged in two layers where the tails of each lipid layer face each other [27, 30, 31]. Liposomes or vesicles are closed bilayer structures; they can consist of multiple bilayers and can range in size from 100nm to several microns in diameter [32]. Micelles are arrangements of lipids where the tails all face in towards a common center. The capacity to form micelles is dependent on the length of the hydrocarbon tails and the sized of the lipid head, with short tails and large heads being the most favorable configuration for micelle formation. Because of this micelles are typically only a few nanometers in diameter [28],while vesicles diameter ranges from about 20nm for small unilamellar vesicles (SUV) to 10s of micrometers for giant unilamellar vesicles (GUVs).

Lipids are synthesized in the smooth endoplasmic reticulum through numerous specialized proteins; they are transported to the membranes as vesicles which are then

incorporated in the target membrane. All membrane structure is controlled by the addition of material in this way and by the removal of materials via the formation of membrane invaginations that then pinch off to become vesicles [33]**.** There are also proteins that have specific roles in the local organization of the lipids bilayer, for instance Flippase is specialized in switching lipids between different leaflets.

Previously, researchers have believed that the primary function of the phospholipid in a cell membrane is structural. Recently, however an array of phospholipids has been found to have important chemical functions in their own right. Certain lipids, such as Phosphatidylinositol 4,5-bisphosphate (PIP_2), have been discovered to carry important biological functions [23, 34-36]. For example they are involved as secondary messengers in the signaling pathways of G protein-coupled receptors [37]and nuclear receptors[38], they have been shown to serve important identification and docking functions in inwardly rectifying potassium channels [39], and they have roles in the activation of certain kinases [40]. Other members of several different lipid categories have also been identified as signaling molecules and cellular messengers. These include sphingosine-1-phosphate (a potent messenger molecule involved in regulating calcium mobilization, cell growth, and apoptosis), diacylglycerol (DAG) and the phosphatidylinositol phosphates (PIPs) (involved in calcium-mediated activation of protein kinase C), and the steroid hormones such as estrogen, testosterone and cortisol (these modulate a host of functions such as reproduction, metabolism and blood pressure).[23, 35]

1.2.3. Proteins

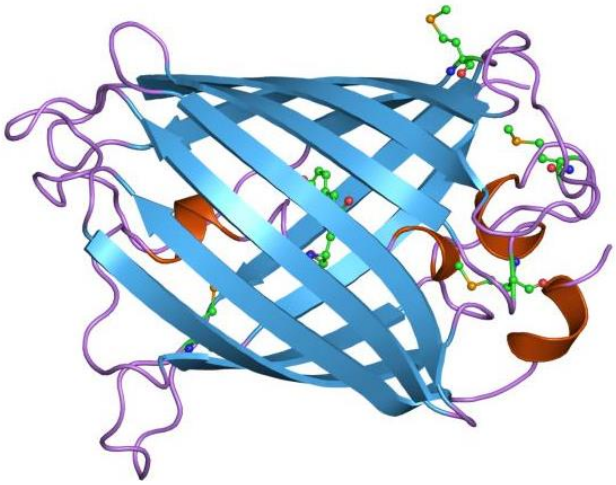

Figure 1.4.: A Green Fluorescent Protein. A Green Fluorescent Protein (GFP) has a beta sheet 'barrel' structure in the middle with alpha helical linkers at either end. The barrel structure protects the fluorescent core.[8] Image: Public Domain

Proteins are organic compounds consisting of amino acids arranged in a linear chain which subsequently folds into a functional three dimensional structure oftentimes the functionality of a protein is more dependent on its structural form as it is on its chemical composition. The production of proteins in cells is governed by the central dogma of molecular biology, namely that deoxyribonucleic Acid (DNA) is transcribed to ribonucleic acid (RNA) which in turn gets translated to an amino acid sequence. The amino acid strand folds according to its lowest energy conformation and various other interactions, often with the aid of other proteins, and assumes a specific three dimensional structure. It is only in that properly folded configuration that the protein can execute its function [41]. For example the green fluorescent protein will only have its fluorescent properties when in the correct three dimensional form depicted in Figure 1.5. Once the protein is folded it may have to have some post-translational chemical modification to allow for chemical structures not covered by the standard 21 amino acids available in eukaryotic cells . Examples for posttranslational modifications are attachment of acyl chains such as miristoyl or generation of formylglycine by formylglycine generating enzyme (FGE) [42].

Membrane proteins are a subclass of proteins which have some association with cellular membranes. More than half of all proteins have some interaction with the cell membrane [33]. Membrane proteins play multiple roles in cell function: structural proteins provide stability to the cell through attachment to the biopolymers of the cytoskeleton, membrane receptor proteins provide a route through which messenger molecules can pass through or relay information through the membrane, cell adhesion molecules identify and interact with other cells (for example the interaction of T cells with Antigen presenting cells in the adaptive immune system of vertebrae), transport proteins play an important role in the maintenance of concentrations of ions and can be either carrier proteins or channel proteins [33].

Membrane proteins can be either peripheral or integral. Peripheral proteins are attached to only one side of the membrane bilayer and their attachment is often facilitated by a lipid anchor attached post-translation. Integral proteins have a hydrophobic region that can often only form in an anhydrous environment such as the hydrophobic core of the lipid bilayer. Thus, in living cells they can often only fold into their correct configuration when integrated into the lipid bilayer of cellular membranes. There are two main types of integral proteins: ones with predominantly alpha helices as transmembrane motif which makes up roughly 27% of all proteins in humans and those that utilize a barrel of beta sheets a hydrophobic structure for membrane embedding [43].

1.2.4. Structure and Dynamics

According to the fluid mosaic model set forth by Singer and Nicolson [7]in 1972, the biological membrane can be considered to behave as a two-dimensional liquid where all lipidic and proteinous elements diffuse more or less freely within the plane of the membrane but are constrained from free diffusion in and out of the bilayer.

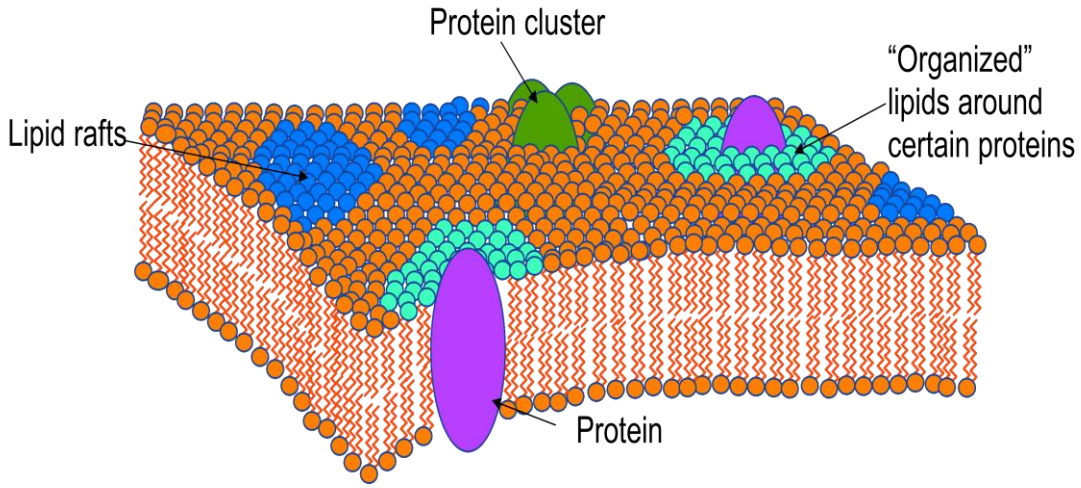

Figure 1.5.: A Model of a Cellular Plasma Membrane. The Singer and Nicholson model of a cellular plasma membrane calls for a "Fluid Mosaic" type of structure where everything diffuses freely. A more modern view of the plasma membrane recognizes spatial and temporal structures of which the most common ones are depicted here [7]

While many of the general precepts of the Singer and Nicholson model still hold, on closer examination it is seen that the plasma membranes contain a variety of structures on several length and time scales[44-47]. Typically such structures - as depicted in Figure 1.5. - are involved in signaling processes at the membrane and can consist of protein-protein complexes [48], lipid-protein complexes [49, 50] or membrane domains with particular composition of lipidic and proteinous elements [51-53]. A variety of proteins will organize shells of particular lipids within their vicinity that are crucial for the proper function of the protein [44]. Lastly, membrane domains compartmentalize cellular processes by serving as organizing centers [54] for the assembly of signaling molecules [55], influencing membrane fluidity and membrane protein trafficking [56]. Lipid micro-domains are thought to be more ordered and tightly packed than the surrounding bilayer, but float freely in the membrane bilayer [57].

Another much studied aspect regarding the biophysics of cell membranes is the dynamic and passive methods of transport in a cell membrane. Thermally driven, lateral random diffusion is responsible for a large amount of the motion of membrane components within the membrane [58-63]. It is essential to many biological functions e.g. PIP_2 [35], nerve growth [64], adhesion plaques [17]. Picket and fence structures (see Fig.1.6.) are part of the actin based cytoskeleton, the regular enclosed areas have been hypothesized to corral membrane elements temporarily to one region. This inhibits long range diffusion and thus prolongs high local concentrations and extended times for chemical reactions [65-67]. Finally, directed motion uses molecular motors that move attached proteins along cytoskeleton structures, such as actin-filament and microtubules while hydrolyzing ATP to ADP[68]. These have been observed when proteins are seen to move in a very direct nonrandom manner, often against the flow of mass movement [69], it is hypothesized that they are actively transported to a region in the cell where they have to perform a specific function. For example integrins move toward the cell periphery in a highly

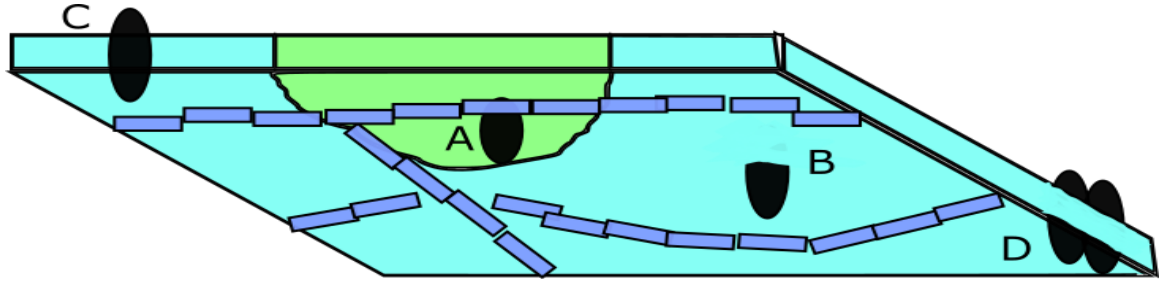

Figure 1.6.: Examples of Membrane Organization A) When proteins are confined in a lipid microdomain they must have a kinetic energy larger than the activation energy of passing the domain barrier in order to leave the domain. B) & C) The filamentous cytoskeleton can provide a barrier to free lateral diffusion of proteins who have a long intracellular domain. The cytoskeleton acts as a fence to these proteins restricting their area of diffusion for a time. Proteins with short enough intracellular domains remain unrestricted. D), Multiprotein complexes are subject to higher viscous forces than their single counterparts. They therefore have a smaller translational diffusion rate than monomeric proteins

directed manner [19, 20]. Frequently, however, mixed forms of these basic transport mechanisms are observed. For example, motors will fall off an actin filament, diffuse randomly for a while until they bind again and resume active transport, thus leading to biased, i.e. directed, diffusion [70].

1.3. Artificial Biomembranes

1.3.1. Biomembranes in the Laboratory

Because native cellular membranes are highly complex in composition and structure, controlled experiments to assess particular aspects of membranes are hard to asses *in vivo*. Thus, a variety of artificial membrane systems have been developed over the past decades for membrane research and technological applications [30]. These artificial systems include monolayers [71], planar bilayers [72] and vesicles [73]. Like cellular membranes, these systems exploit the amphiphilic nature of lipids to form model membranes with a controlled composition.

Artificial model membranes have played an essential role in the work presented in this dissertation. In particular vesicles and supported lipid bilayers have served as starting points for most of the research described herein and are explored in greater detail below.

When insoluble phospholipids are hydrated they start to aggregate once a certain concentration of lipids - the critical micelle concentration - is reached. These aggregates self-assemble into energetically favorable enclosed surfaces allowing close contact of the hydrophobic tails and minimizing their contact with the water, as mentioned above (see Fig. 1.3.). Depending on the length of the tails of the lipids they either form single leaflet spheres called micelles (short tails, small head-group) or closed 3-dimensional membranes of lipid

bilayers known as liposomes (long tails and/or large head groups). Vesicles are characterized based on their size as small unilamellar vesicles (SUVs) with a diameter up to 100nm, large unilamellar vesicles (LUVs) with diameters of several hundred nanometers and giant unilamellar vesicles (GUVs) with diameters up to several tens of micrometers [74-76].

Supported lipid bilayers (SLB's) are created when vesicles approach a suitable flat surface such as clean glass or SiO_2 in aqueous solution. Given the right ionic conditions the vesicles will rupture, and their bilayers merge into one continuous, planar sheet of membrane. During this process a layer of water of a few nanometer thickness is trapped between the supporting surface and the bilayer. This planar configuration is energetically more favorable than the curved arrangement of the bilayer in a vesicle as the packing of the lipid head groups is tighter providing fewer gaps for water molecules to penetrate. Thus, the formed planar bilayer remains stable in aqueous solution remaining fixed to the surface by van der Waals forces. The water layer between the solid support and the successfully formed bilayer acts as a 'lubricant' allowing the lipids in both leaflets to remain fluid, i.e. to diffuse freely within the plane of the membrane. The composition of the vesicles that are used to make SLB's can be easily controlled during their production. The desired ratio of lipids is mixed in chloroform before being evaporated to a monolayer in a round bottomed flask, rehydrated to self-assemble into vesicles and then passed through filters with appropriate pore sizes with high pressure in an extruder to create vesicles with well-defined diameters. Because the lipid composition of the vesicles determines the makeup of the final supported lipid bilayer, SLBs' makeup is easily controlled [8, 31, 72, 77].

Another approach to SLB formation is the utilization of a Langmuir film balance (see Fig. 1.11.) with which two lipid monolayers are sequentially transferred from an air-water

interface onto the supporting surface [78]. This method is capable of producing supported lipid bilayers that have different compositions in each layer, thus resembling more closely the asymmetric bilayer of cellular membranes. The Langmuir deposition technique also allows the formation of bilayers on diverse substrates. Using a Langmuir Blodgett or Langmuir-Schaeffer technique (see figure 1.11.) permits the use of various polymers as bilayer substrates. This eliminates the need for the extremely stiff and smooth surface that the glass presents and opens up a whole variety of materials with different porosities, stiffness's, and chemistry to act as bilayer supports, polymer supports for lipid bilayers will be discussed in more detail below.

As discussed briefly above, lipids will form a monolayer when at an air water interface. A Langmuir film balance takes advantage of this fact to more closely study some of the physical properties of the monolayer. The film balance has a pair of moving barriers at either end that can be moved in order to pack the lipids to a greater or lesser density. The surface pressure can be monitored using a Wilhelmy plate and important physical properties of the lipids can be deduced by careful interpretation of the relationship between surface pressure and area per lipid. The Langmuir film balance permits access to the substrate (the aqueous phase) which allows researchers to vary qualities such as temperature and ionic composition of the liquid. These techniques have helped elucidate some of the basic properties of lipid monolayers.

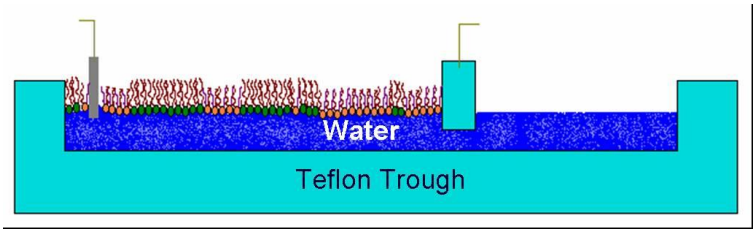

Figure 1.7.: A Langmuir Film Balance. A Langmuir film balance is used to control the packing characteristics of a lipid monolayer by moving a Teflon coated arm. This machine can be used to deposit two distinct monolayers onto a substrate creating an asymmetric bilayer.

1.3.2. Biomembranes as manufactured Biointerfaces

A vast amount of time, effort and capital have gone into the study of the biological membrane with the simple goal of understanding how it behaves and how it will react. A natural consequence of this is that researchers have discovered ways to utilize lipids and lipid structures for a wide array of applications only abstractly related to the original intent of the research. Considering that lipid bilayers are the surface that our own cells have chosen to present to each other, it is apparent that lipid bilayers can serve a very useful role as an interface between living matter and man-made materials. Being able to control and predict the behavior of the bilayer has hitherto been a major obstacle to implementing this logical next step, recent work however has started to utilize this promising platform. There are two major directions that lipid bilayer research has taken so far, they are both discussed briefly below.

1.3.2.1. Biomimetic Membranes as Surface Coatings

Perhaps one of the most promising avenues for the development of lipid bilayers lies in their use as intermediary surfaces between man-made materials and biological tissue. In nature, cells generally only interface with one of two surfaces; another cell which presents a protein studded lipid bilayer, or the extra cellular matrix which presents a biological polymer such as Collagen. Often-times problems arise following medical or dental implantation when the implant is recognized by the immune system as a foreign object which can induce an allergic foreign body response or implant induced coagulation. To help overcome the foreign body response and infection implants are being surface treated to enhance their biocompatibility [79]. One technique involves coating the surface with a lipid bilayer which, post assembly, spontaneously crosslinks at the termini of their acyl chain. This increases its stable lifetime and gives a secure biofunctionalized surface[80], another technique aims to selectively coat areas of titanium oxide

with supported lipid bilayers that can be controlled for composition [81]. A natural progression from this is to a long term stable bilayer that presents protein or glycolipid surfaces specific to the tissue they are to be implanted in to not only decrease the risk of an immune reaction but to actively promote tissue adhesion and regeneration or indeed prevent tissue growth in cases such as cardiac stents. These bio-interactive surfaces could help promote wound healing, cell differentiation, tissue adhesion or any number of applications as yet unconceived. To allow such specific enhancement of a lipid bilayer it is important to have a tool kit of techniques which allow the spatial and temporal rearrangement of the bilayer and its constituents. Such capacity will permit the close replication of a native cell membrane in both composition and behavior. As well as this it is important to know how the fundamental properties of a biomembrane such as fluidity, charge and composition, effect cells in close contact with it. Furthermore the capacity to adhere specific biomolecules to a bilayer would provide the means to enhance the membrane beyond its native capacities

1.3.2.2. Biomimetic Membranes as drug delivery devices

While supported lipid bilayers have proven their worth as an excellent tool for the close optical study of membranes another useful tool in lipid research is the liposome. These closed bilayer spheres have become an important vessel for the delivery of certain types of drugs [82]. Here a closed lipid bilayer encapsulates a solution of the drug to be administered, identifying peptides can help target the drug to specific tissue while other surface modifications can enhance longevity in the system, promote immune system evasion, or activate endocytosis once a target cell is reached [83]. Currently there are more than a dozen different type of liposomal drug delivery systems approved for human use [84]. Liposomes are also being investigated as a means to reduce drug toxicity by scavenging the drug from circulation to reduce its toxic effects [85].

1.4. Polymer Supported Phospholipid Bilayers

1.4.1. Introduction

For the last three decades functionalization of interfaces with mimics of biological membranes has been an ongoing effort. These model-membrane systems have garnered much attention because they provide a useful and interesting interface between the biological world and man-made materials. Thus, they have great potential for basic membrane and cell-biology research as well as a variety of biotechnological and biomedical applications. The simplest of these membrane mimics is the solid supported lipid bilayer that in many ways behaves similar to free lipid membranes. A thin water layer between the substrate and the bilayer serves as lubricant that enables long range lateral diffusion of the lipids. Thus, they preserve the fluidity of biological membranes that is so central to many cellular functions. Since the first fabrication of a solid supported bilayer via successive deposition of two monolayers by Tamm and McConnell [86], solid supported bilayers have been instrumental in a wide variety of studies. This is in part because proteins or other membrane constituents can be placed on or in the membrane, thus providing a highly controlled environment for experimentation. One of the great advantages of using a planar solid supported lipid membrane as opposed to lipid bilayer vesicles is the ability to bring to bear a number of light based analytical techniques such as; Förster resonance energy transfer (FRET) [87], fluorescence correlation spectroscopy (FCS) [88, 89], total internal reflection fluorescence (TIRF) [90, 91] or fluorescence recovery after photo-bleaching (FRAP) [92]. By using a thin (~150μm) support, such as a glass cover slip, means that high magnification optics, with high numerical apertures and small working distances, can be used to bring light to and collect light from those bilayer. For example, supported lipid bilayers have been used to

investigate membrane bound signaling events of cells [93, 94], study protein-lipid interactions on the single molecule level [90] and develop biosensor platforms [95, 96].

However, a significant limitation of such traditional solid supported bilayers can be encountered when trying to incorporate transmembrane proteins into the supported membrane (Figure 1.8.). A typical solid supported bilayer will have an approximately 1-3 nm thick hydration cushion between the support and the bilayer. This does not provide sufficient space for the cytosolic domain of most transmembrane proteins and consequently the protein will contact the substrate surface, deform and eventually denature as indicated in Figure 1.8.b. To overcome this restriction and expand the use of supported lipid bilayers to other research areas and fields, a different type of bilayer support has been developed. In this alternative method a soft polymeric layer is introduced between the solid support and the artificial lipid membrane. The polymer layer provides a low friction interface for the lipid bilayer and any imbedded proteins. The system has proven its adaptability and has been utilized in such diverse applications as; membrane protein binding detection [97], electrophoretic accumulation studies [98, 99], cellular cytoskeleton incorporation[100], and electrochemical biosensors [101]. We will discuss the options available for polymer bilayer supports and try to underscore the particular strengths and weaknesses of the different systems and methods.

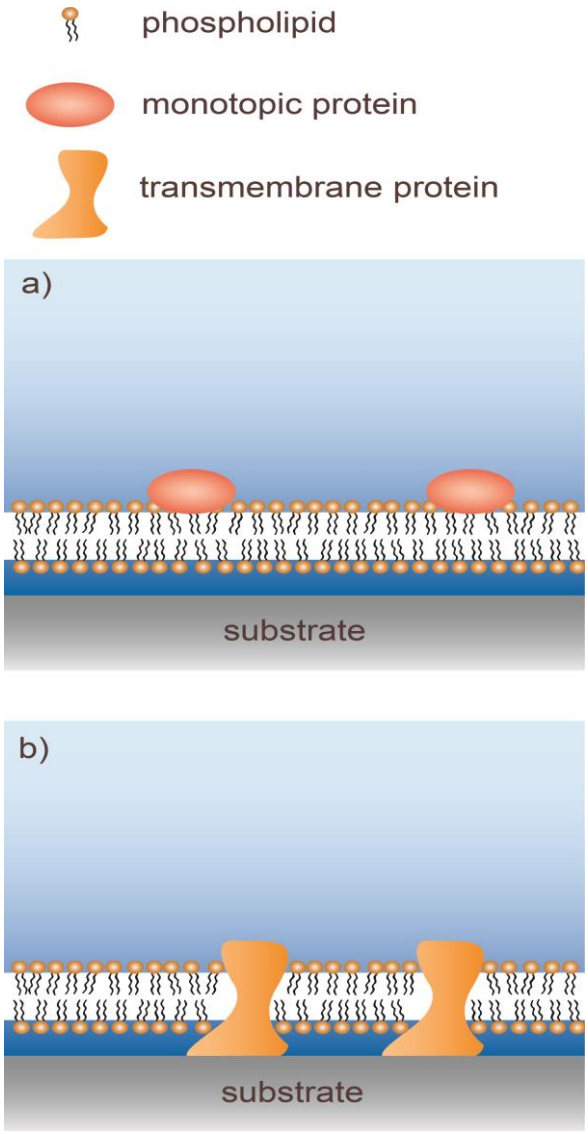

Figure 1.8.: Conventional solid supported lipid bilayer and its limitations. a) the SLB is able to accommodate monotopic proteins so that they stay functional. Both proteins and lipids are laterally mobile in such a scenario. b) In contrast, transmembrane proteins with extended cytosolic domains have not enough space between the substrate and the bilayer. Thus, they will contact the substrate, deform and often denature which leads to loss of function. In addition, such proteins are also immobilized

1.4.2. Polymer Supports for Lipid Bilayers

Most common polymer supports have had their genesis in convenience. Popular biological techniques involve numerous polymerizing substances; consequently some have been adopted for use as membrane cushions. For a successful polymer based lipid bilayer cushion, the polymer must have some few specific characteristics. Firstly, they must be capable of forming a thin layer with surface uniformity suitable for bilayer formation. Secondly, they would ideally have a well-defined elastic modulus that can be replicated at every reiteration of the experiment. Thirdly, the polymer must be hydrophilic, and they must be relatively chemically inert so as not to cause unwanted reactions and interactions with the membrane. Due to their hydrophilicity such polymers typically have high water contents and are known as hydrogels. Hydrogels have refractive indices that deviate only slightly from that of the liquid used to hydrate them, this allows for

good optical coupling between the hydrogel and the aqueous solution, giving aberration free imaging through the gels. Most other light based measurement techniques such as FCS and FRAP are also compatible with these systems. The nature of self-assembly of amphiphilic molecules such as lipids dictates that there must be water present for the formation of a bilayer. Consequently, to avoid de-wetting of the lipid/polymer interface during or after deposition of the bilayer there can be no strong attractive forces between a substrate and the membrane. Care must be taken when using polymers that have charged or polarized functional groups to ensure the attractive forces between these and the lipids are not too great. Typically polymer wetting ability is characterized by the contact angle of a water droplet on its surface. This can give some indication of a good polymer for a bilayer cushion application. Typical contact angles range from 30 – 70 degrees [102, 103].

Polymer supports might be classified with respect to a variety of properties. A first possibility would be a distinction between copolymers (such as styrene-acrylonitrile and nitrile rubber) which are formed using two or more monomer species and homopolymers (such as cellulose, PVC and polyethylene glycol) which consist of only one monomer species. A thorough review of the literature reveals that polymers used for bilayer supports are overwhelmingly of the homopolymer variety although a clear advantage for their use is not obvious per se. Another possible distinction of polymer supported lipid membranes could be made between systems where the polymer layer(s) are formed independently of the bilayer and those that are formed through fusion of vesicles containing lipo-polymers. Another differentiation could be made between polymer supports that attach to the solid support just by adhesion and those polymers that are attached to the solid substrate through an intermediary binding molecule: alkylsilanes for silica and mica substrates [104], or alkylthiols for GaAs or gold substrates [105]. These binding

molecules need to have a functionalized domain for polymer attachment and can be either coated over the entire solid substrate when using independent polymer supports [106] or attached to the distal end of each polymer when using lipopolymer supports [107].

For the purpose of this summary I will separate polymer supported bilayers into two main classes: independent polymer to the bilayer, and coupled membrane-polymer systems where all or parts of the polymers are linked to lipids or hydrophobic molecules that integrate into the bilayer (See Figure 1.9.). A short summary of the different polymer systems are given in Table 1, while the chemical structures are summarized in Figure 1.10.

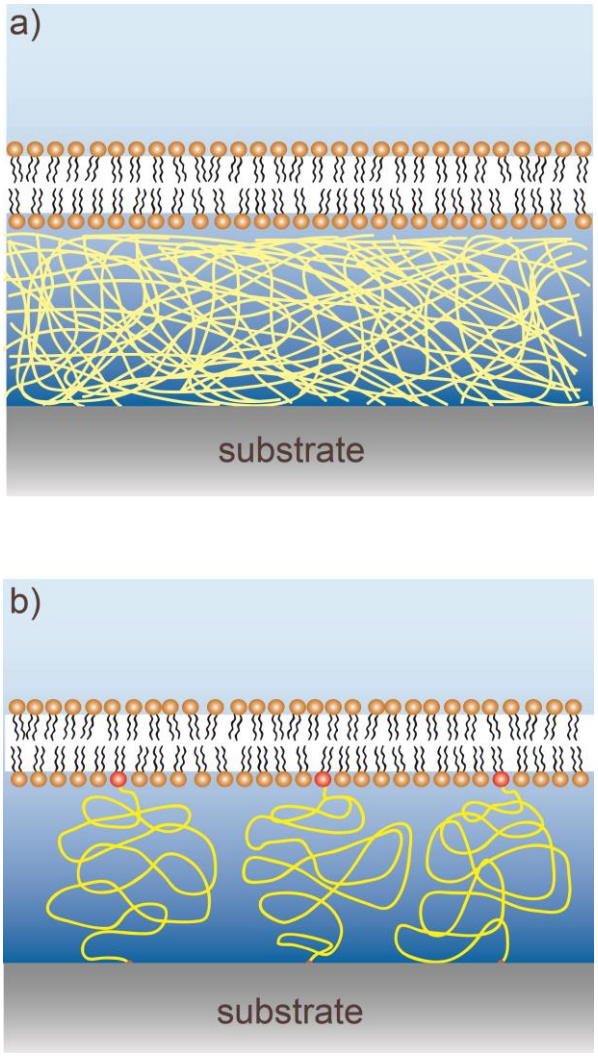

Figure 1.9.: Schematic of the two major classes of polymer supported lipid bilayers. a) The independent support, without linkage between the bilayer and the polymers. b) A coupled membrane-polymer systems where the polymer is covalently linked (red dots) to components of the membrane

1.4.2.1. Independent polymer support

Independent polymer supports are characterized by the fact that they have no direct linkage with the lipid bilayer. This allows for maximal flexibility with respect to polymer choice as well as deposition and manufacture procedures. The polymer in question can be spin coated on [108], deposited by sequential dipping [109] or, for chemically induced polymerization, polymerized

while sandwiched between the substrate and a second solid layer with a nonreactive coating [110]. Following polymer preparation the lipid bilayer is deposited using one of three main techniques: Langmuir-Schaefer, Langmuir-Blodgett, or a hybrid monolayer/vesicle fusion system (*vide infra*)

1.4.2.1.1. Polyacrylamide

Polyacrylamide (see Figure 1.10.a**)** is typically used in gel electrophoresis. In this application the gel structure is controlled by adjusting the ratio of acrylamide monomers and bis cross-linkers in the unpolymerized solution [111]. In an electrophoresis gel this ratio determines the average pore size and if used as membrane support polymer, this ratio can be used to control the elastic modulus of the gel (typically between 1 and 200 kPa [112]). This latter ability made polyacrylamide also very popular as a soft substrate material in studies of cellular biomechanics [113]. To prevent peeling, polyacrylamide requires that the solid substrate be coated with a bonding agent, typically alkylsilane, which covalently binds the cross-linked polymer to the glass. To achieve a smooth surface the unpolymerized solution is sandwiched between the activated solid substrate and another surface coated with a special non-reactive coating, typically a short chain silane polymer which renders the surface inert [114]. Once the nonreactive layer is removed the result is a uniform polymer surface suitable for bilayer deposition. This sandwiching technique is only possible because polymerization and crosslinking of the polyacrylamide is induced chemically and occurs over the time of minutes. In contrast to other polymer systems, the thickness of the cross-linked polyacrylamide gel can be easily controlled during production and thickness from tens to hundreds of micrometers can be achieved. In comparison, other techniques give gel thicknesses in the tens to hundreds of nanometers range

[111]. This wide range of thicknesses increases the number of potential applications for such a system. However, it should be noted that the acrylamide monomer is a toxin that should be handled and processed with care in particular if live cells are involved in a study.

1.4.2.1.2. Poly-L lactic acid (PLLA)

PLLA is another commonly used membrane support (Figure 1.10.b**)**. It is hydrophilic and quite inert and thus provides a good substrate for biological studies [108]. It has some promise in the medical field due to its biocompatibility and biodegradability making it a good candidate as a scaffold for tissue engineering [115]. PLLA can be formed into a uniform support by spin coating a solution onto a solid substrate. The coating then gets annealed before use to complete the polymerization. This yields layer thicknesses in the 100nm range. Having polymer layers this thin allows the use of sensitive optical techniques that rely on the use of objectives with high numerical aperture, such as; sum frequency generation vibrational spectroscopy, total internal reflection fluorescence and glancing angle illumination.

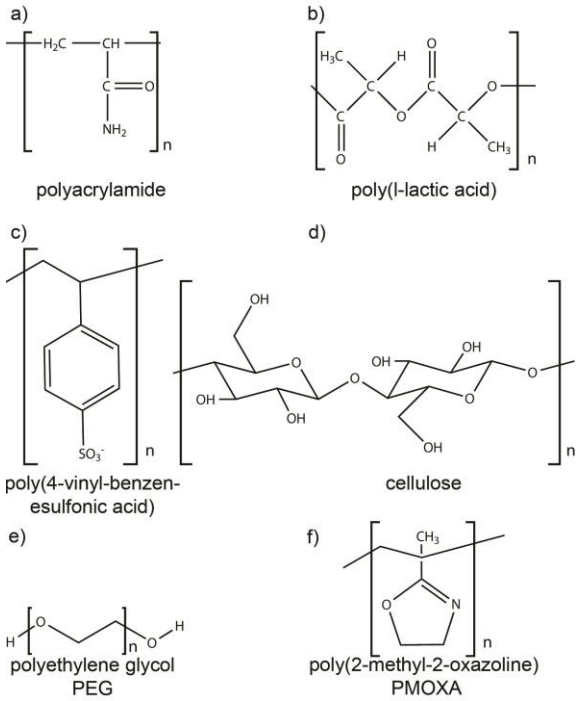

Figure 1.10.: Chemical structure of commonly used polymers for bilayer support. a) Polyacrylamide, b) poylacticacid, c) the polyelectrolyte poly(4-vinyl-benzen-esulfonic acid), d) cellulose, e) PEG and f) PMOXA.

1.4.2.1.3. Cellulose

Cellulose has been one of the most widely used polymers in modern history (Figure 1.10.d**)**. It is found naturally in plant cell walls and is the main constituent of paper and wood products. Cellulose has a diverse number of common uses from cellophane to wall paper paste to food filler. It is an inert hydrophilic polysaccharide, formed from dehydrated dextrose (the right hand form of glucose). It can be formed into thin layers for bilayer support by first substituting their hydroxyl groups for a hydrophobic side chain; this allows them to be dissolved in organic solvents. Once dissolved they can be spin coated onto a substrate or formed into monolayers on a Langmuir trough and deposited onto a substrate; the thickness can be built up through repeated dipping [116]. A variety of cellulose derivatives exist, such as trimethylsilylcellulose (TMSC) and isopentylcellulosecinnamate (IPCC), which provide different properties to the substrate such as solubility in nonpolar solvents and improved surface friction, respectively [116-118]. It has been shown that such cellulose derivatives can be modified post deposition via exposure to HCL vapor to create a hydrophilic surface with a hydrophobic core; this can change the electrical resistance of the bilayer which can be useful for ion channel studies. Cellulose has also been successfully patterned through micro-contact printing; here a polydimethylsiloxane (PDMS) stamp is used to transfer patterns of ‘ink’ monolayers onto the cellulose substrate which act as a diffusion barrier to the lipid bilayer. Patterning permits close spatial control of the bilayer contents, and can be used to promote selective cell growth, to study membrane discrimination, or to isolate proteins or channels from each other [119].

1.4.2.1.4. Agarose

Agarose is a polysaccharide most commonly found in agar, the gelatinous substance used for bacterial cell culture. It is derived from certain species of red algae and is used in such things as ice cream, the brewing process, as well as a food item in its own right [120]. In biological studies agarose is used to make a porous gel for microorganism motility assays; the concentration of agarose in solution determines the final viscosity of the substance [121]. Agarose has been used as a polymer support for bilayers for the last 18 years[122]. It can be deposited on glass by brushing on a solution of agarose type VII in water, this is dried at room temperature, no further modifications are required [122]. This makes agarose arguably the simplest polymer supports to

Table 1.1:Polymers used as membrane supports

Polymer	Thickness	Advantages	Disadvantages	Polymer Support System
Polyacrylamide	1-200µm	Greater thicknesses range	Involved production	I*
PLLA	~100nm	Good thickness control	Limited adaptability	I
Cellulose	10-200nm	versatile	Requires chemical modification	I
Agarose	~100-200nm	Simple to use	Limited adaptability	I
Polyelectrolytes	1-100nm	Excellent thickness control	Leaves a charged surface	I
PEG	10-20nm	Widely available and well researched	Tends to segregate	C
PMOXA	10-20nm	More stable than PEG	Not widely used	C
Protein Coupled	~20nm	Closer biomimetic	Not well researched	C

*** *I* refers to independent polymer supports , *C* refers to coupled polymer supports**

work with.

1.4.2.1.5. Polyelectrolyte Cushions

Another polymer cushioning system involves polyelectrolytes. These are polymers whose monomer subunits have an electrolyte group. The electrolyte groups will dissociate when exposed to an aqueous solution leaving the polymer with a net charge. To form a bilayer cushion the polyelectrolyte is deposited onto the substrate (which is typically charged) in a layer by layer fashion [123, 124]. The substrate is repeatedly dipped between two polyelectrolyte solutions; one a polycation (such as Poly(diallyldimethylammonium chloride)), one a polyanion (such as poly(4-venyl-benzenesulfonic acid, Figure 1.10.c)) [109]. Each dipping causes a monolayer of polyelectrolyte to be adsorbed on the surface through electrostatic attraction and reverses the charge on the surface leaving it ready for the next layer. This layer by layer method is inexpensive, easy and gives excellent thickness control, down to single nanometer precision [109]. Bilayer deposition is then dependent on the relative charges in the system, for a positively charged final polyelectrolyte layer negatively charged lipids are required to get total coverage. This electrostatic coupling may make polyelectrolyte cushions a poor choice for membrane dynamics studies but a good choice for ion channel studies. Surface patterning can be carried out by making use of the electrostatics to selectively layer certain sections through micro contact printing. This approach has the advantage of providing a chemical contrast as opposed to a topographical contrast for membrane patterning.

1.4.2.2. Coupled membrane polymer systems

Coupling between the bilayer and the polymer support is usually achieved by the use of lipopolymers. These are molecules that have a lipid like structure on one end of the polymer chain allowing that part to insert into a lipid bilayer, while the rest of the polymer is free to form

the cushion. In order to get full coverage of the membrane with a supporting cushion the distal portion of the lipopolymer needs to have a reactive end domain allowing it to covalently bind to the solid substrate. Without these tethering points the polymers tend to all reside in the upper leaflet of the bilayer and provide no measurable bilayer/substrate spacing [125]. Even in the presence of the covalent bonding of the polymer to the solid support the system tends to segregate into domains with polymer support and bilayer parts that sit right on top of the solid substrate. The concentration of lipopolymers in the bilayer and the length of the polymer chain can be used to fine tune bilayer/substrate distance for each application

1.4.2.2.1. Polyethylene glycol (PEG)

PEG is one of the most ubiquitous polymers used for lipopolymer constructs. It is a polyether that can be linear or branched and carries little to no charge [126] (Figure 1.10.e**)**. It is non-toxic and has excellent wetting characteristics making it an ideal choice for a wide range of biological applications: PEG is used as an antifouling coating on biomedical devices due to its 'protein repellent' characteristics, i.e. flexibility and hydrophilicity [127-129]. It was first bio-functionalized in the 1970s to aid in drug solubility and stability in immunological studies [130]. The process of covalently attaching a PEG to a biomolecule (known as pegylation) was developed with proteins in mind; however the process is easily adjusted for lipids. The PEG molecule has a hydroxyl group on both ends of the polymer chain that permits hydrogen bonding to a number of end groups suitable for bio reactions such as: amides, esters, and aldehydes. PEGS for lipid studies usually require different reactive groups on either end, some good options include: amine, maleimide, pyridyl disulfide, and carboxylic acids [127]. As with other lipopolymers, the lateral density of pegylated lipids in a supported lipid bilayer determines

whether or not the formation of a polymer cushion will be successful. Too few lipopolymer tethers and the bilayer will sag and contact the solid support. Too many PEGs and free diffusion in the bilayer will be impacted [125].

1.4.2.2.2. Poly(2-methyl-2-oxazoline) (PMOXA)

PMOXA is emerging as an alternative to PEG [131] (see Figure 1.10.f). It shares many of the same properties as PEG, such as hydrophilicity, protein repellence and its nonionic nature. In contrast to PEG however, PMOXA is lacking PEG's ether bonds, which are prone to oxidation, thus rendering PMOXA more stable. In addition, PMOXA can also be modified during synthesis to include terminal groups for attachment [132, 133]. This makes it a potentially easier tether to use in lipopolymers; however it has currently nowhere near the commercial availability as PEG.

1.4.2.2.3. Protein coupled polymer cushion

Recently researches have started to employ membrane incorporated proteins as anchor points to the polymer cushion. Presently, the only known such system is based on poly(N-(2-hydroxyethyl)acrylamide-co -5- acrylamido-1-carboxypentyl-iminodiacetate-co-4-benzoylphenyl methacrylate) (P(HEAAm-co-NTAAAm- co-MABP)) that has been modified with the nickel chelating nitrilotriacetic acid (NTA) groups. This allows binding of cytochrome c oxidase via a poly histidine-tag to the polymer cushion surface. The bilayer between the proteins is then formed using direct vesicle deposition [134].

In this summary I have focused on the most popular methods for providing a polymer bilayer support. Other polymer systems such as dextran and polyethyleneimine (PEI) have also been developed as membrane supports, but have so far not seen widespread use [135, 136].

1.4.3. Bilayer Deposition on Polymer Support

For the deposition of the lipopolymer containing bilayers or of the lipid membrane on the polymer cushion there are three main options that have successfully been used. They all involve the use of a Langmuir film balance to a greater or lesser degree. This is in stark contrast to solid supported bilayers that can often be formed by simple incubation of the clean substrate with small unilamellar vesicles.

The Langmuir-Blodgett technique [137] requires the lipids to be dispersed as a monolayer at the air-water interface of a Langmuir film balance. The Langmuir film balance allows the surface density of the lipid monolayer to be adjusted: eukaryotic cells are thought to have a surface pressure of 32mN/m [138] and surface pressure anywhere between this and 20mN/m have been successfully used for membrane deposition. The surface pressure is adjusted using the parallel barriers and the substrate to be coated is drawn from the liquid phase through the lipid monolayer into the air perpendicular to the surface (Figure 1.11.a), this deposits the first lipid monolayer onto the polymer substrate. The substrate is then dipped back through the monolayer, again perpendicular to the surface, to deposit the second monolayer creating a bilayer (Figure 1.11.d). This technique is suitable for depositing symmetrical as well as asymmetrical bilayers or multilayers.

The second option is the Langmuir-Schäfer technique [139]. This involves the same first step as for Langmuir-Blodgett transfer (Figure 1.11.a), however this time the second dip is done

parallel to the liquid surface (Figure 1.11.c), this way lipids are distributed more evenly in the second monolayer as there is no adjustment required to maintain the surface pressure during the dip. Consequently this produces more homogenous bilayers. Langmuir-Schäfer is sometimes regarded as a variant of the Langmuir-Blodgett technique however Langmuir-Schäfer deposition had typically a better success rate.

The third option is a hybrid Langmuir-Blodgett/vesicle fusion technique [72]. Here the first monolayer is deposited using Langmuir-Blodgett transfer (Figure 1.11.a) and the upper leaflet is formed by incubation with vesicles of the desired upper leaflet lipid composition (Figure 1.11.b).

The preparation of the lipid bilayer in a lipopolymer based support can be achieved using the same techniques as above, but with some small variations. The necessity of binding the polymer to the substrate (typically through salinization for glass) means that there are in general two options: Either the molecule that links the solid support to the polymer cushion is part of the

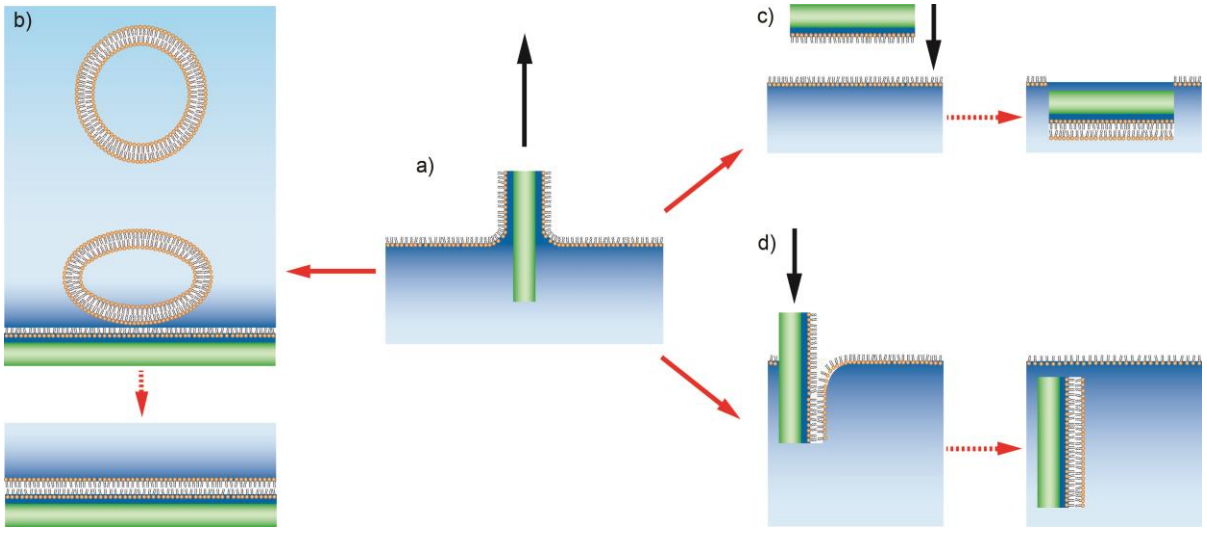

Figure 1.11.: Deposition of a lipid bilayer on a polymer cushion. The first step (a) is the same in all schemes: deposition of a monolayer on the substrate vie Langmuir – Blodgett transfer. The second monolayer can be created either by incubation with small unilamellar vesicles that fuse to form the top monolayer (b), by horizontal Langmuir-Schäfer transfer (c) or by a second Langmuir-Blodgett transfer.

polymer already or it is separately deposited as a film over the entire solid support. There are also different options for how to attach the polymers to the bilayer components. The polymers can either be pre-bound to the solid substrate and then have a modified bilayer element to which they bind [140] or they can be pre attached to the lipid monolayer and then deposited on the pretreated surface.

1.4.4. Advantages and Limitations of Polymer Supports

Obviously, creating a lipid bilayer on a polymer support is much more involved and challenging than producing a bilayer on a solid support or most other membrane mimics. Thus, it is worthwhile to briefly discuss the benefits of such an undertaking. Originally, the creation of polymer supported bilayers was driven by the desire to study membrane bound proteins that have substantially sized cytosolic domain (>10Å, the typical distance between a solid support and a supported lipid bilayer). Studying such large proteins requires that there be no potentially denaturing interactions between the protein and the solid support. Having an inert polymer spacer solves this problem and still permits the protein to diffuse in the bilayer. The introduction of a space between the bilayer and the substrate also means that a reservoir has been created into which ions can flow through ion channels. Therefore with an electrode at the solid support electrophysiological experiments can be conducted in a controlled manner. This makes for an interesting alternative to traditional patch clamping and vertical free-standing black lipid membranes. A further advantage for such studies is the enhanced self-healing seen in polymer supported bilayers. The elimination of bilayer defects increases the electrical resistance across the bilayer; a definite advantage for ion channel characterization.

It has furthermore been shown that similar to solid supported membranes independent polymer supports can also easily be patterned using one of two different techniques: photo mask

lithography or micro contact printing. In the lithographic technique the polymer is chosen such that polymerization or crosslinking can be induced by light [141]. This results in a patterned polymer substrate onto which a bilayer can be easily deposited and constrained by a physical corral. The micro contact printing system uses a polydimethylsiloxane (PDMS) master stamp to transfer a patterned monolayer of 'ink' onto a substrate through direct contact [119]. The ink is adsorbed to the substrate leaving an ink design with micrometer feature size. A variety of protein inks have been developed (e.g. fibronectin, and albumin [142]) that can be deposited directly onto a polymer substrate providing diffusion barriers to a lipid bilayer. Micro-patterns such as these can be used to do direct side by side comparison of different lipid species without intermixing, or alternatively to apply different stimuli to different parts of the bilayer without intermixing of the lipids.

When using lipids that have a high charges (such as phosphatidylinositol 4,5-bisphosphate (PIP_2) which has three negative charges on its head group [143]) there is potentially electrostatic interactions between the supported lipid bilayer and the substrate. In particular since common glass preparation methods such as piranha etching (75% sulfuric acid (H_2SO_4) and 25% hydrogen peroxide (H_2O_2)), hydroxylate the surface leaving it hydrophilic and slightly negatively charged [144]. Separating the charged lipid bilayer from the charged solid support through an inert polymer support of at least several dozens of nanometers introduces enough spatial separation to effectively screen any electrostatic interactions between the solid substrate and the bilayer considering that the Debye screening length at physiological conditions (~150mM NaCl) is about 1nm) [145].

A final advantage of polymer membrane supports is that while they effectively overcome many of the problems inherent to solid supported membranes, they conserve the latter's compatibility

with most of the modern light-based experimental methods. Thus, techniques such as Fluorescence Correlation Spectroscopy (FCS), Föster resonant energy transfer microscopy, fluorescence recovery after photo bleaching or total internal reflection fluorescence microscopy can readily be used with these systems.

The main disadvantage of polymer supported bilayers is the increased complexity of the production process when compared to solid supported bilayers. Many more steps are required for polymer cushion fabrication and lipid deposition presenting many more opportunities for failure of the system. For the independent polymer supports incorporation of the lipid bilayer requires a Langmuir trough. Even in its simplest form this machine requires a moderate outlay in cost and training and requires much more time and resources than vesicle incubation. The total time required for bilayer production with a polymer support is approximately an order of magnitude more than for a solid supported bilayer. This is a severe disadvantage as it increases the personnel cost as well as the materials expenditure.

1.4.5. What Lies ahead for Polymer Cushioned Bilayers?

The clear, distinctive advantage of polymer supports is the ability to incorporate integral membrane proteins into supported lipid bilayers without them losing form or function. The place where this technology advances however will be at the intersection with the techniques discussed above as well as developments that are still ongoing. The combination of polymer supported lipid membranes and semiconductor supports can for example be used as an organic transistor to reliably detect surface charge on a lipid monolayer [146]. Incorporation of this ability with the proper cultured cells could herald new types of cell based biosensors with an electronic output. Patterned polymer supports could be used to develop whole arrays of different biosensors

capable of detecting an enormous range of different properties or reagents on an extremely compact surface.

Polymer cushioned bilayers are new meta-materials that have some features similar to the actin-membrane structure of living cells. Actin is a very dynamic biopolymer and it seems natural to utilize polymers for membrane support that have some added functionality. Using such polymers as cushion could turn polymer supported bilayers into rather active surfaces. For example the pH dependent properties of hydrophilic poly(acrylic acid) (PAA) has been recently used to create an active polymer cushion for bilayer support [147]. One could also envision the use of hydrophilic shape memory polymers such as polyethylene terephthalate-polyethylene glycol copolymer [148] or poly(N-isopropylacrylamide) [149, 150] to actively change the topography of the polymer support which would allow for interesting studies of the active coupling of membrane composition and curvature.

1.4.6. Conclusions

In conclusion, supported lipid bilayers have been an extremely useful tool in membrane characterization. They are limited however when it comes to studying transmembrane proteins. As we reach the limits of what the traditional solid supported lipid bilayer is capable of, we expect greater uptake of polymer cushions and further development of the technology in the coming years.

1.5. Optical Techniques for Biological Imaging and Detection

When studying a biological system it is important to have a measurement technique that is capable of observing the system on the temporal and spatial scale that is appropriate to the structure. On a cellular scale two commonly asked questions are “what does it look like?’ and ‘what is it doing?’. On a molecular scale these questions can be parsed into ‘where is it?’ and ‘how is it moving?’ There are many techniques, such as atomic force microscopy, x-ray crystallography or electron microscopy, to investigate structures on small length scales that are not constrained by the diffraction limit of visible light. These techniques, however, can often only provide limited insights into the dynamics of the system. Either they are based on a scanning approach which limits the timescale on which spatial information can be obtained or they require a specialized environment such as a vacuum, which is not compatible with the systems native environmental conditions. For an investigation of the dynamics of a eukaryotic cell, the environmental requirements for life such as temperature of 37°C, proper pH etc. must be met. In the case of studies of dynamics of components in model membranes similar requirements must be adhered to in order to replicate biological function as closely as possible. To further mirror nature any perturbations to the cell must be minimized to avoid affecting the function under investigation. Similarly any perturbations to the model membranes for measurement purposes must be kept to a minimum.

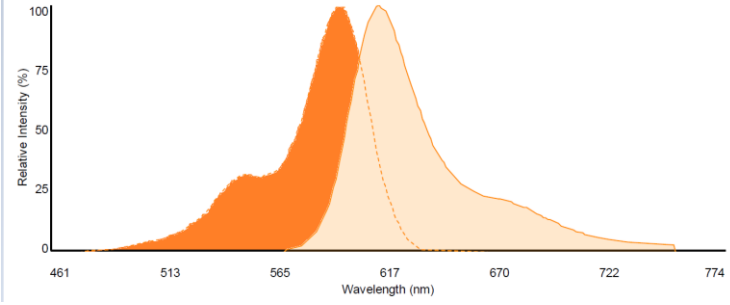

Figure 1.12.: A fluorescence excitation and emission spectra for the Texas-Red fluorophore. The peak excitation lies at 596nm, the peak emission lies at 615nm.

Light based techniques, such as fluorescence imaging, can in general operate under the above conditions. However, it should be noted that these light based techniques need to utilize light intensities that do not exceed the damage threshold of a cell or do not change the characteristics of the model system under investigation [151, 152]. Consequently, only relatively low intensities in the order of 1-10mW in wide field imaging modes are used to ensure the energy density at the focal point remain at safe levels.

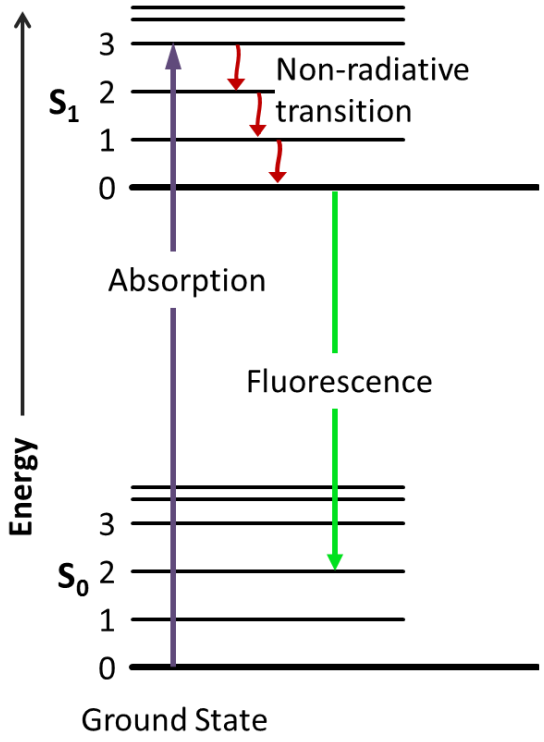

Figure 1.13.:Fluorophore energy levels A typical energy level diagram for fluorescent excitation and emission. Image: Public Domain

1.5.1. Imaging methods

The most frequently used imaging techniques for studying bio-membranes rely on the fluorescent properties of organic dyes [153, 154]. These dyes can be quite tiny when compared to a cell. For example a fluorescein molecule is only about 20 atoms in size and fluoresces with quantum yield of 0.79[155]. The most frequently used dyes for membrane related studies are: Texas Red, the Bodipy and Alexa dyes of different excitation/emission properties. The most common, and most straightforward, method to label a molecule is to covalently attach the dye using a reactive derivative of the fluorophore that selectively binds to a chemical group contained in the target molecule.

In addition to organic dyes fluorescence proteins are also frequently used to label proteins within living cells [156, 157]. Generating the fusion of the protein of interest and fluorescence protein is achieved by utilizing recombinant DNA methods. There a vector is used that contains the target proteins in sequence with the fluorescence protein's DNA. After transfecting the target cell with the vector the DNA will be expressed using the cells translation machinery thus producing a fluorescence version of the protein under investigation. This technique also permits to control the location of the fluorophore within the protein. Fluorescent fusion proteins are also used in *in vitro* experiments by first expressing them in cells (usually prokaryotes) and then purifying them out for use [158].

In general, fluorescent molecules emit light at a lower energy than they absorb (see Fig. 1.13.). The excitation and emission spectra typically have half-maximum absorption/emission spectrum width of 50-100nm for any given fluorophore. The best fluorophores however have a very small band of wavelengths which they can absorb and a correspondingly small band which they emit. Having a narrow excitation and emission spectrum helps reduce spectral overlap when multiple fluorophores are used. This phenomenon - known as cross talk - causes either one fluorophore to get excited from the excitation light of another or the emission light of one fluorophore passes through the filters used for another fluorophore ("fluorescence bleed through"). Both instances can lead to

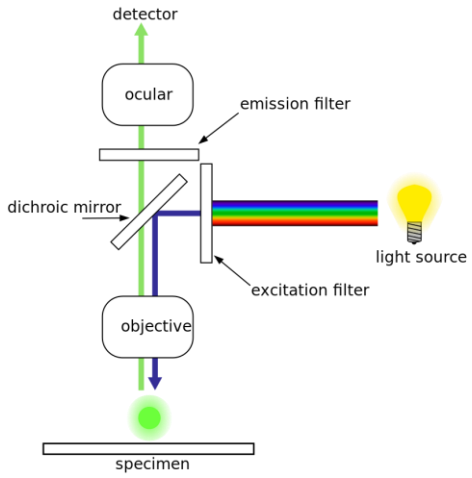

Figure 1.14.: The principle of Excitation and Emission White light is filtered to just excite at the desired wavelength, the effect is enhanced by filtering out the excitation light when viewing the sample Image: Public Domain

ambiguity in the fluorescence source when imaging or measuring samples in which multiple fluorophores are used.

To successfully excite the target fluorophore often a broad spectrum lamp is used together with an appropriate filter set to allow transmission around the appropriate wavelength (see Fig. 1.15.). In contrast, lasers provide a much narrower excitation spectrum as they emit only light of specific wavelength. In addition, they are able to provided higher photon densities. However, conventional lasers are limited by the fact that they do not have a wide spectrum of wavelengths, thus the fluorophore must be selected to correspond with the laser or vice versa.

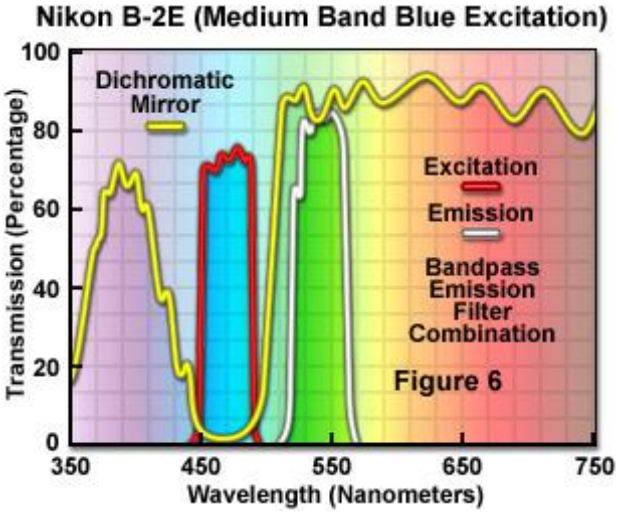

Figure 1.15.: Fluorescent Filter Cube Spectral Composition An example of the spectra of the components of a typical filter cube.

1.5.2. Single Particle and Fluorophore Tracking

In single particle tracking (SPT) and single fluorophore tracking (SFT), a molecule of interest is labeled with a tag that is visible under a light microscope. SPT uses a large tag, typically a gold particle or a fluorescently labeled particle and covalently attaches this to the molecule of interest. Light incident on the particle is reflected or fluorescently emits an observable signal back to the observer [159-161]. In contrast, the technically more demanding

SFT uses the signal of single fluorophores that are attached to the molecule of interest by either of the methods described above [162]. Typically the individual tags used in SPT and SFT are smaller than the wavelength of the light used to image them. However, their images are Airy disks of resolvable magnitude. Using image analysis these disks can be used to determine the position of the molecule of interest with sub-diffraction limited precision, typically 10-50 nm [163]. The positions in sequential frames are then assembled into the track of the molecule in time. The transport characteristics of the molecule is then determined from analysis of this track [164]. The benefits of SPT/SFT are instilled in the very nature of the technique. Firstly, the fact that single particles have to be resolved means that extremely low concentrations must be used. These low concentrations mean that there is very little impact on the system as a whole due to the addition of the tracking agents. Secondly, position of individual molecules can be resolved with a resolution below the diffraction limit. Finally, the amount of data is only limited by the lifetime of the tags and the residence of a molecule in the field

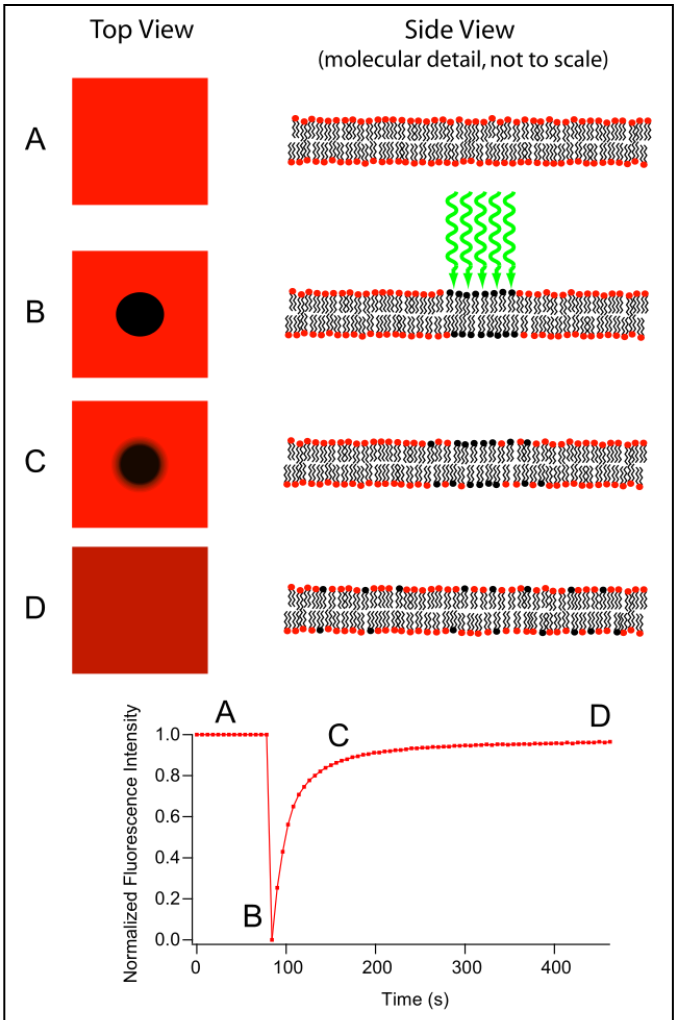

Figure 1.16.: Fluorescent Recovery After Photobleacing. FRAP relies on the recovery characteristics of a photo-bleached area of a fluid bilayer to convey information about its dynamics. Image: Public domain

of view.

The downside to SPT/SFT is that it is very difficult to determine structural information using this technique. It is also true that, by necessity, the field of view for such systems is very narrow. This means that alternative techniques must be used for larger scale diffusive studies.

1.5.3. Fluorescence Recovery After Photo-bleaching (FRAP)

Fluorescence Recovery After Photo-bleaching, FRAP, is another technique for measuring the fluid dynamics of a bilayer [165, 166]. It is based on the fact that the excited states of molecules are more chemically reactive. Thus, if excited continuously by light, fluorophores will at some point undergo irreversible photo-induced chemical reactions (usually with oxygen in the solution) resulting in a non-fluorescent compound. This leads to a limited number of excitation/ emission cycles fluorophores can on average go through before they lose their fluorescent properties. This phenomenon is called photo-bleaching and it is irreversible. While photo-bleaching is usually a negative effect for imaging, it can be used to determine the fluidity of a bilayer. To that end a specific region of the sample is photo-bleached while the rest of the sample is masked (usually by an aperture in the illumination path). After the region has been bleached one can record the recovery of the fluorescence in that region. By fitting the time dependent recovery curve to a theoretical model, the lateral diffusion coefficient and the mobile fraction (the portion of the fluorescent molecules that are diffusing) can be determined. Depending on the fluorophore used, the fraction of labeled lipids in a bilayer can be less than one mol percent of the total lipid amount, again allowing the majority of the bilayer to be unaffected and thus conserving its native properties. This technique can be used in this manner to determine the diffusion coefficient of lipids in a bilayer. For this work however the more accurate FCS

technique was used for diffusion coefficient measurement. TIRF was exclusively used to determine that the bilayer integrity was intact and that the lipids were fluid.

1.5.4. Total Internal Reflection Fluorescence Microscopy (TIRFM)

Total Internal Reflection Fluorescence microscopy, TIRF, is an illumination technique that uses the evanescent wave at a point of total internal reflection to excite fluorophores [89, 91, 167, 168]. An evanescent wave can be described as a near-field standing wave which decays exponentially with distance from the boundary at which the wave was formed. Evanescent waves are most intense within one-third of a wavelength from the surface of formation. For visible light this translates into effective illumination within about 100nm-200nm of the interface. Evanescent waves can occur in the contexts of optics and other forms of electromagnetic radiation, acoustics and quantum mechanics. In essence they are due to the fact that a wave cannot be discontinuous at a boundary. The evanescent field has the same wavelength as the light that creates it, providing straightforward excitation mechanics for fluorescent microscopy. At an optical surface where light refraction is so pronounced as to be greater than 90° total internal reflection occurs. Snell's law:

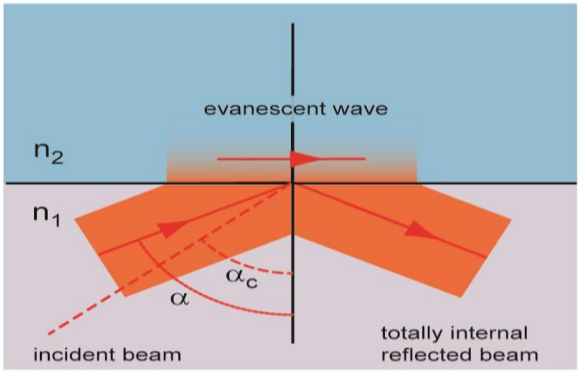

Figure 1.17.: Total Internal Reflection. Snells law describes the behavior of light at the interface between two areas of different optical density. Where total internal reflection occurs an evanescent wave is formed

$$n_1 \sin(\Theta_1) = n_2 \sin(\Theta_2) \quad \text{(equ. 1.1.)},$$

describes the relationship between the angles of incidence and refraction for a wave travelling through a boundary between two different isotropic media. The refraction angle is dependent on the incidence angle and the phase velocities of the two media. When dealing with light waves in optics the phase velocities are usually equated to the inverse refractive index. As light travels from an area of high refractive index to low refractive index the light experiences an angular displacement away from the normal. Depending on the ratio of refractive indices this can require the *sin (θ)* to have a value greater than 1 which is impossible to satisfy. This requires the notion of the 'critical angle' of incidence at which the refraction is 90° and above which total internal reflection occurs.

Because of the strong dependence of the evanescence wave intensity on distance TIRF is useful in imaging the surface of a cell with very high contrast as only the area in contact with the glass gets illuminated. A light intensity of a few milliwatts is required for the excitation light as the vast majority of it is reflected at the point of refraction.

Because of the very specific way that the area is illuminated, there is very little fluorescence from anywhere other than the volume close to the interface. A cell, in aqueous solution, adhered to a glass cover slip at which TIRF occurs at the glass/water interface, will mostly have just the fluorophores in the plasma membrane that is in contact with the glass illuminated. This is especially useful for looking at cell motion and surface binding [169].

To introduce the light to the sample at the required angle the infinity corrected optics in the objective lens can be utilized. Infinity optics systems convert light from an objectives focal point into parallel bundles of rays. These parallel light rays can then travel through different light paths within the microscope body without undergoing distortion or requiring multiple internal focal points. In order to perform TIRF we need a collimated beam with an adjustable angle to emit from the objective into the sample. The infinity property of the objective lens can be used in reverse: a focused laser beam is incident on the rear focal plane of the objective and this produces a collimated beam from the objective main lens. As the focal point of the laser is moved from the center of the back focal plane of the objective, the resultant parallel beam takes on an angle of propagating with respect to the optical axis of the microscope and the objective lens. By controlling this angle the critical angle can be met for any variety of refractive index differences that are suitable to produce total internal reflection.

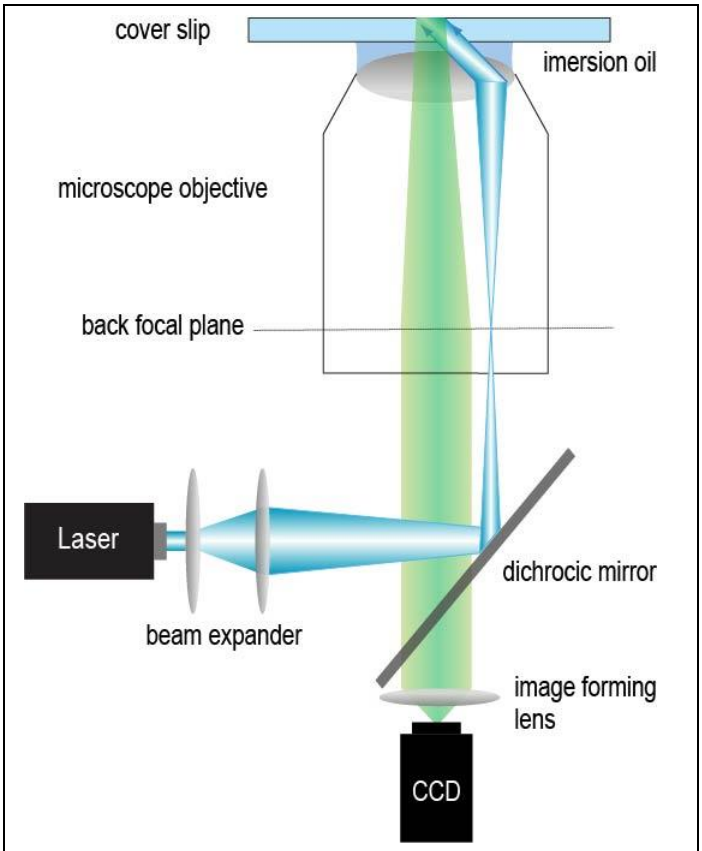

Figure 1.18.: TIRF Microscopy Laser light is focused on the back focal plane of the objective lens. By changing the distance from the optical axis at which the focused light falls, the output angle can be adjusted until total internal reflection occurs.

1.5.5. dSTORM

Fluorescence microscopy offers a number of powerful tools for the observation of the large and small scale behavior of biological systems. All light based microscopy systems have traditionally shared the major constraint of the diffraction limit. The diffraction limit renders it impossible to distinguish between two light sources that are separated by a distance smaller than approximately 200-300nm. This makes it impossible to determine the fine structure of cellular systems using traditional light microscopy. There are non-light based techniques capable of finer resolutions but these typically require an environment that is incompatible with biological integrity. Since the late 1970's there has been steady progress toward overcoming the optical limitations of traditional microscopes[170]. Over the last 40 years a number of techniques have been developed which either actually permit image resolution below the diffraction limit or effectively permit it[171]. Those that produce actual super resolution images typically used photon emitters that are themselves scaled below the diffraction limit or have an emission/depletion pattern that limits the light incidence in a similar manner[172, 173]. Techniques that provide effective super-resolution utilize properties of the fluorophore in order to produce single fluorescent events that can then be artificially localized based upon the point spread function of the system. One effective super-resolution technique in particular is very accessible as it can be implemented without the need for optical or mechanical systems more specialized than a TIRF system. This technique is called direct STochastic Optical Reconstruction Microscopy, dSTORM. In order to preform dSTORM common cyanide based fluorophores such as Cy-5 or Alexa Fluor 647 are attached to the sample in the conventional manner. The sample is then placed in an oxidizing and reducing buffer system. Following intense excitation from the light source, fluorophores can reach a triplet excited state. While in the triplet state the fluorophore is susceptible to reduction from the buffer

system. This causes the fluorophore to enter a non-radiative 'dark' state for prolonged periods. The oxidation of the fluorophore will cause the fluorescent state to be recovered releasing the photon. The buffer contains an oxidizing agent to rarify the environmental oxygen and therefore maintain the dark state of the fluorophores. The stochastic fluorescence of the dyes returning from the stable dark state allows individual fluorescent events to be captured and localized to a position at the center of their point spread function. A super resolution image is constructed by the processing of thousands of frames of stochastic flickering of the fluorophores each of which is converted to one super resolution pixel.

1.5.6. Fluorescence Correlation Spectroscopy (FCS)

Fluorescence Correlation Spectroscopy, FCS, is one of the main fluorescent techniques used in this work [174-179]. FCS uses a tightly focused laser beam to excite fluorescently labeled molecules that pass through the focal area (see Fig. 1.19.). Due to its Gaussian intensity profile, a focused laser beam will have an area of maximum intensity, called the excitation volume, directly at the focal point. The sample is labeled and illuminated sparsely enough that the fluctuations in the fluorescent signal due to labeled molecules passing in and out of the laser spot are significant. In other words, since fluctuations around the mean are proportional to the inverse square root of the number of objects, this number is kept small.

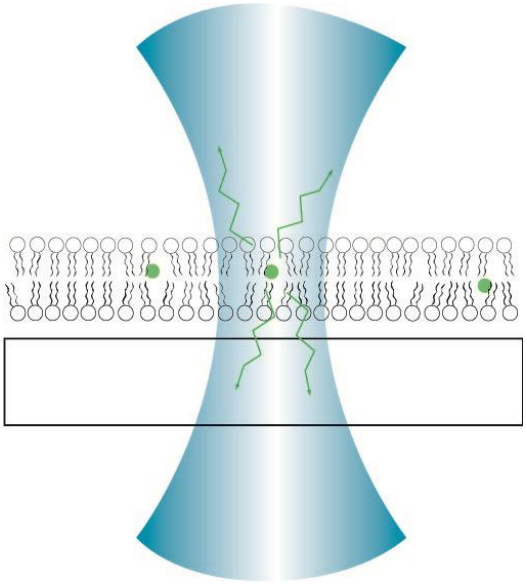

Figure 1.19.: Fluorescence Correlation Spectroscopy Illumination. In FCS fluorescent molecules diffuse through a focused laser beam and produce fluorescent fluctuations

Photons emitted by the excited fluorophores are captured with sensitive detectors and given a timestamp on arrival. This photon arrival time series is then converted into a fluorescent intensity over time measurement (see Fig.1.20.). Finally, a time series of intensity fluctuations around the mean is calculated. This data set is then auto-correlated producing a correlation curve from which the diffusion rate and the concentration can be extracted. The sparse labeling required for FCS makes it a minimally invasive procedure suitable for measurements on both artificial systems and cells. In 3-D diffusion measurements the fluorophore concentration can be in the nano-molar region.

1.5.6.1. Fluorescence Correlation Spectroscopy theory

In fluorescent correlation spectroscopy (FCS) the experimental hardware produces a time series of fluorescence intensity fluctuations. In order to calculate the auto-correlation this time series is duplicated (see Fig. 1.21.) and time shifted by a lag time "τ". The two resulting data sets are compared mathematically and a resulting auto-correlation coefficient, *G* is calculated for a given lag time, τ. This process is repeated for increasingly larger τ resulting in the autocorrelation function $G(\tau)$, which in the context of FCS is defined as:

$$G(\tau) = \frac{\langle F(t)F(t+\tau)\rangle - \langle F(t)\rangle^2}{\langle F(t)\rangle^2} = \frac{\langle \delta F(t)\delta F(t+\tau)\rangle}{\langle F(t)\rangle^2} = \frac{1}{const.}\int \delta F(t)\delta F(t+\tau)dt \qquad \text{(equ.1.2.)}$$

Here, $F(t)$ is the fluorescence intensity at time t and $\delta F(t)$ is the deviation of the fluorescence intensity from its mean. In essence the autocorrelation quantifies the similarity between the two data sets as a function of the lag time τ. Correlation curves have a theoretical maximum which is approached for the smallest value of τ, this is because the smaller the τ step the more similar the graphs.

1.5.6.2. Optical setup

To successfully illuminate a supported lipid bilayer sample for FCS, a laser beam, focused as tightly as possible, must be incident on the artificial membrane with the focal point situated in the plane of the membrane. The easiest way to achieve this is by using the microscope objective to focus the laser. Modern high powered microscopes have infinity-corrected internal optics. This infinity optics means that positional information of an object in the focal plane is translated into an angular displacement of parallel beams. This allows the optical path length to be changed

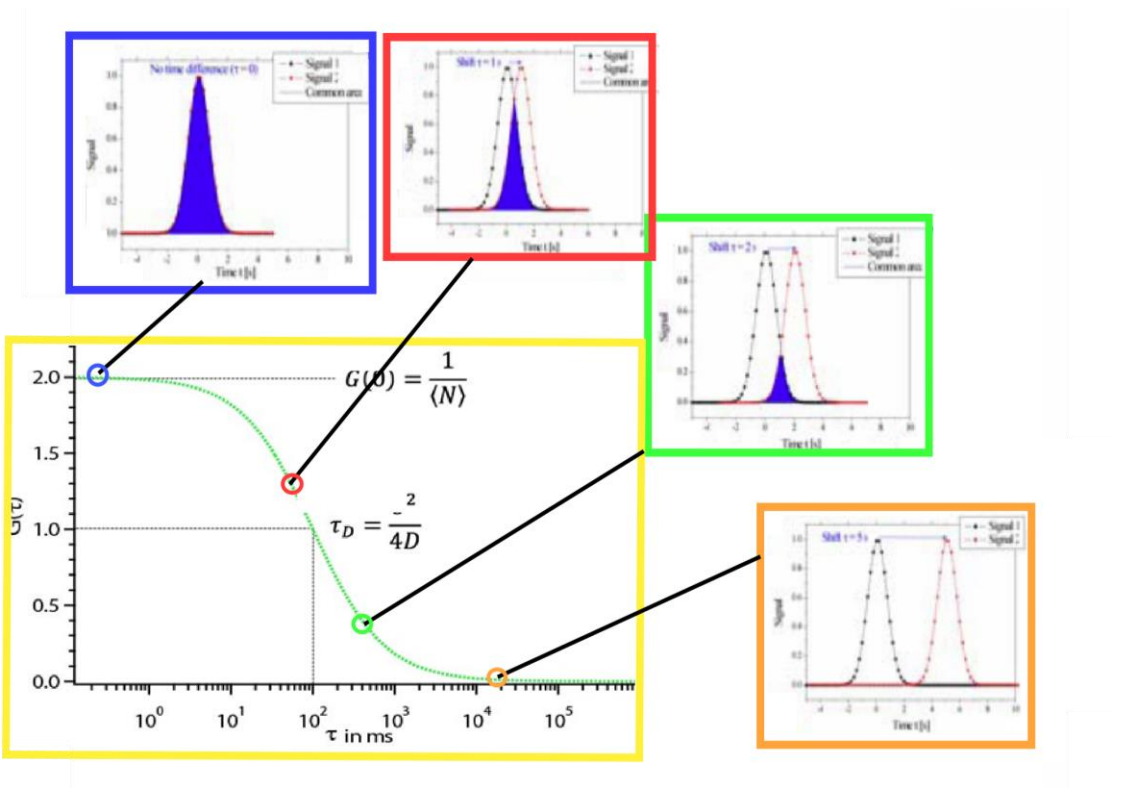

Figure 1.21.: The development of an autocorrelation curve for a single event: A typical correlation curve is depicted in the main image (highlighted yellow), it shows a decrease in correlation as lag time increases. In the top left (dark-blue highlighted) area we see near perfect correlation of an event at the smallest lag time. In the two middle (red and green) regions the area that correlates decreases as the lag time increases. In the far right (orange) region there is no correlation of the event at the long lag time.

without affecting the focal planes (in particular the front focal plane of the objective) in the microscope optics. In other words, in an infinity-corrected objective light that has been gathered from a point in the objectives focal plane exits the objective as a parallel bundle of light rays. Since in a ray optics picture optical paths can be reversed, the objective can be used to introduce a fully collimated laser beam at the rear of the objective to have it render a tightly focused spot in the front focal plane of the objective. The laser beam should be carefully controlled to provide an aberration free, uniform intensity profile.

On the detection side a highly sensitive photo detector is required as the sparse labeling requirement for FCS outputs a very low intensity signal, on the order of 10,000 – 100,000 counts per second (a typical light bulb would emit approximately 10^{20} photons per second). These signals, once detected, are relayed to specialized signal processing hardware where each photons arrival time is recorded. With the extremely low light levels involved, any spurious and erroneous fluorescent signal not originating from the labeled molecules at the laser focal point can have extremely negative effects on data fidelity. With this in mind the detection is typically set up confocally, where a pinhole is placed at an intermediary focal point providing a spatial barrier to off-focal point light. This leads to exclusion of erroneous fluorescent

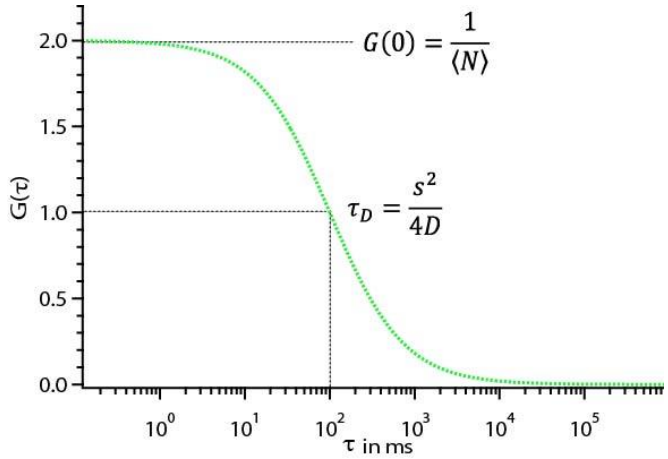

Figure 1.22.: Auto correlation of a 2-D diffusive sample. The Y intercept has a dependence on the number density of objects in the confocal volume. The full width half max of the decay is dependent on *s*, the radius of the confocal volume, and *D* the diffusion rate.

signals and thus to a better contrast in the image plane

1.5.6.3. Data processing

When taking an FCS measurement real time correlation is required for final adjustments. To have real time correlation a combination of ultra-fast hardware and software are needed, they should be capable of time resolution in the picoseconds range. The emitted photons must be gathered and converted into the proper data format. This processed must be carried out quickly enough so that there is no overlap between detections. Once the hardware has processed and assigned a time stamp to each detected photon, the software has to perform a correlation on the intensity change over time data. Afterwards the resultant correlation curve gets fitted to a theoretical model. For example, the 2-D free diffusion $G(\tau)$ is defined as:

$$G(\tau) = \frac{\langle \delta F(t) \delta F(t+\tau) \rangle}{\langle F(t) \rangle \langle F(t) \rangle} \propto \frac{1}{\langle N \rangle} \frac{1}{(1+\frac{\tau}{\tau_D})} \quad \text{(Equ. 1.3.)}$$

Here $\tau_D = s^2/4D$ where D is the diffusion rate of the fluorescently labeled species and s^2 is the measurement area .

In this fitted curve the half max intensity gives $\tau = \tau_D$ simplifying the equation to give, among other things, the diffusion rate D. Where the correlation curve intercepts the y-axis the mathematics lose their dependence on τ, this allows for simplification that gives $G(0) = 1/N$ with N = the numerical density of fluorophores in the illumination area.

To eliminate signals from electrical and detector noise in the detectors a pair of detectors can be used. Afterpulsing is a form of detector noise that typically occurs in an avalanche photo diode when some of the generated charge carriers are trapped in a depletion layer [180]. These trapped carriers are released by thermal excitations creating a second avalanche event which is closely

correlated with the original event. Since noise in the two detectors is uncorrelated. By splitting the light signal evenly between two detectors and then cross-correlating the two resultant data streams, electrical artifacts such as shot noise and after-pulsing can be suppressed [89].

1.5.7. Photon Counting Histogram Analysis

A complimentary technique to FCS is Photon Counting Histogram analysis (PCH). Utilizing the

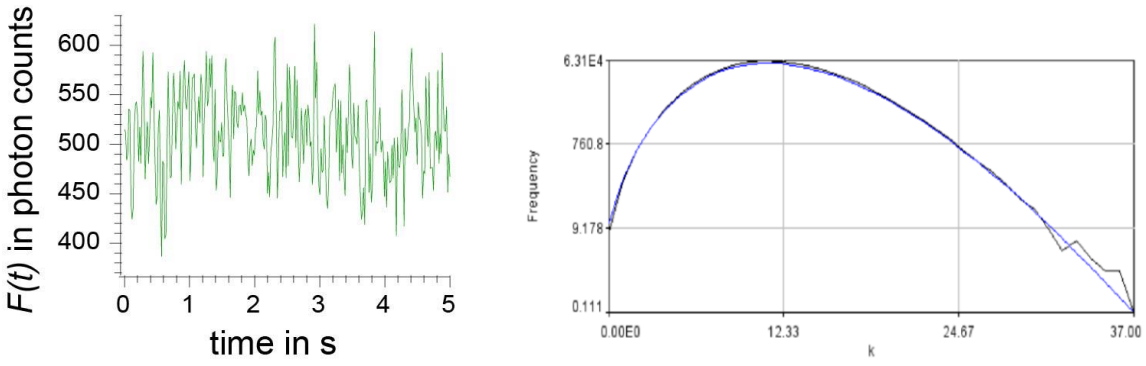

Figure 1.23. The Formation of a Photon Counting Histogram: Photon arrival times are translated into intensity over time graph. These counts can be displayed as a histogram of photon counts, the analysis of which can give the molecular brightness ε, and the average number of photon counts ‹*k*›

same raw data set as is acquired for FCS, i.e. single photon arrival times, PCH analysis permits the extraction of additional fluorescent properties from the system. Namely the average number of molecules within the excitation volume and the number of photons detected per molecule (aka the molecular brightness). This allows a user to distinguish between fluorescent molecules that have a diffusion rate too close to separate using FCS but which have a differing molecular brightness [181-183]. The benefits of such a capacity are twofold; molecules can be distinguished by the selection of fluorophores of the same wavelength but of differing fluorescent brightness allowing one excitation/detection path to detect multiple diffusive molecules, and molecular brightness can be used to distinguish between fluorophores is varying states of aggregation. The capacity to detect aggregation is tempered by the sparse labeling requirement necessary for FCS as only a small percentage (typically between 0.01 and 0.5 Mol% dependent on the system and the fluorophore) of the molecules of interest are labeled. In conjunction with the diffusion data from FCS analysis the PCH is a powerful tool in illuminating behavior on a molecular level.

1.5.7.1. PCH: Theoretical considerations

A constant illumination source will produce photon counts detected with a Poisson distribution of probabilities. A Poisson distribution predicts the degree of spread around a known average rate of occurrence and is described by equation (1.3)

$$p(N) = \frac{\langle N \rangle^N \cdot e^{-N}}{N!} \quad (Eq. 1.3)$$

Where N = number of events and p(N) = probability of N events

In an FCS experiment the probability of detecting a certain number of photons is the convolution of the probability of the number of particles in the excitation volume and the probability of the detection of a photon by the hardware. Both of these are Poisson distributions of probability. The convolution of these two Poisson distributions produces a broader probability distribution known as a Super-Poisson. The entire system is further complicated by the fact that the illumination profile of an FCS excitation volume is not a constant. In fact a laser beam in the TEM_{00} mode already has a Gaussian beam intensity profile and the act of focusing it produces a 3-D Gaussian-Lorentzian excitation volume. This position dependent variation in the light intensity within the excitation volume causes the Super-Poissonian distribution of detection intensities to further broaden.

In order to determine the correct representation of a system it is appropriate to start with a simplified version of a system and add complexity. For PCH we can start by calculating the probability distribution of intensities for a single particle with a specified molecular brightness in the excitation volume. To do this we integrate over all possible positions of the particle in the excitation volume. The probability of detecting k photons at any position is given by the Poisson distribution, the intensity of the excitation volume at that point, and the molecular brightness.

Since the excitation volume is not well distinguished it is necessary to define an arbitrary volume over which the integral must take place (V_0), this must be substantially larger than the excitation volume. Considering the fact that we are assessing the probability of detection we must also now treat the excitation volume as the point spread function (PSF) that it would take after traveling through the optics of the detection system. The formula for this system is represented as equation (1.4.):

$$PCH^{(1)}(\varepsilon, k) = \frac{1}{V_0} \int_{V_0} Poi(k, \varepsilon PSF(\overrightarrow{r)) \, d\vec{r}} \quad Equ.(1.4.)$$

Where ε = molecular brightness, and *k* = number of detected photons. When a second fluorescent particle is added to the system then it is necessary to convolve both intensity probability distributions in order to determine every possible position of both particles, this produces equation (1.5.):

$$PCH^{(2)}(\varepsilon, k) = \left(PCH^{(1)} \otimes PCH^{(1)}\right)(\varepsilon, k) = \sum_{i=0}^{k} PCH^{(1)}(\varepsilon, k-i) \, PCH^{(1)}(\varepsilon, i) \quad Equ.(1.5.)$$

Equation (4) can be expanded to an arbitrary number of particles, *n*, by convolving the intensity distribution of the single particle with the *n*-1 particle intensity distribution.

In order to incorporate the fluctuation in particle numbers in the excitation volume (which is described by a Poisson distribution) it is necessary to calculate the average of the '*n*' particle distributions. Each average is weighted by the probability of having that '*n*' given the average number of particles in the system which we will call *N*. This gives rise to the multiple particle equation for PCH equation (1.6.):

$$PCH(\langle N\rangle\varepsilon,k)=\sum_{N=0}^{\infty}Poi(N,\langle N\rangle)PCH^{(N)}(\varepsilon,k)\quad Equ.(1.6.)$$

If there are diffusive species present with different brightness's, whether from aggregation (in which they are simply multiples of ε_1) or due to having a different fluorescent marker, they can be considered mathematically by convolving the different species. This gives the final and most complete approximation of the photon counting histogram from an FCS experiment, equation (1.7.).

$$PCH(N1,2,\varepsilon1,\varepsilon2,k=PCHN1,\varepsilon1,k\otimes PCHN2,\varepsilon2,k\quad Equ.(1.7.)$$

This mathematical approximation can be fitted to an experimental PCH in order to extract the molecular brightness, ε, and the photon count, *k.* This knowledge can then be used to determine the number of particles in the excitation area by simply dividing the total photon count intensity by the calculated molecular brightness.

1.6. Dual Color FCS/TIRF machine

In order to fully understand the research that is carried out in this work it is necessary to understand the optical system that permits the various experiments that will

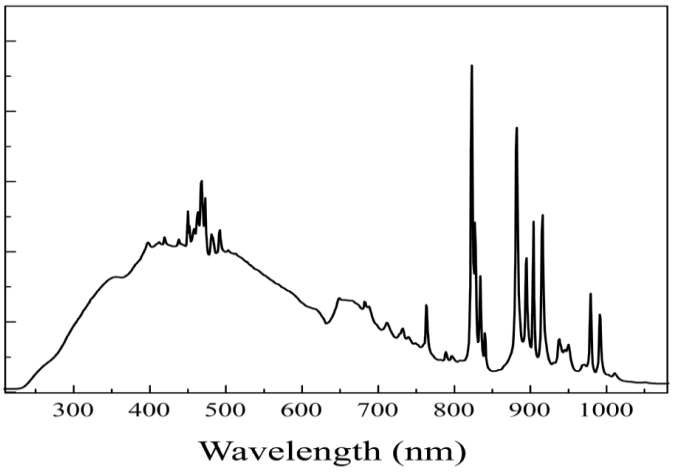

Fig. 1.24.:Xenon Arc Lamp Spectral Distribution: a Xenon spectrum shows even light distribution through the visible spectrum Image: Public Domain.

be discussed in subsequent chapters. The building of a multi-wavelength combined TIRF/FCS microscopy platform is motivated by the symbiotic relationship between the two techniques. TIRF imaging gives a broad perspective of the movements and interactions of membrane elements over a relatively large area. FCS on the other hand looks at one, very small area and measures the movement of molecules through it. A combination of these two techniques can provide crucial information of the large and small scale dynamics in membranes.

The dual capacity to perform both high resolution and high contrast measurements on the same sample nearly consecutively will provide better insight into the processes that drive the dynamics of molecules in a membrane. To be able to do both with two wavelengths of excitation light will allow multiple species to be measured simultaneously. From this added dimension lipid-lipid, protein-protein and lipid-protein interactions can be studied in the context of the cell membrane. Opening up the avenue of investigation into how these dynamics are influenced instead of just what the dynamics are.

1.6.1. Design

The design and construction of a dual color FCS/TIRF illumination and detection system was undertaken based around a Nikon Ti Eclipse microscope (Nikon Ltd. Japan). The microscope, two illumination systems, two cameras and the shutter control system were purchased from MVI Inc. based in Avon, Massachusetts. The Nikon Ti

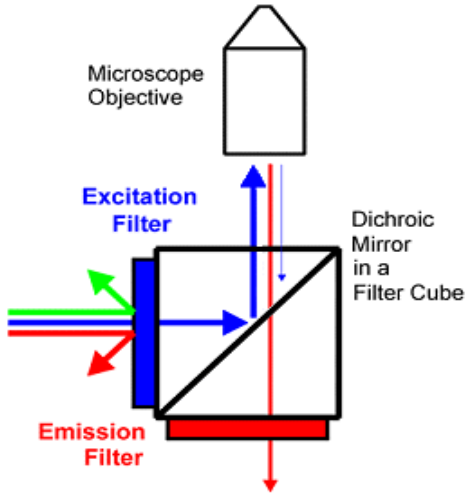

Figure 1.25.: Filter Cube Anatomy: A filter cube consists of a dichroic mirror and matching excitation and emission filters. Each fluorophore has its own customized filter cube.

features their CFI-60 infinity optics system. This enhances the versatility of the system as it allows the outputs to be placed ergonomically without requiring a complex lens system.

The microscope was ordered to include two illumination methods: Through-light and Epi-illumination. Through-light illumination is the standard illumination method that has been used since the early days of microscopy. Light from an outside source is shone on the sample to be viewed. A bright source is required to view objects under high magnification. Epi is a Greek prefix that means ‘on’, ‘among’, or ‘through’, in this context it refers to light illuminating the sample ‘through’ the same optical pathway used for imaging. In this type the sample is illuminated and imaged from the same side. Dichroic mirrors and wavelength specific filters are used to separate the illumination light from the emitted light when using epi-illumination.

There are two separate lamps, one for each illumination scheme: the epi illumination uses a Xenon lamp that provides light in a broad spectrum (see Fig. 1.24.). A broad spectrum is required of use in conjunction with a filter cube turret that allows different combinations of excitation filter, dichroic mirror and excitation mirror to be chosen depending on which fluorescent label is being used (see Fig. 1.25.). The lamp is located in a separate housing from the microscope and the light is channeled into the scope

Figure 1.26.: A Nikon Eclipse Ti microscope. The various optical paths are highlighted. A rotating prism selects the output port.

using a liquid light guide (a light transmitting tube that has a liquid core and cladding much like an optical fiber but it doesn't suffer from the packing dead space that fiber optics have). The second lamp, built into the body of the scope, is for the more conventional through light illumination and is powered by a halogen bulb.

The microscope features three output ports along with the eyepiece, ports are located on either side of the microscope are on the bottom. The selected position is controlled by a motorized prism that sends 100% of the light to the chosen port. When in the bottom port configuration no prism is inserted in the optical pathway. This minimizes photon loss and thus the bottom port is the best suited for high quality, low-light imaging.

Situated directly above the prism assembly is the epi-illumination filter cube turret. This contains a rotating disk with spaces for six filter cubes; each filter cube can be rotated into the optical path. The dichroic mirror in the filter cube is responsible for introducing the epi-fluorescent illumination into the optical pathway, reflecting it from its introduction point at the liquid light guide.

Above the filter cube turret is a spacer between the filter cube turret and the objective

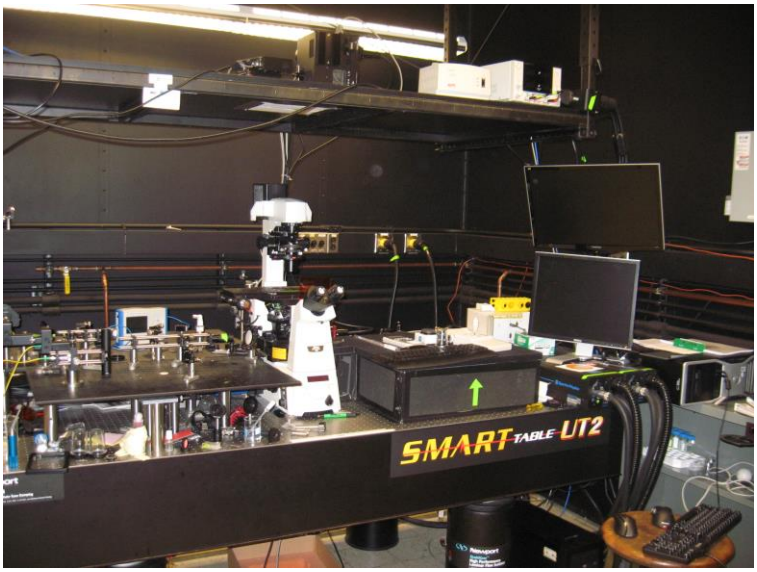

Figure 1.27.: The Optics Table The optics table with the microscope in the middle, the lasers on the extreme right, the FCS acquisition (with the green arrow) on the right, and the FCS &TIRF excitation optics on the left.

turret that extends the optical path length at the point where beams are parallel beam bundles. This extended “infinity space” is provided to allow other excitation sources, in our case lasers, to be introduced into the optical paths of the microscope. The additional space is accessible from the left and right, but closed at the front and has a circular opening to the rear. It is located approximately 8” above the bottom of the scope. This is where all subsequent laser excitation sources will be coupled into the microscope.

Finally there is a motorized objective lens turret, this moves up and down for focusing and rotates for objective lens selection. The sample is held by a motorized stage that moves in the x-y plane but not the z direction.

To allow a variety of fluorophores to be used in TIRF and FCS, a tunable laser source was deemed to be the best option as the required excitation wavelength can be selected as required. A gas laser with a variable resonator length allows different wavelengths to be selected by adjusting the resonator to correspond with the available laser wavelengths. A mixed gas gain medium provides a broad spectrum selection of wavelengths. Two Spectra physics Stabilite 2018 Krypton/ Argon ion gas laser were purchased (Spectra Physics, Santa Clara, CA), these lasers have stimulated emissions at 647nm, 568nm, 530nm, 520nm, 514nm, 488nm, 476nm, and 457nm. The gas mixture allows this broad range of wavelengths. The Krypton facilitates the higher wavelength emissions, from ~520nm up, while the argon-ion is responsible for the lower wavelengths. Wavelength selection is achieved by adjusting a prism at the lasers high reflector end which changes the cavity length until it corresponds with the desired wavelength.

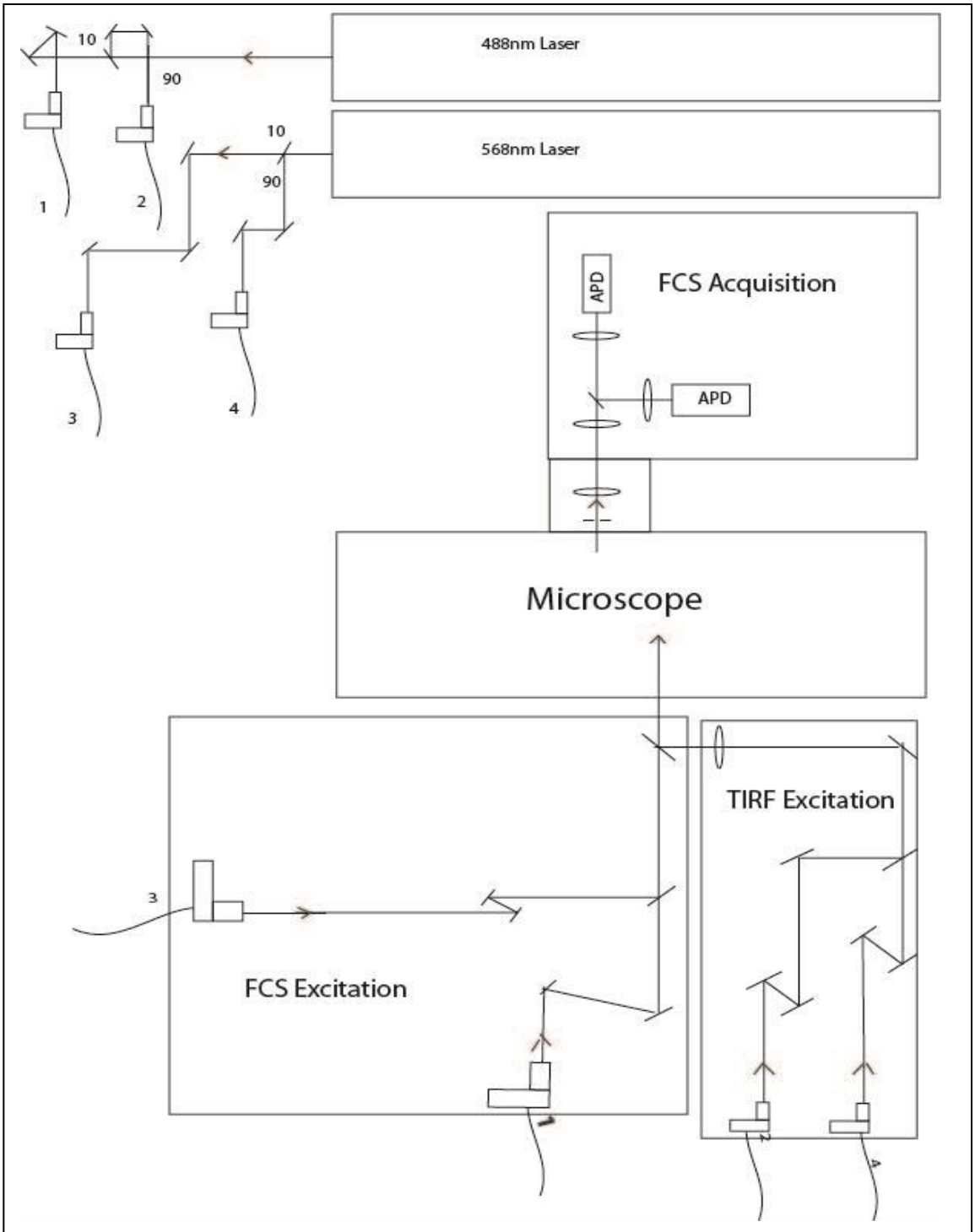

Figure 1.28.: Optics Schematic: A schematic showing the placements of the various components of the FCS/TIRF system on the optics table.

Some physical considerations and infrastructure requirements influenced the design of the system. Given the nature of FCS it is important that external vibrations be minimized in the sample as these could easily be confused with intensity fluctuations. A vibration damping optical table was therefore used to house all the components. Independent optical systems were separated spatially in the table to facilitate convenience in maintenance and troubleshooting.

1.6.2. General requirements

The microscopes epi illumination uses a combination of a broad spectrum lamp, dichroic mirrors and band pass filters to select the proper excitation light for the fluorophore used. For the FCS and TIRF illumination we use the two Spectra Physics Stabilite 2018 He-Ar ion lasers. Each laser is tunable to 8 different wavelengths by adjusting the length of the cavity (see above). The intensity of each wavelength is not identical however, with only four wavelengths having powers greater than 0.3W. The maximum output is 300mW at 488nm, this is the wavelength used for exciting GFP and fluorescein. The 647nm line and the 514nm line are also approximately 0.3W; these wavelengths are suitable for the Alexa 647 fluorophore (which is suitable for dSTORM) and the yellow fluorescent protein (YFP) respectively. Biological imaging does not require high intensities, in fact too high of an intensity can be harmful to cells. TIRF requires intensity in the milli-watt range as the majority of the light gets reflected at the imaging surface; FCS requires intensity in the microwatt range as sparse illumination helps keep the fraction of fluorescing molecules moving in and out of the observation volume at a significant portion of the total observed.

To get the appropriate power level for each excitation path from a single source, the laser beam should be split with the majority of the light energy going for TIRF illumination.

To this end a disproportionate 90/10 reflecting beam splitter was placed outside the output aperture of each laser.

The four resulting beams are separately steered and coupled into optical fibers using two steering mirrors each to direct the beam toward the coupler. Each fiber only carries one wavelength, however to accommodate the ability to change the wavelengths of the lasers for different fluorophores, the optics used were all achromatic; to eliminate lengthy adjustments due to differing refraction angles and focal points when changing wavelength.

To optimize the focusing power of subsequent optics the decoupled beams undergo expansion: a much tighter focal point is produced when the light being focused covers the entire focusing lens. However it should also be noted that certain optical aberrations are associated with lens edges and these areas should not be illuminated; approximately 80% of the lens surface was used for focusing. TIRF and FCS both use focusing lenses. In the case of TIRF a lens chosen specifically to focus the laser beam on the back focal plane of the objective and in FCS the focusing lens used is the microscopes objective lens itself. These two lenses have different optical properties and sizes and therefore to get the optimal laser beam diameter for each we require separate beam expanders for the FCS and TIRF illumination paths. .

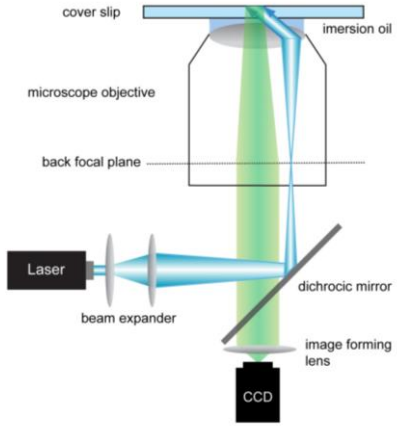

Figure 1.29.:TIRF Ray Diagram: A typical TIRF ray diagram showing light being focused on the rear surface of the objective lens exiting collimated and at an angle when displaced from the optical axis to produce total internal reflection.

1.6.2.1. TIRF excitation

As mentioned previously, with Nikon infinity corrected optics a focused laser spot at the rear optical surface of the objective produces a collimated laser beam at the focal point of the objective due to the fact that Infinity optics use parallel light bundles inside the body of the scope. The angle of propagation with respect to the optical axis of a laser beam manipulated in this way depends on where the focal spot lies on the back focal plane of the objective. By adjusting the point where the focal spot falls on the rear focal plane away from the optical axis, the output beam exhibits an angular displacement away from the optical axis (see Figure 1.29.).

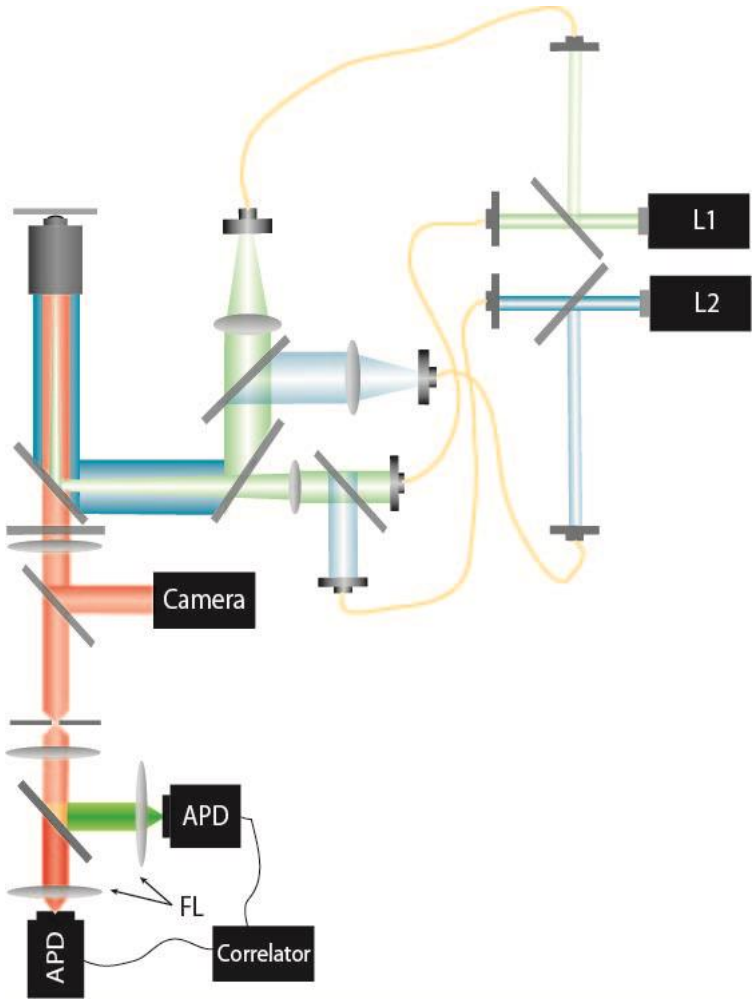

Figure 1.30.: Basic Optics Setup: A conceptual schematic of the dual color FCS/TIRF optics layout. In this schematic there is no distinction between the optics in the microscope and those external.

To be able to adjust the position of the focal point the entire TIRF excitation optics were placed on an elevated 'breadboard' (a solid plate with attachment points for opto-mechanical devices) at a

height that allowed for direct coupling into the microscope via the open space below the objective turret. The breadboard was mounted on an x-y stage with support posts on each corner using a single ball bearing on a smooth aluminum plate to allow free movement. Once the laser has been expanded and refocused it is steered towards the dichroic mounted in the microscope and carefully aligned into the microscopes optical path.

1.6.2.2. FCS Excitation

FCS requires a collimated laser beam on the rear of the microscope objective. This produces a focused laser spot at the image point of the objective. To achieve a tighter focal spot the laser beam was expanded to ~15mm diameter, this corresponded to about 80% of the back aperture of the objective. The excitation light was transferred from the beam expander using two mirrors, these allowed the beam to be adjusted to lie centered on the optical axis. All coupling optics were mounted on two inch high stainless steel posts, with 1" diameter. They are highly stable and help to reduce any vibrations in the excitation light which can cause false signal fluctuations which would show up as strong intensity correlations and thus giving erroneous measurement results. For FCS experiments beam stability is crucial to good experimental data. The microscope was fitted with a 'stage-up' kit that provided the space necessary to incorporate a coupling optic within the body of the microscope. The coupling dichroic was mounted in a Thor Lab 'Kinematic Base' these bases have a base plate that has magnets that allows the dichroic to be removed and replaced with repeatable, high accuracy. Another benefit of these mounts is that different dichroics for different fluorophores can have their own mounts and can be swapped in and out without having to dismantle any of the mounting hardware and thus realignment can be minimized.

For TIRF illumination to work properly all interfaces from the objective to the point of reflection should be of a similar index of refraction, this prevents unwanted reflections at other interfaces. TIRF specific objective lenses were obtained with the microscope. These objectives use a refractive index matching immersion oil to bridge the gap between the objective lens and the glass slide where the samples rest. The FCS technique is dependent on a stable focal spot size and shape. By omitting extraneous steering mirrors and expansion optics we minimized the points where optical distortions and aberrations or mechanical vibrations can occur. We consequently chose to situate the FCS optics directly in front of the coupling dichroic

With the majority of the excitation light reflected at the interface in TIRF the output signal has a tendency to be weaker than traditional epifluorescent imaging when using similar concentrations of fluorophores. Because of this a high numerical aperture objective and a highly sensitive camera are typically required. As mentioned previously, two types of camera were ordered with the microscope: one high resolution, one for low light intensity. The first is a Photometrics CoolSNAP EZ camera which has 1392 x 1040 pixels at 6.25µm x 6.25µm with 12bit digitization at 20MHz. This is mounted on the left hand port. Mounted at the bottom port is the second camera, a Photometrics Cascade II with 1024 x 1024 pixels with a size of 13µm x 13µm. This camera uses an on-chip amplification scheme that can be used to amplify low light signals. The Cascade camera is the more useful in daily operation as it can detect the sparsely doped bilayers generally used in biological experiments.

The microscope system consists of many different electronic and mechanical components. In order to control these efficiently a software package which can operate all of these is bundled with the microscope. Nikons ‘Elements’ software controls the camera exposure times and also allows adjustment of the signal gain as well as some simple image manipulations

Fluorescence correlation spectroscopy is a very low-light measurement system and the signals collected are typically only 10,000 – 100,000 photons per second. Any background noise, be it electrical or photonic, must be kept to an absolute minimum to ensure a clean signal and meaningful measurements. To eliminate the simplest and possibly the most troubling form of nose, ambient light, a light –proof box was built in which to house all the detection optics and electronics.

Central components of the FCS detection are the pair of highly sensitive photo-detectors connected to a device that time stamps and dynamically correlates both channels. The Time-Stamp/Correlator is a hardware single photon counter purchased from Pico Quant; the model is the PicoHarp 300. For detectors we have two avalanche photo diodes (APDs) from Perkin Elmer (Waltham Ma).They are connected via signal attenuators/inverters to the PicoHarp 300 as the APDs operate on a 5V positive TTL pulse while the PicoHarp requires 2V negative pulses for counting. Each photo diode has a dark count of ~50counts per second. The PicoHarp electronics time stamp every input signal, i.e. photon, with a time resolution of down to 4ps. It then sends it to a PC with acquisition software from Picoquant which stores all the events on a PC for future processing while also giving a real time sampling for system adjustments. One of the possible post processing modalities is the calculation of the fluorescence intensity time series from the photon arrival times and subsequent calculation of the auto- and cross correlations of the two input channels.

The Nikon Ti has an output port on the right hand side of scope for use in the FCS detection. At that output the light from the scope is focused and usually a camera is placed at this focal plane. In our case a pinhole is placed at this focal point (in this case where the image is a point, i.e. the emission from the small area illuminated by the tightly focused laser spot) to act as a spatial

filter. The pinhole used has a 50µm aperture that prevents the majority of the light cone from off focal point light from passing through while allowing light from the focal point through freely. The light from the pinhole is restricted and then divided by a non-polarizing 50/50 beam splitter into two detection paths. In each of them a final convex lens focuses the light on the sensor area of the APDs. The APDs are mounted on highly stable 562 Series ULTRAlign™ Precision XYZ Positioning Stages from Newport Inc. (Irvine Ca.). This allows them to be positioned precisely in the focal point to maximize the detected signal and thereby maximizing the signal to noise ratio.

1.6.3. System Calibration

The primary information contained in microscopy images is location and intensity of light. Thus, in order to obtain quantitative information, it is important to translate dimensions on the camera images into real distances. This is achieved by performing calibrations against a known standard. Traditionally, microscope calibration involves the determination of the size of features of the sample at a known magnification by comparison of a scale built into the ocular lens (i.e. the eyepiece lens) to a certified stage micrometer (a microscope slide with a scale etched onto its surface). In our system, this calibration is facilitated by the Nikon elements software which translates the size of the field

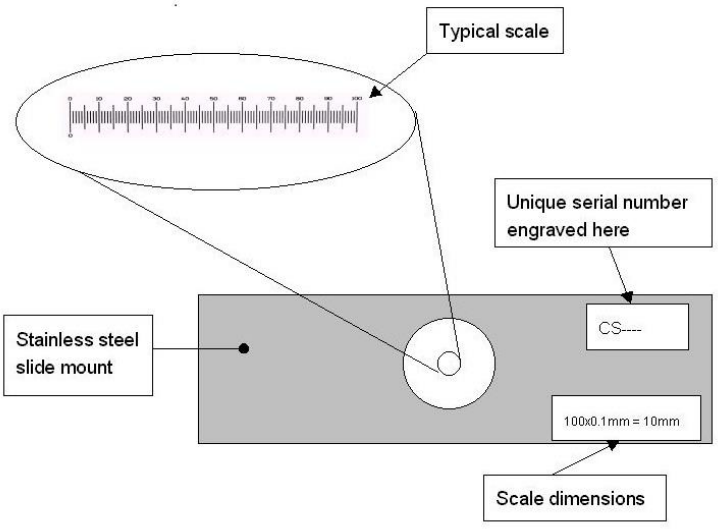

Figure 1.31.: Microscope Calibration Scale: A schematic of a stage micrometer from SPI Inc. The scale on the micrometer is used to define the apparent size of a pixel under a specific magnification.

of view into the size of each camera pixel. A 1mm calibration grid was purchased from SPI supplies (West Chester, PA) with 100 graduations of 10µm each(see figure 1.31.) . To calibrate an objective lens, the lenses' particulars such as magnification, numerical aperture, phase annulars etc. are entered into the software. An image of the calibration grid is brought into focus under through-light illumination. The software then allows the two extremes of the known distance to be defined in the image plane. From this known distance the average size of an individual pixel is then determined automatically. Each objective lens must be calibrated in this way, and care must be taken when inserting and removing objectives into the objective turret that the software is updated correspondingly. Each camera requires separate calibration also as they have different pixel size and the CCD chip for each camera may lie at a slightly different position on the imaging plane.

Once the objectives have been fully calibrated, measurements can be taken on images by using the cursor to define a length or an area. The Elements software then determines the physical size based on the corresponding pixel size, namely 13µm x 13µm for the Cascade II camera.

In an FCS system there are generally only two unknowns: the observation volume (often referred to also as confocal volume) and the diffusion rate of the fluorescence species being observed. To calibrate the system one of these unknowns must be determined which can then be used to calculate the other. Given the fact that our experiments are designed to determine the diffusion rates of different lipids, it becomes clear that the determination of the observation volume in necessary. The means of determining the diffusion coefficients depends on the type of measurement being done, namely if we are measuring diffusion in two or three dimensions. However, the essence of the calibration of the observation volume remains the same. A

fluorophore whose diffusion coefficient in solution is well known is measured at varying

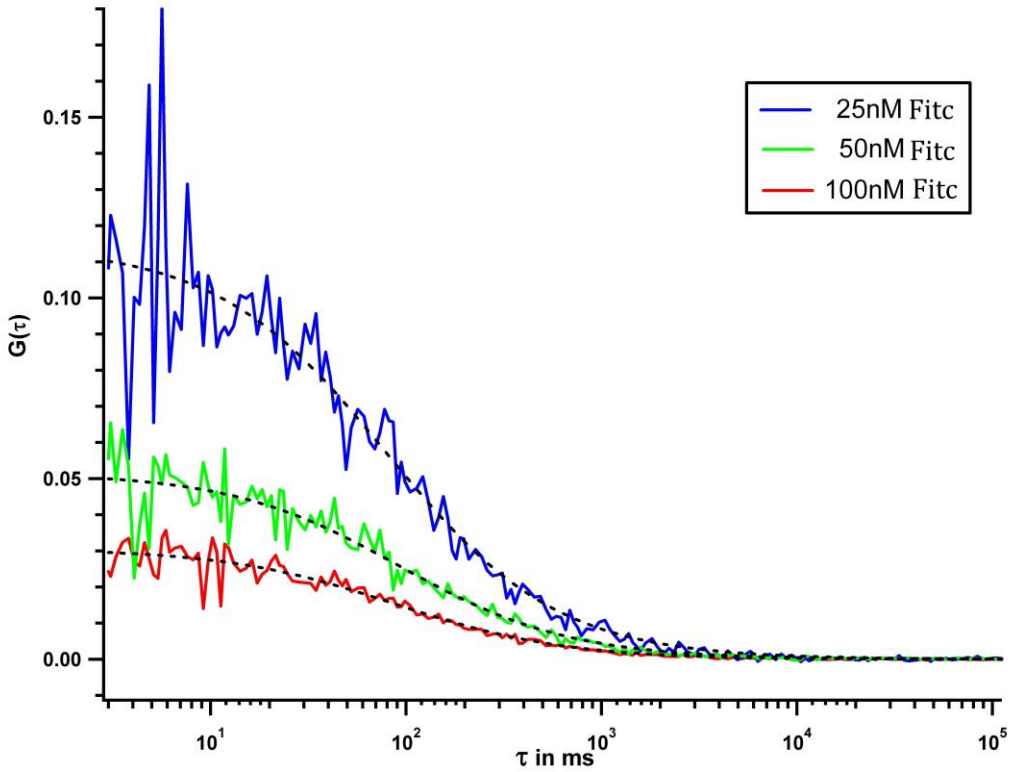

Figure 1.32.: FCS Calibration: Correlation traces of varying concentrations of fluorescein in 10mM Tris buffer at pH 10. These curves were used to calibrate the system by determining the observation volume. The inverse relation of the y-intercept to the number of fluorescence objects can be clearly seen.

concentrations to give an averaged observation volume.

The FCS system is controlled by PicoQuants SymPhoTime software. The software saves the data stream from the PicoHarp 300 onto a Raid-array of hard-drives on the PC. The data can then be auto correlated, cross correlated as well as other manipulations. Once the correlation curve has been calculated the software can be used to fit a theoretical curve based on the mathematical model of the diffusion properties of the fluorophore. The theoretically fitted curve

can then be used to determine the observation volume by entering the expected numerical value for the diffusion rate into the software.

To calibrate the system for a three dimensional measurement a series of fluorescein solutions are made at decreasing concentrations 10mM Tris buffer at pH 10. Typically these concentrations range from ~500nanoMolar (nM) down to 5-10nM. In particular we measured solutions at 500nM, 200nM, 100nM, 50nM, 20nM, 10nM and 5nM. Each measurement produces an observation volume in femtoliters when the diffusion rate is entered into the software. The diffusion rate has been well determined in literature and a value of 425um^2/s was used for the calibration [184]. The three plots seen above in Fig. 1.32. were fitted using the 2-D diffusion

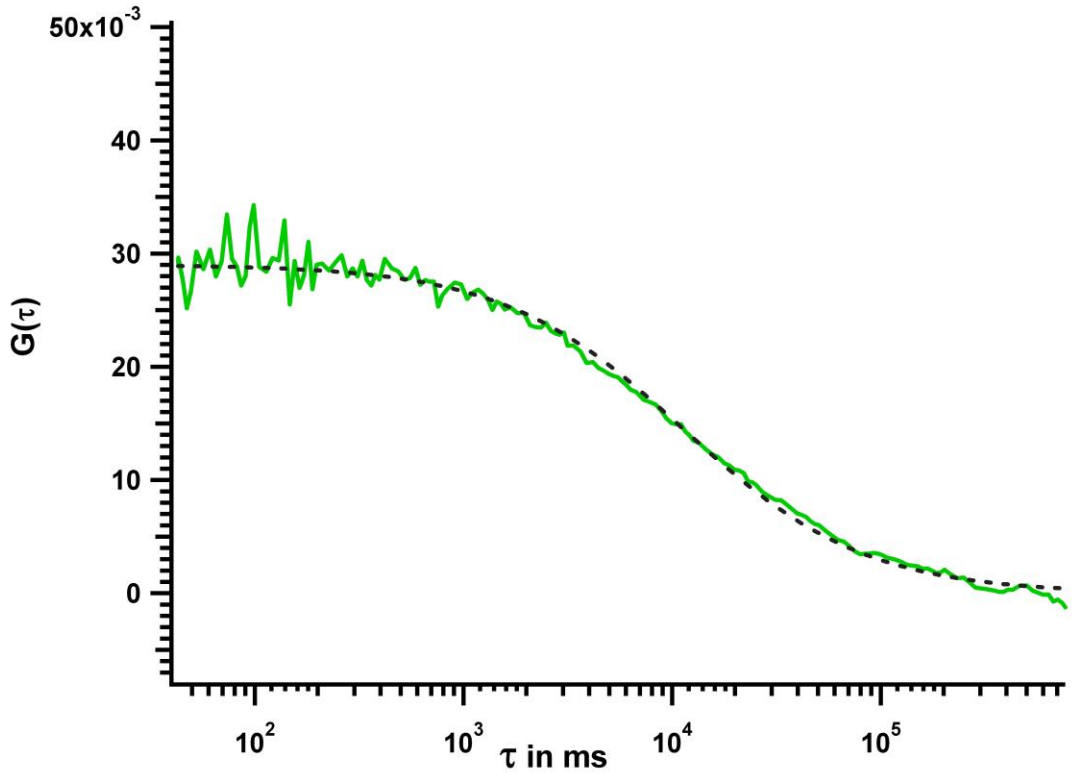

Figure 1.33.: FCS Calibration Verification: FCS curve of a 99.995 mol% DOPC/ 0.005 mol% SLB. The fitted curve confirms the observation volume of the FCS system at 14.5μm^2±0.5.

model. This gives an acceptable value for the detection volume as the elliptical shape of the excitation volume has an aspect ratio of approx. 20:1 meaning that the vast majority of the fluctuations are due to diffusion in the x-y plane. From this a detection area, ω, was determined to be 14.5±0.5 μm^2.

To verify that our FCS system works properly and allows for reliable measurements of lipid diffusion in membranes, we used the above determined observation area to determine the diffusion coefficient of a fluorescent labeled lipid to its values given in the literature. This was done using a supported lipid bilayer consisting of 99.995 mol% DOPC (Avanti lipids, Alabaster, Al) and 0.005 mol% β-Bodipy-fl-C12 –DHPC (Invitrogen, Carlsbad, Ca.). The minor constituent of the bilayer is a fluorescently labeled DHPC lipid with green Bodipy covalently attached to one of the hydrocarbon chains. A series of three, one minute FCS measurement were performed on this system. The fitted curve gives a diffusion coefficient of 3.21 ± 0.08 $\mu m^2/s$. This compares very well to a *D* of 3.3±0.1 $\mu m^2/s$ reported previously [185].

The open and modular design of the optical systems means that they can be easily altered or changed completely depending on the need. The basic elements are suitable for a number of applications other than those they were designed for. For instance, the tightly focused and controllable laser beam engineered for FCS acquisition is also suitable for an optical tweezers. The adjustable (relatively) high intensity laser beam designed for TIRF is also suitable for super resolution microscopy acquisition using the dSTORM technique described above.

The design and building of this system provided me with the necessary experience and hardware to pursue the diverse experimental investigations that will be seen in this work.

1.7. Scope of proposal

This work aims to make a broad effort at progressing some of the essential aspects of cellular and bilayer research. By answering basic function questions, engineering novel artificial bilayer solutions and looking at the broader cellular structure simultaneously the entire spectrum of necessary research can be inter woven using similar research equipment and techniques.

1. The basic behavior of the bilayer will be investigated, namely the role of Ca^{2+} ions in the dynamics of the phospholipid Phosphatidylinositol 4,5-bisphosphate (PIP_2), an important signaling molecule in its own right but also a facilitator to protein recognition and adhesion [35]. It has been shown previously that relatively large concentrations of Ca^{2+} will induce aggregation of PIP_2 in supported lipid bilayers [186]. By determining the boundaries of this aggregation phenomenon, and by determining its relevance to physiological concentrations of Ca^{2+} and PIP_2, a system can be developed which would allow researchers to actively control the spatial arrangement of molecules in the bilayer with the potential to expand to proteins or peptides anchored to the bilayer. This work will also help illuminate one of the unknown factors in Ca^{2+} signaling: how the cell differentiates between Ca^{2+} signaling pathways.
2. A novel lipid-protein anchoring system has been developed and refined permitting the genetic encoding of an anchor point on the protein that is only activated post translation. This ‘Aldehyde Tag’ will permit the site specific anchoring of a protein or peptide onto a bilayer surface, allowing researchers to couple the dynamic and chemical properties of both..

3. The effect of bilayer surface charge on the adhesion and proliferation of fibroblast cells will be investigated, this will assist in the development of improved drug delivery liposomes as well as determining the best way to encourage or discourage cellular growth on a surface.
4. Some additional experiments will be outlined which, while not at an advanced enough state to deserve a chapter of their own, they do merit inclusion in this work due to their novel nature or their promising initial results. These include a super-resolution study of the spectrin based membrane skeleton of fibroblast and cardiac cells, and an investigation into how the structural properties of a polymer substrate can influence the dynamics of the lipid bilayer it supports.

This research conducts vital investigative work that will permit the development of advanced and interactive bio-membranes with the capability to improve mechanical and chemical coupling between manmade materials and biological tissue. Along the way important signaling systems and basic biological properties will be investigated.

1.8. Structure of rest of document

The remainder of this document will consist of three chapters one each dedicated to one major experimental field of my research. A fifth chapter will incorporate the projects that were too small or insufficiently developed to deserve an individual chapter. And finally the sixth chapter will cover the overall discussion and conclusion for the work as a whole. Individual project chapters will be self-contained with respect to motivation, materials and methods, results and discussion/outlook.

Chapter 2: The Effects of Ca^{2+} on the dynamics of PIP_2 Containing Lipid Bilayers

Summary

Phosphatidylinositol 4,5-bisphosphate (PIP_2) is an anionic phospholipid found in most abundance on the cytosolic leaflet of the plasma membrane. Research has shown that PIP_2 is involved in multiple cellular functions from intracellular calcium signaling to protein activation to protein anchoring. It has been hypothesized that PIP_2 can form pools of increased concentration as a means to differentiate between its various functions. Previous studies have observed aggregation of PIP_2 in elevated Ca^{2+} environments but the quantities of both used has far exceeded those found in nature. In this work we aim to investigate the aggregation hypothesis at concentration of both Ca^{2+} and PIP_2 found in nature. Fluorescence Correlation Spectroscopy (FCS) will be used as the primary tool in determining the diffusion rate of PIP_2 containing supported lipid bilayers. Aggregation of the PIP_2 should result in retardation of the diffusion rate. Fluorescently labeled PIP_2 was included and its diffusivity taken as representative of the behavior of all the PIP_2 in the system. Ca^{2+} was introduced in a controlled manner increasing to a physiologically relevant concentration of 1350 nM. The data acquired from FCS analysis was also used in a Photon Counting Histogram (PCH) analysis. PCH analysis informs on the quantity of fluorescing molecules being detected during an observation. From this data observed an interesting behavior in the system where the aggregation rate increased for low Ca^{2+}

concentrations before decreasing at higher concentrations. PHC analysis suggested that this might be due to a previously only theorized interaction between the anionic PIP_2 and the zwitterionic DOPC lipid in the bilayer.

2.1. Introduction and motivation

While the structural importance of lipids and lipidic molecules for membranes is well established, it is also true that there are many members of these species that are important because of their biological functions. Great examples for roles that lipids play in cellular processes are Protein Kinase C activation by diacyl-glycerol, apoptosis induced by Ceramide accumulation, Glycosphingolipids aiding in cell recognition and phosphatidylethanolamine facilitating cytokinesis [47, 187-191]. It is hard to deny, however, that currently phosphoinositides (PIs) reign supreme in the realm of lipids with distinct biological functionality [36, 192-194]. These glycerophospholipids feature an inositol ring at their head group which provides potentially 5 locations for phosphorylation. The possible permutations give then rise to the different PI subspecies with the apparent omnipresent PIP_2 and its especially popular form representing the version with phosphate groups on carbon 4 and 5 (properly known as phosphatidylinositol (4,5)-bisphosphate). $PI(4,5)P_2$ has been shown to have important roles in; membrane trafficking (endocytosis, regulated exocytosis), membrane-cytoskeleton interface (microvilli formation, membrane attachment to cytoskeleton, and phagocytosis), and cell

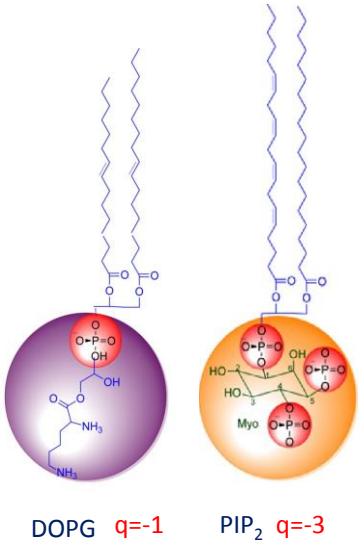

Figure 2.1.: PIP_2 & DOPC: PIP_2 bears three phosphates on its inositol ring which contributes to it highly negative charge.

signaling (protein kinase localization and activation, regulation of ARF GTPases, and EGFR regulation of membrane ruffling) [35, 36, 195]. Given the multitude and diversity of process in which even a single sub-species such as $PI(4,5)P_2$ is involved in, one central questions becomes inevitable: How does the cell funnel these diverse functionalities through one particular molecule species while avoiding unwanted crosstalk between the different cellular processes involved? One possible and arguable the most likely answer is: "via spatial-temporal regulation". In other words, through spatially separated pools of, for example PIP2, that -for the most part- are regulated and controlled independently [193]. This would allow for specific PIP_2 related functionality to be executed at one end of the cell, while at a different location a separate pool of PIP_2 is involved in another set of biochemical reactions.

The biological implications of unraveling such a mechanism are quite apparent: understanding how the various PIP_2 functions are differentiated will permit the further study and adaptation of these systems. From a biomedical engineering standpoint there is also a substantial application based incentive for unraveling this mechanism. If there exists in nature a highly reactive biomolecule capable of dynamic rearrangement and domain formation due to some natural stimuli then such a system would have numerous engineering applications. This system could be used to 'switch' between two or more states of organization or protein activation [196, 197] dependent on conditions, either induced or environmental.

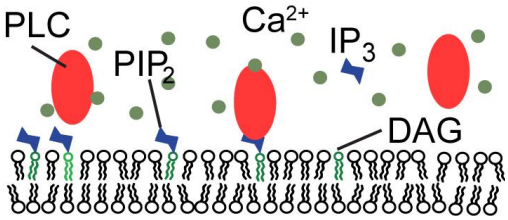

Figure 2.2.: Calcium Signalling: Key events during calcium signaling: Phospholipase-C (PLC) hydrolyses phosphatidylinositol 4,5-bisphosphate (PIP2) in the presence of calcium ions. The reaction products are inositol 1,4,5-trisphosphate (IP3) and diacylglycerol (DAG)

Lipid based biomimetic membranes are currently being used as platforms to interface with cells and tissue (in the case of drug delivery) that make it necessary to provide native lipid environments. SLBs are a most promising technology for increased interface with live cells. Recent work has seen their use as a mimic for cell-cell contacts where cadherin proteins, which play a vital role in binding cells together, have been attached to the lipid bilayer to investigate cellular response to variations in their concentrations [198]. In another investigation the epidermal growth factor tyrosine kinase (EGFR), a member of the type 1 ErbB kinase receptor family that is deregulated in certain types of cancer [199], was incorporated into a supported lipid bilayer. The investigators looked at how the presence or absence of EGFR on a bilayer surface influenced the capacity of human breast epithelial cells to attach [200]. Other work has seen the supported lipid bilayer used as a platform for investigating neuronal crest cell differentiation [201], the 3D presentation of ligands on temperature partitioned lipid bilayers [202], and the mimicking of the contacts between the cell and the extra cellular matrix using; peptide [203], individual proteins [204], and networked proteins [205] enhanced supported lipid bilayers. These investigations provide an activated surface to a cell that permits the cell to reorganize the elements. To build upon this utility it would be very useful to mimic also the controlled dynamic properties, such as dynamic restructuring, of real cell membranes. These systems are the means that cells use to communicate between themselves [206] and so if we want to create better cell surface mimics then replication of these properties is essential.

Experimental observation of distinct areas of (PtdIns(4,5)P_2) enrichment in living cells support the idea that this highly reactive anionic lipid is capable of dynamic reorganization [207, 208]. Yet, given the lateral fluidity of lipid membranes such as the cellular plasma membrane, the question then becomes: what physicochemical mechanisms might a cell exploit to form,

maintain and regulate these 'pools' or domains of high PIP_2 concentration? Currently a few different possibilities have been proposed. For one, a phase separation mechanism that relies on cholesterol dependent fluid –fluid de-mixing of lipids could play a role [186, 209]. Others, however, might employ at least in part the fact that at physiological conditions each phosphate group contributes about one negative charge, thus making highly phosphorylated PIs such as PIP2 strongly anionic. For example, it has been shown that myristoylated alanine-rich C kinase substrate (MARCKS) rely not on specific PIP_2 binding sites but are able to organize the highly negative PIP_2s by exploiting highly positively charged regions of the peptide [35, 210].

Another intriguing avenue is the aggregation of phosphoinositides due to the action of bivalent ions [211, 212]. This is in particular appealing as it directly couples biological functions such as calcium signaling to the spatial organization of membranes. Recent investigations have provided some basic insight in the interactions of highly acidic lipids in the presence of bivalent ions such as calcium and magnesium [212, 213]. However, the range of ion concentrations in these studies, lies mostly between 10µM and 10mM [186, 211-213]). These magnitudes are already interesting as they can be found for short periods of time during cellular signaling proximal to calcium channels, and in the extracellular space up to ~ 2mM [214, 215]. However, much more typical calcium concentrations for intracellular signaling are mostly in the range of 100nM to 1µM [214]. This corresponds well with, for example, the concentration of calcium in diastolic cardiac cells measured to be 100nM [216], or in the dendritic spine of a neuron during an action potential event measured to be ~1000nM [217] or even ~900nM for extended durations in apoptotic events [218].

Thus, our work logically extents these previous studies to the range of ion concentrations most commonly found in eukaryotic cells. Therefore, we hope to illuminate to what extend ion

induced aggregation processes of, for example, PIP2 can indeed play a role in cellular signaling process in those circumstances.

Further to the obvious biological significance of ion induced aggregation, this mechanism could provide an exciting opportunity to develop a non-mechanical means to actively induce structure formation in biomembranes. If the behavior of the PIP_2 can be well characterized at different Ca^{2+} concentrations then it should be possible to induce these aggregations through close control of the ions concentration and disperse them on command by sequestering the Ca^{2+} via a chelator such as ethylene glycol tetraacetic acid (EGTA). This would provide interesting possibilities in the development of temporal and spatial patterning of bilayers, the organizing of membrane associated proteins, or the temporary sequestration of specific membrane elements.

In order to study the aggregation of PIP_2 it is necessary to use a highly sensitive, minimally invasive technique; Fluorescence Correlation Spectroscopy (FCS) fulfills these needs. FCS is an optical technique that correlates the Brownian fluorescence fluctuations in a very small

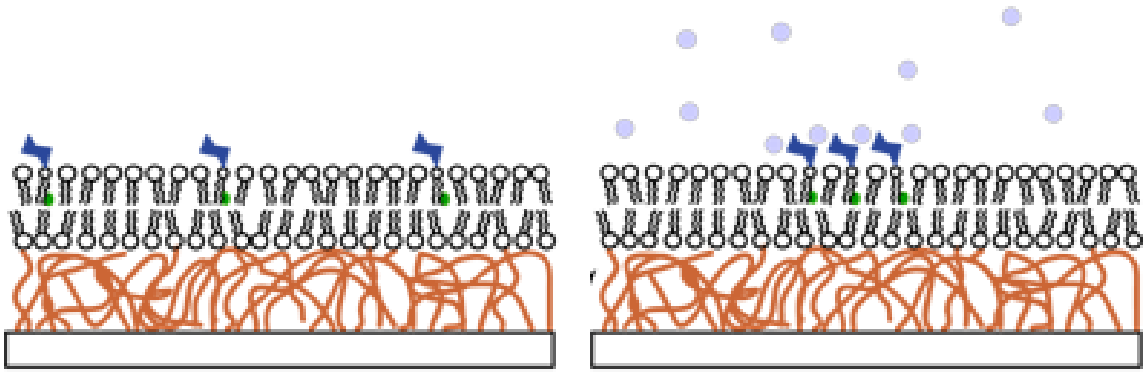

Figure 2.3.: Experimental Set-up: Our proposed experimental system would seek to identify the formation of calcium induced aggregates of PIP_2 through the use of Fluorescence Correlation Spectroscopy (FCS). Aggregate diffusion rates should be significantly decreased in comparison to freely diffusing lipids due to an increased cross sectional area in the bilayer.

sample volume. Analysis gives the diffusion rate of the observed molecules and the average concentration. Due to its reliance on fluorescence fluctuation it is desirable to have very small numbers of fluorescent molecules, typically only 0.001 Mol% of the total lipids will have an attached fluorophore [175-178].

A complimentary technique to FCS is Photon Counting Histogram (PCH) analysis. This technique reveals the measured photon counts per molecule and the average number of molecules within the observation volume using the same data as is acquired during FCS measurements[181, 219, 220]. This permits molecules to be distinguished not by the difference in their diffusion rate but by their molecular brightness. This is particularly advantageous when trying to determine the state of aggregation of a fluorescent molecule as distinct brightnesses can be determined [221].

2.2. Materials and Methods

2.2.1. Materials.

1,2-dioleoyl-sn-glycero-3-phosphocholine (DOPC) and 1,2-dioleoyl-sn-glycero-3-phospho-(1'-myo-inositol-4',5'-bisphosphate) (PIP_2) were obtained from Avanti Polar Lipids (Alabaster, AL). 2-(4,4-difluoro-5,7-dimethyl-4-bora-3a,4a-diaza-s-indacene-3-dodecanoyl)-1 hexadecanoyl- sn-glycero-3-phosphocholine (Bodipy FL C_{12} HPC) was acquired from Life Technologies (Grand Island, NY) and Bodipy FL -glycero-3-phospho-(1'-myo-inositol-4',5'-bisphosphate) ($GloPIP_2$) from Echelon Biosciences (Salt Lake City, UT). All lipids were dissolved and stored (-20 °C) in chloroform, except PIP2 and $GloPIP_2$ for which a 65:35:8 chloroform:methanol:water (by unit volume) mixture was used to ensure thorough suspension of the highly anionic lipid. All organic solvents were HPLC grade, and used without further purification. Poly(L-lactic acid) (PLLA) was obtained from Sigma-Aldrich (St. Louis, MO) and

used as a polymer support for the SLB. Calcium ion concentrations were adjusted by mixing a low calcium buffer solution (110 mM KCl, 20 mM MOPS, 20 mM NaCl and 10 mM K_2H_2EGTA) and a high calcium solution (110 mM KCl, 20 mM MOPS, 20 mM NaCl, and 10 mM K2CaEGTA) in the appropriate ratio [222]. All aqueous solutions were prepared using organic-free doubled-deionized (DI) water of high specific resistivity (approx. 18.0 mΩ/cm).

2.2.2. Preparation of Polymer Supported Lipid Bilayers.

The preparation of the PLLA supported bilayers is in large part based on the method by *Wang et al.* [223]. In brief, No. 1 (170μm thickness) glass cover slides with 25 mm diameter (Fisher Scientific International Inc., Hampton, NH) were first sonically cleansed in isopropanol for 20 minutes, then thoroughly washed with DI water and then etched in Piranha solution (3:1 ratio of H_2SO_4 to 30% H_2O_2) for 5 minutes. Following repeated rinsing with DI water the coverslips were dried in an oven at 120° C overnight. A drop of 30 μl of a 1wt% PLLA in chloroform solution was spin coated at 3000 rpm onto the dried cover slips yielding a polymer coat of approximately 100 nm [223]. The polymer coated substrate was then annealed for 12 hrs. at 50°C.

Lipid bilayers were deposited on the glass supported PLLA cushion using the hybrid Langmuir- Blodgett / Langmuir–Schaefer transfer [77]. To that end the PLLA coated coverslip was first submerged vertically in the low calcium buffer subphase of a Langmuir film balance (KSV Minitrough: Biolin Scientific, Stockholm, Sweden) using a motorized dipping mechanism. Then a solution of the desired lipid composition dissolved in chloroform was carefully spread on the surface of the subphase. Subsequent evaporation of the chloroform for 12 min leads to the formation of a lipid monolayer at the air-water interface. The monolayer was compressed by the two actuated barriers of the Langmuir trough until the final deposition surface pressure of

30 mN/m was reached. The coverslip was then pulled through the water/monolayer/air interface at a speed of 2 mm/min to deposit a first lipid monolayer on the PLLA cushion. A microlayer of the low Ca buffer is trapped between the polymer and the lipid monolayer ensuring the integrity of the lipid monolayer and the subsequent lipid bilayer. The substrate was then rotated into a horizontal orientation and then stamped again through the monolayer on the subphase to deposit the second bilayer leaflet. Finally, the resulting coverslip with the PLLA cushioned bilayer was then mounted in an Attofluor sample holder (Life Technologies, Grand Island, NY) for further characterization.

2.2.3. Fluorescence Correlation Spectroscopy (FCS).

In order to measure the lateral mobility of the fluorescent labeled lipid (either GloPIP2 or Bodipy FL C_{12} HPC) in the bilayer via FCS, 0.1 mol% of the tagged lipid was included in the initial lipid solution for spreading. FCS experiments were performed on our in house built apparatus. In brief, the laser beam (488nm wavelength) from a Krypton/Argon mixed gas laser (Stabilite 2018, Spectra Physics, Santa Clara, Ca is guided through an optical fiber (Thorlabs, Newton, NJ) then enlarged via a Galilean beam expander to fill about 60% of the microscope objective's back aperture. Using a dichroic mirror (Chroma Technology Corp., Rockingham, VT) the laser beam is then coupled into the optical path of an inverted TiE microscope (Nikon Corp., Tokyo, Japan). A 60x, 1.2NA, water immersion objective (Nikon Corp., Tokyo, Japan) focuses the collimated beam of 10 μW power into a diffraction limited spot in the objective's focal plane.

As individual fluorescently labeled lipids diffuse within this excitation spot they emit photons which are collected by the objective. After passing through the dichroic mirror the emission

light is spectrally filtered through a FITC filter cube (Nikon Corp, Tokyo Japan) and then spatially filtered by a confocal pinhole aperture (50 μm diameter, Thorlabs, Newton, NJ). A 50/50 beam-splitter divides the incoming light, which is finally focused into two avalanche photo diodes (APD) (Perkin&Elmer, Canada). A hardware single photon counter (PicoHarp 300 (PicoQuant, Berlin, Germany))) records the arrival of each detected photon. The system software then translates the photon arrival pulses into intensity fluctuations and calculates the cross-correlation between the two APD signals. The resulting correlation curves are fitted to analytical expressions in IGOR Pro (WaveMetrics, Lake Oswego, OR) using a nonlinear Levenberg-Marquardt algorithm.

For lipid composition we performed correlation measurements on at least 3 individual samples. At each location within a particular sample a minimum of 10 separate correlation measurements of 60 s duration were taken and mean values and corresponding standard deviations for every point of the experimental curves were calculated.

Since we assume that the fluorescently labeled lipids in the membrane undergo 2D-diffusion on the length scale probed by FCS, we use

$$G(\tau) = \frac{1}{N}\left(1 + \frac{\tau}{\tau_D}\right)^{-1} \qquad \text{(Equ. 2.1.)}$$

as the analytical form of the temporal cross-correlation $G(\tau)$ [224, 225]. It depends on the average number of fluorophores in the excitation area, N, and the diffusion correlation time, τ_D. It should be noted that we followed the convention to omit the factor '+1' contained in the original equation for simplicity and compensated by subtracting 1 from the experimental curves. Using the reciprocal standard deviations as weights, we fitted the average correlation curve for each experiment to equation 2.1. to extract the correlation time τ_D associated with the diffusion

process. This correlation time is equivalent to the time it takes for the mean square displacement of a diffusing molecule to reach the size of the effective observation area, ω, of the FCS apparatus. Consequently we evaluated $D=\omega/4\tau_D$ to obtain the diffusion coefficient D from the measured time τ_D. The observation area, ϖ, was determined independently before and after each measurement series using a 10 nM fluorescein solution (50 mM TRIS, pH 10), employing the fluorophores known diffusion coefficient of 425 $\mu m^2/s$ as standard [226]. For each experimental condition the diffusion constants of the individual experiments were averaged. The error bars shown in Figure 2.6 and 2.9 represent the spread of the values for D at each condition and composition, respectively.

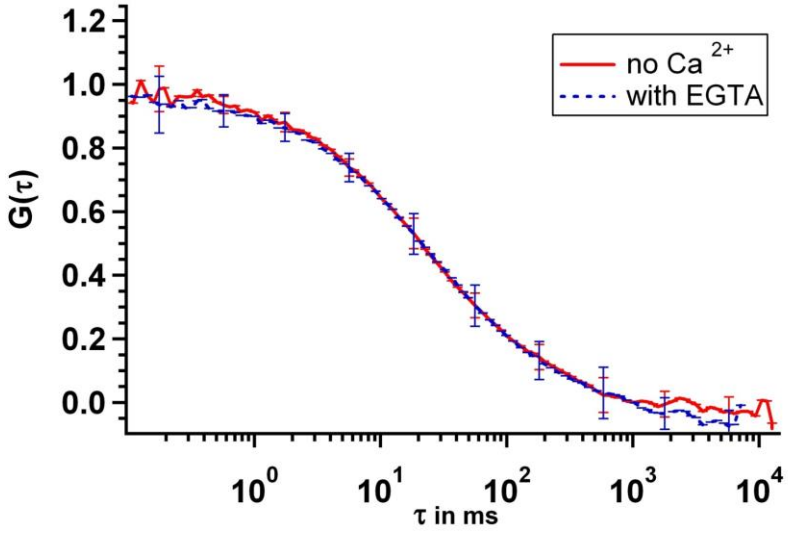

Figure 2.4.: Environmental Ca^{2+} Test: To test for the presence of calcium in our water system 1mM EGTA, a powerful calcium chelator, was added to the buffer of a PIP_2 containing SLB. FCS measurements were taken before and after the addition of EGTA with no change in the diffusion rate detected. This indicated there was no appreciable amount of free calcium ions in the system.

2.2.4). Photon Counting Histogram (PCH) Analysis.

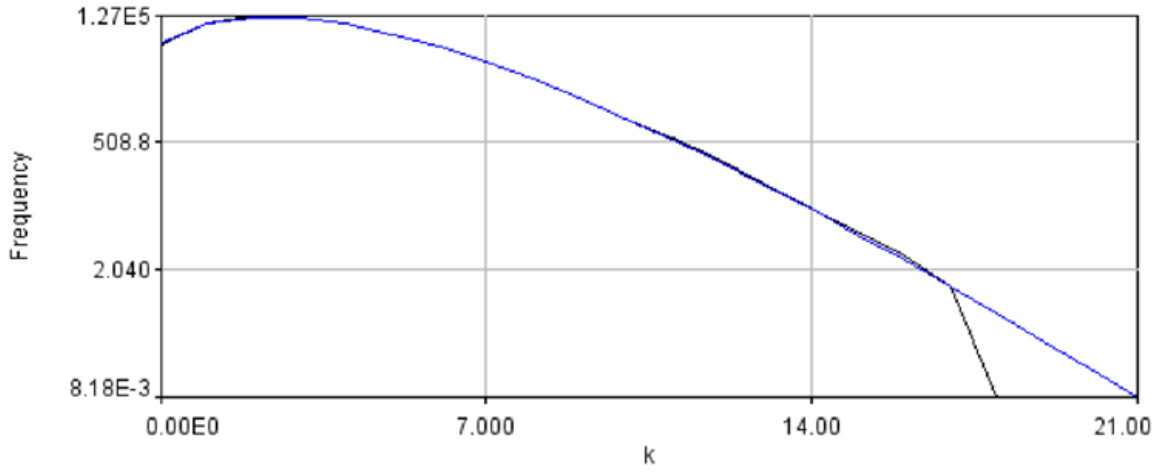

Figure 2.5.: A PCH Curve: An example of a PCH curve (black line) and the corresponding fitted curve (blue line). The number of photon count events per binning period, k (1ms in this example), comes from the same data as the FCS acquisition. Broadening of the curve from the standard Super Poissonian distribution is indicative of diffusive species with increasing brightness

The Photon Counting Histogram (PCH) is a complimentary technique to FCS, using the same acquisition data in its analysis. Where FCS looks at the fluctuation frequency and duration, PCH looks at the intensity of these fluctuations over the duration of an experiment [181]. The recorded intensities can be represented as a histogram of counts v. frequency. The form of the histogram is determined by a convolution of the Poissonian shot noise of the system and the Poissonian for the particle number fluctuation in the excitation volume; this produces a super-Poissonian curve which is further broadened by extra fluorescent species. This PCH curve can be fitted to a theoretical model as described by Chen et. al. in 1999 [181]

Experimental data was fitted using an ImageJ plugin made kindly available by Jay Unruh, Stowers Institute for Medical Research. The software uses number and brightness analysis [227] which extracts these two parameters from the moments of the photon count distribution. Here the average molecular brightness, ε, is given by

$$\langle \varepsilon \rangle = \frac{\sigma^2 - \langle I \rangle}{\gamma \langle I \rangle} = \sum_i f_i \varepsilon_i \,, \qquad \text{(Equ.2.2.)}$$

Where σ^2 is the variance, I is the intensity, ε_i is the molecular brightness of species i, f_i is the fractional intensity of species i, , and γ is the gamma factor defined elsewhere [228]. The average intensity divided by the average molecular brightness furnishes the average number of particles, N.

The software allows the fitting of up to three diffusive species as well as the linking of variables across multiple curves. In this case the molecular brightness, ε, as determined from the 0 Ca^{2+} curves, was linked across all curves from an experimental series. Molecular species of 2ε and 3ε were then fit to the system to give the number of objects containing two and three times the number of fluorescent molecules as the 0 Ca^{2+} case.

2.3) Results and Discussion

To test the aggregation of PIP_2 containing bilayers a number of different lipid compositions were studied. In order to infer from our work some biological significance, PIP_2 concentrations were set at 2 mol%. This is the accepted concentration for PIP_2 in eukaryotic plasma membranes [36]. FCS measurements were conducted on supported lipid bilayers containing a total of 2 Mol% PIP_2: 0.01 Mol% of the PIP_2 was the tail labeled fluorescent variety 'GloPIP_2', 1.99 Mol% of the unlabeled variety with phosphates at the 4 and 5 positions, the most common arrangement. The remaining 98 Mol% of the lipids were 1,2-Dioleoyl-sn-glycero-3-phosphocholine DOPC: phosphocholines are the major lipid component of eukaryotic plasma membranes and the zwitterionic DOPC provides a neutral stable foundation for many bilayer experiments. The diffusion rate of the GloPIP_2 was measured by FCS at 0, 17, 38, 65, 100, 150, 225, 351, 602, and

1350 nM of Ca^{2+}. Two alternative compositions were also investigated, firstly a lipid bilayer with composition: 97.99Mol% DOPC, 2Mol% PIP_2, and 0.01Mol% Bodipy-HPC (a fluorescently labeled phosphocholine) was tested to investigate the behavior of the 'bulk' or 'solvent' lipid. The second system investigated omitted the PIP_2 and just looked at the response

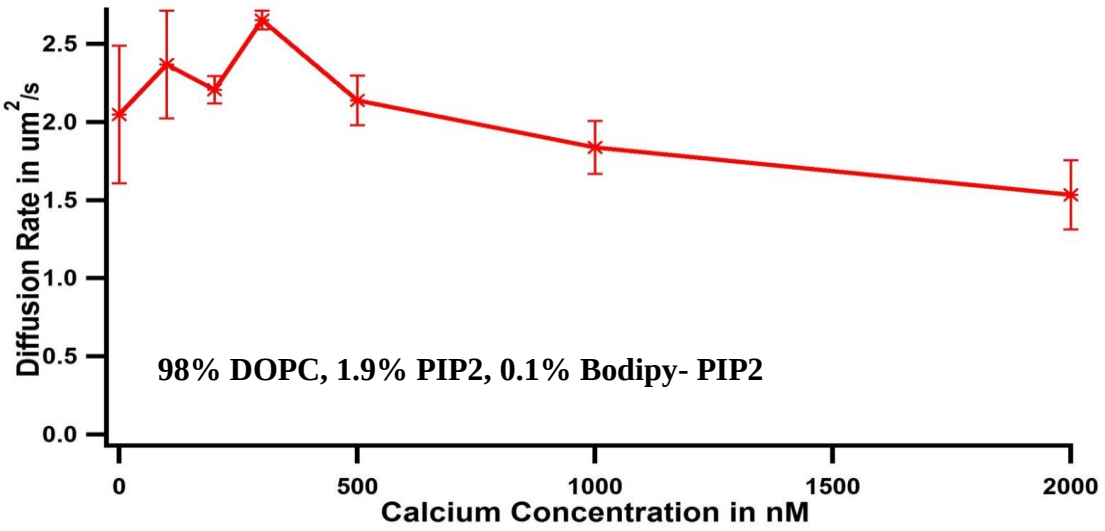

Figure 2.6.: PIP_2 Diffusion on a Solid Substrate: The 2-D diffusion of a fluorescently labeled PIP_2 on a solid support shows an initial increase in diffusion rate with the addition of calcium.

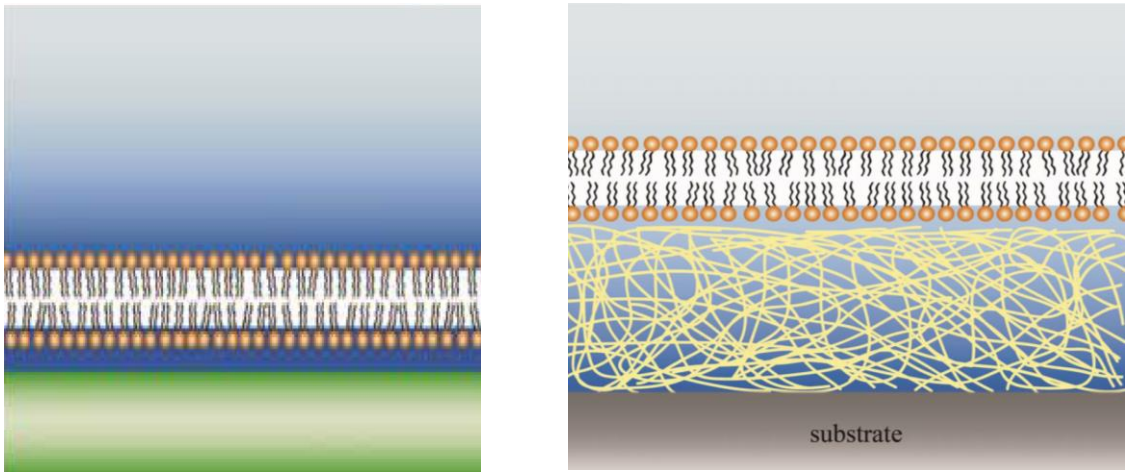

Figure 2.7.: Introduction of a Polymer Support: A polymer support (yellow lines on the right side schematic) was introduced to the system to mediate suspected glass induced effects. A ~100nm thick coating of Poly-L-Lactic Acid (PLLA) was placed on the SiO_2 substrate.

of a neutral bilayer to calcium variations; the bilayer was 99.99Mol% DOPC and0.01Mol% Bodipy-HPC. At least 10 FCS acquisitions were taken for each system at every calcium concentration and averaged to provide an average diffusion speed for the labeled lipid. Different locations on each bilayer were also tested in order to screen out bilayer regions with non-typical

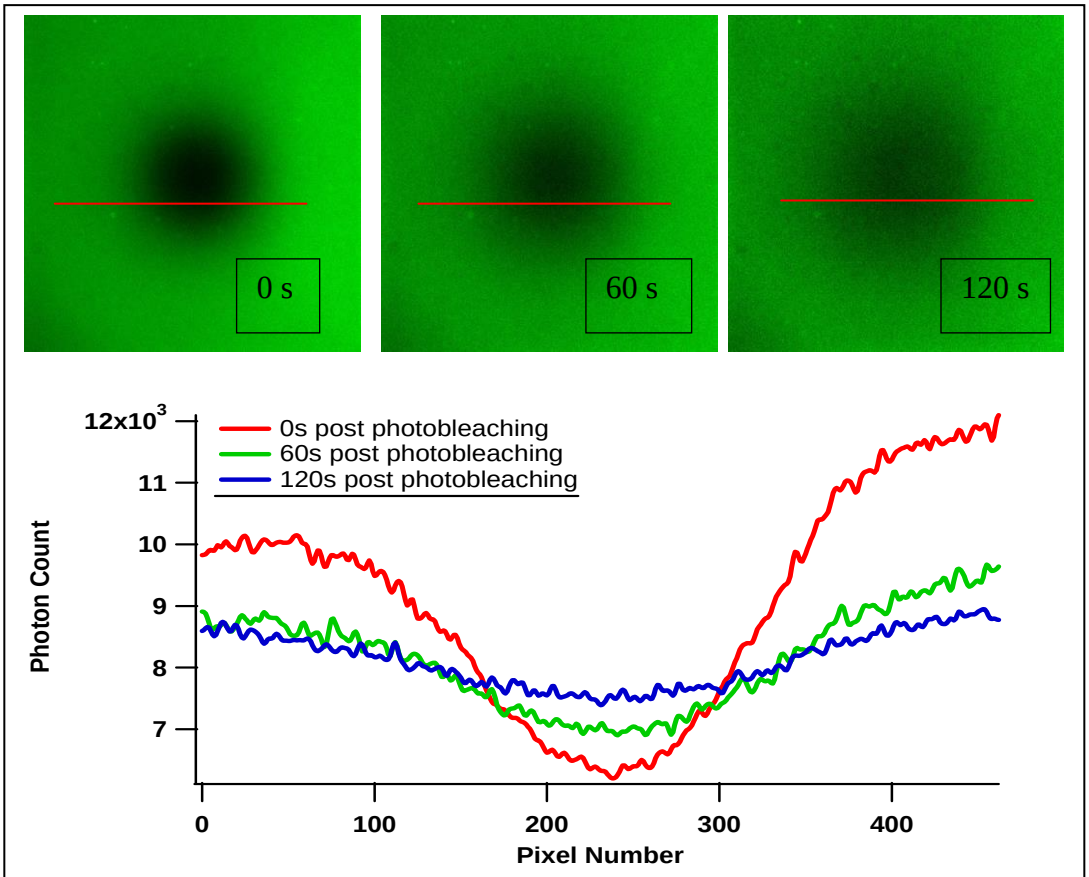

Figure 2.8.: FRAP: Fluorescence recovery after photo-bleaching of a PLLA supported lipid bilayer. The top row of fluorescence images shows the recovery of the bleached center spot over time (left to right). This visual impression is validated by plotting the fluorescence intensity along the red lines in the images above. Clearly visible is the recovery of the fluorescence signaling with respect to the unbleached region: A hallmark for a fluid membrane and indicator of the successful deposition of a connected supported lipid membrane on PLLA polymer support.

diffusion characteristics.

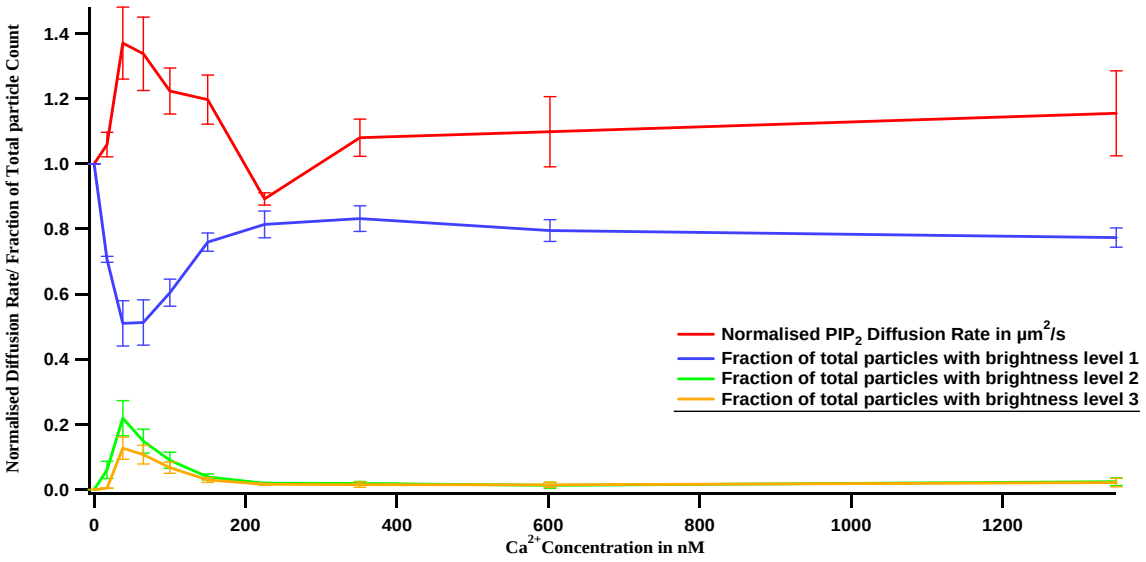

Figure 2.9.: Combined FCS/PCH data for fluorescent PIP2: Here we see that the addition of calcium causes a decrease in the number of particles with resting state brightness (brightness level 1) and an increase in the number of articles with 2X (level 2) and 3X (level 3) the brightness measured with no Ca^{2+} in the system. Surprisingly the increase in brightness corresponds to an *increase* in the diffusion rate indicating greater freedom of movement for the PIP_2 lipids.

The behavior of PIP_2 was seen to act in a manner completely unexpected at very low Ca^{2+} concentrations. The FCS data (see figure 2.6) shows that instead of the formation of diffusion retarding aggregates, the addition of very low levels of Ca^{2+} (~17 – 150nM) causes an *increase* in the diffusion rate. Above 400 nM the diffusion rate returns to approximately its starting value without any evidence of significant change, up to the maximum [Ca^{2+}]. This behavior was initially attributed to a residual coulomb force interaction between the negatively charged lipid bilayer and the silica glass substrate which becomes hydroxylated following cleaning with Piranha etch (75% Sulphuric Acid, 25% Hydrogen peroxide) leaving it negatively charged [144]. It was thought that the bilayer might be possibly initially under an electrostatic tension that was screened by the addition of calcium ions permitting more unobstructed diffusion

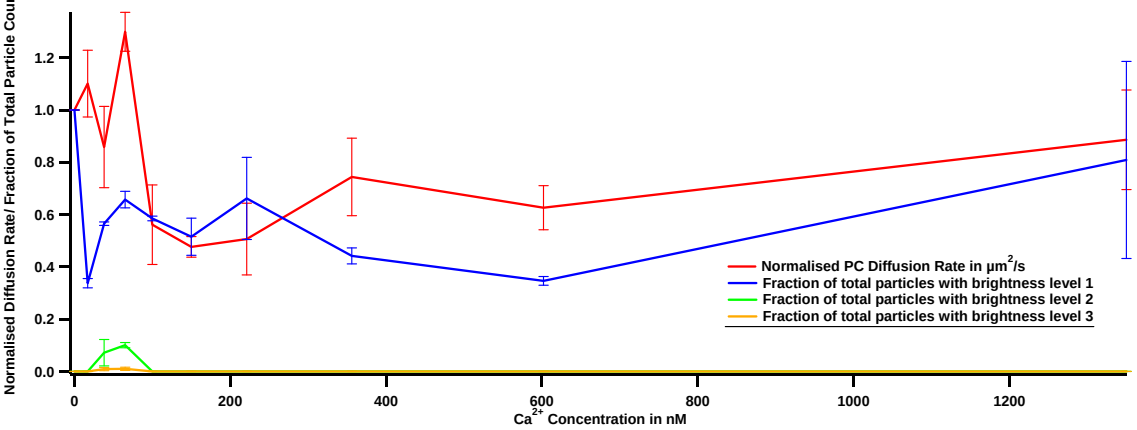

Figure 2.10.: Combined FCS/PCH data for fluorescent PC with PIP2 present: PCH analysis of the bilayer containing PIP_2 and a fluorescently labeled PC lipid shows that there is an increase in the number of particles with 2X resting brightness. This increased brightness corresponds to an increase in the diffusion rate at these calcium concentrations.

of the PIP_2 before the Ca^{2+} began to induce aggregation. In order to combat this electrostatic interference a polymeric spacer was introduced between the glass and the lipid bilayer (see figure 2.7). Following a thorough literature search and experimental evaluation of a few polymer candidates, a poly-l-lactic acid (PLLA) substrate was chosen because of its electrical insulation properties, its ease of production, and its reliability in producing, in our hands, defect free bilayers [223, 229]. The PLLA based polymer cushion has previously only seen very limited use as membrane support and never used in studies of membrane dynamics before. However, as can be seen in Figure 2.8., fluorescence in the central photobleached spot recovers over time. This is indicative of fluorescently labeled lipids diffusing in the bleached spot and thus it can be concluded that the membrane deposited on PLLA is indeed fluid and connected. This first result is validated also by the FCS measurements described below which give diffusion coefficients for the labeled lipid species in the order of a few $\mu m^2/s$, which is typical for supported lipid bilayers. Following further experimenting with this polymer substrate the same initial increase in diffusion

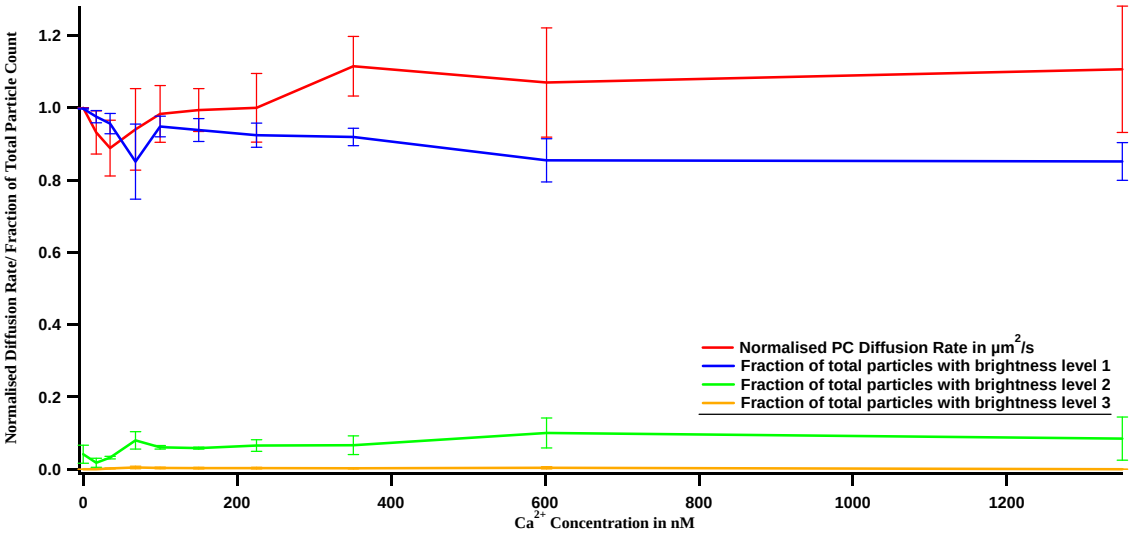

Figure 2.11.: Combined FCS/PCH data for fluorescent PC with PIP2 absent: When PIP_2 is omitted from the bilayer the behavior of the system appears to have effectively no dependence on the calcium concentrations. Of interest is the fact that there is a diffusive component bearing 2X the resting brightness for all measured Ca^{2+} concentrations.

rate was observed (see figure 2.9). A second analysis technique was introduced to try to illuminate this phenomenon; Photon Counting Histogram (PCH) analysis uses the same data as FCS but gives the brightness of fluorescent molecules in an excitation event instead of the diffusion rate as is derived from FCS. The PCH analysis software allows the user to fit the PCH characteristics of up to three simultaneously diffusing species. By linking the brightness of the second and third diffusive species to the brightness of the diffusing species when there is no Ca^{2+} in the system it is possible to fit for aggregates incorporating one, two, or three fluorescent lipids. PCH analysis reveals that the increase in diffusion rate is not associated with an increase in singly diffusing fluorescent PIP_2, but rather a decrease (see Figure 2.9). Increased PIP_2 diffusion rates appear to correspond with the formation of molecular assemblies with twice and triple the brightness of the initial (with no added calcium) detected molecules. Further when we completed the same analysis for the PIP_2 system with the fluorescent PC lipid we observed a similar behavior (see figure 2.10). Again an increase in the diffusion rate is associated with a decrease in

single brightness diffusing objects. When we analyzed the system that contained no PIP_2 there appeared to be no significant change in the properties or the ratios of single/multiple brightness objects (see figure 2.11). Interestingly however, the PCH analysis does reveal that the system is best fit as one containing a small fraction of objects with twice the brightness of the 0 Ca^{2+} condition

These observed phenomena could have two possible origins: they could be a genuine result of the formation and disruption of electrostatically induced lipid aggregates due to the presence of PIP_2 and the addition of Ca^{2+}, or they could be due to a photochemical effect that causes the fluorophore to vary in their brightnesses. Lipid bilayers that contained only DOPC and HPC-Bodipy showed no calcium dependent variation in the lipid diffusion rate. The only time these variations are observed is when the system contains PIP_2. Further the fluctuations are not dependent on the fluorescent species in the system: we see them for $GloPIP_2$ and Bodipy HPC lipids. These facts would suggest that the phenomenon is related to the presence of the acidic lipid. The major difficulty in understanding the system is in reconciling the fact that the formation of aggregates, as indicated by PCH, actually corresponds to an increase in the diffusion rate for both the PIP_2 and the PC lipids. One possible scenario that could begin to explain the observed behavior is that PIP_2 forms a weak ionic bond with the zwitterionic DOPC which forms the majority of the supported lipid bilayer. This ionic bond would occur due to the physical separation of the positive and negative charges in the DOPC head group. While in bulk and at a distance

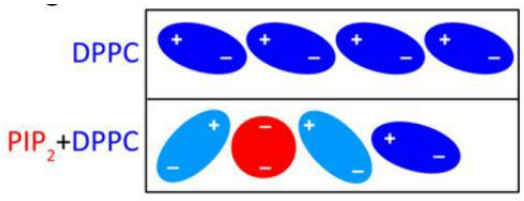

Figure 2.12.: PIP_2 Induced Nanoclusters: PIP_2 can induce organization in adjacent zwitterionic lipids due to its highly charged nature [6]

the DOPC appears to be neutral, up close there are areas with charged residues. This bond between the PIP_2 and DOPC could become disrupted by the addition of the positively charged calcium ions which, once sufficient concentration is reached, start to form areas of PIP_2 enrichment. This interpretation is supported by computer simulation performed by Lupyan et al (see figure 2.12) [230]. Here they observed evidence of PIP_2 and DOPC forming microcluster under physiological salt conditions. If this is indeed the case then the small hydrodynamic radius of Ca^{2+} would make them better capable of disrupting such a bond than the larger Na ions already in the solution. The diffusion behavior might be further explained by the difference in the nature of the aggregates that are being observed. If the PIP_2/DOPC micro-clusters are dependent on their close proximity to each other (i.e. less than one Debye length, approx. 1nm) then they would be forming structures that would have an increased cross sectional area compared to a singly diffusing lipid. This would result in an appropriately retarded diffusion rate. PIP_2 clusters induced by Ca^{2+} addition would more likely take the form of an area of enrichment of the PIP_2 as opposed to tightly bound structures. If this were the case then diffusing PIP_2s would be more likely to encounter a repulsive negatively charged PIP_2 in their close vicinity which could lead to an overall increase in the diffusion rate within the areas of enrichment. One further observation is that in a system such as is studied here the Ca^{2+} is likely to reach a saturation point where the PIP_2 all have sufficient calcium molecules to effectively encapsulate them and screen their charge. This could be a reason that the increased diffusion rate returns to approximately the starting rate above 351nM Ca^{2+}. If all the PIPs are screened then there can be no charge induced aggregations

While the exact mechanisms behind the observed change in the brightness of the objects and the dynamics of the system remain subject to further study, the intriguing nature of the

interaction between PIP_2 .and calcium remains clear. The complexity and unexpected behavior of this system shows that this vital biological system is deserving of sustained further study. Our work has taken a look at the system at the concentrations and in conditions that are much closer to nature than any that previous work. Rather than settling the debate as to the role of ion induced aggregation for PIP_2 function, this work perhaps presents more questions than it answers. One thing that is abundantly clear however is that the PIP_2 and Ca^{2+} levels studied here are more capable of complex behavior than was previously suspected. Further, this work shows that physiological concentrations might indeed be capable of the great variety in behavior that would be necessary to control the disparate roles of this intriguing phospholipid.

For further work on this issue I believe it would be prudent to perform dual color Fluorescent Cross Correlation Spectroscopy (FCCS) experiments [231]. FCCS would only show dual color correlation if the two fluorophores were moving in tandem. This technique would be able to determine the state of aggregation of different lipidic elements by tracking the cross correlation in the motion of two different fluorescently labeled lipids. With, for example, a green and a red fluorescent PIP_2 a researcher could detect the formation of aggregates of PIP_2 more directly. Further by having a green PIP_2 and a red PC lipid, for example, the formation of PIP/PC micro-domains could be directly investigated.

•

Section 3: A Biosynthetic Membrane-Anchor/Protein System Based on a Genetically Encoded "Aldehyde Tag"

Summary

The covalent binding of an aldehyde side-chain containing protein to a lipid with an aminooxy -modified head group opens a versatile avenue to bio-functionalize lipid membranes without compromising function and dynamic properties of both the protein and the lipid membrane. It was recently found that the site-specific insertion of a 6 amino acid consensus sequence (LCTPCR) into a protein is sufficient to target it for post-translational modification by formylglycine-generating enzyme (FGE). FGE will enzymatically turn the cysteine in the consensus motif into a formylglycine, thus leading to the site-specific introduction of an aldehyde side chain for further chemical modification. We have engineered the consensus sequence to the N and C terminals of Enhanced Green Fluorescence Protein (EGFP) which was co-expressed with FGE in *E. Coli* and further reacted with FGE *in vitro*. Lipids were chemically modified to bear a reactive aminooxy group and then conjugated with the aldehyde tagged EGFP. The resulting EGFP-lipid constructs were successfully incorporated into solid supported lipid bilayer as verified by fluorescence microscopy. Membrane integrity, as well as protein and lipid motilities, were investigated using both fluorescence recovery after photo-bleaching

(FRAP) and fluorescence correlation spectroscopy (FCS). This site specific lipidation strategy promises to allow for the use of a variety of possible lipid anchors as well as to provide unprecedented freedom in the choice of the lipidation site on the protein.

3.1) Introduction

One of the hallmarks of eukaryotic life is the presence of compartmentalizing lipid bilayer membranes enclosing areas of specialization within the cell. All the cellular organelles including the nucleus, Golgi apparatus, mitochondria etc. are encapsulated in a lipid bilayer. These membranes have a hydrophobic core that helps them resist the diffusion of water soluble elements through the bilayer. In order for the cell to effectively communicate between its internal organelles as well as with the outside environment it is necessary to overcome the natural barrier of the bilayer. To this end cellular membranes have evolved intricate protein and lipid mediated mechanisms capable of transferring information across a bilayer. These can take the form of transport proteins that permit the selective passage of particular molecules or ions through the membrane integrated protein. They can also take the form of a receptor protein where protein stimulation on one side of the membrane produces a conformational change on the other side thus relaying the signal. Along with signaling proteins there are also a large array of anchoring proteins, adhesion proteins, and enzymes that are integrated or associated with the membrane.

Proteins integrated with the membrane have the capacity, provided they are not bound to a larger fixed structure such as the ECM, to diffuse within the plane of the membrane. This property is highly functional as it permits variations in the local concentrations of particular proteins. For instance an Antigen Presenting Cell (APC) will, following detection and absorption of a pathogen, present peptide fragments of the pathogen on their Major Histocompatibility Complexes (MHCs) distributed evenly across their surface. Following attachment and

recognition with a T-Cell the MCHs will reorganize to the area of the APC in contact with the T-Cell. The elevated regional concentration of the antigen presenting MHC increases the speed and efficiency of the system wide immune response. Another example is the Inwardly Rectifying Potassium (IRK) channel, this protein passes positive ions towards the interior of the cell in order to maintain the resting membrane potential of the cell. The IRK channel requires Phosphatidylinositol 4,5-bisphosphate (PIP_2) binding to activate. This will ensure that there is increased passage of the positive K^+ ion into regions with elevated concentration of the negative PIP_2 lipid.

In order for researchers to more efficiently study these and other membrane based dynamic systems it is desirable to be able reconstitute them in a controlled manner on an surface accessible to experimentation and measurements. This is where supported lipid bilayer systems come in, as discussed in chapter 1. Bilayer composition can be closely controlled and some proteins can be integrated. However, there are many proteins that have only a loose association with the membrane. These weak associations can be through a conformational change that exposes a previously shielded hydrophobic region, such is the case with the polybasic domain of the MARCKS protein. Sometimes this more fragile association can be brought about through weak ionic interaction with membrane anchoring lipids such as with Cytochrome c. In addition, there are many circumstances where only parts of membrane proteins, such as those with extracellular binding domains that are of interest for a particular experiment. In all these circumstance circumstances it would be very desirable to bind the protein of interest to a supported lipid bilayer but there is no reliable natural bilayer binding domain built into the protein structure.

For high quality investigations into protein-protein interactions, or protein-cell interactions it would be thus of great advantage to be able to site specifically anchor proteins to a fluid bilayer substrate. This would have some major benefits for existing and future research. For studying reaction dynamics a supported lipid bilayer is an excellent system to maintain the fluid reorganization of the elements but to reduce the dynamic velocities involved. An effective reduction in diffusion speeds from hundreds of $\mu m^3/s$ for 3-dimensional diffusion of small molecules at room temperature to a few $\mu m^2/s$ for 2D diffusion on a bilayer lipid provides a significantly slower mixing and interaction rate on a surface that is optically accessible. This could be especially applicable to studying transient protein interactions where the binding duration could be expanded by the slower diffusion rates. For protein-cell interaction investigations site specific binding would allow the orientation of the protein to be controlled with respect to the cell allowing greater insight into binding mechanisms. Concentrations could also be dialed in and proteins would be able to travel along the bilayer surface in tandem with proteins on the surface of the living cells helping to emulate the conditions a cell would experience when interacting with another cell.

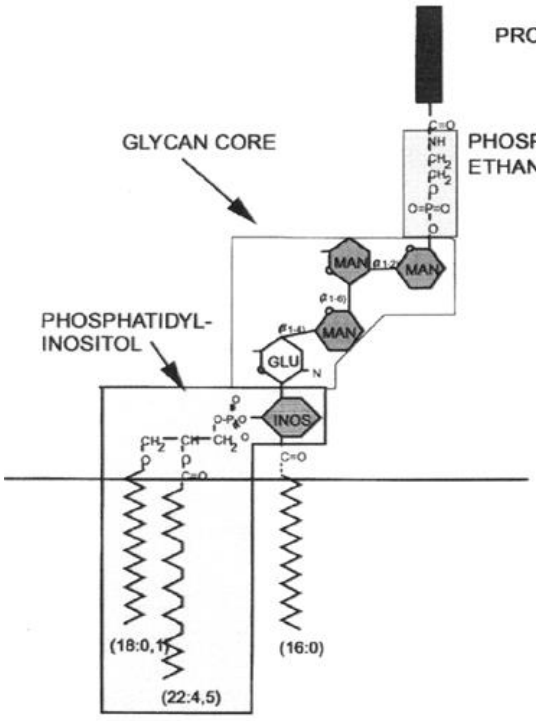

Figure 3.1.: A GPI anchor: A diagram of a glycosylphoshaptidylinositol (GPI) anchor [9]. A GPI anchor contains a sugar region (the glycan core that is made up of mannose and glucose molecules) that binds the protein to the fatty acid or acyl chains. Used with permission of Elsevier

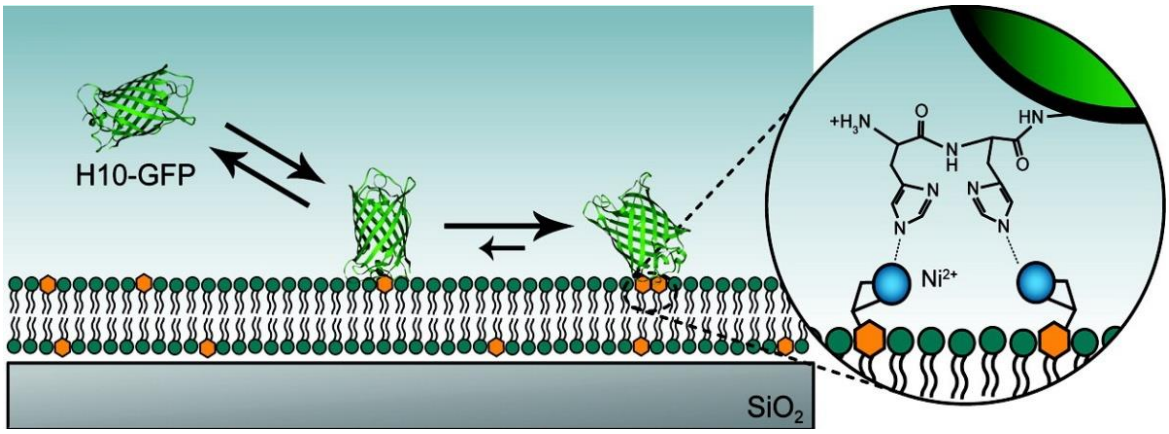

Figure 3.2.: Histidine Tag + Nickel Method: Green fluorescence proteins (GFP) were modified with a polyhistidine tag (containing 10 His residues) at the carboxyl or amino terminus. His- tagged GFPs may bind up to two nickel atoms located on the membrane surface. Binding is reversible as indicated by the arrows. In the figure, lipids with nickelated head groups are labeled in orange [12].

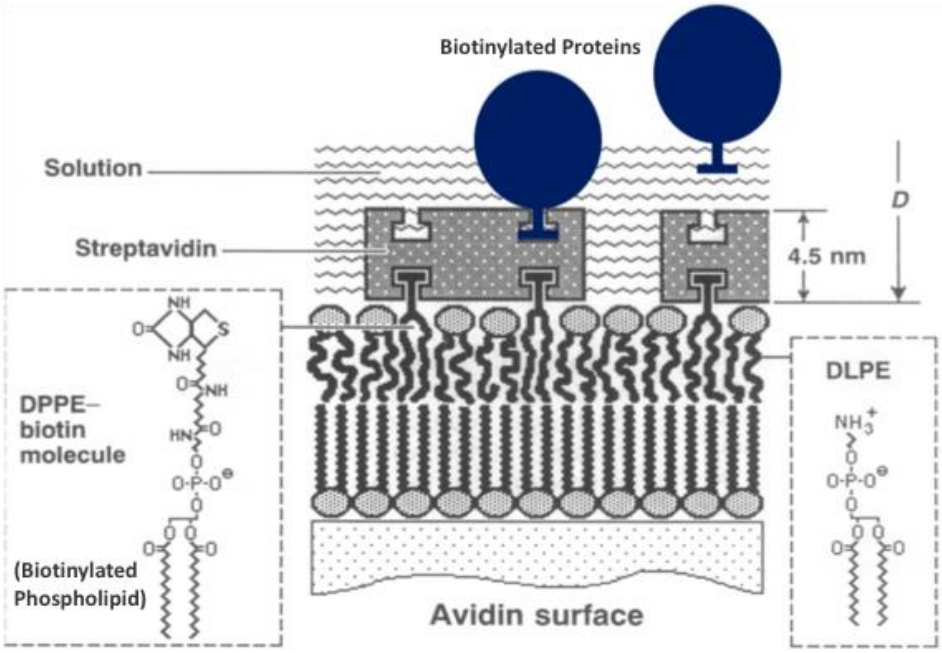

Figure 3.3.: Biotin + streptavidin method: Proteins (balloon-shaped) containing a biotin (upside-down T shaped anchor) bind with streptavidin found on the membrane surface. As seen in the diagram, streptavidin is attached to the membrane via linkages with biotinylated lipids on the surface. Currently, the variety of biotinylated lipids that are commercially available is limited. used with permission: copyright PNAS: {Helm, 1991 #369}

There currently exist a number of technologies for attaching proteins to lipid bilayers. Each of these systems comes with a set of limitations that either makes it unsuitable for certain applications or unreliable in execution. One of the most popular systems is the poly-histidine tag; here a residue of at least six histidines can be genetically attached to the C or N – terminus of proteins. This 'His'-tag can then bind to nickel molecules engineered into lipid head groups. The binding of the His-tag to the nickel bearing lipid effectively fixes the attached protein to the

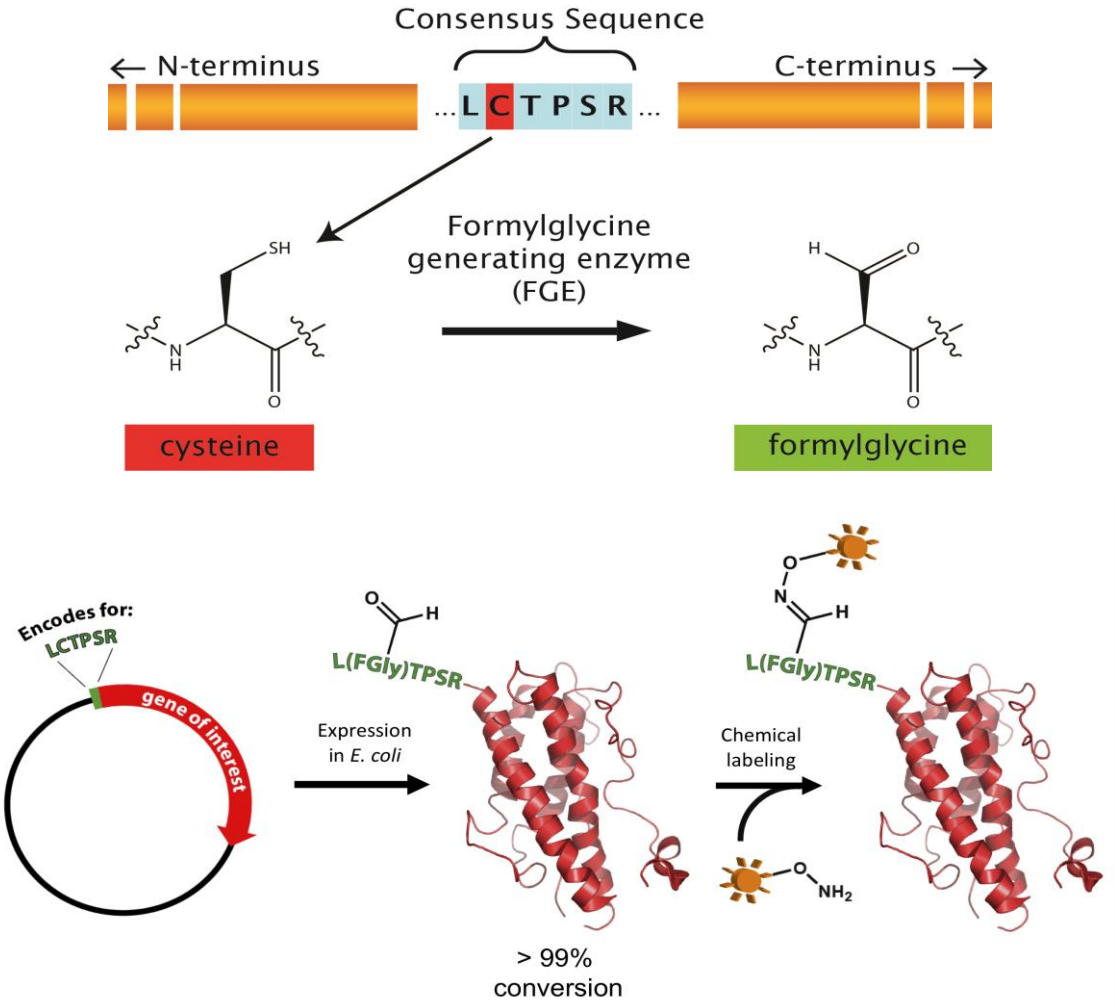

Figure 3.4.: Aldehyde Tag: The Aldehyde Tag technology as developed by Carrico *et al* is summarized in this schematic. The consensus sequence, LCTPSR, contains a cysteine that is oxidized to formylglycine by FGE. The sulfatase motif is cloned into the protein of interest and the cysteine is converted into a FGly, which is coupled with another molecule, site-specifically and quantitatively.

bilayer. A major drawback to this technique is that the His/Ni bond has a relatively weak binding affinity. Thus, small changes in pH or temperature can severely effect the concentrations of bound protein[12]. Another popular protein anchoring method is through the introduction of a glycosylphosphatidylinositol (GPI) anchor (Figure 3.1.). Here the GPI is a genetically encoded posttranslational modification to a protein[232]. The GPI is always attached to the protein C terminus and acts like a lipid-like membrane anchor. The anchor section consists of a phosphatidylinositol with two hydrophobic fatty acid chains. This technique is limited in a number of significant ways; it is specific to both the protein attachment position and the membrane anchor chemistry, further the direct attachment of a hydrophobic region to the exterior of the protein requires multiple extra steps for purification and membrane incorporation. The latter is particular involved, as the GPI-anchored protein is not water soluble and thus from the time of synthesis needs to be kept in detergent micelles and then carefully exchanged into proteoliposomes to finally be able to be used for supported membrane production[233, 234]. Another popular technique involves the use of a biotin/streptavidin/biotin linkage. Here the strong non-covalent bond between biotin and streptavidin is utilized to attach a protein to a lipid. Proteins and lipids can have a biotin molecule attached by using various chemical conjugations to produce a non-specific biotinylation at a carbohydrate, carboxylate, amine, or a sulfhydryl [235]. One considerable drawback of this technique is that streptavidin is a tetramer by nature, with all four locations being active binding sites. This produces a lot of unspecific binding and cross binding between multiple lipid anchors and proteins. Another considerable drawback of this system for use in membrane augmentation is that streptavidin and its related biotin binding proteins tend to aggregate at relative low surface concentrations [236, 237]. Together, these

limitations make the biotin/streptavidin/biotin membrane attachment strategy suitable for only a very small set of protein attachment problems.

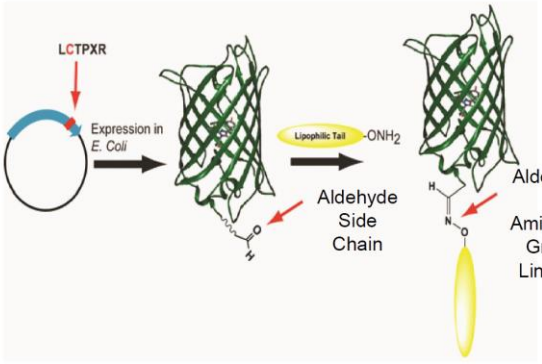

Figure 3.5.: Proposed Protein/Lipid anchor: A genetically encoded aldehyde can be used to attach a lipidic anchor site specifically to a green fluorescent protein.

The development of a genetically encoded aldehyde tag by the research group of Carolyn Bertozzi at the University of California, Berkeley in 2007 introduced a novel technique to hybridize proteins [238]. The technique centers on a six amino acid consensus sequence that can be introduced into the genetic code of a protein via vector DNA. Once expressed this amino acid sequence can be recognized and acted upon by a formylglycine generating enzyme (FGE) which converts the cysteine in the sequence into formylglycine: an non canonical amino acid with an aldehyde side chain. This site specific placement of an aldehyde permits careful chemical modification of the protein at a controlled location [239]. There is already a large array of commercially available aldehyde reagents such as hydrazide and aminooxy reagents. The rarity of aldehydes in biomolecules and their absence in almost all proteins makes them excellent site specific reaction points. A number of uses for this system have already been developed such as; protein- protein conjugation, protein PEGylation and protein fluorophore conjugation [239-241]. However, protein lipid conjugation has not yet been undertaken. A genetically encoded aldehyde lipid anchor system neatly overcomes many of the most apparent problems of the previously mentioned techniques: the aldehyde/aminooxy reaction

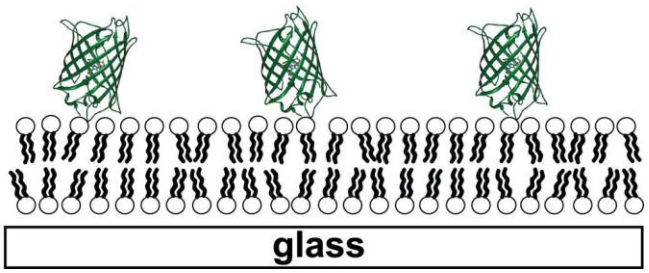

Figure 3.6.: Proposed Experimental Model: EGFP would be covalently bound to an aminooxy containing lipid in a supported lipid bilayer via a genetically encoded aldehyde tag on the C or N terminus

is highly specific, the technique can be undertaken in a part wise fashion where the lipids and the proteins can be brought together when in their respected locations in the biomembranes mimic avoiding the incorporation problem, and finally the aldehyde tag is a direct anchor point for an aminooxy or hydrazide on a lipid head group producing a one to one binding ratio. This technology offers a flexible system by which arbitrary proteins can be potentially incorporated onto a controlled biomimetic membrane surface while maintaining the chemical properties of the protein and the dynamic properties of the lipid bilayer. Being able to choose the lipidic anchor enables a whole new set of behaviors to be brought to bear in the study of protein interactions; namely, the phase separation behavior of certain lipids. Lipid-lipid demixing can be induced via careful temperature control and could potentially be used to induce anchored protein interactions in a precise manner. The freedom in the choice of lipid anchors and the site of attachment to the protein combine to make this an exciting new technique to manufacture enhanced biomembranes. A system permitting the dynamic rearrangement of a proteinous surface in response to externally controllable stimuli (such as temperature for tail mediated lipid phase separation or ion concentration for electrostatic rearrangement) promises a new range of possibilities for the study of cellular communication and in producing interactive biomimetic surfaces.

3.2. Materials and Methods

3.2.1. Materials

For bilayer production: 1,2-dioleoyl-sn-glycero-3-phosphocholine (DOPC) and 1,2-dioleoyl-sn-glycero-3-phosphoethanolamine (DOPE) were purchased from Avanti Polar Lipids (Alabaster, AL). Marina Blue® 1,2-dihexadecanoyl-sn-glycero-3-phosphoethanolamine was purchased from Invitrogen (Carlsbad, Ca). All lipids were dissolved and stored (-20 °C) in chloroform. All organic solvents were HPLC grade, purchased from Sigma-Aldrich (St. Louis, MO) and used without further purification. For lipid aminooxy modification: Boc -2- (aminooxy) acetic acid, carbonyldiamidazole (CDI), hydrochloric acid (HCl), magnesium sulfate ($MgSO_4$), and TFA (Trifluoroacetic acid) were purchased from Sigma-Aldrich (St. Louis, MO). For in vitro formylglycine reaction: Tris(hydroxymethyl)aminomethane (Tris), , Bovine Serum Albumin (BSA), Dithiothreitol (DTT), and Potassium Acetate ($C_2H_3KO_2$) were purchased from Sigma-Aldrich (St. Louis, MO). For aminooxy – aldehyde conjugation: 2-(N-morpholino)ethanesulfonic acid (MES), and 5-methoxyanthranilic acid (5MA) were purchased from Sigma-Aldrich (St. Louis, MO). Aqueous solutions were prepared using organic-free deionized (DI) water of high specific resistivity (approx. 18.0 MΩ/cm).

3.2.2. Protein Modification

The purpose of these experiments is to show that a genetically encoded aldehyde tag is an appropriate and effective means of anchoring a protein to a supported lipid bilayer. In order to establish that the protein is attached and diffusing in 2D, and that the protein is intact and performing its function it is prudent to select the Enhanced Green Fluorescent Protein (EGFP) for modification [242]. If the structure of the EGFP is unperturbed it will fluoresce and be easily studied by fluorescence correlation spectroscopy (FCS), otherwise it will remain dark. Protein

modification was carried out in Escherichia coli (*E.Coli*) following the development of a number of plasmids encoding aldehyde tag motifs at various positions on the protein. EGFP fused with the consensus sequence was co-expressed with Formylglycine Generating Enzyme (FGE) in the bacterium with the aim of producing fully modified proteins. C & N terminal modification plasmids were designed by Dr. Forstner and optimized by DNA 2.0 (Menlo Park, CA)

3.2.3. Chemical Lipid Modification

.The chemical head group modification resulting in an aminooxy group on

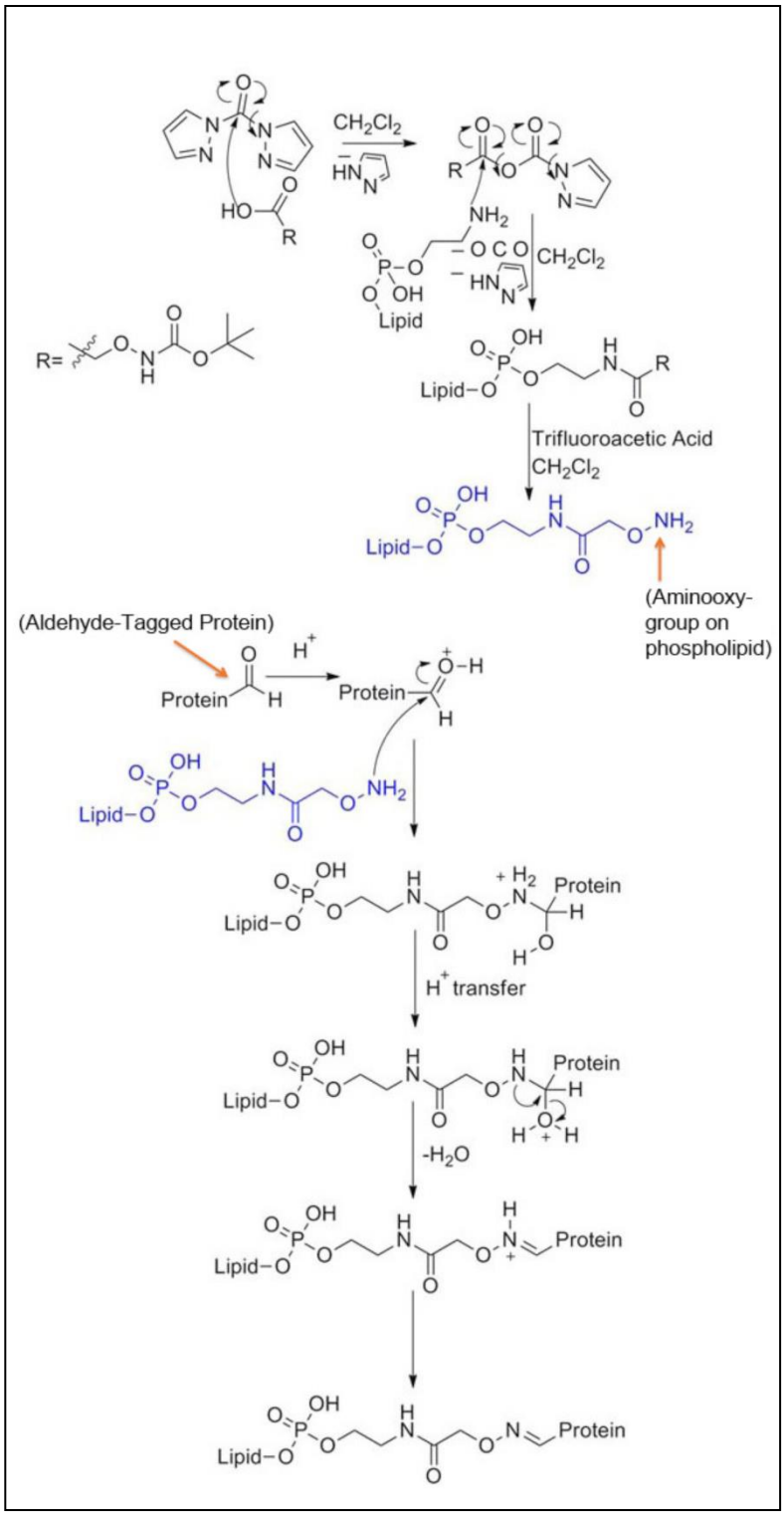

Figure 3.7.: Aldehyde Production Chamistry: Reaction Schematics for the Aminooxy-Modification of a Lipid and Subsequent Conjugation to a Aldehyde-Tagged Protein

commercially available lipids was developed and executed by Prof. Dr. Bader in the Department of Biomedical and Chemical Engineering at Syracuse University. 1,2-Dioleoyl-sn-glycero-3-phosphoethanolamine (DOPE) phospholipids were aminooxy-modified to bear the ($-ONH_2$) group required to bind the aldehyde side chain of the EGFP. The aminooxy group was attached to the lipid via conjugation of the ethanolamine group to BOC protected aminoxy acetic acid, followed by removal of the BOC group with trifluoroacetic acid (TFA). In brief, 0.04032 mmol (7.7mg) Boc -2- (aminooxy) acetic acid and 0.04032 mmol (6.5 mg) carbonyldiamidazole (CDI) were dissolved in 5ml methylenechoride (CH_2Cl_2) in a round bottom flask under a nitrogen environment and stirred at room temperature for 30 mins. In a separate round bottom flask 0.01344 mmol (10mg) of the DOPE lipid was dissolved in 1ml methylenechoride under nitrogen and added to the CDI/BOC-2-(aminooxy) acetic acid solution via cannula. The reaction mixture was stirred at room temperature overnight. Afterwards, the solution was washed with 50ml 1M hydrochloric acid (HCl), 0.1 M NaOH, and brine (salt water). The organic layer was dried over $MgSO_4$, filtered, and concentrated to yield BOC-protected aminooxy modified DOPE lipids as a colorless residue. Formation of the desired intermediate was confirmed by ^1H NMR. Without additional purification, the residue was dissolved in methylene chloride and TFA (1:1) was added. After stirring at room temperature for 2 hours, the solvents were removed via evaporation to give the aminooxy modified DOPE lipids, as confirmed by ^1H NMR.

3.2.4. Small Unilamellar Vesicle Preparation

For the production of supported lipid bilayers it is first necessary to form small unilamellar vesicles (SUVs) with the lipidic ratios desired on the finished bilayer. Lipids are stored at various concentrations (typically 0.1 – 10mg/ml) in organic solvent (typically chloroform). The desired mol% ratio of lipid in the bilayer is determined and the appropriate volume of each lipid mixture

is calculated. In a clean round bottom flask (piranha etched and dried at 80^0C overnight) the predetermined volumes of each lipid solution are combined and mixed for approximately 30s to ensure thorough distribution. The solvent is then removed through approximately 30mins in a roto-vap with a water bath temperature above the transition temperature of the lipids in solvent. The result is a lipid multilayer on the interior of the flask, typically the lipid are rehydrated in 1ml of dd-H_2O which causes the spontaneous formation of lipid multilayer liposomes. The liposome solution is first homogenized by vigorous pipetting. The lipid solution is then extruded with a high pressure extruder (LIPEX^{TM} extruder, Northern Lipids Inc., Burnaby, BC, Canada) through a 0.1µm pore diameter membrane. Ten extrusion cycles are sufficient to produce monodisperse, unilamellar vesicles.

3.2.5. Bilayer Formation

The formation of a supported lipid bilayer on glass was performed via the following procedure: No.1 Glass coverslips (Fisher Scientific, Pittsburgh, PA), held in a Teflon cover glass holder (Fisher Scientific, Pittsburgh, PA), were prepared by first ultrasonically cleaning them in isopropanol, next thorough washing in dd-H_2O (typically 5 rinses) is followed by a 5min etch in Piranha solution (25% Hydrogen Peroxide, 75% Sulphuric Acid). An intense cleaning in dd-H_2O followed (typically 10 rinses) the etching. The lipid vesicle solution is next diluted 3:1 with buffer solution (typically 20mM TRIS, 120mM NaCl, pH 7.4) and a drop of this mixture (30µl for a 25mm diameter coverglass) is placed on a sterile plastic petri dish. A freshly etched (less than approx. 3hrs) coverglass is then dried under an anhydrous nitrogen stream before being placed on top of the vesicle containing droplet. The formation of the bilayer is effectively instantaneous although certain lipid mixtures can benefit from a 3-5min incubation period at this point. The petri-dish with the coverglass is next submerged in a large bowl (1-1.5l) of buffer

solution (the same as previously) where the coverglass is carefully pried off the petri dish. Utmost care must be taken at this point to ensure that the newly formed bilayer has no contact with the air, any loss of water contact will result in the immediate degradation of the bilayer. The coverglass is gently swirled in the buffer to remove unfused lipid vesicles before being place in an Attofluor cell chamber (Life Technologies, Grand Island, NY) while ensuring a constant aqueous environment

The composition of the bilayer was chosen such that it provided a number of different functionalities. Firstly the bilayer should be chemically inert and neutral, to this end the main lipidic constituent of the system was selected to be 1,2-dioleoyl-sn-glycero-3-phosphocholine (DOPC) a chemically inert neutral lipid. Secondly it was desirable to be able to independently confirm the integrity of the bilayer, thus 1mol% of a fluorescently labeled lipid, 1,2-dihexadecanoyl-sn-glycero-3-phosphoethanolamine (Marina Blue® DHPE, Life Technologies, Grand Island, NY), was included. This fluorescent lipid with an absorption maximum at a wavelength of 360 nm and emission at 445 nm was selected to avoid spectral overlap with the EGFP that absorbs maximally at 488 nm and emits mostly around 509 nm [243, 244]. Finally the aminooxy lipid was included to provide a potential fluorescence that would be appropriate for the detection systems available. Based on past experience a concentration of 1mol% fluorescent lipid was judged to be adequate for our needs. Given the desire (see below) to have a 10:1 aminooxy-lipid: aldehyde tagged protein ratio for complete protein incorporation we included 10 mol% of the aminooxy modified lipid to the system.

3.2.5. Protein-Lipid Conjugation

The binding of the aldehyde to the aminooxy requires the formation of a water molecule to remove the –OH group of the aldehyde for attachment to the aminooxy. Thus, an environment

with high concentrations of free hydrogen is necessary for the reaction which advantages a slightly acidic environment for binding. To this end the aldehyde conjugation was performed in a MES buffer solution at pH 6.3 (20 mM MES, 50 mM NaCl) as a compromise between low pH for conjugation and maintaining the structural integrity of the protein which is most stable at pH 7.4. Given the versatile nature of the aldehyde tag system there is no necessity to undertake protein/lipid conjugation at any particular point in the bilayer production process. Two general options were identified as appropriate points for the coupling of the system, either before formation of the supported lipid bilayer (while the lipids are in liposome formation) or after the production of the bilayer. While both options would provide additional information about the versatility of the system, ultimately it was deemed that the addition of the proteins to a pre-formed bilayer would present fewer potential points of potential difficulties and a more direct route to demonstrate feasibility of the overall approach. Amongst the many unknowns of the procedure was the appropriate concentration of proteins to aminooxy lipids. Given the larger expense in time and effort involved in protein or main goal initially was to capture as much protein from solution as possible. Thus modified lipids were introduced in the membrane at a 10-fold excess to the number of proteins in solution.

3.2.6. Imaging and FCS

Standard epifluorescence imaging was undertaken using the built in imaging pathways on the microscope (Nikon Ti-Eclipse, Nikon, Tokyo, Japan). Fluorophore specific filter cubes were used for the two imaging channels. Fluorescence Correlation Spectroscopy (FCS) was used to measure the dynamic diffusion rate of the EGFP in order to determine bilayer attachment (there is approximately two orders of magnitude difference between bilayer diffusion and free 3-D diffusion) The FCS detection system was built in house and it is described in greater detail in

chapter 1. The analysis and extraction of diffusion coefficients followed the procedures laid out in Chapter 2, Section 2.2.3.)

3.2.7. In Vitro Conversion of Cysteine to Formylglycine

In initial experimental attempts it was found that there was a large portion of unbound EGFP present after the protein-lipid conjugation step. The most apparent reason for this was unmodified cysteine in the consensus sequence of a subpopulation of the EGFP. This could have been caused by insufficient exposure of EGFP to FGE during co-expression. To achieve higher conversion ratios the harvested EGFP was incubated again with FGE in a 10:1 ratio *in vitro*. The protocol was provided by Dr. Rabuka (Redwood Scientific, Emeryville, CA) and adapted with modifications. Briefly, a reaction buffer consisting of 50 mM Tris, 68 mM NaCl, 0.2 mg/ml BSA, and 2 mM DTT was produced at 10X concentration at pH 8.0. 81.75 µg EGFP, 1.45 µg FGE, 5 µl of 10X reaction buffer and 5.641 of dd-H_2O (to bring total volume to 50 µl) were combined in the following manner: first the EGFP solution is diluted with dd-H_2O to 30 µl, this is warmed to 30^0C followed by addition of the 10X buffer, the FGE solution and the remaining dd-H_2O to make up 50 µl. This reaction takes place for 8 hrs. at 30°C before being quenched by the addition of 4 µl of 1 mM KOAc at pH 6.4. Following the in vitro FGE reaction the protein was purified by serial dilution of the reaction chemicals in a 30 kD dialysis tube in 1 l of dialysis buffer (50 mM Tris, 68 mM NaCl, pH 7.4) which was exchanged every 4 hrs. for 12 hrs. total. The resultant aldehyde tagged EGFP was incubated on with an aminooxy-lipid containing SLB for 8 hrs. before thorough washing and imaging/FCS. Following additional investigations a chemical catalyzer for the aldehyde/aminooxy reaction was trialed. 5-methoxyanthranilic acid (5MA), 125 mM at pH 7.4 and room temperature, was found to decrease the time needed for bilayer integration to 30 mins and eliminate the need for the lower (6.4) pH for conjugation.

Subsequent experiments determined that 3 mM of 5MA in buffer solution (20 mM Tris, 100 mM NaCl, pH 7.4) was sufficient to provide a 30:1 ratio of catalyst to aminooxy lipid which was sufficient for economic protein/lipid coupling.

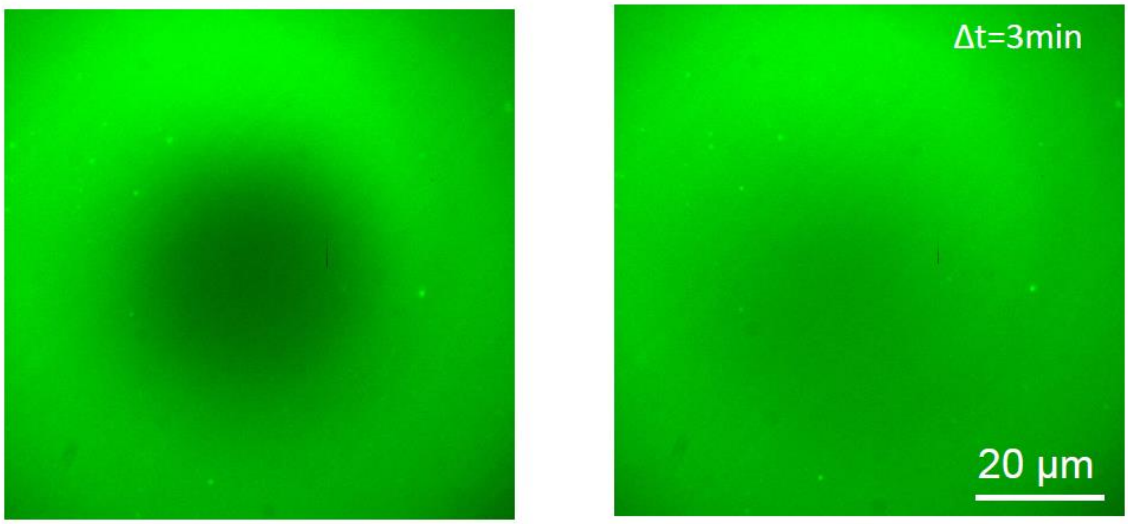

Figure 3.8.: TIRF Shows Succussul EGFP Integration: EGFP has successfully been integrated onto a supported lipid bilayer via an aldehyde attached lipid anchor. Here an area of the bilayer has been carefully photobleached (left hand picture). The recovery of fluorescence in this area shows that the fluorescent molecules are capable of 2-D diffusion indicating an intact lipid bilayer.

3.3. Results and Discussion

N and C terminus modified EGFP were successfully anchored to a SLB via an aminooxy bearing 1,2-Dioleoyl-sn-glycero-3-phosphoethanolamine (DOPE) phospholipid. The attached GFP retained its fluorescence and was measured to have a diffusion rate comparable to a membrane bound lipid. The modification and attachment methods were refined to eliminate unattached EGFP with the inclusion of an additional FGE reaction stage and the addition of 5-methoxyanthranilic acid (5MA) into the system buffer solution to act as a catalyzer for the aldehyde/aminooxy binding reaction.

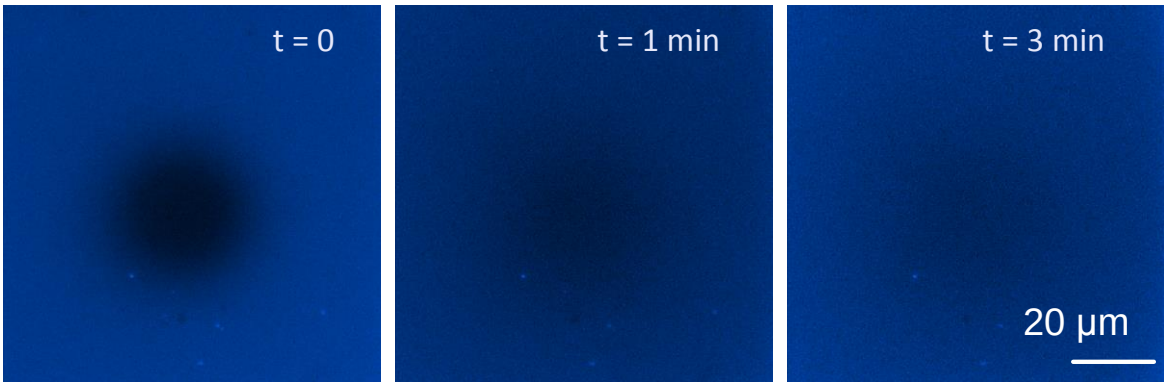

Figure 3.9.: TIRF Shows Bilayer Remains Intact: The integrity of the underlying bilayer is ascertained through the addition of a Marina Blue labeled lipid. Here the photo-bleaching and recovery of a specific area shows that the bilayer remains intact and fluid following the successful conjugation of aldehyde modified GFP to the bilayer incorporated aminooxy-DOPE

We found that during the initial experimental stages that the amount of non-reactive GFP in the system was causing disruption to the bilayer. The unassociated protein was attaching through small membrane defects directly to the glass. These regions of fixed proteins rendered detection of the lipid anchored fraction of the GFP impossible. A number of steps were taken to combat

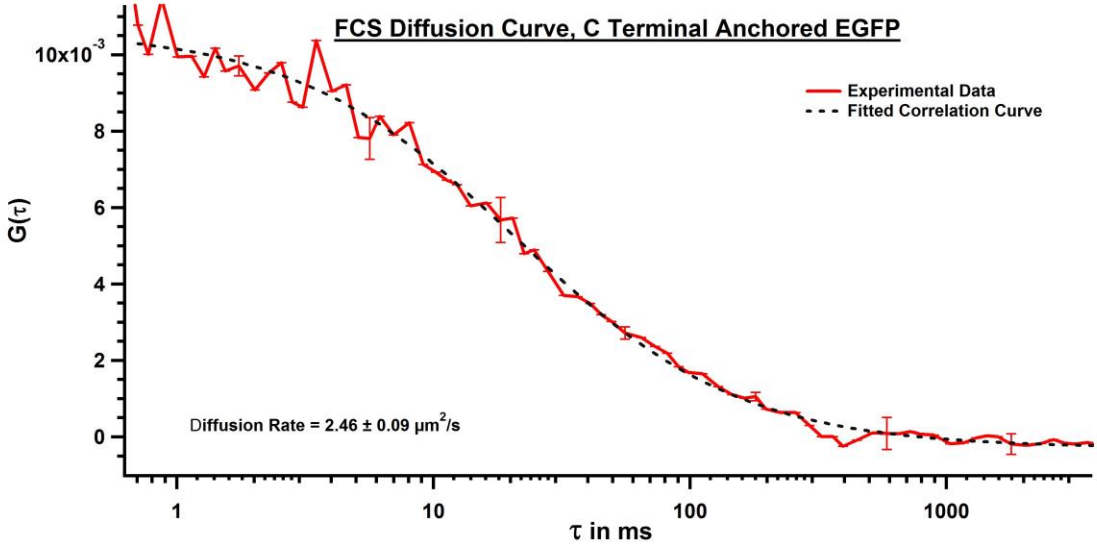

Figure 3.10.: FCS Diffusion Measurement of Aldehyde Anchored EGFP: An example of an FCS correlation curve for an EGFP bound to a solid supported lipid bilayer via an aldehyde tag on its C terminal. The diffusion rate was measure to be 2.46µm^2/s. This is comparable to expected lipid diffusion rates of approximately 3µm^2/s

this problem. A blocking buffer containing bovine serum albumin (BSA) was introduced to the bilayer before the addition of the GFP. This is a well-known way to pre-occupy small holes in the bilayer [245]. The intent was that the BSA would bind to any areas where there were bilayer defects thus preventing the GFP from binding to the glass. This blocking buffer was accompanied with an extensive washing routine before imaging or FCS detection. These attempts alone however proved insufficient to the task. It was determined that an additional in vitro FGE reaction was necessary. Subsequent to the secondary FGE reaction it was found that the GFP was attaching to the bilayer without the large amount of surface bound protein that was obscuring previous experiments. Recent work by Kool et el in Stanford has identified a number of aldehyde/aminooxy catalysts that can be used in low concentrations and at room temperature [246]. Of these catalysts 5-methoxyanthranilic acid (5MA) was the most promising due to its efficiency and low necessary concentration, thus having the least potential for unwanted side effects [246]. Work by Glen Research (Sterling Va.) showed that the addition of 5MA for an hour can have up to a 4x increase in the amount of aldehyde/aminooxy conjugations. For our work we added the catalyst to the buffer solution for EGFP incorporation. Following 30mins of incubation we then washed the bilayer thoroughly with buffer solution (20mM Tris, 100mM NaCl, pH 7.4). After optimizing all the steps as described above, the procedure results in a clean bilayer showing fluorescence recover under FRAP protocols as seen in Figure 3.8.. Also, the mobility of the lipid attached EGFP could now be determined. The diffusion coefficients as measured with FCS are similar to most commonly observed SLB bound lipids (for example 2.46 ± 0.09 $\mu m^2/s$ in one measurement for C terminal attached EGFP, 3.17 ± 0.90 $\mu m^2/s$ in one measurement for N terminal attached EGFP vs.~ 3 $\mu m^2/s$ for a typical phospholipid [247]). The experiments were expanded to include EGFP with aldehyde modifications on the C and N

terminals with the average diffusion rate for N terminal anchored EGFP across all independent measurements being 2.49 ± 0.15 $\mu m^2/s$ and the average diffusion rate for C terminal anchored EGFP across all independent measurements being 2.63 ± 0.16 $\mu m^2/s$ with an accumulated average between both N and C terminally anchored proteins of 111.85 ±8.15 EGFP molecules per μm^2. With the N terminal anchored proteins having 113.17± 10.42 molecules per μm^2, and the C terminal anchored proteins having 110.54± 1.78 molecules per μm^2.The matrix lipid DOPC has a cross-section area on supported lipid bilayers of around 50 $Å^2$ at room temperature[248]. Thus, one can deduce an upper bound of about 2×10^6 DOPC lipids per μm^2 in the upper leaflet of the SLB. At 10 mol% that would give about a maximum of 2×10^5 aminooxy modified lipids. Thus, under these experimental conditions and procedures about 0.05% of all mobile aminooxy modified lipids were successfully conjugated with an EGFP. Given that structurally EGFP is roughly a cylinder with a length of 4.2 nm and a diameter of 2.5 nm [249], one can estimate the cross-sectional area of a terminally anchored EGFP to about 10 nm^2

resulting in 0.1 % estimated coverage of the SLB's surface by EGFP. These results show that an aldehyde labeled protein can be successfully attached to a aminooxy modified protein while maintaining the function of both. This is a significant step in the application of this exciting new technology. The development of a functional protocol will allow other researchers to begin implementation of the aldehyde tag lipid anchoring system.

The continuing work for this project has a number of different outlooks. Firstly the immediate work of showing that aldehyde/aminooxy anchors can be used with diverse lipids and proteins could be addressed. This can be undertaken in a relatively straightforward manner now that a successful integration protocol has been established. A secondary outlook would be to begin to show the excellent function that such a system has to offer. For example the careful selection of lipid anchors has the potential to permit the dynamic rearrangement of the attached proteins. By exploiting the temperature induced phase separation that occurs for certain lipids, the protein bearing lipids could be caused to enter the lipid domains below the phase transition or

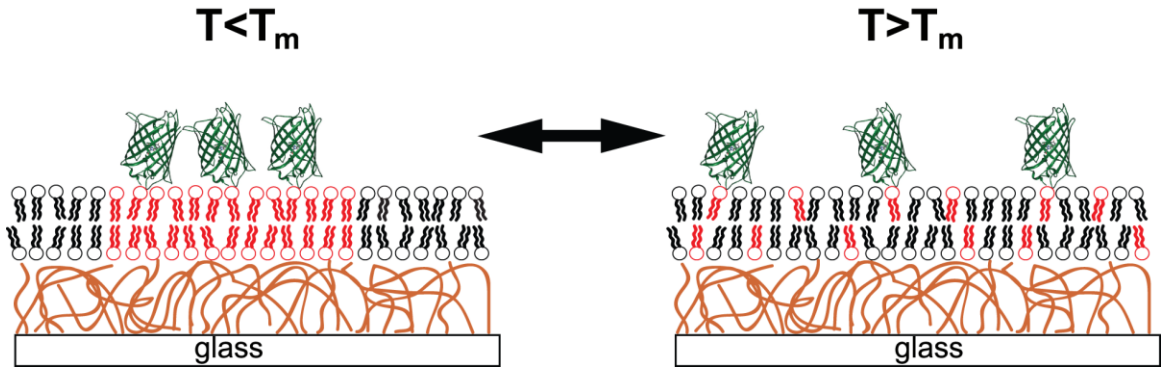

Figure 3.11.: Potential Aldehyde Tag Applications: Lipid phase separation can be induced by careful control of the temperature T. By gently lowering and raising the temperature with respect to the transition temperature T_m of the lipid bilayer, it is expected that the anchor-EGFP constructs follow the phase separation events and distribute according to the chemical identity of their specific lipidic anchor motif.

distribute homogeneously above the transition temperature as shown in Figure 3.11.. This would permit the controlled spatial rearrangement of planar protein systems. This would be an excellent system for studying cell/protein interactions. Thirdly, it would be beneficial to determine a technique for incorporating vesicles bearing lipid anchored proteins into a preexisting bilayer. Such a system would allow SLBs with multiple different protein or peptide types to be formed. These proteins could then be induced into a state of mass aggregation via lipid phase separation allowing their interactions to be carefully timed and closely investigated.

Section 4: The Effect of Bilayer Charge on the Adhesion and Proliferation of Adherent Cells

Summary

Biophysical science is a perpetual effort to mimic the behavior of biological systems in a manner that permits the replication and study of the structures involved. To this end researchers are constantly trying to create a better analogue of in vivo conditions for in vitro investigations. Recent work has seen the inclusion of adhesion and signaling molecules to supported lipid bilayers in order to better study the behavior of living cells. Relatively little is known, however, about what effects different lipid bilayer properties have on cells that are attached to them. In this work we investigate the effect of bilayer charge on the adhesion and proliferation of adherent cells. This work aims to provide a foundation of basic knowledge on which future enhanced bio-surfaces can be developed. The properties of both enhanced and decreased cellular adhesion can be desirable depending on the proposed application. For the study of intracellular signaling then enhanced adhesion would be desirable. For biomedical application in areas where tissue growth is undesirable, such as cardiac stents, then decreased cellular adhesion is advantageous. In order to study the effect of lipid bilayers on the proliferation of cells, NIH 3T3 mouse fibroblast cells were incubated on bilayers of different mol% ratios of anionic and cationic lipids. The cellular proliferation over the course of 48 h was measured. The morphology of the cells was also studied under high magnification to determine the quality of adhesion. Control experiment included bare

glass surfaces and collagenated substrates. In a first step towards biologically functionalized lipids glycolipid enriched bilayers' effect on cell behavior were investigated as well. It was found that during the first 24 h period that the charged bilayers all produced an extensive decrease in the cell count. For the second 24 h period the bilayers with the anionic lipids showed positive population growth while those with cationic lipids continued to show a decrease in cell numbers. The inclusion of glycolipids into the lipid bilayer increased the cell growth dramatically for all time periods.

4.1 Introduction

Since the 1980's supported lipid bilayers have provided a reliable system for the study of lipids and membrane associated proteins [250-252]. These versatile experimental tools allow investigators to create compositionally controlled analogues of the cellular membrane, simplifying the system from the tens of thousands of constituents found in nature [253-256] to one of a controlled number of elements produced in vitro. By selecting the elements of a lipid bilayer the basic interactions between membrane components can be determined in a controlled and measurable manner. Currently there exists a large body of work detailing many lipid-lipid and lipid-protein interactions [257-265]. With this strong foundation in place there has been a consistent push in this research toward greater mimicry of natural cell surfaces [78, 266]. The addition and incorporation of proteins, peptides, carbohydrates and

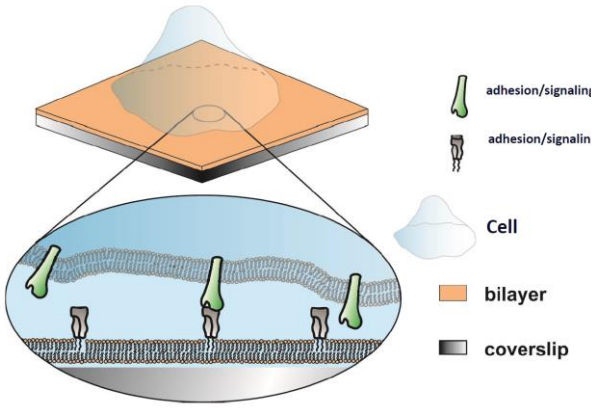

Figure 4.1.: Enhanced Bilayers: Bilayers can be enhanced with adhesion or signaling proteins to aid in the study of their action in living cells.

sterols all serve to duplicate and illuminate the actual behaviors of biological membranes in living tissue. Researchers aim to develop biomembranes capable of impersonating any desired cellular interface. This will permit numerous natural interactions, such as cellular adhesion, T-Cell response, and stem cell differentiation to be investigated and simulated [267-271]. A suitable biomembrane could be developed to induce a specific response in a cell that would allow close temporal and spatial control facilitating experimental observation in a manner previously impossible. Another possible application for this is in the lipidic coating of man-made materials; here a supported lipid bilayer would be formed on a surface that is to be in close contact with biological tissue. A well designed biomembrane would promote certain biological responses such as healing and cell adhesion while preventing others such as infection and clotting. Ultimately a controllable surface capable of perfectly mimicking the cell surfaces in natural tissue would permit the full integration of artificial devices with the human body. The implications of such capability could include neural implants that can transmit thought into some external action (or vice versa) such as would be desirable in limb replacement, machine control, paralysis bypass or enhanced sight or vision.

Closed lipid structures already have an important medical application; they are used in liposomal drug delivery [82, 272-279]. Here a closed lipid bilayer encapsulates a solution of the drug to be administered, identifying peptides can help target the drug to specific tissue while other surface modifications can enhance longevity in the system, promote immune system evasion, or activate endocytosis once a target cell is reached [83, 280-288]. Currently there are more than a dozen different type of liposomal drug delivery systems approved for human use [84]. Liposomes are also being investigated as a means to reduce drug toxicity by scavenging the drug from circulation to reduce its toxic effects [85].

The common link between the above applications is that they are both based on the interaction of a lipid bilayer and biological tissue. Despite the fact that the lipid bilayer is the main structural component of these systems most investigators attempt to provide functionality via protein or carbohydrate inclusions on the bilayer surface. Oftentimes the lipids themselves have been overlooked as a means to impart cellular response. In order to build a reliable interfacial biomembrane it is desirable to keep complexity as low as possible but as high as necessary. Thus, if the lipid composition can serve both a structural and a chemical role then greater efficiency can be achieved. As of yet there has been almost no work detailing how living cells interact with pure supported lipid bilayers without any proteinous or other augmentations. Cells are commonly cultured on supported lipid bilayers where the bilayer is expected to have sometimes a passive role and sometimes an active role in promoting biocompatibility [15, 289, 290]. Without concrete characterizations of these effects the use of bilayers will remain minor. The possibility of bilayer composition being able to influence cell adhesion also has significance to biomedical engineers looking to promote a certain type of behavior in their system. For example a joint implant with a biocompatible lipid coating that speeds up the adhesion of the muscle tissue while preventing the formation of clots and also providing an antibacterial layer. Another application might be a cardiac stent with an engineered lipid coating on its inner surface that provides favorable conditions for endothelial cell growth but prevents smooth muscle cell growth.

It is with these facts in mind that we endeavor to undertake an investigation to observe how fundamental properties of a supported lipid bilayer will affect some of the basic behaviors of cells cultured on top. In particular there is a distinct lack of knowledge about how the electrical charge of lipids in a bilayer effect cells in direct contact with it. Cellular surfaces have

been measured to consistently bear a slightly negative charge [291]. With all cells being anionic on their surface it seems evident that there should be adhesion mechanisms that rely on the charge found on other cells when identifying and establishing intercellular adhesions. Specifically we will investigate the role that charge has in the adhesion and proliferation of cells; two important considerations for surface studies.

The cell lines used in experiments were NIH 3T3 fibroblasts cells. These cells were used because their morphology is strongly influenced by their adhesion quality. They have roughly a 16 hour doubling time at optimal culturing conditions which is useful for experiment cycles, and most importantly they are widely studied and well understood making the cell line a good experimental model.

Previous studies of cells on bilayer substrates have been forced to restrict themselves to either small areas or small iteration numbers. In order to perform an accurate cell count researchers have been forced to either restrict the area so that a manual count can be performed, or to add a nuclear dye to permit automated counting [292, 293]. This is both highly tedious and costly in terms of supplies. These techniques also mean that in order to perform multi day experiments you either need a limited number of samples small enough to count rapidly by eye, or you need to make multiple samples that can be stained and counted at each time point. The ideal situation would be one where it was possible to automatically count multiple samples in parallel without altering them in any way. This is now possible thanks to innovations in cell identification and counting software. In particular Molecular Devices (Sunnyvale, CA) have developed a system that can use phase contrast illumination and advance machine vision software to identify cells through their size and shape [294]. The device, a SpectraMax, MiniMax 300 Imaging Cytometer, will be used in these experiments to permit an unprecedented number of parallel experiments to

take place. This will be done without the use of any cellular dye which allows the progressive tracking of the behavior of a particular sample through multiple time points, and will help to eliminate some of the variability typically seen in hybrid supported bilayer/cell systems. With this approach we demonstrate for the first time that some of these kinds of experiments can be translated to a high throughput method to which statistical analysis can be applied.

3T3 fibroblasts cells were incubated on supported lipid bilayers with varying percentages of either singly negatively or singly positively charged lipids. Bilayer charge is also affected by the charge of the underlying substrate, the cleansing process commonly used in bilayer preparation has been found to produce a negatively charged substrate. The work of Parasarathy et al in 2005 equated this surface charge of the piranha etched glass to 4 mol% of negatively charged lipids in a bilayer surface [291]. It is common practice in the field of supported lipid bilayers to equate electrostatic potential in or on the bilayer to an equivalent concentration of charged lipids (in mol%) [295-298]. The reason for this lies in the difficulties of measuring a surface charge on a planar surface in an ionic aqueous solution: titration of the lipid charge through bulk solution pH can have system wide side effects, and surface force apparatus studies require specialized equipment (such as an atomic force microscope). Taking the negative charge of the glass into consideration a series of bilayers with net charge composition of 10 mol% negative charge, 5 mol% negative charge, 10 mol% positive charge, 5 mol% positive charge and net neutral were produced. Proliferation measurements were conducted at 4 hours, 24 hours and 48 hours post-seeding. High magnification images were taken at 24 hours and 48 hours to evaluate the morphology of cells and the integrity of the supported lipid bilayer. The same proliferation and morphology experiments were conducted with fibroblasts incubated on sonically cleansed glass, piranha etched glass, and collagen treated glass to provide control values and reference images.

We found that during the first 24 h period that the charged bilayers all produced an extensive decrease in the cell count. For the second 24 h period the bilayers with the anionic lipids showed positive population growth while those with cationic lipids continued to show a decrease in cell numbers. The inclusion of glycolipids into the lipid bilayer increased the cell growth dramatically for all time periods.

4.2 Materials and Methods

4.2.1 Materials

1,2-dioleoyl-sn-glycero-3-phosphocholine (DOPC), 1,2-dioleoyl-3-trimethylammonium-propane (DOTAP), 1,2-dioleoyl-sn-glycero-3-ethylphosphocholine (eDOPC), 1,2-dioleoyl-sn-glycero-3-phospho-(1'-rac-glycerol) (DOPG), and 1,2-dioleoyl-sn-glycero-3-phospho-L-serine (DOPS) were purchased from Avanti Polar Lipids (Alabaster, AL). (2-(4,4-difluoro-5,7-dimethyl-4-bora-3a,4a-diaza-s-indacene-3-dodecanoyl)-1-hexadecanoyl-sn-glycero-3-phosphocholine) (β-BODIPY® FL C12-HPC) was purchased from Life Technologies (Grand Island, NY). monosialotetrahexosylganglioside (Ganglioside GM1) (Ovine Brain) and 1,2-dioleoyl-sn-glycero-3-phosphoethanolamine-N-lactosyl (Lactosyl- DOPE) were purchased from Avanti Polar Lipids (Alabaster, AL).

4.2.2 Cell Line

The cell line used in these experiments was NIH 3T3 Mouse Fibroblasts (ATCC, Manassas, VA). This cell line serves as an excellent experimental model for both proliferation and adherence experiments. This suitability is due to a number of different factors; they are a highly motile cell line, they are contact inhibited resulting in rapid and thorough surface coverage, and primarily because they are adherent by nature and form abundant focal adhesions [299-302]. The

morphology of adherent fibroblasts on hard and also soft substrate has been thoroughly studied [303-305]. There is a tight connection between adhesion, cell health and morphology enabling visual interpretation of the quality of a substrate for fibroblast growth [306-309]. Fibroblast motility is also connected to adhesion and cytoskeletal reorganization and again both of these aspects have been studied in much detail [310-312].

4.2.3 Cell Culture

Cells were grown in Dulbecco's Modified Eagle's Medium with 10% FBS at 37^0C under 5% CO_2 enriched atmospheric air. Overnight and throughout the experiments when the cells were not being used, they were maintained in a Forma Series II Water Jacketed CO_2 Incubator purchased from Thermo Scientific (Pittsburgh, PA). The 3T3 fibroblasts were split with a sterile technique inside the laboratory's Thermo Scientific 1300 Series A2 hood (Thermo Scientific, Pittsburgh, PA) at all times. Before all materials were placed inside the hood they were sterilized either by being autoclaved or by a 70% reagent alcohol (Fisher Scientific, Pittsburgh, PA) and 30% double-distilled water solution, strict aseptic procedures were followed at all stages of sample perpetration and experimentation. The cells were split on an as-needed basis in order to be maintained between 30% and 90% confluence and to ensure a nutrient rich environment. For these investigations the cells were all between their 8^{th} and 12^{th} passages, this avoided the increased proliferation rates seen in low passage number cells and the retarded growth rates seen in high passage number cells [313]. . The splitting ratio was chosen to provide sufficient cells to perform planned experimental procedures.

4.2.4 Glass Substrate Preparation

With special consideration being given to the inherent surface charge of Piranha Etched glass a thorough preparation process was followed to ensure consistency through all experimental

iterations. The initial cleaning was through ultra-sonic agitation. For this process, a Fisher Scientific Digital Ultrasonic Cleaner FS30D (Fisher Scientific, Pittsburgh, PA) was used. No 1 fused silica glass coverslips (Fisher Scientific, Pittsburgh, PA) with either 15 mm (for multiwell plate) or 25 mm (for Attofluor cell chamber) diameter were held within a Teflon coverslip holder and placed inside a beaker with isopropyl alcohol (Fisher Scientific, Pittsburgh, PA). A degasing cycle (5 mins at a vibrational frequency with increased low pressure sound waves that cause gas scavenging bubble formation in the liquid) was performed to remove dissolved gases from the liquid that may fall out of solution and form bubbles on the glass surface thus preventing proper solvent access to areas of the glass. The coverslips were then sonicated for 15 minutes, which ultrasonically cleansed them by releasing adhered particles and disrupting organic material that may have come in contact with the glass surface. Sonication was followed by thorough washing in double-deionized water in preparation of Piranha Etch.

Immediately following sonic cleansing the coverslips were cleaned in a Piranha solution. This step was performed immediately prior to bilayer deposition. Piranha etch consists of a 3:1 (by volume) sulfuric acid and hydrogen peroxide mixture. Piranha etch is a highly oxidizing solution which will oxidize any organic material remaining on the glass surface and will also hydroxylate the surface rendering it hydrophilic [144]. Coverslips arranged in a Teflon holder were placed in a beaker containing a mixture of 150 mL concentrated sulfuric acid (Sigma-Aldrich) and 50 mL hydrogen peroxide (Sigma-Aldrich). Following 5 mins of soaking in the Piranha etch the coverslips were finally washed 10 times in double-deionized water. This procedure was performed inside a designated hood and using appropriate safety aprons, gloves and face shields at all times

4.2.5 Supported Lipid Bilayer Preparation

Positive surface charge was adjusted by inclusion of either 1,2-dioleoyl-3-trimethylammonium-propane (DOTAP), or 1,2-dioleoyl-sn-glycero-3-ethylphosphocholine (eDOPC) (Avanti Polar Lipids, Alabaster, AL), both of which bear a single positive charge in their head group at physiological conditions. Negative charge was provided by inclusion of 1,2-dioleoyl-sn-glycero-3-phospho-(1'-rac-glycerol) (DOPG) or 1,2-dioleoyl-sn-glycero-3-phospho-L-serine (DOPS) (Avanti Polar Lipids, Alabaster, AL). At the environmental conditions of the experiment both of these lipids bear a single negative charge in their head group. All bilayers contained 0.1 Mol % of (2-(4,4-difluoro-5,7-dimethyl-4-bora-3a,4a-diaza-s-indacene-3-dodecanoyl)-1-hexadecanoyl-sn-glycero-3-phosphocholine) (β-BODIPY® FL C12-HPC) (Life Technologies, Grand Island, NY) a green fluorescent lipid (488 excitation/ 512 emission) in order to confirm the integrity and fluidity of the bilayer under a microscope.1,2-dioleoyl-sn-glycero-3-phosphocholine (DOPC) (Avanti Polar Lipids) was used as the major lipid component for the bilayers making up the remainder of the system. DOPC is a net neutral lipid with low biological interactions and excellent fluidity at 37°C [314]. All bilayers were placed on the glass substrate immediately following etching to ensure that the negative charge on the glass did not degrade before placement of the insulating lipid bilayer. All bilayer compositions were adjusted so that they take into account the 4 mol% equivalent negative charge in the glass, to-wit the net 10 mol% negative charge bilayer contained in fact 6 mol% of negatively charged lipids and the net 10 mol% positive charge bilayers contained 14 mol% positively charged lipids to compensate for the negative glass. Consequently the net neutral (net 0 mol% charged lipid) bilayers actually all held 4 mol% of the cationic lipid. Glycolipid bilayers were formed to contain 5 mol% of the

respective glycolipid following the accepted concentration for this type of molecule found in mammalian plasma membranes [315].

4.2.6 Proliferation Experiment

3T3 fibroblasts were seeded in 24-well cell culture plates each containing a 15mm diameter glass coverslip with corresponding supported lipid bilayers of different net surface charges. An initial cell count was taken at 4 h post seeding using the automated dye-free cell counting function of a Spectromax Minimax 300 (Molecular Devices, Sunnyvale, CA) plate reader kindly loaned by the research group of Prof. Movileaneau in the Physics Department of Syracuse University. This time point permitted an accurate count of the number of cells deposited at each imaging location in the well without risk of inaccuracy due to suspended cells or cellular proliferation. Further proliferation was measured at 24-hour and 48-hour post seeding time points. Cell proliferation was also analyzed from cells cultured in three additional 24-well cell culture plates. The three additional culture plates served as controls, and had cells cultured on piranha etched glass coverslips, ultrasonically cleansed glass coverslips, and collagen treated glass coverslips (Etched glass coverslips were dried at 80^0C overnight, the surface was saturated with 0.5ml of 200µg/ml Collagen in a 90/10 Ethanol/ddH_2O solution and allowed to dry overnight in the cell culture hood). Initial experiments were conducted to determine a suitable seeding density for these conditions, seeding density should be as high as possible to ensure healthy cell growth while avoiding confluencey greater than 90% which would inhibit further cell growth and be a detriment to reliable counting. A quantity of 7,500 cells per well, corresponding to an approximate average cell density of 4,237 cells/ cm^2 was found to permit 48 hours of growth and division without overcrowding the surface at even the most favorable growth conditions. This

concentration was within the range recommended by PromoCell Inc. (Heidelburgh, Germany) of between 3,500 and 7,000 cells / cm^2.

The Minimax 300 plate reader uses a stain free cell counting technique, called StainFree™ Technology that permits reliable cell counts without any additional dye or perturbation of the cells. The software is doing so by identifying the contrast profile of cells. Cell images were taken using a 4x phase contrast through-light module. Green channel (488nm excitation/ 512 nm emission) images were also acquired to test for the presence of a lipid bilayer. Each plate was counted at 4h, 24h and 48h post inoculation. 16 representative images (0.875mm X 0.875mm) were acquired for each well and contrast based edge analysis software determined the number of cells per image. The well counts for each time point were summed and compared to the count from 24h previous. Wells with cell counts in excess of two standard deviations of the median were excluded from analysis. The standard deviation and standard error of the mean were calculated for each plate. Inherent error in the system comes from miscounting of the cells, due to poor contrast or overcrowding. A comparison of automated counts versus visual counts showed a concurrence within approximately 5%, this is less than the difference in cell count between wells on any plate.

4.2.7 Adhesion Experiment

The 24 well plates provided an excellent system to observe a high number of different bilayer systems in a short amount of time. However, the system required the use of a plastic multi-well plate with a glass coverslip placed inside. This thickness of material proved to be too thick for high power microscopy where the focal point is very close (1-2 mm) to the objective lens of the microscope. In order to perform a closer examination of the cell morphology under the different bilayer condition it was necessary to produce a series of experiments on substrates suitable for

high power microscopy. Larger (25 mm diameter) fused silica coverslips (Fisher Scientific, Pittsburgh, PA) were prepared with the respective bilayers and were imaged at 24-hour and 48-hour time points. In order to enhance the contrast and to distinguish between living and dead cells a Live/Dead Cell stain kit (Life Technologies, Carlsbad, CA) was used. This kit targeted esterase activity and cell membrane integrity in order to distinguish between living and dead cells. In order to distinguish between multiple cells in a cluster a blue nucleus dye (Hoechst 33342, Life Technologies, Carlsbad, CA) was also included. Following verification of the

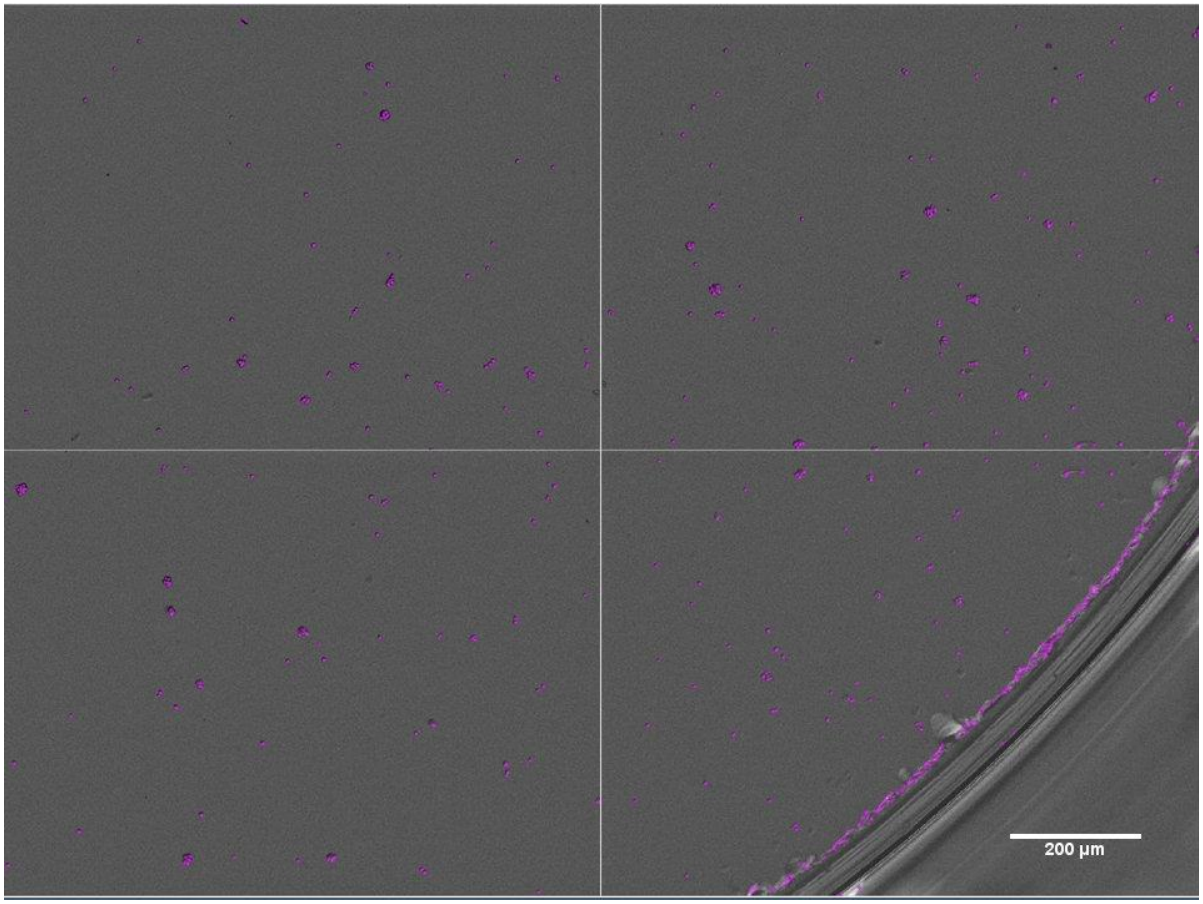

Figure 4.2.: Automated Cell Counting: The SpectraMax cell counting software identifies cells by detecting the change in contrast due to the cell edge using phase contrast microscopy. Erroneous cell counts were taken at the edge of the glass substrate due to the roughness of the edge. Purple indicates cells identified by the software in the grey-scale image. The software identifies stitches together multiple images to provide a wide field overview of the substrate.

integrity of the bilayer by fluorescence imaging the cells were stained and imaged on a Nikon Eclipses Ti inverted biological microscope. A 60x water immersion objective was used to determine general features of the cells and their morphology. Closer examination was achieved by the introduction of an internal 1.5x lens, which boosted the magnification to 90x total. Images were acquired at the three different fluorescent channels (Red, Green, and Blue) using Nikon Elements software. Following image acquisition the three separate images were stitched into a three color overlay using the same software.

4.3 Results and Discussion

While measuring fibroblast proliferation, the software used by the Spectromax Minimax 300 could not distinguish between the edges of glass coverslips and living cells as can be seen in Figure 4.2. Many of the cell counts that were made at the edge of the glass coverslips were erroneous. Because of this areas where the image contained the edge of the glass substrate were eliminated from further analysis. To determine the rate of cellular proliferation, the total amount of cells from the usable areas in each of the 24 wells was summed up after being incubated for 4 hours, enough time to permits the cells to settle and begin binding but not long enough to alter the cell count significantly from the seeding amount. That amount was then compared to the cell count in that same well at 24 and 48-hour time points and a percentage change in the cell population is calculated for each of the intervals. The capability to perform these experiments on 24 well plates allowed an unprecedented number of experiments to be performed in parallel. This is one of the first examples of a high throughput supported lipid bilayer experimental system capable of producing statistically relevant iteration numbers in a single run. High experimental iteration numbers help to overcome the large natural fluctuations in behavior seen in biological systems, thus they help to extract the more general response.

4.3.1) Control Groups

In order to have a good understanding of the proliferation behavior of these cells under different substrate condition we undertook a number of control experiments. We looked at bare glass surfaces as they are at two different stages of the bilayer production process: after sonic cleansing and after Piranha etching. In addition, we coated a glass substrate with collagen to duplicate a commonly used cellular growth substrate. As well as providing proliferation baselines these substrates were also used to observe cellular morphology on these solid substrates as a basis of comparison for later experiments. Cellular proliferation was seen to be consistently good on all the solid substrates (see Figure 4.3.). An unexpected result was that the two bare glass substrates actually produced higher proliferation rates than the collagenated glass

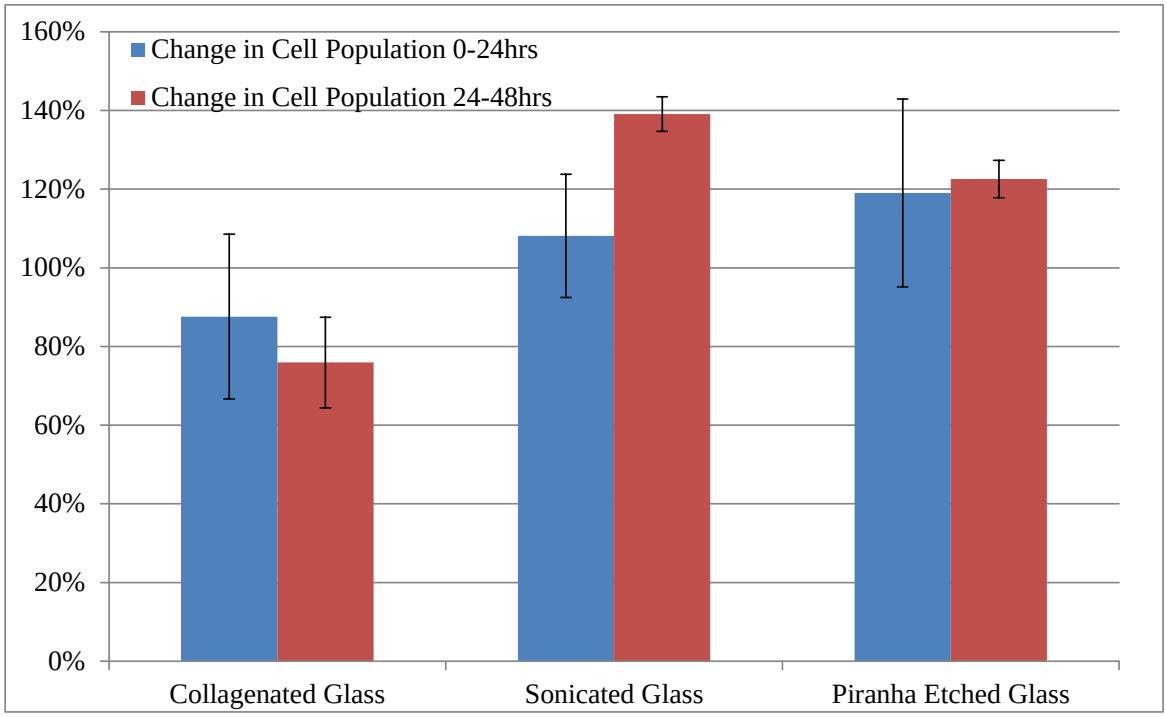

Figure 4.3.: Cell Population Change on Control Substrates: Change in cell population for fibroblast cells adhered to control substrates from 0-24 hrs and from 24-48 hrs. Solid substrates showed consistantly positive cell growth with doubling rates approaching those found in culture flasks. Surprisingly the bare glass substrate showed slighttly higher proliferation than the collagenated glass

substrate. Solid supports showed an approximate doubling time of 24h. Each value is the calculated mean across all 24 wells. In Figure 4.4. representative examples of 3T3 cells attached to the different solid supports can be seen. Here their shape can be seen to be highly influenced by thorough attachment they make with the substrate. These cells will typically have a number of lamellipodia when surface adhered and will often bear a vaguely triangular shape when migrating with the direction of the motion generally occurring towards the broad base of the ‘triangle’. When not adhered to a substrate 3T3 cells will have a minimum-energy spherical form.

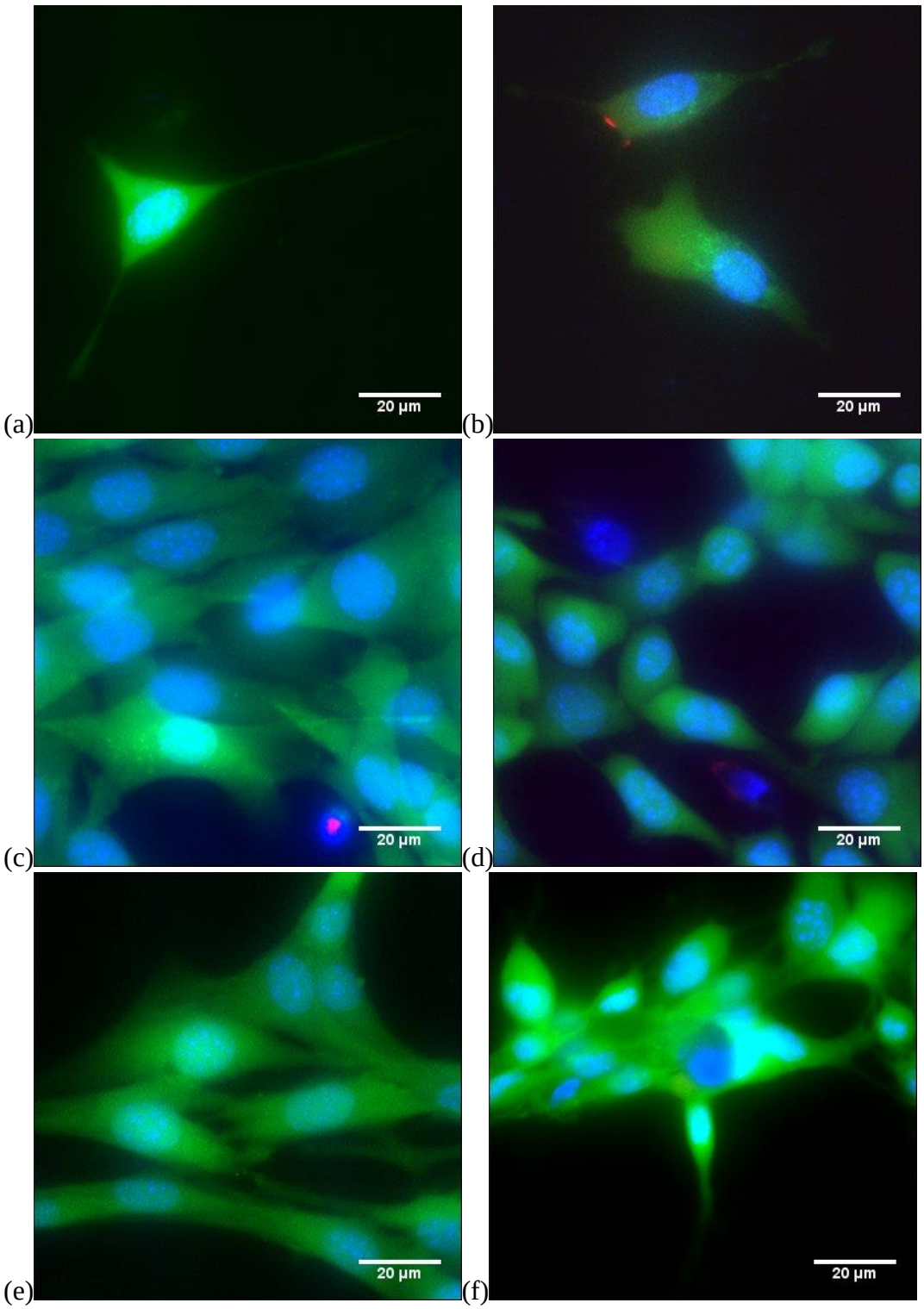

Figure 4.4.: Cell Morphologies on Control Substrates: Morphology of 3T3 fibroblasts on different solid substrates: (a) Fibroblast cells on a collagenated glass substrate at 24 h and (b) 48 h, (c) Fibroblast cells on a Piranha Etched Glass substrate at 24 h and (d) 48 h, Fibroblast cells on a sonically cleansed glass substrate at 24 h and (f) 48 h. Green dye indicates living cells, blue dye indicates the nucleus and red indicates dead cells.

4.3.2 Supported Lipid Bilayers.

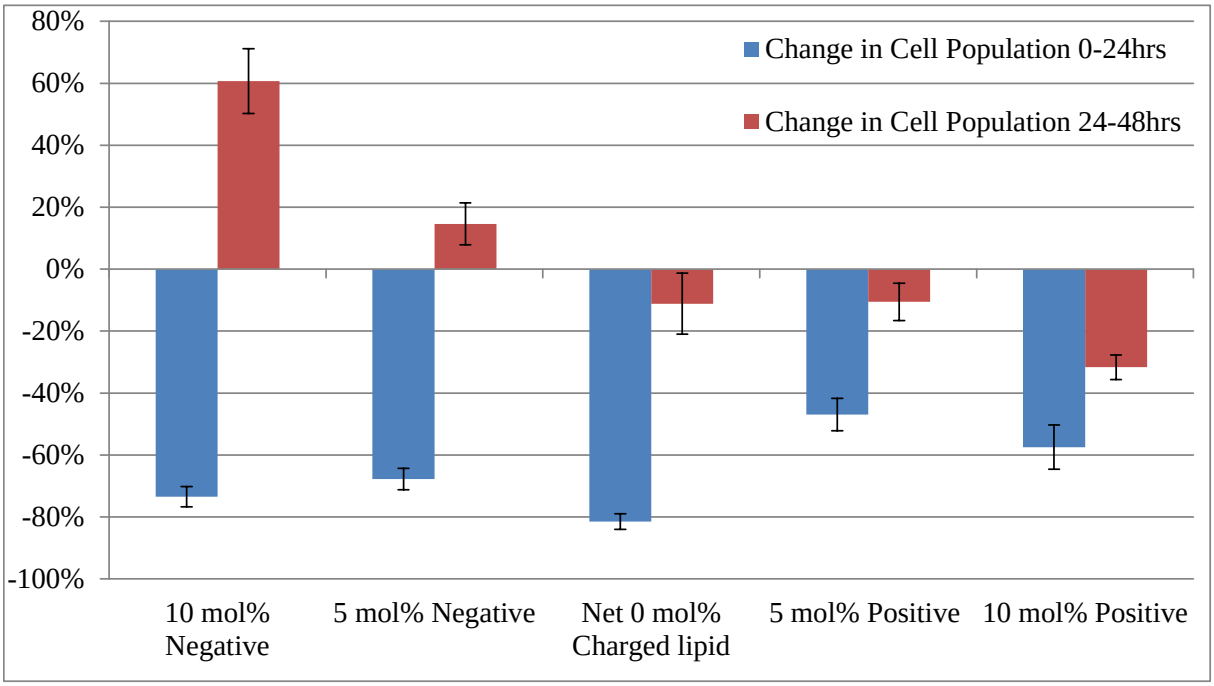

Figure 4.5.: Cationic lipid: DOTAP, Anionic lipid: DOPG: Proliferation percentage of cells adhered to charged bilayers from 24 hours to 48 hours, all bilayer substrates showed a decrease in cell numbers during the initial 24 hour period.

4.3.2.1) Proliferation: The determination of the proliferation rates for the cells grown on supported lipid bilayer substrates was undertaken in the same manner as for the control experiments. Namely each well was summed at each time point and compared to the total cell count from that well 24h previously. Over the first 24h time period almost all SLB substrates showed significant reduction in the number of cells counted. There are a number of possible reasons for this, none of which are directly apparent from these experiments. Firstly, this could be due to a mass migration of cell away from the fluid bilayer surface and toward the edge where due to the constraints of the experimental system we are unable to count them, this seems unlikely as there was still areas of cellular coverage at the 48h time period for all bilayer compositions. Secondly this could be due to mass necrosis of cells that are unsuitable for life on a SLB surface, leaving only those cells with the capacity for life in such an environment, this too

seems unlikely as the imaged cells are clearly capable of forming some number of adhesions which must be through the bilayer onto the substrate. Or thirdly, cells that were unable to adhere to the surface undergo necrosis leaving only those that were able to bind to the underlying glass substrate through bilayer defects. This hypothesis has some support in the literature where it was found that fibroblasts died when unable to form attachments on inert surfaces [304]. Despite the initial reduction in cell numbers there was some recovery observed in proliferation during the second 24 h period. Here the amount of charged lipids in the bilayer appears to have a major influence on the proliferation rates of the cells. The more negatively charged lipids present, the greater the proliferation. Surfaces with net positive charge appear to be incompatible with growth of 3T3 fibroblasts. This may be due to the fact that most cellular surfaces bear a negative charge

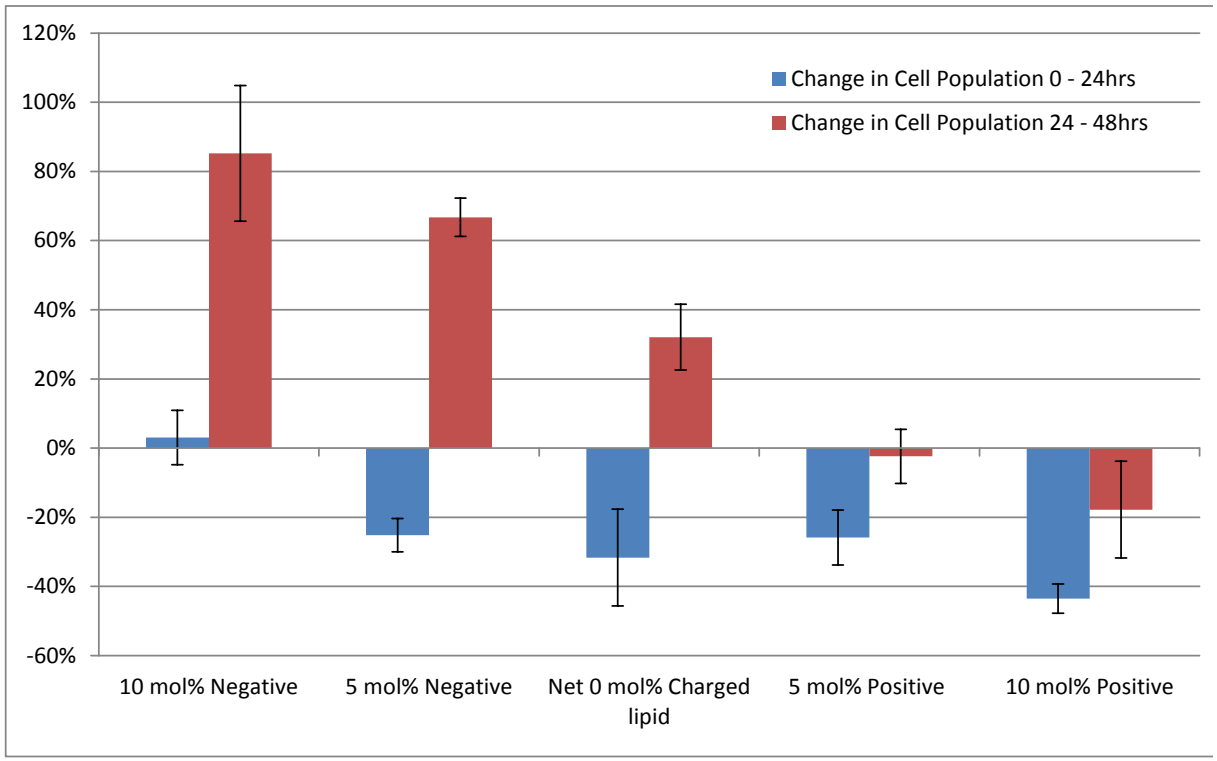

Figure 4.6.: Cationic lipid: eDOPC, anionic lipid: DOPS, the change in cell population is in general consistent with the previous charged lipid panel however there is some slight variations that may be explained by the lipid chemistry. In particular the net neutral bilayer now shows positive cell growth in the 24-48 h period.

and therefor the mechanisms for adhesion are optimized for this type of environment. Cytotoxicity studies for cationic lipids have seen that the charge in the lipid head group and its localization are major influences on toxicity. Where charge is concentrated in a single nitrogen atom, such as in an amine or ammonia (as in DOTAP) the lipid is more toxic, where the charge is dispersed in a heterocyclic ring the lipid exhibits lower toxicity [316]. The case for a lipid toxicity influence on adhesion can be made from the difference in the proliferation for the 'net 0 mol% charged lipids' bilayer for the two different bilayer compositions. At the 24-48h cell growth for the DOTAP containing bilayer the cells show negative growth. At the same time point for the eDOPC containing bilayer the cells show positive growth. In this instance the percentage of effective charged lipid in the two systems are identical but we see two very

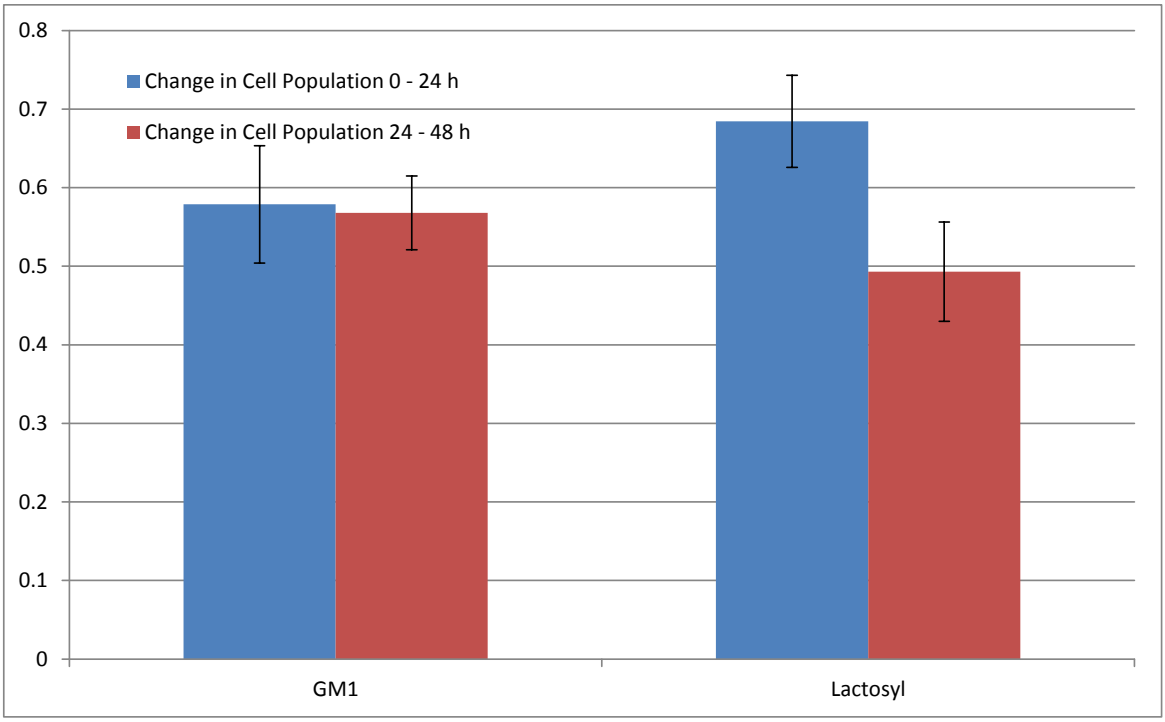

Figure 4.7.: Glycolipid Containing Bilayers: For cells cultured on SLBs containing 5 mol% of a glycolipid the cellular proliferation was seen to be steady for the GM1 enriched surface across all time points measured. While the Lactosyl enriched surface showed reduced population growth for the 24-48 h period. The effectiveness of glycolipid enriched surfaces is comparable to the collagenated surface typically used for cell culture.

different behaviors that can only be explained by the difference in the lipids in the bilayer. It should be noted that the change in cell numbers for the positively charged bilayers exhibit a large variation in cell counts and a corresponding large error range. This means that some caution must be taken when drawing conclusions based on this data.

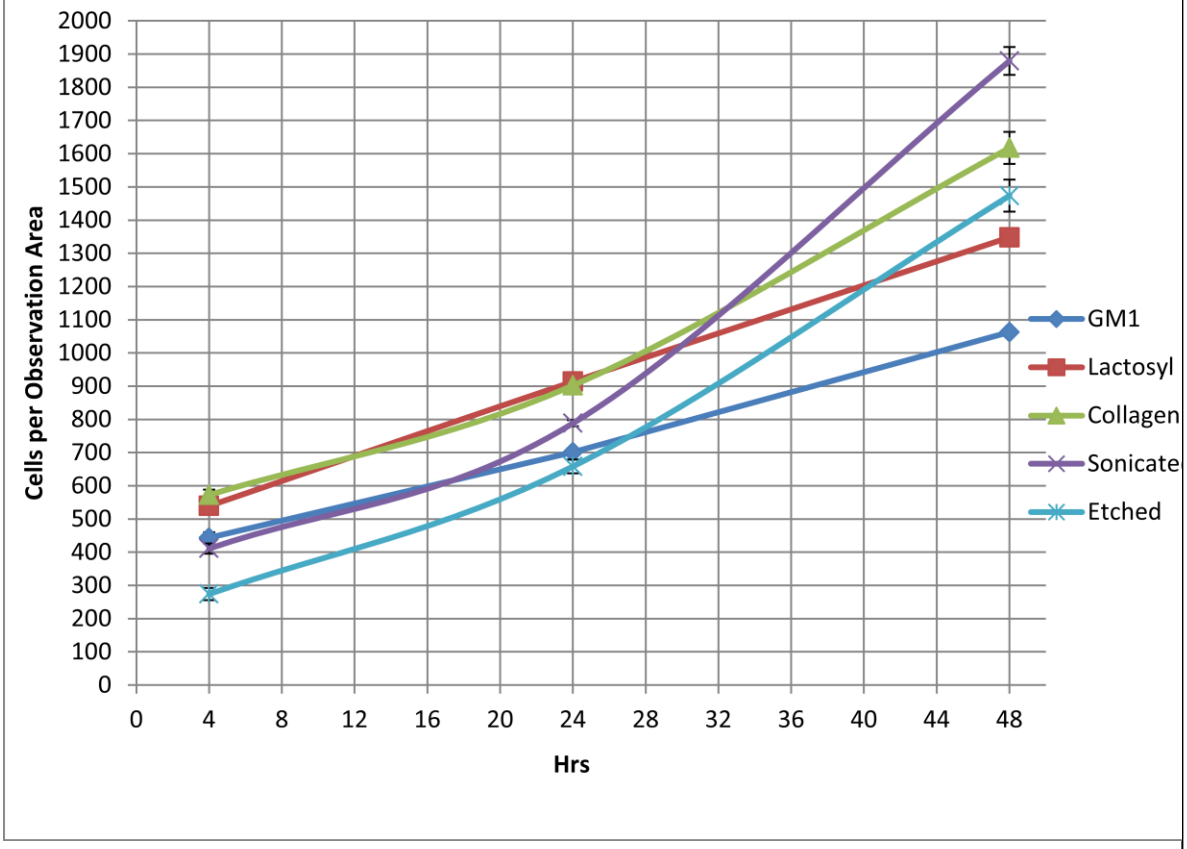

Figure 4.8: Day to Day average Cell Count per observation area: Solid Substrates and Glycolipid containing bilayers

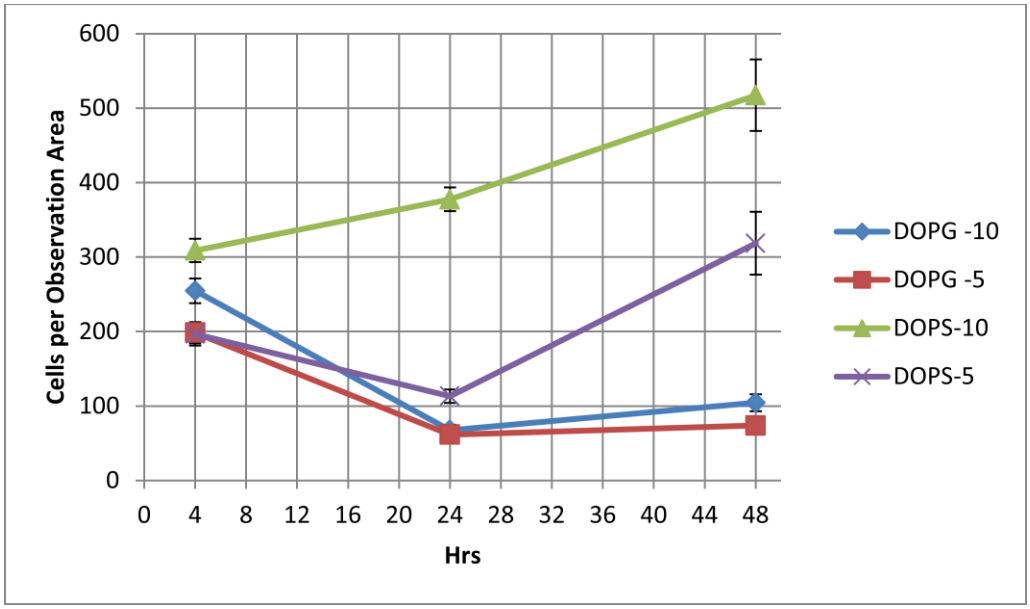

Figure 4.9: Day to Day average Cell Count per observation area: Negatively Charged Bilayers

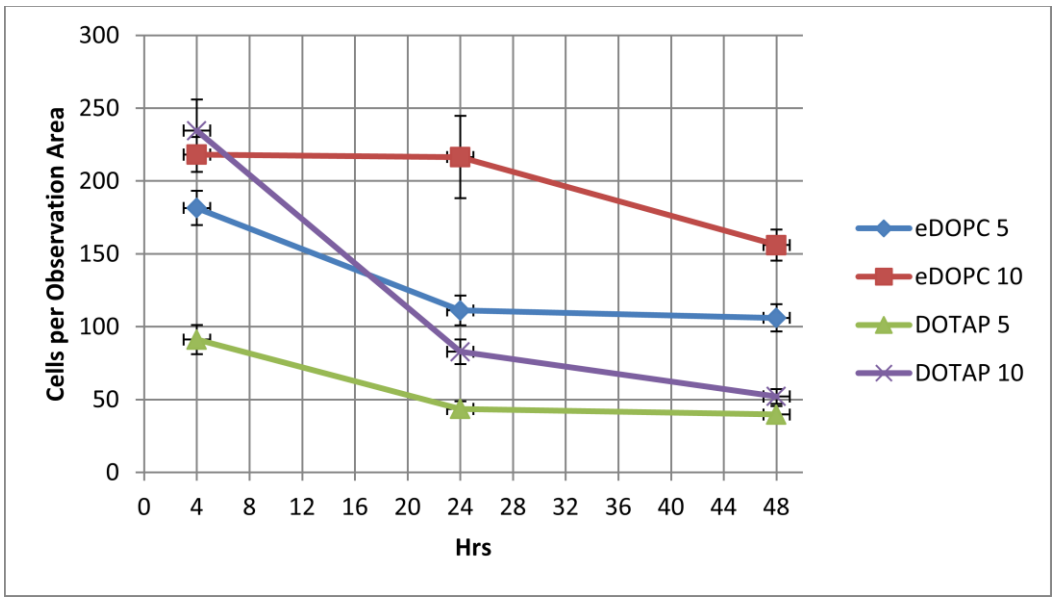

Figure 4.10: Day to Day average Cell Count per observation area: Positively Charged Bilayers

Glycolipids are commonly identified in the literature as being essential for cellular recognition and adhesion. In order to test this and investigate whether they can help functionalize a SLB we elected to include two commercially available glycolipids in our study. The effect of GM1 and Lactosyl-DOPE was significant (see Figure: 4.7.). The greatest difference between these surfaces and the charged bilayer surfaces was that there was no reduction in cell numbers at any point. In this respect the glycolipid enriched bilayers performed as well as the solid supports as a cell culture surface.

(a) 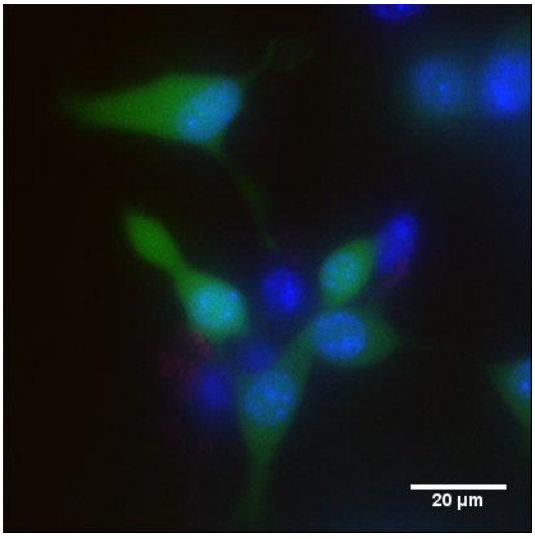

(b) 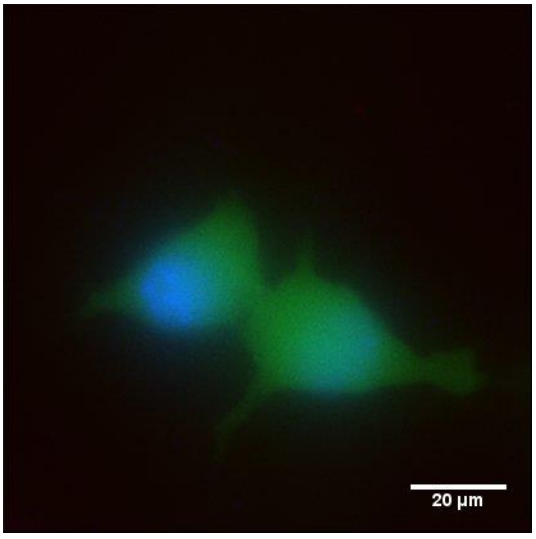

Figure 4.8.: Cells on 10 mol% negatively charged lipid bilayers (a) 24hrs and (b) 48hrs post seeding

(a) 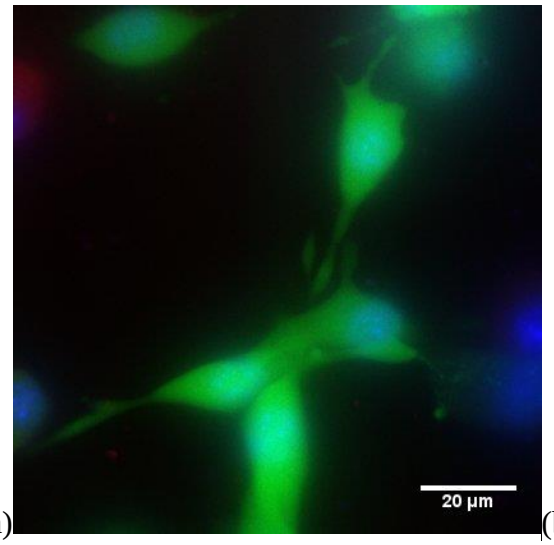

(b) 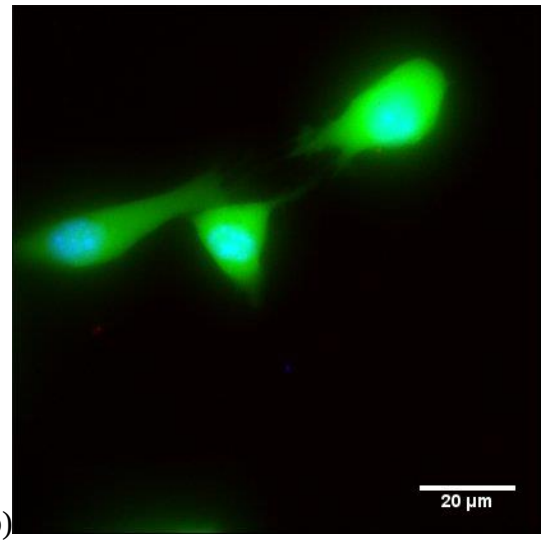

Figure 4.9.: Cells on 5 mol% negatively charged lipid bilayers (a) 24hrs and (b) 48hrs post seeding

4.3.2.1) Adhesion: Analysis of the proliferation data showed a clear preference for the more negatively charged lipid surfaces. A close examination of the cells and an assessment of their adhesion might elucidate the mechanism behind this preference. In figure 4.8. can be seen examples of cellular adhesion on the 10 mol% negatively charged lipids bilayer at 24 (Figure

(a) 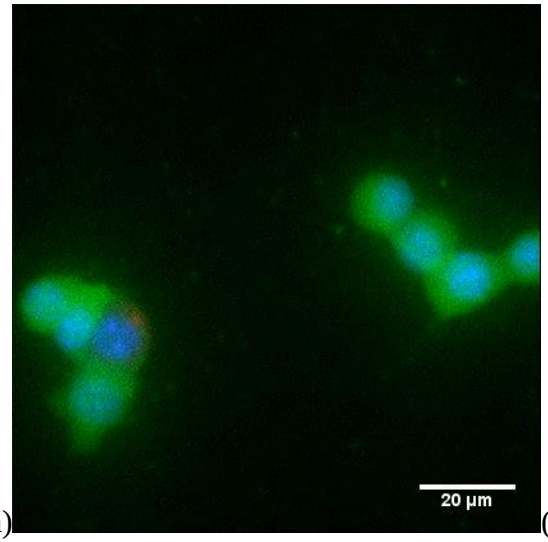

(b) 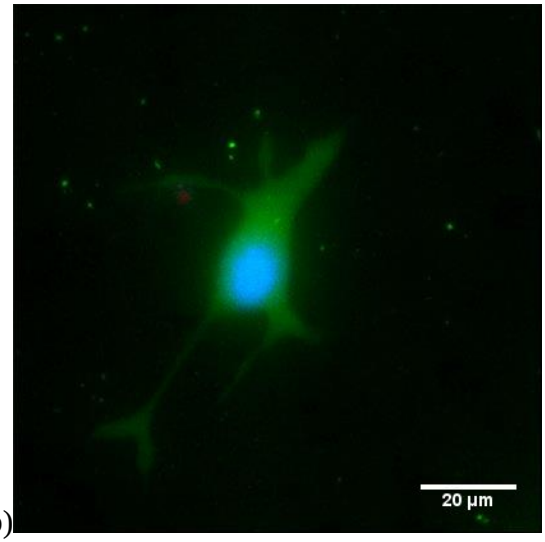

Figure 4.10.: Representative fluorescence images of 3T3 cells (nucleus in blue) on 0 mol% net charged lipid bilayers (a) 24hrs and (b) 48hrs post seeding

(a) 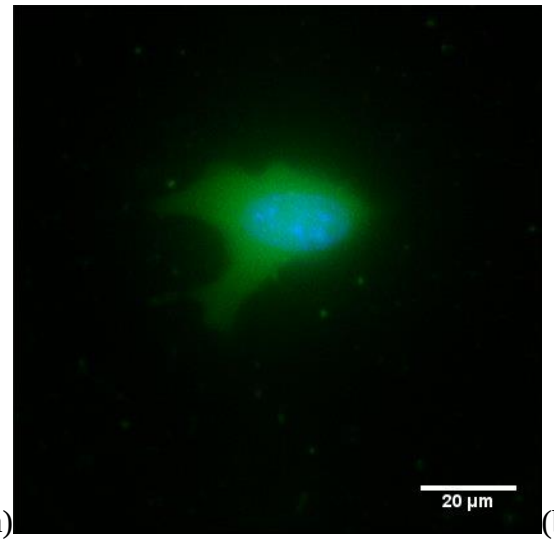

(b) 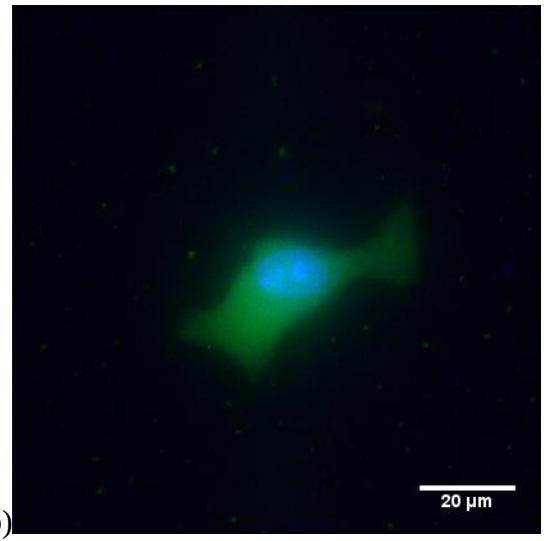

Figure 4.11.: Cells on 5 mol% positively charged lipid bilayers (a) 24hrs and (b) 48hrs post seeding

4.8.a) and 48 h (Figure 4.8.b) post seeding can be seen. Cells at the 24h time point appear to have had some trouble attaching to the surface as is indicated by the lengthy protrusions and the spherical aspect of many of the cell bodies. At the 48h time point the cells have taken on a more typical flattened profile similar to that seen in the solid supports indicating that they now have multiple points of adhesion. In Figure 4.9 we can see examples of cellular adhesion on the 5 mol% negatively charged lipids bilayer at 24 h (Figure 4.9.a) and 48 h (Figure 4.9.b) post seeding. Cells at the 24h time point appear to already have some adhesion points indicated by the presence of lamellipodia however there is also a spherical aspect to the cell body indicating still a certain lack of sufficient surface attachment. At the 48h time point the cells appear to have many more points of attachment as indicated by the presence of lamellipodia with multiple filopodia. In figure 4.10. we can see examples of cellular adhesion on the 0 mol% net charged lipids bilayer at 24 h (Figure 4.10.a) and 48 h (figure 4.10.b) post seeding. Cells at the 24h time point appear to have little to no attachment points with most of the cells showing no protrusions and a generally spherical aspect. At the 48h time point there appears to have been some development

in the number of attachment points but the cell body retains its spherical form. In Figure 4.11. we can see examples of cellular adhesion on the 5 mol% net positively charged lipids bilayer at 24 h (Figure 4.11.a) and 48 h (Figure 4.11.b) post seeding. This substrate had a sparse distribution of attached cells with very few multi cell aggregates. At 24 h and 48h the cells appear to have multiple attachment points but their form appears to be somewhat misshapen in comparison to the cells on solid supports. Cells appear to lack the directionality that is common to 3T3 cells, instead having multiple protrusions in disparate directions. . In figure 4.12. we can see examples of cellular adhesion on the 10 mol% net positively charged lipids bilayer at 24 h (Figure 4.12.a) and 48 h (Figure 4.12.b) post seeding. This substrate too had a sparse distribution of attached cells with very few multi cell aggregations. At 24 h and 48h the cells also appear to have multiple attachment points but their form appears to be misshapen. Protrusions are nonlinear and

(a) 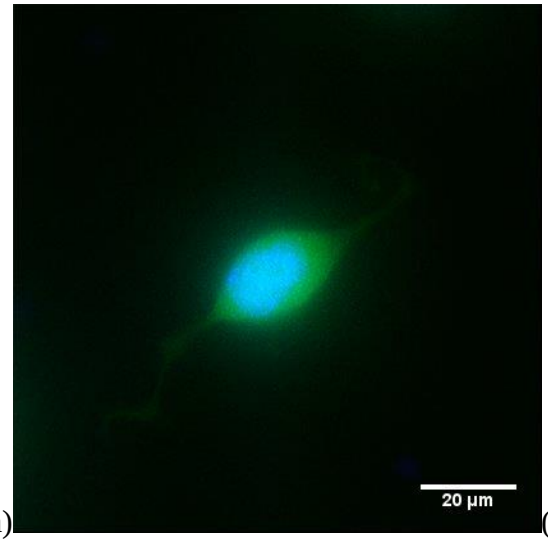

(b) 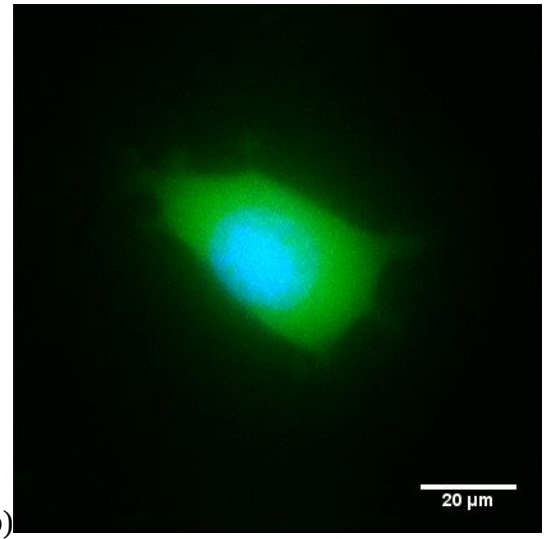

Figure 4.12.: Cells on 10 mol% positively charged lipid bilayers (a) 24 h and (b) 48h post seeding

in varying directions. While the morphology of the cell is helpful in determining the state of adhesion for some cells it is a highly interpretive method and is subject to huge variation between cells in any particular sample. The above images are representative of some of the morphologies seen but they are subject to the procedures of the fluorescent staining and its multiple washing steps which could have removed cells with weak attachment.

For the bilayers containing glycolipid surfaces the proliferation rates were found to be positive at all time-points. This can be seen reflected in the morphology of the cells which indicate multiple points of adhesion at both the 24 and 48 hour time points. For the GM1 containing bilayer the cells showed many of the same morphologies as seen on the solid supports with perhaps an increase in the number of long protrusion seen from the cells (see Figure 4.13.). In the Lactosyl-DOPE containing bilayers the cells showed a distinct increase in the number of

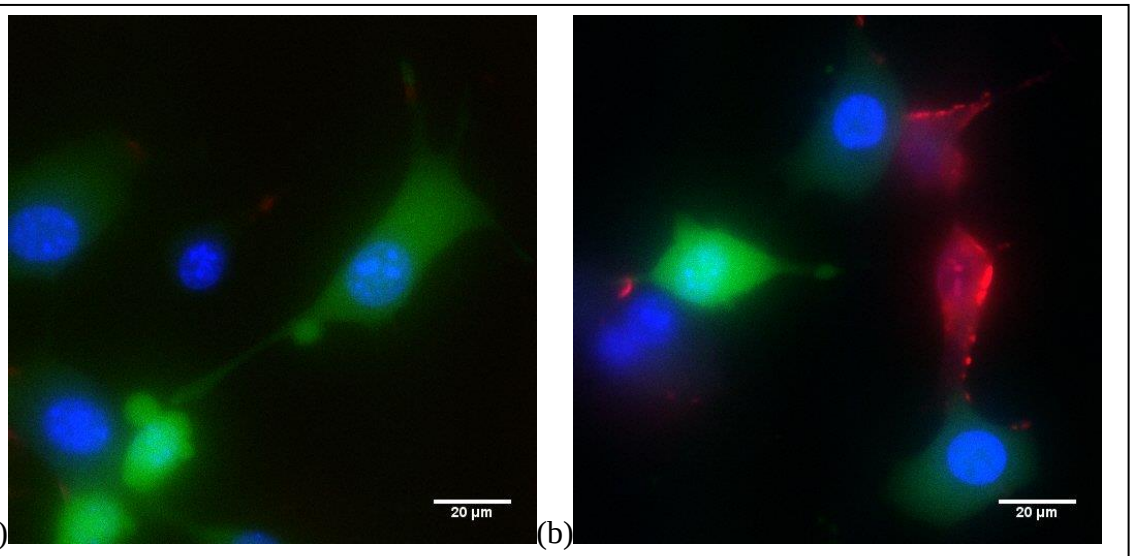

Figure 4.13.: 3T3 Cells on a 5 mol% GM1 glycolipid containing SLB. 24 h (a) and 48 h (b)

elongated protrusions (see figure 4.14.) which might suggest that they were unable to detach their adhesion points easily.

The capacity for 3T3 cells to form attachment points appears to be a major indicator of their proliferation rate. While it is without doubt that the negatively charged bilayers provided a more suitable foundation for cell growth it is not yet apparent what the precise mechanism for this behavior is. One thing that is of significance however is that this finding goes against those of researchers who have looked at charged solid surfaces. Previous studies have found that positively charged surfaces have higher cell adhesion and proliferation rates than negatively charged ones [317-320]. The form of the cells on the negative bilayers also most closely resembles that of the solid substrates, especially at the 48h observation point. This suggests that the cells are more capable of forming attachments through negatively charged surfaces while positive surfaces pose a more difficult obstacle for the cells. Given that cells present a slightly negatively charged plasma membrane in nature it seems logical that negatively charged biomolecules are something that the cells have some capacity to manipulate. It is possible that the positive charged lipids disrupt the mechanisms that the cell relies on to form adhesions and potentially some other processes such as protein kinase C activation as suggested in cytotoxicity experiments [321]. Study of the images of cells on positively charged bilayers shows a number of unusually shaped protrusions that have multiple angles and changes in direction. There is a possibility that these may be formed due to the fusion of the cationic supported lipid bilayer and the plasma membrane of the cell. Cationic lipids are used in liposomal drug delivery and in DNA transfection to identify and integrate with a cellular plasma membrane thus depositing the payload into the cell interior [322]

While the mechanisms behind these observations require further investigation, the effect of bilayer charge almost certainly has an influence on cell adhesion and proliferation. This knowledge has important implications for a whole host of biomedical applications. Bilayer composition can now be chosen to promote or inhibit cellular attachments. One possible use for this could be in the study of cell adhesion dynamics. Here a protein embedded bilayer could be developed such that the cell will form attachments with surface bound proteins that remain rearrangeable due to the fluidity of the bilayer. Lipid composition could be chosen to inhibit attachment of the cell thus leaving the proteins to rearrange freely and the dynamic reaction of the cell surface to be studied. There are also biomaterials implications where the simple choice between two lipids on a surface could help retain biocompatibility while either helping integrate the material with tissue or helping keep the material free of unwanted tissue growth. In the case of a cardiac stent for example, the exterior of the device would benefit from quality tissue

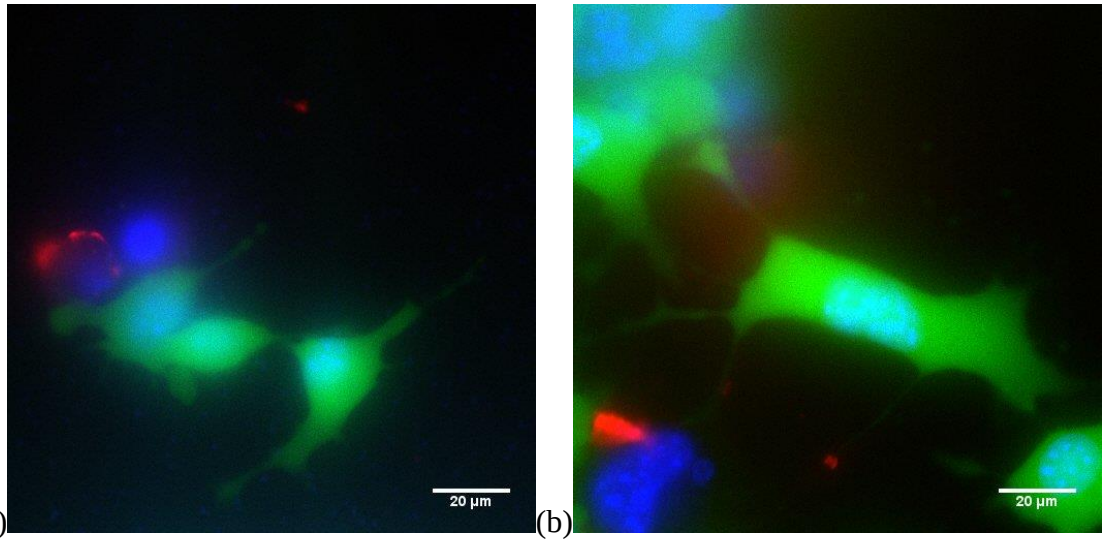

Figure 4.14.: 3T3 Cells on a 5 mol% DOPE-Lactosyl containing SLB 24 h (a) and 48 h (b). The cells generally showed multiple elongated and jagged protrusion atypical for a healthy fibroblast

adhesion while the interior of the device would benefit from a tissue preventing surface. The

addition of functional proteins and peptides to bilayer surfaces can add a wealth of utility to such a hybrid system. While we discuss the cellular proliferation of these systems it should be noted that the automated system only takes a cell count. There is no way to distinguish between an increase in cell number due to precipitation, migration, or proliferation. Given the experimental setup it seems unlikely that anything but proliferation and necrosis could account for the variation in the cell numbers.

This research opens the door to some interesting and useful applications. The possibility of developing bilayer compositions that induce different behaviors for distinct tissue types would permit the next stage in integration between biological tissue and man-made materials to take place. Enabling such development will be this work where we also established high throughput technology for rapid screenings of living cells on an artificial bilayer system.

Chapter 5, Minor Projects

5.1 Super-Resolution Imaging of Cellular Spectrin

5.1.1 Introduction

Historically the most versatile and accessible tool for the study of cellular and subcellular biological systems has been optical microscopy [169, 323-330]. Through the improvement of the optical components and the refinement of microscope design steady optimization of image quality, specifically resolution, had been possible for several centuries. The single constraining factor that has been restricting microscopy to advance significantly in the last decades is a fundamental property of light itself: namely that it is a wave. The fact that light is a wave means that when it passes through an opening that is approximate to the size of a wavelength or, more likely in a modern microscope, when it passes through an object with varying optical densities the wave will diffract. Diffraction is a result of constructive and destructive interference that alters the propagation of the wave. The consequential alteration in the light from a point-like light source as it passes through the microscope is known as the point spread function (PSF).. The diffraction of light from two point sources renders it impossible to distinguish the separate points when they are within a certain distance of each other. Ernst Abbe in 1873 determined this so called optical diffraction limit for a microscope to be :

$$d = \frac{\lambda}{2n\ sin\theta} \ldots Equ. 5.1.$$

Where d is the radius of a diffraction limited spot, λ = the wavelength of the incident light, n stands for the refractive index of the medium through which the light is travelling, and θ describes the angle of convergence of the incident light. In modern microscopy the properties 'n sinθ' are typically expressed as the 'Numerical Aperture' (N/A) of the microscope objective lens. Typical values for objectives with high resolving power are between 1.4 and 1.6 which produces a microscopy diffraction limit range of $d = \lambda/2.8$ to $\lambda/3.2$. It is also the case that these N/A objectives all rely on an immersion fluid in order to achieve a high refractive index, n. In contrast objectives that have air between the objective lens and the sample, n will be most equal to 1. Thus, their numerical aperture is limited to values smaller than one resulting in a much higher diffraction limit at the same wavelength. Visible light has a wavelength of roughly between 390 nm and 700 nm giving a maximum diffraction limit, for the lowest wavelength of visible light, of~ 121- 139nm. Thus, even assuming the most optimal conditions and hardware, it is impossible to resolve structures and features smaller than 120nm with conventional though-light microscopy. Yet a whole plethora of essential biological systems fall below this diffraction limit. For example; eukaryotic cell organelles and small bacteria (approx. 100nm), proteins (approx. 10nm) and lipids (approx. 1nm) all are impossible to resolve using traditional light microscopy.

In order to overcome this diffraction limit researchers have been developing a number of techniques. Certain non-optical techniques have been in use for decades. However, the downside with Atomic Force Microscopy (AMF) or Scanning Electron Microscopy (SEM) for instance is that they either require an environment that is incompatible with a cellular environment (such as the conductive coating required for SEM or the vacuum condition even for the most standard of electron microscopy techniques) or they have a very poor temporal resolution (such as the single line scanning speed in an AMF). In order to continue to take advantage of the benefits of optical

microscopy, such as large scale observations, biocompatible environmental conditions and high temporal resolution, researchers have developed light based systems that can overcome the diffraction limit. These 'Super-Resolution' techniques typically fall under two broad categories: those that actually permit image resolution below the diffraction limit, and those that (through clever manipulation of the light signal) effectively permit it [171]. Techniques that produce actual super resolution images typically use photon emitters that are themselves scaled below the diffraction limit or have an emission/depletion pattern that limits the light incidence in a similar manner[172, 173]. Techniques that provide effective super-resolution utilize properties of the fluorophore in order to produce single fluorescent events that can then be localized based upon the point spread function of the system. One effective super-resolution technique in particular is very accessible as it can be implemented without the need for optical or mechanical systems more specialized than a TIRF system. This technique is called direct STochastic Optical Reconstruction Microscopy, dSTORM. It uses flickering fluorophores on the molecule of interest to produce images where only a very few of the fluorophores are illuminated at any time. Over a few thousand frames of image capture different fluorophores should be in their 'on' state for each frame. These images can be then processed to localize each point source to its theoretical center. The super resolution image is created by assigning a single nano-scale pixel to each of the localizations. In order to perform dSTORM common cyanide based fluorophores such as Cy-5 or Alexa Fluor 647 are attached to the sample in the conventional manner. The sample is then placed in an oxidizing and reducing buffer system which enhances and prolongs the blinking. Following intense excitation from the light source, fluorophores can reach a triplet excited state. While in the triplet state the fluorophore is susceptible to reduction from the buffer system. This causes the fluorophore to enter a non-radiative 'dark' state for prolonged periods.

The oxidation of the fluorophore will cause the fluorescent state to be recovered releasing the photon. The buffer contains an oxidizing agent to rarify the environmental oxygen and therefore maintain the dark state of the fluorophores. The stochastic fluorescence of the dyes returning from the stable dark state allows individual fluorescent events to be captured with video fluorescence microscopy and localized to a position at the center of their point spread function. A super resolution image is constructed by the processing of thousands of frames of stochastic flickering of the fluorophores each of which is converted to one super resolution pixel.

The development and free distribution of techniques such as dSTORM have opened up a vast new realm of possibilities for the study of biological systems. One question that dSTORM can help to illuminate is that of the role of Spectrin in the membrane skeleton of non-erythroid cells.

Spectrin was originally identified in red blood cells where, in the absence of an actin cytoskeleton, it provided all of the mechanical strength of the cell. After its discovery it was believed to solely exist in erythrocytes, however soon new isoforms were identified in non-erythrocytes, these are known as Spectrin II, Calspectin, Brain Spectrin, and Fodrin. The most studied variety remains however that found in erythrocytes: Spectrin I.

Spectrin I is typically 200-260 nm in length and 3-6 nm in width and is the main structural component of the erythroid membrane skeleton [331]. In the red blood cell they form a heterotetramer which comprises two αI- and two βI-subunits arranged in anti-parallel, head to head α-β dimers [332]. In erythrocytes spectrin tetramers of αI- and βI subunits form geometric structures (40-42), while in non-erythrocytes no larger-scale organization beyond the Spectrin tetramers has been thus far identified. Spectrins can bind to a large variety of proteins either directly or indirectly. One such is ankyrin -which anchors spectrins to the plasma membrane via

a variety of membrane proteins [333-337]. Other examples include actin [338], certain lipids [339-341], tyrosine kinases [342], voltage-dependent sodium-channels [343], Tes and EVL [344].Most of our knowledge of Spectrin derives from studies on red blood cells. In stark contrast, the spectrin membrane skeleton in non-erythrocytes has been much less studied so far. However, in general it is assumed that spectrins underneath the cellular plasma membrane of non-erythrocytes organize also in tetramers where each dimer is formed by one α-II and one β-II spectrin [345, 346]. This non-erythroid membrane skeleton protects the plasma membrane [347], helps accumulate proteins and organizes the membrane [348] in such ways as coordinating ion exchangers [349, 350] adhesion molecules [351] and cytoskeletal elements [352]. Moreover, it is known that spectrin expression and regulation are important for fundamental cellular functions [353-355] and consequently spectrin mutations lead to a variety of human diseases such as Spinocerebellar ataxia [356] while knockdown of the non-erythroid αII-spectrin is in fact lethal [355].

Given the great structural importance and the fascinating geometry that Spectrin brings to erythrocytes, it is somewhat surprising that a large scale investigation into the distribution and formation of Spectrin in non-erythrocytes has not been thus far undertaken. Such work would be critical in recognizing the importance of Spectrin to non-erythroid cellular structure and motility. Having full knowledge of the extent of Spectrin prevalence and the nature of its structure will help in fashioning future investigations of cell motility as well as informing on basic cell physiology.

Utilizing the novel and powerful technique of dSTORM we endeavor to investigate how the Spectrin molecule is organized in a number of different cell types. Namely we investigate Spectrin distribution in NIH 3T3 murine Fibroblast cells and in murine cardiomyocyte cells with

the goal of resolving the structure of the spectrin based membrane skeleton in these cells on a nanometer scale.

5.1.2 Materials and Methods

NIH 3T3 Mouse fibroblast cells and adult mouse Cardio myocyte cells were grown in Dulbecco's Modified Eagle Medium (DMEM) from Life Technologies (Carlsbad, CA). Culture media was supplemented with 5% vol. penicillin streptomycin solution, and 10% vol. fetal bovine serum (FBS) also from Life Technologies (Carlsbad, CA).

Cells for imaging were cultured on a collagen coated 25 mm No.1 glass coverslip (Fisher Scientific, Hampton, NH). Once 70-80% cell coverage was achieved the cells were fixed for 2 h in a 3% formaldehyde solution, washed in phosphate buffered saline (PBS) and permeabilized for 1 h with a 0.5% solution of Triton x-100 surfactant from Sigma Aldrich (St. Louis, MO).

Primary immunostaining occurred overnight at 4^0C with a 1:60 dilution of the rabbit-anti mouse spectrin antibody (either anti-all spectrin isophorms, anti - α1 spectrin or anti-α2 spectrin, Abcam, Cambridge, MA) with 1% bovine serum albumin (BSA). Before the addition of the secondary antibody the sample was washed extensively in PBS. Secondary immuno-staining occurred for 1hr in a 1:25 dilution of the Alexa 647 goat anti rabbit in buffer. The sample was again washed extensively with PBS.

Storm buffer formulation was adapted from a protocol by Sauer et al [357]. Namely: 800 µL dilution buffer (50 mM NaCl, 100 mM Tris, pH 8.0),200 µL of 50% (m/v) Glucose,10 µL of beta-mercaptoethanol (BME),20 µL of Oxygen Scavenger (GLOX) solution (100 µL of dilution Buffer (see above),7 mg glucose oxidase, 25 µL of catalase (16 mg/mL)). Fixed and stained cells were placed in an Attofluor cell chamber (Life Technologies, Carlsbad, Ca) which was filled

with storm buffer. The sample chamber was immediately sealed with a glass cover to prevent additional oxygenation of the buffer from atmospheric sources.

Imaging for storm acquisition was undertaken through a modification of the TIRF (see section 1) excitation optics for the microscope. A 647 nm wavelength laser beam was incident on the sample at full power, approximately 1.4 W, for 10 - 15 seconds. This induced the photostable state in the fluorophores which began the stochastic blinking necessary for dSTORM. Following the initial high power exposure the laser was placed into a total internal reflection arrangement permitting high contrast imaging of the cells. In order to reconstruct a high quality dSTORM image it was essential to acquire a minimum of 10,000 frames of single fluorophore localizations. This necessitated the restriction of the detection area on the camera to in order to permit the processing of images at fast enough rates.

For dSTORM image reconstruction there are a number of different software options freely available on the internet. For our purposes we found that the rapidSTORM program available from Steve Wolter at the University of Wuerzburg [358] was the most suitable because of its ease of use and its support for the file types in use. Images were converted from their raw format into a multi-page tiff file. The experimental parameters are adjusted in the software and the reconstructed super resolution image is formed with a resolution (usually 3 nm per pixel which roughly corresponds to the location accuracy of a single stationary fluorophore under these conditions) specified by the user.

5.1.3. Results and Discussion

(a) 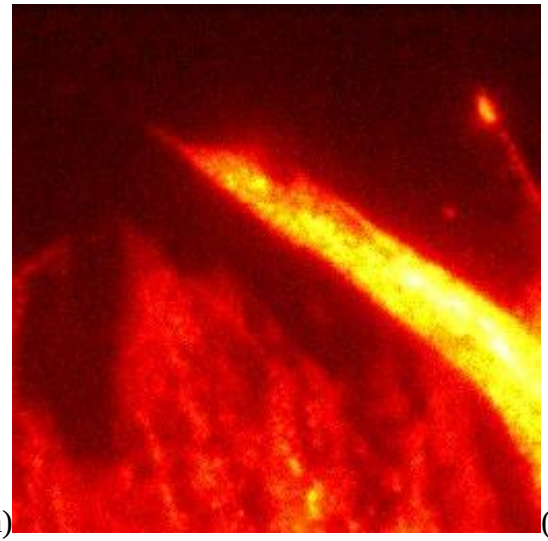 (b) 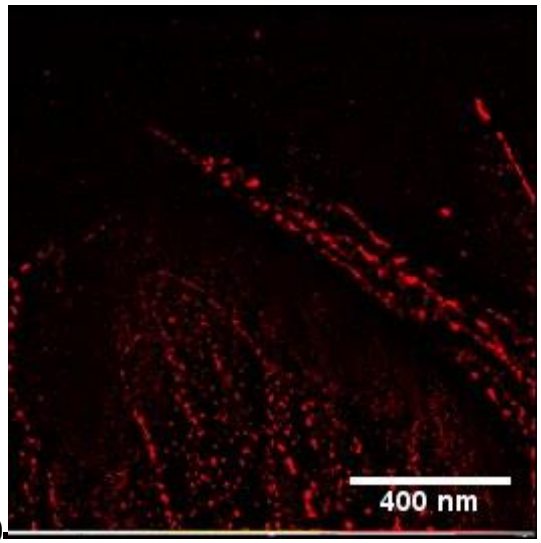

Figure 5.1.: murine cardiomyocyte with all spectrin isophorms labeled. (a) Standard epifluorescence 150x image. (b) dSTORM super-resolution image of same area. The scale bar applies to both images.

Super resolution imaging of the Spectrin in murine 3T3 fibroblast cells and murine cardiac cells revealed a highly pervasive and intricate structure. A number of different primary antibodies to label different spectrin populations were used: one that labeled all spectrin isophorms, one against α1 (a.k.a. erythroid) spectrin and one against α2 spectrin (i.e. non-erythroid). The presence of spectrin in almost all areas of the cell close to the lower plasma membrane was noted. One important first observation is made if the images in Figure 5.3. are compared to the 3T3 images in Figure 5.4.. It appears that when all spectrin isophorms are labeled, larger extended structures are visible. However, if only specific isoforms are labeled no such structures appear. Thus, one is left to conclude that an extended membrane skeleton, possibly one similar to the one of erythroids, is composed of a mixture of different spectrins. While there are of course many questions regarding the organization and function of non-erythroid spectrins awaiting

further probing, this work has significance in its own right as it has produced the first high resolution structural images of the spectrin network in conventional non-erythroid cell lines.

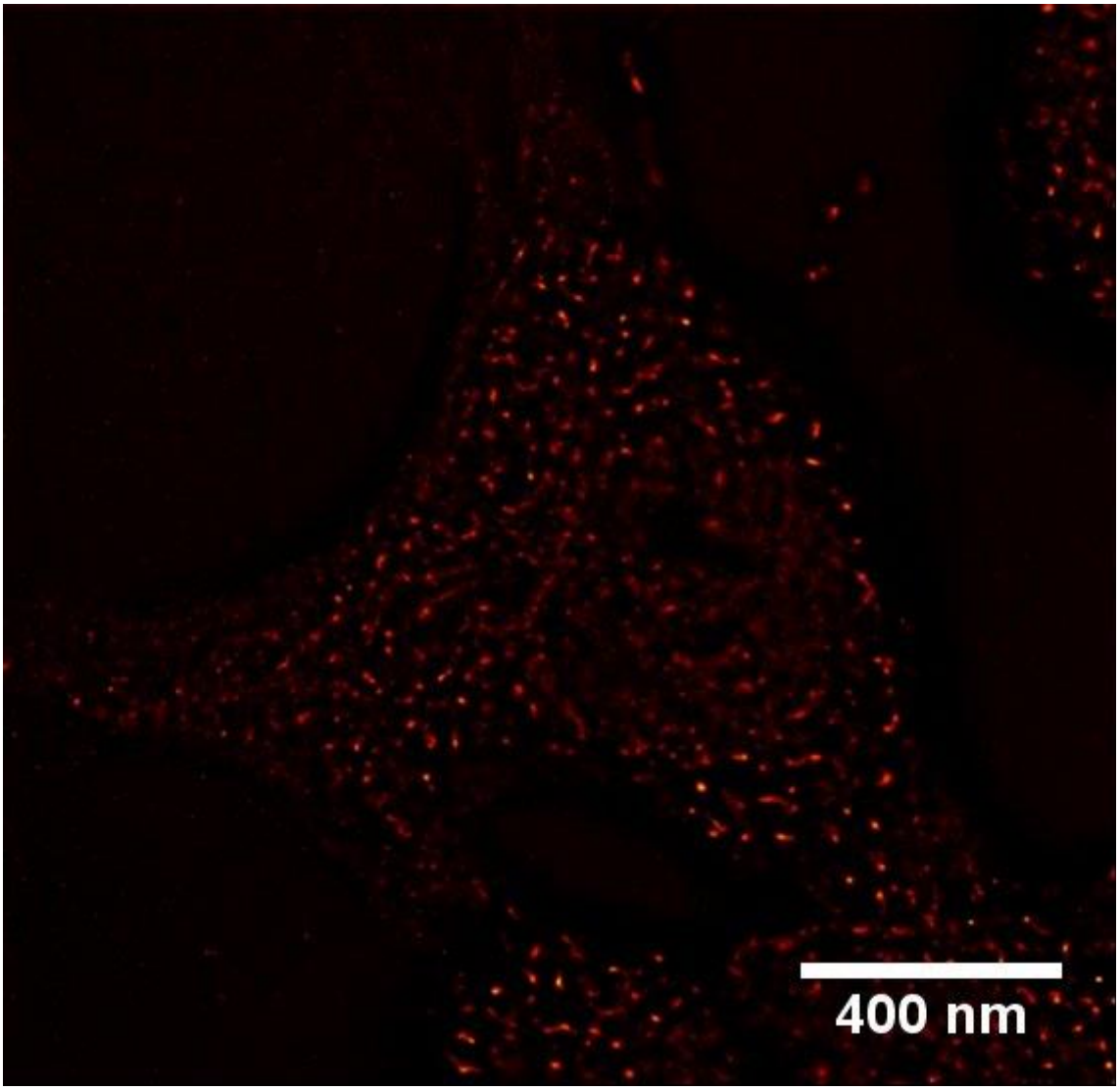

Figure 5.2.: A 3T3 cell with all spectrin isophorms labeled. The protein is widely distributed and it appears that the spectrins form larger, extended structures, possibly similar to the non-erythroid membrane skeleton.

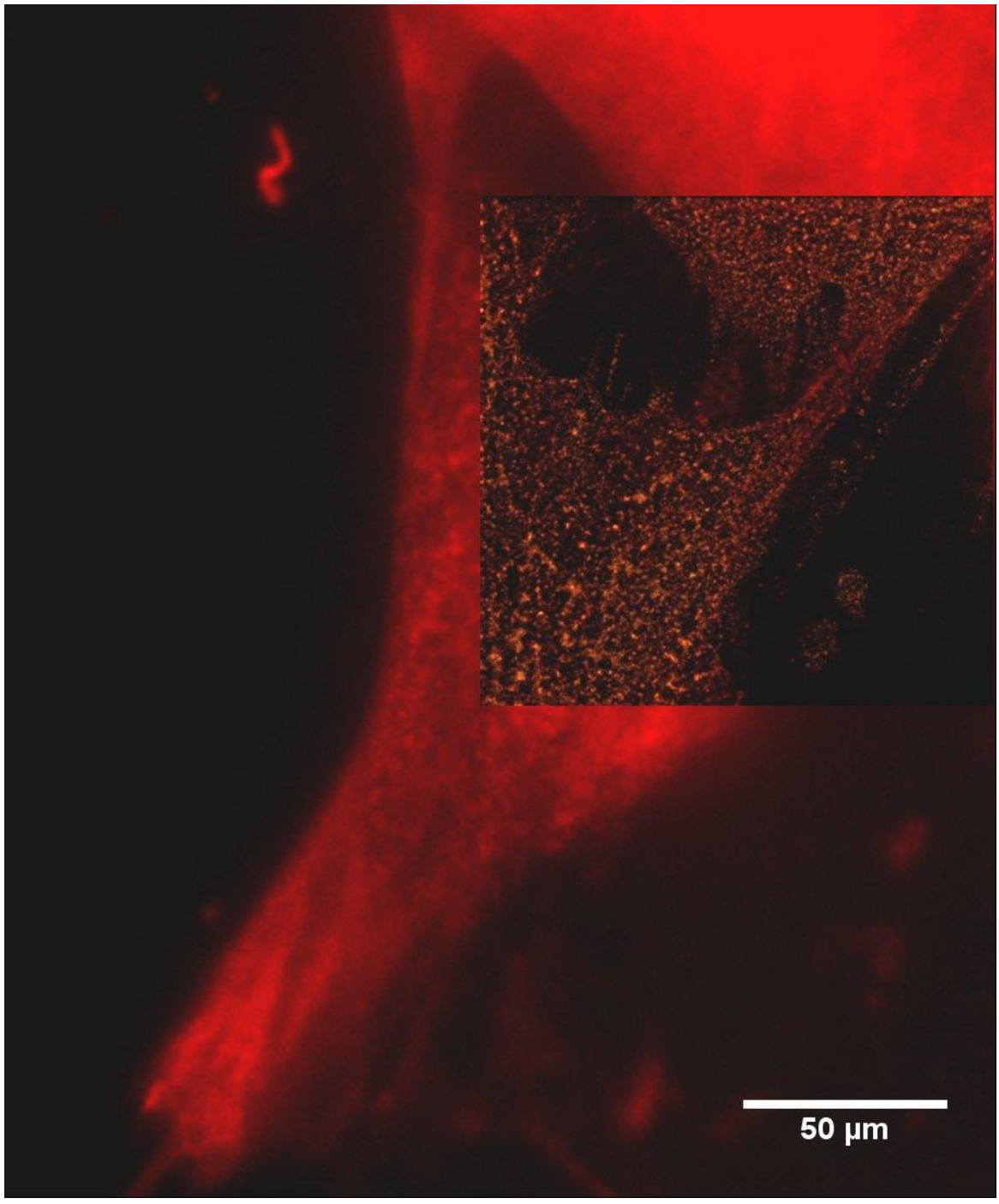

Figure 5.3.: The Power of dSTORM: A mouse Cardiomyocyte is shown under high magnification Epifluorescence imaging (main picture) and under dSTORM super-resolution imaging (inset).

5.2 Hybrid Lipo-Polymer cell substrate

5.2.1 Introduction

The Fluid Mosaic Model proposed by Singer and Nicholson in 1972 laid out the basis of our understanding of the basic dynamics and structures of cell membranes. It is now generally accepted that cell membranes are composed of a bilayer of phospholipids with proteins dispersed throughout. The lipids have the ability to freely diffuse laterally throughout the membrane while being constrained to the plane of the membrane. See chapter 1 for a more in-depth discussion of cell membranes and their structures.

In-vivo studies of lipid bilayers have presented copious difficulties as cellular surfaces are vastly complex. Consequently the behaviors of individual lipids or proteins are hard to observe and track, and well controlled studies are challenging. A common technique to simplify the system is to place compositionally controlled lipid bilayers on glass substrates. This methodology allows for a close control of the specific lipids in the bilayer while maintaining bilayer fluidity. In

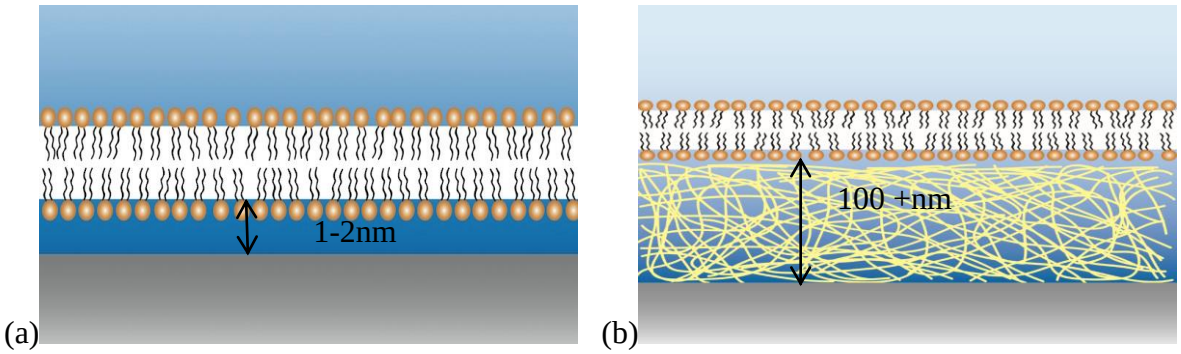

Figure 5.4.: Polymer Supported Bilayer: (a) A schematic of a typical solid supported lipid bilayer. (b) A schematic of a polymer supported lipid bilayer

studies of cellular systems the gold standard for any experiment is to make an observation of a behavior in a living cell. It would be highly advantageous to researchers to be able to add complexity to a supported lipid bilayer in order to induce behaviors in a live cell. Incorporating proteins, peptides or transmembrane chemical gradients to a supported lipid bilayer would massively increase their potential and functionality. A major drawback of solid supported bilayers is that the bilayer is placed within 1-2nm if an inflexible SiO_2 substrate. This proximity automatically prohibits the incorporation of a large number of membrane associated proteins that have a transmembrane element as any protein part extending into the space between membrane and glass will rapidly denature onto the substrate, thus render it dynamically trapped and biologically often defunct. Further, the rigidity of the substrate prevents the dynamic deformation of the bilayer in response to cellular action. If we are to more closely mimic an organic cellular plasma membrane then a more flexible alternative to the solid supported bilayer is needed that also mechanically starts to mimic the actual cellular surface more closely. One promising avenue for development is in using various polymers as a membrane support. Polymer supports can be controlled in such a way as to permit sufficient space for transmembrane proteins, they can be controlled for elasticity, and they can allow for fluid exchange in the space below the bilayer permitting chemical gradients across the membrane. While the possibilities for polymer supported bilayers are vast, the technology is still in its relative infancy. In order to develop future systems it is necessary to characterize some of the basic behaviors of lipid bilayers on polymer substrates. One of the most fundamental properties of a lipid bilayer is its fluidity: the average rate of dynamic diffusion of individual lipids. Variations in fluidity can lead to such behaviors as phase separation, selective protein binding, and control of some membrane dependent signaling systems.

A popular biocompatible polymer is polyacrylamide (PA), PA will form a hydrogel when acrylamide strands are cross-linked with bis in an aqueous environment. The mechanical properties of the gel can be controlled by regulation of the ratio of polymer to crosslinker as well as the liquid fraction of the system.

In this study we attempted to ascertain if there is a relationship between the average pore size of a polyacrylamide gel and the diffusion rate of a phospholipid bilayer deposited on the gel. Gel porosity was ascertained from the work of N.C. Stellwagen [359].

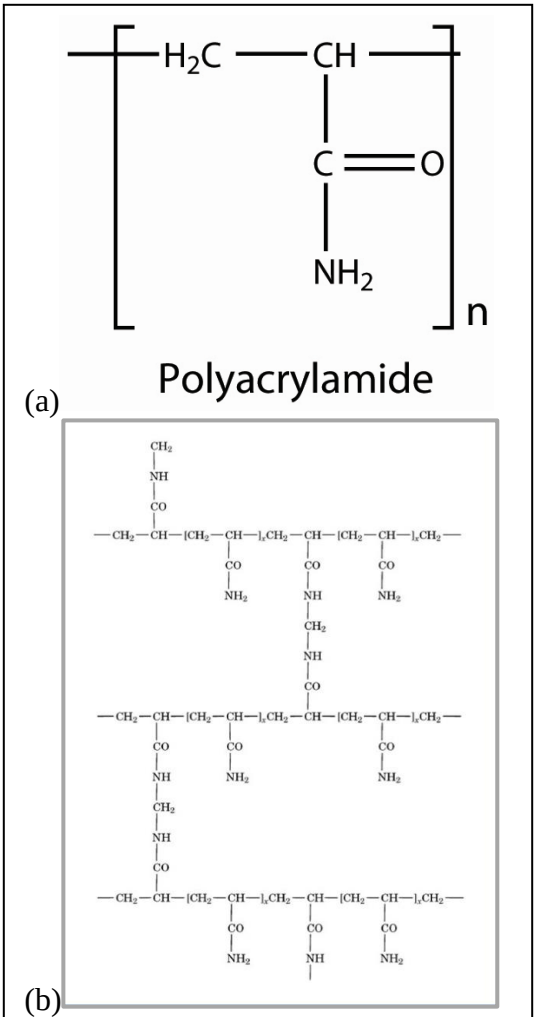

Figure 5.5.: Polyacrylamide (a) Polyacrylamide will crosslink with Bisacrylamide to form a hydrophilic polymer gel (b)

5.2.2 Materials and Methods

Materials: 1,2-dioleoyl-sn-glycero-3-phosphocholine (DOPC) and 2-(4,4-Difluoro-5-Methyl-4-Bora-3a,4a-Diaza-s-Indacene-3-Dodecanoyl)-1-Hexadecanoyl-sn-Glycero-3-Phosphocholine (β- Bodipy fl C_{12}- HPC) were purchased from Avanti Polar Lipids Inc. (Alabaster Al.). Acrylamide solution (40%) and bis-acrylamide solution (2%) were purchased from Fisher Scientific (Pittsburgh Pa.).

Fluorescence excitation was produced using a Spectra Physics (Mountain View, Ca.) tunable gas Laser. Signal acquisition was carried out using two Perkin Elmer (Waltham Ma.) avalanche

photo diodes connected to a Picoquant (Berlin, Germany) Picoharp 300 hardware correlator. Data processing was done using PicoQuants SymPhoTime software and in-house developed software.

Methods: Polyacrylamide (PA) gels were prepared by combining predetermined amounts of the stock solutions of acrylamide and bis with DDI water to achieve a desired total solids concentration %T (w/v %) and a cross linker concentration %C (w/w%). An accelerant (TEMED) and a catalyst (ammonium persulphate) were added to initiate the polymerization reaction. Following preparation of the PA substrate a lipid bilayer was deposited using the hybrid Langmuir-Blodgett/Schaeffer as described in chapter 1. Fluorescence Correlation Spectroscopy (FCS) was used to measure the diffusion rate of fluorescently labeled lipids. It uses the fluctuations in observed light signals from fluorescent molecules, as they pass in and out of a focused laser beam, to calculate their diffusion rate and concentration. Measurements were taken on a PA-supported lipid bilayer. The deposited bilayer consisted of 0.1 mol% β- Bodipy fl C_{12}- HPC, 99.9 mol% DOPC.

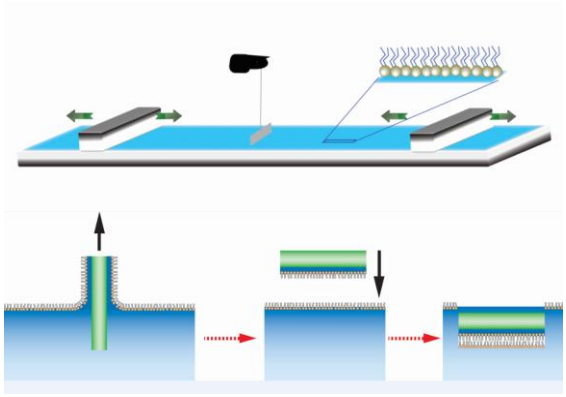

Figure 5.6.: Bilayer Deposition: Once a PA gel is prepared two lipid monolayers are deposited using the Langmuir- Schäfer technique on a Langmuir film balance to form a bilayer. Lipid composition of the bilayer is thus easily controlled

5.2.3 Results and Discussion

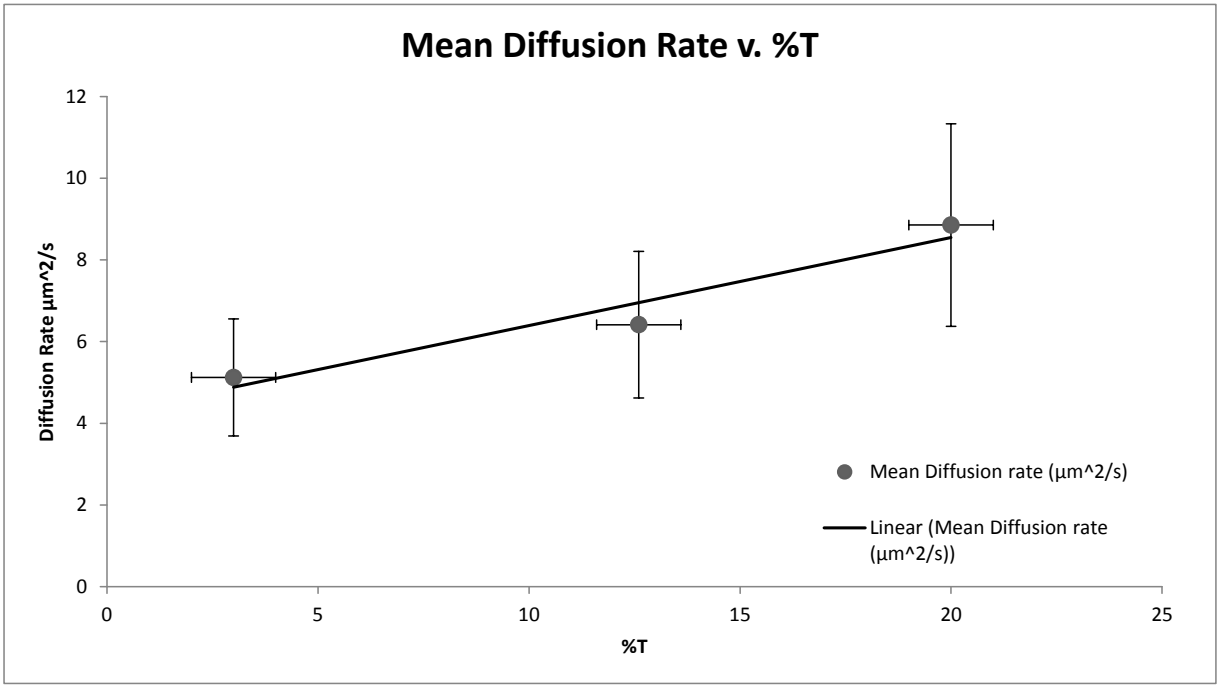

Figure 5.7.: Diffusion Rate V. Pore Size: stable and intact PA supported bilayers proved difficult to produce; the few dependable results seem to indicate a relationship between increasing %T (and therefore decreasing pore size) and increasing diffusion rate. However, the number of data points (N=7) are too small to be dependable

PA-supported lipid bilayers proved more difficult to produce than first estimated. After multiple attempts to produce stable fluid bilayers only a handful of successful results were produced. The measured corresponding diffusion rates are graphed in Figure 5.8.

There appears to be a correlation between increasing %T (and therefore decreasing pore size) and increasing diffusion rate. However, with only seven successful measurements it appears premature to draw solid conclusions.

When bilayers failed to form there was evidence of fluorescent lipid micelles diffusing in the aqueous phase. These are byproducts of failed bilayers but nonetheless can tell us something about the surface to which they did not adhere.

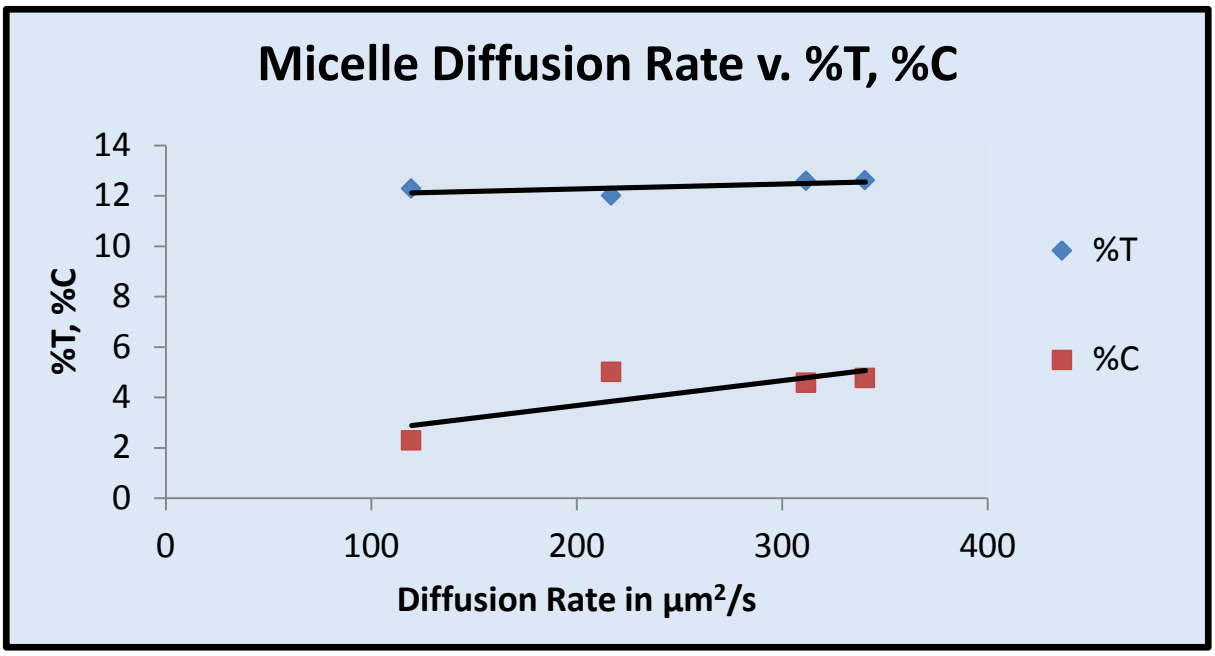

Figure 5.8.: Micelle Diffusion Rate: Floating micelle diffusion rate from failed bilayer depositions appears to bear a slight dependence on %C (mass of Bis Crosslinkers) as opposed to %T

Figures 5.9. and 5.10. show the diffusion rate with respect to polymer composition as well as

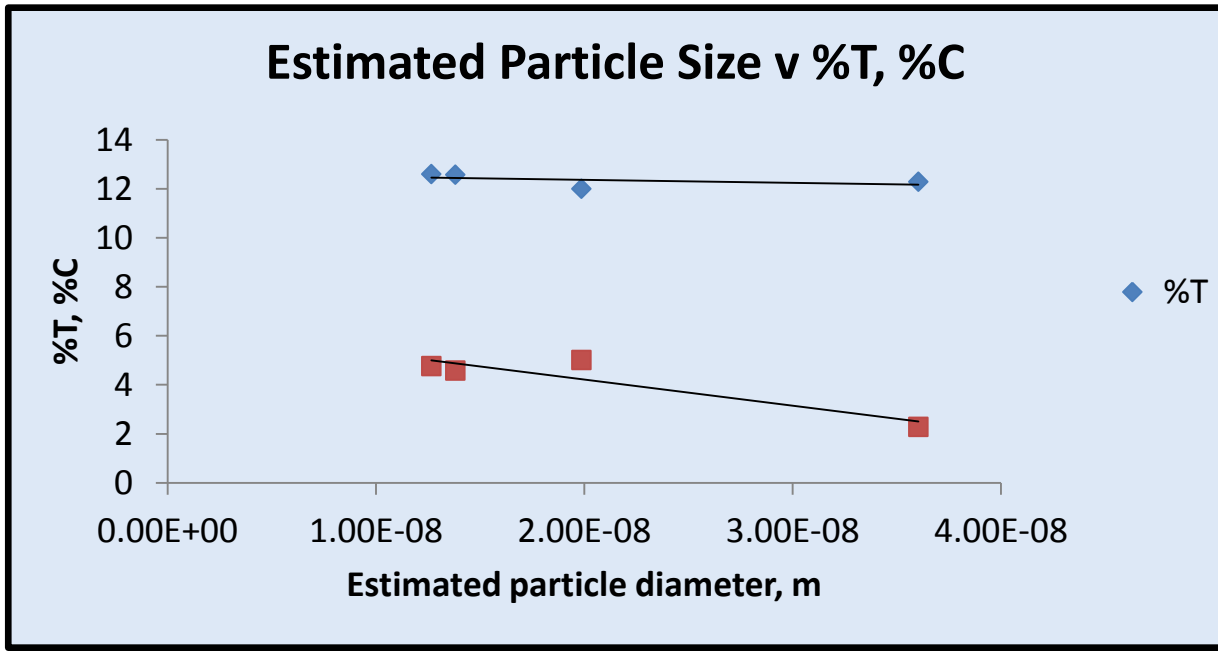

Figure 5.9.: Particle Size Estimate: Micelle diameter was estimated from the diffusion rate using the Stokes-Einstein equation for the Brownian motion of a spherical particle. It appears that particle size decreases as the cross-linked ratio increases

estimated micelle size (determined using Stokes-Einstein theory for Brownian motion of spherical particles in aqueous solution). Here it appears that %C has a greater effect on the system.

We had hoped to see that with increasing %T, %C there would be a decrease in pore size of the gel and a corresponding change in lipid diffusion rate. Results were suboptimal due to unsuccessful bilayer formation. This difficulty may have been because of the structure of the polymer surface; too-large pores may have not provided sufficient scaffold to support a bilayer and instead facilitated micelle formation. This mechanism is supported by the dependence of the micelle diffusion rate and estimated size on the polymer composition.

Attempting to follow exact protocols from reported PA supported bilayer studies proved unsuccessful. Future studies may include alternative bilayer deposition techniques, varying %T, %C concentrations, examination of the gel surface, and exploring alternative polymers.

Chapter 6: Discussion and Conclusions

6.1 General Discussion

Biological membranes have shown themselves to be highly sophisticated and intricate entities. In this work I have developed a multifaceted experimental approach to advance both our understanding of these systems and their utility as manufactured interfaces. This dissertation takes into account a number of diverse projects that share the common aspect of all focusing on the lipid based biological membrane. The membrane is so vastly complicated and holds so much potential for interesting applications that it will surely be studied for many decades or even centuries to come. This work makes a small attempt at developing some of that potential for interesting applications while also trying to illuminate one of the more interesting signaling problems currently being studied.

6.2 PIP_2 Dynamics

The investigation into the dynamics of PIP_2 at physiological Ca^{2+} concentrations illuminates a very important cellular signaling system and provides evidence for a previously only theorized molecular organization in the bilayer. We saw that the minute quantities of Ca^{2+} that are found at physiological conditions are indeed capable of altering the behavior of PIP_2. The most interesting finding however was what appears to be preexisting diffusion retarding microclusters between the highly anionic PIP_2 and the zwitterionic DOPC. This mechanism cold have the property of restricting the PIP_2 to a certain region of the cell membrane when Ca^{2+} levels decrease (and stop screening the interaction) and then when the Ca^{2+} levels increase

beyond a threshold of approximately 200 nM the PIP_2 are freed to diffuse more freely and perhaps even form areas of enrichment at high enough calcium levels. This dynamic rearrangement of the phospholipids due to a simple increase in ion concentration provides an interesting insight into its function within the cell but it could also lead the way to a new method of active control of the dynamic properties of bilayer constituents. This would follow in the footsteps of almost all of the biological tools we have in use today: once a system is understood enough it can then be co-opted for alternative uses (such as fluorescent proteins, immunostaining, and nucleic acid transfection). The PIP_2 phospholipid has a rich potential for novel and varied artificial applications as it has such an abundance of functions in nature (see chapter 2) binding upwards of 280 different proteins [35]. Of particular note in this work is that the behavior of PIP_2 was characterized for physiological conditions, a situation that is critical for *in vivo* uses. If full integration is to be made with a biological system then the basic conditions for life must be met. The high negative charge of PIP_2 due to the three phosphate groups in its amphiphilic region also has the potential to make it a versatile reaction point in the bilayer

The work on PIP_2 will continue for many years to come as the many biological functions of this molecule are just now becoming apparent [360-362]. This experimental series could benefit from a two-color fluorescence cross correlation spectroscopy (FCCS) study [231, 363, 364]. Here PIP_2 lipids with spectrally separate fluorophores on their hydrophobic regions would be observed as they diffuse in varying calcium environments. If the lipids move together they will have positive correlation in the cross color correlation curve. This would permit the precise pinpointing of the onset of aggregate formations. The work could also be expanded to include a PIP_2 with one fluorophore and a PC lipid with a spectrally dissimilar fluorophore on its acyl chain. This would again show it there is indeed coordinated movement between the two lipid

species. The incorporation of cholesterol into the system would also test whether any clusters are robust enough to exist in a membrane system that more closely resembles the plasma membrane [365-367].

6.3 Aldehyde Tag

With the long term goal of producing fully interactive, lipid bilayer based biological interfaces there is always a need to add functionality to the system. In this study we showed that the site specific genetic placement of an aldehyde on a protein can be an excellent tool to add a hydrophobic lipid domain to an arbitrary location on the protein. We determined a successful protocol for the modification and attachment of both N and C terminus of an EGFP, showing that the integrity of the protein remained intact as did the fluidity of the bilayer it was anchored to. The success in these two factors proves that this is a valid, completely novel protein lipidation technique. The aldehyde tag system has the potential to become the new standard for protein anchoring as it lacks the many drawbacks that other protein/bilayer attachment systems have . The versatility of the system comes from the potential for specific placement of the aldehyde and the potentially large choice of anchoring lipids. The development of a genetically encoded protein lipidation point promises to enable the combination of the properties of both the lipid and the protein which could lead to numerous exciting applications in the future. As a first endeavor, the temperature dependent demixing of certain lipid species could be exploited to show that protein distribution on the bilayer surface can be controlled at will. This demixing could be expanded to produce regions of enrichment on a surface by control of the lipid species and the patterning of the substrate. The findings of the PIP_2 research could also be brought to bear in the reorganization of proteins on a lipid bilayer substrate. Here the ionic environment (i.e. Ca^{2+} concentrations) could directly feedback into a rearrangement of proteins on the surface, perhaps

producing a reaction from a cell in close contact. This work is not limited to proteins however, peptides could also be modified to bear the genetic marker and thus covalently bonded to a lipid. This would permit the formation of peptide bearing bilayers where the peptide could be cross-linked to increase the durability and the resilience of the bilayer surface, while retaining the biocompatibility and protein resistance of a lipid bilayer.

6.4 Charged Lipid Bilayers

The often touted potential for lipid bilayers as biological interfaces has not, in fact, received the in-depth investigations that would enable their widespread uptake as a cellular culture/investigation platform. We introduced a novel, high throughput technique to investigate lipid bilayer supported cellular growth. The parallel investigation of 24 separate cell/bilayer systems permitted the application of statistical analysis in a way previously rendered impossible by the logistics of such a task. This allowed the natural variations of a biological system to be overcome. By studying the impact of charged lipid concentrations on cellular proliferation a new possibility for phospholipid bilayer induced tissue control has been discovered. This work has shown that 3T3 fibroblast cells have a strong preference for a bilayer surface with greater concentrations of negatively charged lipids; the presence of positively charged lipids appeared to be incompatible with 3T3 existence. Further we have shown that the presence of physiological concentrations of GM1 or Lactosyl-DOPE glycolipids produced a lipid bilayer surface capable of cell growth as high as any solid substrate investigated. We have shown that through careful selection of the constituent lipids in a bilayer the surface can be made to promote or discourage cellular adhesion. This opens up some exciting possibilities for surface treatments of medical implants where the lipid bilayer would provide a biocompatible surface that would encourage or discourage cellular growth as desired. This work should also be beneficial to researchers using

supported lipid bilayers as substrates to investigate living cell behavior. To continue on with this promising investigation it would be prudent to expand the investigation into other cell lines. Osteoblasts, Smooth muscle cells, and epithelial cells would all be excellent candidates due to their proximity to common medical implants. Further, while the charge of the lipids appears to be the major factor in the cellular response, there also seems to be some dependence on the chemistry of the lipid head region. An investigation into the response of different cells to different bilayer compositions would pave the way for surfaces that can encourage the growth of one particular cell type while hindering others.

6.5 Outlook

While each of these projects deserved to be studied simply based on their own merits, it is when they are taken as a whole that they become significant. It is at the intersection of the disciplines required to conduct this research that the next major steps in our understanding and capacities will come. It is also at the intersections of these types of investigations that the interfacing of artificial materials and organic tissues will become possible. In combination these studies represent a meaningful advance in the theory and utility of lipid bilayers in nature and in application.

6.6 Case Study: Stents

In order to directly outline the applicability of these investigations a case study will be briefly discussed. For this purpose I have chosen to look at medical Stents. A Stent is a tube placed in the body with the purpose of enlarging or creating a passage. The most common form of stent, and the one to which I will be referring henceforth is the cardiac stent. Currently the state of the art is polymer coated drug eluting stents, these contain a therapeutic agent within the pores of the

polymer that get released either through free diffusion or through degradation of the polymer. The purpose of the drugs is to prevent the growth of smooth muscle cells into the luminal space to prevent restenosis- the re-narrowing of the blood vessel. The major drawback to such a system is that the drugs also prevent the growth of the epithelium without which the site is never truly healed. This leaves the area susceptible to the aggregation of platelets and the formation of thrombosis which can have terrible consequences for the patient. A tissue targeting lipid bilayer coating would overcome these limitations in multiple different ways. The main constituent of natural plasma membranes is a phospho-choline lipid; these have been shown to be highly hemocompatible, reducing clot formation. They are also the main component of most supported lipid bilayer systems. The charge composition of the bilayer can be selected for increased positively charged lipids thus prohibiting cellular growth. Further, the lipid bilayer can also be patterned to have areas of different lipid composition and therefore tailor the tissue adhesion profile of the implant. Another intriguing possibility of this system is the utility of having a targetable surface directly at the implant site; this would open up the possibility of targeted drug delivery to the bilayer. The aldehyde tag lipid-protein anchoring system would be an ideal candidate for such highly specific membrane targeting. Direct targeting would mean that site specific therapeutics could be controlled externally, through liposomal drug injection, and with high specificity as aldehydes occur extremely rarely in the human body. Another interesting possibility is the inclusion of lipids that can respond to natural stimuli, such as calcium fluctuations. A protein embedded lipid

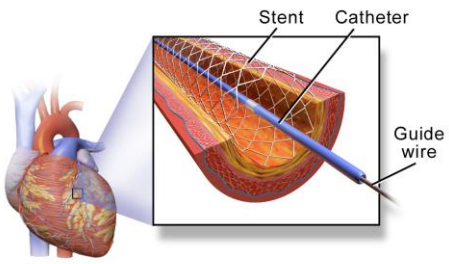

Figure 6.1: A Cardiac Stent: a stent is used to expand a restricted coronary artery.[3]

bilayer over a drug containing polymer could act as a responsive surface where lipid organization, such as is found with PIP_2 with response to Ca^{2+} concentrations, could be the trigger to open bilayer embedded protein channels. Such a response could be engineered to be reactive to a natural stimulation, such as clotting which requires calcium as a cofactor, or to an externally controlled stimulus.

One of the most distinguishing factors of this research is that it can be conducted on polymer supports. This serves two functions: first the polymer technology, particularly PLLA which I have already shown to be an excellent lipid substrate, is currently in use in drug eluting stents. This means that any functionality that can be provided to the polymer will directly interface with the existing implant technology with the potential for immediate application. Secondly the physical properties of the polymer substrate provide a highly customizable surface that can be tailored to influence the spatial and mechanical properties of the bilayer. For instance the diameter of the polymer pores can couple into the diffusive properties of the bilayer, opening the possibility for patterned polymers that can have different surface properties in different regions. Another example is mechanical coupling of the polymer stiffness into the bilayer via integrin proteins, this would produce a surface that is now chemically and mechanically more like a natural membrane. Such developments would have not only an industrial application but also great investigative potential for the study of cellular responses to mechanical and chemical stimulation

6.7 Conclusions

In this work we have shown that:

1. PIP2 aggregations contain a high potential for dynamic rearrangements of bilayer elements via simple solute control
2. Aldehyde tag offers a modular approach to protein or peptide binding to any phospholipid based object: micelle, vesicle, or bilayer.
3. The quantities of lipids with positive or negative charge in a lipid bilayer are critical to a cells propensity to adhere and proliferate on that surface. Further the inclusion of glycolipids enhances the cellular capability of a fluid bilayer surface to that of a solid substrate.
4. Super-resolution microscopy on spectrins in non-erythroid cell lines shows that there is fine scale structure that is composes of several spectrin isophorms.
5. Polymer supported bilayers have great potential for diversity in the means that are used to create biomimetic surfaces as well as enhanced biointerfaces.

All of these findings can be combined to advance the field of biomedical engineering with respect to cellular interfacing.

References

1. Tien, H.T. and A.L. Ottova, *The lipid bilayer concept and its experimental realization: from soap bubbles, kitchen sink, to bilayer lipid membranes.* Journal of Membrane Science, 2001. 189(1): p. 83-117.
2. TIRF Schematic 2008.
3. staff, B.c., *Stent in Coronary Artery.* Wikiversity Journal of Medicine, 2014.
4. Campell, N.A., *Biology*. 4th ed. 1996, Menlo Park: Benjamin Cummings Publishing Company.
5. Lodish, H., et al., *Molecular Cell Biology*. 4th ed. 2000, New York: W. H. Freeman and Company.
6. Lupyan, D., et al., *A Molecular Dynamics Investigation of Lipid Bilayer Perturbation by PIP2.* Biophysical Journal. 98(2): p. 240-247.
7. Singer, S.J. and G.L. Nicolson, *Fluid Mosaic Model of Structure of Cell Membranes.* Science, 1972. 175(4023): p. 720-&.
8. Brian, A.A. and H.M. McConnell, *Allogenic Stimulation Cyto-Toxic T-Cells by Supported Planar Membranes.* Proceedings of the National Academy of Sciences of the United States of America-Biological Sciences, 1984. 81(19): p. 6159-6163.
9. Wyrick-Glatzel, J., J.K. MacDonald, and J.J. Chen, *Paroxysmal nocturnal hemoglobinemia: A molecular definition of the clinical biology of the disorder.* Labmedicine, 2006. 37(4): p. 237-243.
10. Gest, H., *The remarkable vision of Robert Hooke (1635-1703) - first observer of the microbial world.* Perspectives in Biology and Medicine, 2005. 48(2): p. 266-272.
11. Vasil, I.K., *A history of plant biotechnology: from the Cell Theory of Schleiden and Schwann to biotech crops.* Plant Cell Reports, 2008. 27(9): p. 1423-1440.
12. Nye, J.A. and J.T. Groves, *Kinetic control of histidine-tagged protein surface density on supported lipid bilayers.* Langmuir, 2008. 24(8): p. 4145-4149.
13. Cunningham, B., et al., *Liposomal Formulation Increases Local Delivery of Amphotericin from Bone Cement: A Pilot Study.* Clinical Orthopaedics and Related Research, 2012. 470(10): p. 2671-2676.
14. Lundquist, A., et al., *Biotinylated lipid bilayer disks as model membranes for biosensor analyses.* Analytical Biochemistry, 2010. 405(2): p. 153-159.
15. Madwar, C., G. Gopalakrishnan, and R.B. Lennox, *Interfacing Living Cells and Spherically Supported Bilayer Lipid Membranes.* Langmuir, 2015. 31(16): p. 4704-4712.
16. Wu, J.C., et al., *Antibody conjugated supported lipid bilayer for capturing and purification of viable tumor cells in blood for subsequent cell culture.* Biomaterials, 2013. 34(21): p. 5191-5199.
17. Kloboucek, A., et al., *Adhesion-induced receptor segregation and adhesion plaque formation: A model membrane study.* Biophys. J., 1999. 77(4): p. 2311-2328.
18. Schnaar, R.L., *Glycolipid-mediated cell-cell recognition in inflammation and nerve regeneration.* Archives of Biochemistry and Biophysics, 2004. 426(2): p. 163-172.
19. Smilenov, L.B., et al., *Focal adhesion motility revealed in stationary fibroblasts.* Science, 1999. 286(5442): p. 1172-1174.

20. Maheshwari, G., et al., *Cell adhesion and motility depend on nanoscale RGD clustering.* Journal of Cell Science, 2000. 113(10): p. 1677-1686.
21. Syriani, E., et al., *Profilin induces lamellipodia by growth factor-independent mechanism.* Faseb Journal, 2008. 22(5): p. 1581-1596.
22. van Meer, G., D.R. Voelker, and G.W. Feigenson, *Membrane lipids: where they are and how they behave.* Nature Reviews Molecular Cell Biology, 2008. 9(2): p. 112-124.
23. Gamper, N. and M.S. Shapiro, *Target-specific PIP2 signalling: how might it work?* Journal of Physiology-London, 2007. 582(3): p. 967-975.
24. Gambhir, A., et al., *Electrostatic sequestration of PIP2 on phospholipid membranes by basic/aromatic regions of proteins.* Biophysical Journal, 2004. 86(4): p. 2188-2207.
25. McCloskey, M. and M.M. Poo, *Protein Diffusion in Cell-Membranes - Some Biological Implications.* International Review of Cytology-a Survey of Cell Biology, 1984. 87: p. 19-81.
26. Nelson, D.L. and M.M. Cox, *Lehninger Principles of Biochemistry*. 5th ed. 2008: W. H. Freeman.
27. Cevc, G. and D. Marsh, eds. *Phospholipid Bilayers-Physical Priciples and Models*. Cell Biology: A Series of Monographs, ed. E.E. Bittar. Vol. 5. 1987, John Wiley & Sons: New York.
28. Jones, M.J. and D. Chapman, *Micelles, Monolayers and Biomembranes*. 1995, New York: WIley-Liss Inc.
29. Tanford, C., *The Hydrophobic Effect: Formation of Micelles and Biological Membranes.* 1991, Malabar: Krieger.
30. Chan, Y.H.M. and S.G. Boxer, *Model membrane systems and their applications.* Current Opinion in Chemical Biology, 2007. 11(6): p. 581-587.
31. Tamm, L.K. and H.M. McConnell, *Supported phospholipid bilayers.* Biophysical Journal, 1985. 47(1): p. 105-113.
32. Lipowsky, R., *Vesicles and Biomembranes.*, in *Encyclopedia of Applied Physics*, G.L. Trigg, Editor. 1998, Wiley-VCH Verlag GmbH: New York. p. 199 - 222.
33. Alberts, B., et al., *Molecular Biology of the Cell*. third ed. 1994, New York & London: Garland Puplishing, Inc.
34. Liscovitch, M., et al., *Novel Function of Phosphatidylinositol 4,5-Bisphosphate as a Cofactor for Brain Membrane Phospholipase-D.* Journal of Biological Chemistry, 1994. 269(34): p. 21403-21406.
35. McLaughlin, S., et al., *PIP2 AND proteins: Interactions, organization, and information flow.* Annual Review of Biophysics and Biomolecular Structure, 2002. 31: p. 151-175.
36. Czech, M.P., *PIP2 and PIP3: Complex roles at the cell surface.* Cell, 2000. 100(6): p. 603-606.
37. Berridge, M.J., *Inositol Triphosphate and Calcium Signaling.* Nature, 1993. 361(6410): p. 315-325.
38. Clapham, D.E., *Calcium Signaling.* Cell, 1995. 80(2): p. 259-268.
39. Soom, M., et al., *Multiple PIP2 binding sites in Kir-2.1 inwardly rectifying potassium channels.* Febs Letters, 2001. 490(1-2): p. 49-53.
40. Chinen, Y., et al., *Phosphoinositide Protein Kinase PDPK1 Is a Crucial Cell Signaling Mediator in Multiple Myeloma.* Cancer Research, 2014. 74(24): p. 7418-7429.
41. Zimmer, M., *Green fluorescent protein (GFP): Applications, structure, and related photophysical behavior.* Chemical Reviews, 2002. 102(3): p. 759-781.

42. Carlson, B.L., et al., *Function and structure of a prokaryotic formylglycine-generating enzyme.* Journal of Biological Chemistry, 2008. 283(29): p. 20117-20125.
43. Almen, M.S., et al., *Mapping the human membrane proteome: a majority of the human membrane proteins can be classified according to function and evolutionary origin.* Bmc Biology, 2009. 7: p. 14.
44. Anderson, R.G.W. and K. Jacobson, *Cell biology - A role for lipid shells in targeting proteins to caveolae, rafts, and other lipid domains.* Science, 2002. 296(5574): p. 1821-1825.
45. Brown, D.A. and E. London, *Functions of lipid rafts in biological membranes.* Annual Review of Cell and Developmental Biology, 1998. 14: p. 111-136.
46. Edidin, M., *Shrinking patches and slippery rafts: scales of domains in the plasma membrane.* Trends in Cell Biology, 2001. 11(12): p. 492-496.
47. Jacobson, K., O.G. Mouritsen, and R.G.W. Anderson, *Lipid rafts: at a crossroad between cell biology and physics.* Nature Cell Biology, 2007. 9(1): p. 7-14.
48. Gross, D.J. and W.W. Wecc, *Cell surface clustering and mobility of the liganded LDL receptor measured by digital video fluorescence microscopy.*, in *Spectrocopic Membrane Probes.*, L.M. Loew, Editor. 1988, CRC Press: Boca Raton. p. 19-45.
49. Dumas, F., et al., *Consequences of hydrophobic mismatch between lipids and melibiose permease on melibiose transport.* Biochemistry, 2000. 39(16): p. 4846-4854.
50. Duque, D., et al., *Molecular theory of hydrophobic mismatch between lipids and peptides.* Journal of Chemical Physics, 2002. 116(23): p. 10478-10484.
51. Epand, R.M., et al., *Protein-induced formation of cholesterol-rich domains.* Biochemistry, 2001. 40(35): p. 10514-10521.
52. Fan, J., M. Sammalkorpi, and M. Haataja, *Domain formation in the plasma membrane: Roles of nonequilibrium lipid transport and membrane proteins.* Physical Review Letters, 2008. 100(17).
53. Pani, B. and B.B. Singh, *Lipid rafts/caveolae as microdomains of calcium signaling.* Cell Calcium, 2009. 45(6): p. 625-633.
54. Pike, L.J., *Lipid rafts: bringing order to chaos.* Journal of Lipid Research, 2003. 44(4): p. 655-667.
55. Allen, J.A., R.A. Halverson-Tamboli, and M.M. Rasenick, *Lipid raft microdomains and neurotransmitter signalling.* Nature Reviews Neuroscience, 2007. 8(2): p. 128-140.
56. Winckler, B., P. Forscher, and I. Mellman, *A diffusion barrier maintains distribution of membrane proteins in polarized neurons.* Nature, 1999. 397(6721): p. 698-701.
57. Ikonen, E., *Roles of lipid rafts in membrane transport.* Current Opinion in Cell Biology, 2001. 13: p. 470-477.
58. Anderson, C.M., et al., *Tracking of cell surface receptors by fluorescence digital imaging microscopy using a charge-coupled device camera. Low-density lipoprotein and influenza virus receptor mobility at 4 degrees C.* Journal of Cell Science, 1992. 101(Pt 2): p. 415-25.
59. Barak, L.S. and W.W. Webb, *Diffusion of Low-Density Lipoprotein-Receptor Complex on Human- Fibroblasts.* Journal of Cell Biology, 1982. 95(3): p. 846-852.
60. de Brabander, M., et al., *Lateral diffusion retrograde movements of individual cell surface components on single motile cells observed with nanovid microscopy.* J. Cell Biol., 1991. 112 (1): p. 111-124.

61. Gheber, L. and M. Edidin, *A model for membrane patchiness: lateral diffusion in the presence of barriers and vesicle traffic.* Biophysical Journal, 1999. 77: p. 3163-3175.
62. Kusumi, A., Y. Sako, and M. Yamamoto, *Confined lateral diffusion of membrane receptors as studied by single particle tracking (nanovid microscopy). Effects of calcium-induced differentiation in cultured epithelial cells.* Biophysical Journal, 1993. 65(5): p. 2021-40.
63. Schutz, G.J., et al., *Properties of lipid microdomains in a muscle cell membrane visualized by single molecule microscopy.* EMBO Journal, 2000. 19(5): p. 892-901.
64. Tani, T., et al., *Trafficking of a ligand-receptor complex on the growth cones as an essential step for the uptake of nerve growth factor at the distal end of the axon: A single-molecule analysis.* Journal of Neuroscience, 2005. 25(9): p. 2181-2191.
65. Kusumi, A., et al., *Single-molecule tracking of membrane molecules: plasma membrane compartmentalization and dynamic assembly of raft-philic signaling molecules.* Seminars in Immunology, 2005. 17(1): p. 3-21.
66. Kusumi, A., et al., *Hierarchical organization of the plasma membrane: Investigations by single-molecule tracking vs. fluorescence correlation spectroscopy.* FEBS Letters, 2010. 584(9): p. 1814-1823.
67. Saxton, M.J., *Lateral diffusion in an archipelago. Single-particle diffusion.* Biophysical Journal, 1993. 64(6): p. 1766-80.
68. DeMond, A.L., et al., *T cell receptor microcluster transport through molecular mazes reveals mechanism of translocation.* Biophysical Journal, 2008. 94(8): p. 3286-3292.
69. Yu, C.H., et al., *Altered Actin Centripetal Retrograde Flow in Physically Restricted Immunological Synapses.* Plos One, 2010. 5(7).
70. Qian, H., M.P. Sheetz, and E.L. Elson, *Single particle tracking. Analysis of diffusion and flow in two-dimensional systems.* Biophysical Journal, 1991. 60(4): p. 910-21.
71. Brockman, H., *Lipid monolayers: why use half a membrane to characterize protein-membrane inteactions?* Current Opinion in Structural Biology, 1999. 9: p. 430-443.
72. Castellana, E.T. and P.S. Cremer, *Solid supported lipid bilayers: From biophysical studies to sensor design.* Surface Science Reports, 2006. 61(10): p. 429-444.
73. Wesolowska, O., et al., *Giant unilamellar vesicles - a perfect tool to visualize phase separation and lipid rafts in model systems.* Acta Biochimica Polonica, 2009. 56(1): p. 33-39.
74. Jesorka, A. and O. Orwar, *Liposomes: Technologies and Analytical Applications.* Annual Review of Analytical Chemistry, 2008. 1: p. 801-832.
75. Szoka, F. and D. Papahadjopoulos, *Comparative properties and methods of preparation of lipid vesicles (liposomes).* Annual Review of Biophysics and Bioengineering, 1980. 9: p. 467-508.
76. Watwe, R.M. and J.R. Bellare, *Manufacture of Liposomes - A Review.* Current Science, 1995. 68(7): p. 715-724.
77. McConnell, H.M., et al., *Supported Planar Membranes in Studies of Cell0-Cell Recognition in the Immune System.* Biochimica Et Biophysica Acta, 1986. 864(1): p. 95-106.
78. Tancrede, P., et al., *Formation of asymmetrical planar lipid bilayer-membranes form chracterized monolayers.* Journal of Biochemical and Biophysical Methods, 1983. 7(4): p. 299-310.

79. Schuler, M., et al., *Biomedical interfaces: titanium surface technology for implants and cell carriers.* Nanomedicine, 2006. 1(4): p. 449-463.
80. Halter, M., et al., *Engineered lipids that cross-link the inner and outer leaflets of lipid bilayers.* Langmuir, 2004. 20(6): p. 2416-2423.
81. Rossetti, F.F., et al., *Interactions between titanium dioxide and phosphatidyl serine-containing liposomes: Formation and patterning of supported phospholipid bilayers on the surface of a medically relevant material.* Langmuir, 2005. 21(14): p. 6443-6450.
82. Klibanov, A.L., et al., *Amphipathic polyethyleneglycols effectively prolong the circulation time of liposomes.* FEBS Lett, 1990. 268(1): p. 235-7.
83. Templeton, N.S., et al., *Improved DNA: Liposome complexes for increased systemic delivery and gene expression.* Nature Biotechnology, 1997. 15(7): p. 647-652.
84. Torchilin, V.P., *Micellar nanocarriers: Pharmaceutical perspectives.* Pharmaceutical Research, 2007. 24(1): p. 1-16.
85. Forster, V., P. Luciani, and J.C. Leroux, *Treatment of calcium channel blocker-induced cardiovascular toxicity with drug scavenging liposomes.* Biomaterials, 2012. 33(13): p. 3578-3585.
86. Tamm, L.K. and H.M. McConnell, Supported Phospholipid Bilayers. Biophysical Journal, 1985. 47(1): p. 105-113.
87. Gordon, G.W., et al., *Quantitative fluorescence resonance energy transfer measurements using fluorescence microscopy.* Biophysical Journal, 1998. 74(5): p. 2702-2713.
88. Forstner, M.B., et al., *Lipid lateral mobility and membrane phase structure modulation by protein binding.* Journal of the American Chemical Society, 2006. 128(47): p. 15221-15227.
89. Groves, J.T., R. Parthasarathy, and M.B. Forstner, *Fluorescence imaging of membrane dynamics*, in *Annual Review of Biomedical Engineering*. 2008, Annual Reviews: Palo Alto. p. 311-338.
90. Rozovsky, S., et al., *Single Molecule Kinetics of ENTH Binding to Lipid Membranes.* Journal of Physical Chemistry B, 2012. 116(17): p. 5122-5131.
91. Axelrod, D., T.P. Burghardt, and N.L. Thompson, *Total Internal-Reflection Fluorescence.* Annual Review of Biophysics and Bioengineering, 1984. 13: p. 247-268.
92. Axelrod, D., et al., *Mobility measurement by analysis of fluorescence photobleaching recovery kinetics* Biophysical Journal, 1976. 16(9): p. 1055-1069.
93. Mossman, K.D., et al., *Altered TCR signaling from geometrically repatterned immunological synapses.* Science, 2005. 310(5751): p. 1191-1193.
94. Salaita, K., et al., *Restriction of Receptor Movement Alters Cellular Response: Physical Force Sensing by EphA2.* Science, 2010. 327(5971): p. 1380-1385.
95. Shao, Y., et al., *Conducting polymer polypyrrole supported bilayer lipid membranes.* Biosensors & Bioelectronics, 2005. 20(7): p. 1373-1379.
96. Trojanowicz, M. and A. Mulchandani, *Analytical applications of planar bilayer lipid membranes.* Analytical and Bioanalytical Chemistry, 2004. 379(3): p. 347-350.
97. Baksh, M.M., M. Jaros, and J.T. Groves, *Detection of molecular interactions at membrane surfaces through colloid phase transitions.* Nature, 2004. 427(6970): p. 139-141.
98. Stelzle, M., R. Miehlich, and E. Sackmann, *2-Dimensional Microelectrophoresis in Supported Lipid Bilayers.* Biophysical Journal, 1992. 63(5): p. 1346-1354.

99. van Oudenaarden, A. and S.G. Boxer, *Brownian ratchets: Molecular separations in lipid bilayers supported on patterned arrays.* Science, 1999. 285(5430): p. 1046-1048.
100. Fischer, M., et al., *Design of biofunctional assemblies on solids through recombinant spherical bacterial protein lumazine synthase.* ChemPhysChem, 2001. 2(10): p. 623-627.
101. Borisenko, V., et al., *Simultaneous optical and electrical recording of single gramicidin channels.* Biophysical Journal, 2003. 84(1): p. 612-622.
102. Good, R.J., *Contact-Angle, Wetting, and Adhesion - A Critical-Review.* Journal of Adhesion Science and Technology, 1992. 6(12): p. 1269-1302.
103. Rios, P.F., et al., *The effect of polymer surface on the wetting and adhesion of liquid systems.* Journal of Adhesion Science and Technology, 2007. 21(3-4): p. 227-241.
104. Piehler, J., et al., *A high-density poly(ethylene glycol) polymer brush for immobilization on glass-type surfaces.* Biosensors & Bioelectronics, 2000. 15(9-10): p. 473-481.
105. Sackmann, E. and M. Tanaka, *Supported membranes on soft polymer cushions: fabrication, characterization and applications.* Trends in Biotechnology, 2000. 18(2): p. 58-64.
106. Kuhner, M., R. Tampe, and E. Sackmann, *Lipid Mono- and Bilayer Supported on Polymer Films: Composite Polymer-Lipid Films on Solid Substrates.* Biophysical Journal, 1994. 67(July): p. 217-226.
107. Wagner, M. and L. Tamm, *Tethered Polymer-Supported Planar Lipid Bilayers for Reconstitution of Integral Membrane Proteins: Silane-Polyethyleneglycol-Lipid as a Cushion and Covalent Linker.* Biophysical Journal, 2000. Volume 79(September): p. 1400–1414.
108. Wang, T., et al., *Single Lipid Bilayers Constructed on Polymer Cushion Studied by Sum Frequency Generation Vibrational Spectroscopy.* Journal of Physical Chemistry C, 2011(115): p. 7613–7620.
109. Kohli, N., et al., *Arrays of lipid bilayers and liposomes on patterned polyelectrolyte templates.* Journal of Colloid and Interface Science, 2006(301): p. 461–469.
110. Wang, Y.L. and R.J. Pelham, *Preparation of a flexible, porous polyacrylamide substrate for mechanical studies of cultured cells.* Molecular Motors and the Cytoskeleton, Pt B, 1998. 298: p. 489-496.
111. Towbin, H., T. Staehelin, and J. Gordon, *Electrophoretic Transfer of Proteins from Polyacrylamide Gels to Nitrocellulose Sheets - Procedure and Some Applications.* Proceedings of the National Academy of Sciences of the United States of America, 1979. 76(9): p. 4350-4354.
112. Muniz, E.C. and G. Geuskens, *Compressive elastic modulus of polyacrylamide hydrogels and semi-IPNs with poly(N-isopropylacrylamide).* Macromolecules, 2001. 34(13): p. 4480-4484.
113. Kandow, C.E., et al., *Polyacrylamidc hydrogels for cell mechanics: Steps toward optimization and alternative uses*, in *Cell Mechanics*, Y.L. Wang and D.E. Discher, Editors. 2007. p. 29-+.
114. Tse, J. and A. Engler, *Preparation of Hydrogel Substrates with Tunable Mechanical Properties.* Current Protocols in Cell Biology, 2010. 10(16): p. 1-16.
115. Yang, F., et al., *Fabrication of nano-structured porous PLLA scaffold intended for nerve tissue engineering.* biomaterials, 2004. 25(10): p. 1891-1900.
116. Rehfeldt, F. and M. Tanaka, *Hydration Forces in Ultrathin Films of Cellulose.* Langmuir, 2003(19): p. 1467-1473.

117. Tanaka, M., et al., *Frictional drag and electrical manipulation of recombinant proteins in polymer-supported membranes.* Langmuir, 2007. 23(10): p. 5638-5644.
118. Hillebrandt, H., et al., *High Electric Resistance Polymer/Lipid Composite Films on Indium-Tin-Oxide Electrodes.* Langmuir, 1999(15): p. 8451-8459.
119. Groves, J., L. Mahal, and C. Bertozzi, *Control of Cell Adhesion and Growth with Micropatterned Supported Lipid Membranes.* Langmuir, 2001(17): p. 5129-5133.
120. Falshaw, R., R.H. Furneaux, and D.E. Stevenson, *Agars from nine species of red seaweed in the genus Curdiea (Gracilariaceae, Rhodophyta).* Carbohydrate Research, 1998. 308(1-2): p. 107-115.
121. Gu, W.Y., et al., *New insight into deformation-dependent hydraulic permeability of gels and cartilage, and dynamic behavior of agarose gels in confined compression.* Journal of Biomechanics, 2003. 36(4): p. 593-598.
122. Ide, T. and T. Yanagida, *An Artificial Lipid Bilayer Formed on an Agarose-Coated Glass for Simultaneous Electrical and Optical Measurement of Single Ion Channels.* Biochemical and Biophysical Research Communications, 1999(265): p. 595–599.
123. Katagiri, K. and F. Caruso, *Monodisperse polyelectrolyte-supported asymmetric lipid-bilayer vesicles.* Advanced Materials, 2005. 17(6): p. 738-+.
124. Lee, G., Y. Lee, and B. Kyung, *Layer-By-Layer Assembly Of Zeolite Crystals On Glass With Polyelectrolytes As Ionic Inkers.* Journal of the American Chemical Society, 2001. 123(40): p. 9769–79.
125. Watkins, E.B., et al., *Structure and Thermodynamics of Lipid Bilayers on Polyethylene Glycol Cushions: Fact and Fiction of PEG Cushioned Membranes.* Langmuir, 2011. 27(22): p. 13618-13628.
126. Jimenez, J., et al., *Construction and Characterization of Soft-Supported Lipid Bilayer Membranes for Biosensors Application.* IEEE 2006(1): p. 4119-22.
127. Ryan, S.M., et al., *Advances in PEGylation of important biotech molecules: delivery aspects.* Expert Opinion on Drug Delivery, 2008. 5(4): p. 371-383.
128. Ngadi, N., et al., *Are PEG Molecules a Universal Protein Repellent?* International Journal of Biological and Life Sciences, 2009. 5(3): p. 106 - 110.
129. Pasut, G. and F. Veronese, *State of the art in PEGylation: The great versatility achieved after forty years of research.* Journal of Controlled Release, 2012. 161(161): p. 461–472.
130. Davis, F.F., *Commentary - The origin of pegnology.* Advanced Drug Delivery Reviews, 2002. 54(4): p. 457-458.
131. Konradi, R., et al., *Poly-2-methyl-2-oxazoline: A Peptide-like Polymer for Protein-Repellent Surfaces.* Langmuir, 2008(24): p. 613-616.
132. Purrucker, O., et al., *Supported Membranes with Well-Defined Polymer Tethers–Incorporation of Cell Receptors.* ChemPhysChem, 2004. 5(3): p. 327 - 335.
133. Naumann, C.A., et al., *The Polymer-Supported Phospholipid Bilayer: Tethering as a New Approach to Substrate-Membrane Stabilization.* Biomacromolecules, 2002. 3(1): p. 27-35.
134. Kibrom, A., et al., *Hydrogel-supported protein-tethered bilayer lipid membranes: a new approach toward polymer-supported lipid membranes.* Soft Matter, 2011. 7(1): p. 237-246.
135. Majewski, J., et al., *Structural Studies of Polymer-Cushioned Lipid Bilayers.* Biophysical Journal, 1998. 75(5): p. 2363–2367.

136. Adlkofer, K., et al., *Electrochemical passivation of gallium arsenide surface with organic self-assembled monolayers in aqueous electrolytes.* Applied Physics Letters 2000. 76(22): p. 3313.
137. Jin, Y.G., Y.X. Qiao, and X.P. Hou, *The effects of chain number and state of lipid derivatives of nucleosides on hydrogen bonding and self-assembly through the investigation of Langmuir-Blodgett films.* Applied Surface Science, 2006. 252(22): p. 7926-7929.
138. Brockman, H.L., et al., *Interactions of olopatadine and selected antihistamines with model and natural membranes.* Ocular Immunology and Inflammation, 2003. 11(4): p. 247-268.
139. Hughes, A.V., et al., *Floating lipid bilayers deposited on chemically grafted phosphatidylcholine surfaces.* Langmuir, 2008. 24(5): p. 1989-1999.
140. Lin, Y., et al., *Physisorbed Polymer-Tethered Lipid Bilayer with Lipopolymer Gradient.* Materials, 2012. 5(3): p. 2243-2257.
141. Morigaki, K., et al., *Patterning solid-supported lipid bilayer membranes by lithographic polymerization of a diacetylene lipid.* Angewandte Chemie-International Edition, 2001. 40(1): p. 172-174.
142. Chen, C.S., et al., *Geometric control of cell life and death.* Science, 1997. 276(5317): p. 1425-1428.
143. Thornell, I.M., et al., *PIP2 hydrolysis stimulates the electrogenic Na+-bicarbonate cotransporter NBCe1-B and -C variants expressed in Xenopus laevis oocytes.* Journal of Physiology-London, 2012. 590(23): p. 5993-6011.
144. Seu, K.J., et al., *Effect of surface treatment on diffusion and domain formation in supported lipid bilayers.* Biophysical Journal, 2007. 92(7): p. 2445-2450.
145. Trebotich, D., G.H. Miller, and M.D. Bybee, *A Penalty Method to Model Particle Interactions in DNA-Laden Flows.* Journal of Nanoscience and Nanotechnology, 2008. 8(7): p. 3749-3756.
146. Hillebrandt, H., M. Tanaka, and E. Sackmann, *A novel membrane charge sensor: Sensitive detection of surface charge at polymer/lipid composite films on indium tin oxide electrodes.* Journal of Physical Chemistry B, 2002. 106(2): p. 477-486.
147. El-Khouri, R.J., et al., *pH Responsive Polymer Cushions for Probing Membrane Environment Interactions.* Nano Letters, 2011. 11(5): p. 2169-2172.
148. Leng, J.S., et al., *Shape-memory polymers and their composites: Stimulus methods and applications.* Progress in Materials Science, 2011. 56(7): p. 1077-1135.
149. Mather, P.T., X.F. Luo, and I.A. Rousseau, *Shape Memory Polymer Research*, in *Annual Review of Materials Research*. 2009, Annual Reviews: Palo Alto. p. 445-471.
150. Davis, K.A., et al., *Dynamic cell behavior on shape memory polymer substrates.* biomaterials, 2011. 32(9): p. 2285-2293.
151. Aabo, T., et al., *Effect of long- and short-term exposure to laser light at 1070 nm on growth of Saccharomyces cerevisiae.* Journal of Biomedical Optics, 2010. 15(4).
152. Neuman, K.C., et al., *Characterization of photodamage to Escherichia coli in optical traps.* Biophysical Journal, 1999. 77(5): p. 2856-2863.
153. Giepmans, B.N.G., et al., *Review - The fluorescent toolbox for assessing protein location and function.* Science, 2006. 312(5771): p. 217-224.
154. Resch-Genger, U., et al., *Quantum dots versus organic dyes as fluorescent labels.* Nature Methods, 2008. 5(9): p. 763-775.

155. Kellogg, R.E. and R.G. Bennett, *Radiationless Intermolecular Energy Transfer .3.Determination of Phosphororescence Efficiencies.* Journal of Chemical Physics, 1964. 41(10): p. 3042-&.
156. Massoud, T.F. and S.S. Gambhir, *Molecular imaging in living subjects: seeing fundamental biological processes in a new light.* Genes & Development, 2003. 17(5): p. 545-580.
157. Zhang, J., et al., *Creating new fluorescent probes for cell biology.* Nature Reviews Molecular Cell Biology, 2002. 3(12): p. 906-918.
158. Zhang, J., et al., *Fusion Partners as a Tool for the Expression of Difficult Proteins in Mammalian Cells.* Current Pharmaceutical Biotechnology, 2010. 11(3): p. 241-245.
159. Daumas, F., et al., *Confined Diffusion Without Fences of a G-Protein-Coupled Receptor as Revealed by Single Particle Tracking.* Biophys. J., 2003. 84(1): p. 356-366.
160. Saxton, M.J. and K. Jacobson, *Single-particle tracking: Applications to membrane dynamics.* Annual Review of Biophysics and Biomolecular Structure, 1997. 26: p. 373-399.
161. Crocker, J.C. and D.G. Grier, *Methods of digital video microscopy for colloidal studies.* Journal of Colloid and Interface Science, 1996. 179(1): p. 298-310.
162. Schutz, G.J., et al., *Single molecule microscopy of biomembranes (review).* Molecular Membrane Biology, 2000. 17(1): p. 17-29.
163. Cheezum, M.K., W.F. Walker, and W.H. Guilford, *Quantitative comparison of algorithms for tracking single fluorescent particles.* Biophysical Journal, 2001. 81(4): p. 2378-2388.
164. Martin, D.S., M.B. Forstner, and J.A. Kas, *Apparent subdiffusion inherent to single particle tracking.* Biophysical Journal, 2002. 83(4): p. 2109-2117.
165. Forstner, M.B., et al., *Simultaneous single-particle tracking and visualization of domain structure on lipid monolayers.* Langmuir, 2003. 19(12): p. 4876-4879.
166. Reits, E.A.J. and J.J. Neefjes, *From fixed to FRAP: measuring protein mobility and activity in living cells.* Nature Cell Biology, 2001. 3(6): p. E145-E147.
167. Axelrod, D., *Total Internal-Reflection Fluorescence Microscopy.* Methods in Cell Biology, 1989. 30: p. 245-270.
168. Axelrod, D., *Selective imaging of surface fluorescence with very high aperture microscope objectives.* Journal of Biomedical Optics, 2001. 6(1): p. 6-13.
169. Axelrod, D., *Total internal reflection fluorescence microscopy in cell biology.* Traffic, 2001. 2(11): p. 764-774.
170. Ash, E.A. and G. Nicholls, *Super-Resolution Aperature Scanning Microscope.* Nature, 1972. 237(5357): p. 510-&.
171. Yamanaka, M., N.I. Smith, and K. Fujita, *Introduction to super-resolution microscopy.* Microscopy, 2014. 63(3): p. 177-192.
172. Lieberman, K., N. BenAmi, and A. Lewis, *Fully integrated near-field optical, far-field optical, and normal-force scanned probe microscope.* Review of Scientific Instruments, 1996. 67(10): p. 3567-3572.
173. Hell, S.W. and J. Wichmann, *Breaking the diffraction resolution limit by stimulated emission: stimulated-emission-depletion fluorescence microscopy.* Opt Lett, 1994. 19(11): p. 780-2.
174. Kahya, N. and P. Schwille, *Fluorescence correlation studies of lipid domains in model membranes (Review).* Molecular Membrane Biology, 2006. 23(1): p. 29-39.

175. Krichevsky, O. and G. Bonnet, *Fluorescence correlation spectroscopy: the technique and its applications.* Reports on Progress in Physics, 2002. 65(2): p. 251-297.
176. Medina, M.A. and P. Schwille, *Fluorescence correlation spectroscopy for the detection and study of single molecules in Biology.* Bioessays, 2002. 24(8): p. 758-764.
177. Schwille, P., J. Korlach, and W.W. Webb, *Fluorescence correlation spectroscopy with single-molecule sensitivity on cell and model membranes.* Cytometry, 1999. 36(3): p. 176-182.
178. Webb, W.W., *Fluorescence correlation spectroscopy: inception, biophysical experimentations, and prospectus.* Applied Optics, 2001. 40(24): p. 3969-3983.
179. Elson, E.L. and D. Magde, *Fluorescence Correlation Spectroscopy .1. Conceptual Basis and Theory.* Biopolymers, 1974. 13(1): p. 1-27.
180. Contini, D., et al., *Memory effect in gated single-photon avalanche diodes: a limiting noise contribution similar to afterpulsing.* Physics and Simulation of Optoelectronic Devices Xxi, 2013. 8619: p. 9.
181. Chen, Y., et al., *The photon counting histogram in fluorescence fluctuation spectroscopy.* Biophysical Journal, 1999. 77(1): p. 553-567.
182. Kask, P., et al., *Fluorescence-intensity distribution analysis and its application in biomolecular detection technology.* Proceedings of the National Academy of Sciences of the United States of America, 1999. 96(24): p. 13756-13761.
183. Thompson, N.L., A.M. Lieto, and N.W. Allen, *Recent advances in fluorescence correlation spectroscopy.* Current Opinion in Structural Biology, 2002. 12(5): p. 634-641.
184. White, N.S. and R.J. Errington, *Fluorescence techniques for drug delivery research: theory and practice.* Advanced Drug Delivery Reviews, 2005. 57(1): p. 17-42.
185. Paulick, M.G., et al., *Synthetic analogues of glycosylphosphatidylinositol-anchored proteins and their behavior in supported lipid bilayers.* Journal of the American Chemical Society, 2007. 129(37): p. 11543-11550.
186. Levental, I., et al., *Calcium-Dependent Lateral Organization in Phosphatidylinositol 4,5-Bisphosphate (PIP2)- and Cholesterol-Containing Monolayers.* Biochemistry, 2009. 48(34): p. 8241-8248.
187. Shevchenko, A. and K. Simons, *Lipidomics: coming to grips with lipid diversity.* Nature Reviews Molecular Cell Biology, 2010. 11(8): p. 593-598.
188. Khan, W.A., G.C. Blobe, and Y.A. Hannun, *Activation of Protein-Kinase-C by Oleic-Acid - Determination and Analysis of Inhibition by Detergent Micelles and Physiological Membranes - Requirement for Free Oleate.* Journal of Biological Chemistry, 1992. 267(6): p. 3605-3612.
189. Chan, S.Y.V., et al., *Apoptosis induced by intracellular ceramide accumulation in MDA-MB-435 breast carcinoma cells is dependent on the generation of reactive oxygen species.* Experimental and Molecular Pathology, 2007. 82(1): p. 1-11.
190. Hakomori, S. and Y. Igarashi, *Functional role of glycosphingolipids in cell recognition and signaling.* J Biochem, 1995. 118(6): p. 1091-103.
191. Emoto, K., et al., *Redistribution of phosphatidylethanolamine at the cleavage furrow of dividing cells during cytokinesis.* Proceedings of the National Academy of Sciences of the United States of America, 1996. 93(23): p. 12867-12872.
192. McLaughlin, S. and D. Murray, *Plasma membrane phosphoinositide organization by protein electrostatics.* Nature, 2005. 438(7068): p. 605-611.

193. Hinchliffe, K.A., A. Ciruela, and R.F. Irvine, *PIPkins, their substrates and their products: new functions for old enzymes.* Biochimica Et Biophysica Acta-Molecular and Cell Biology of Lipids, 1998. 1436(1-2): p. 87-104.
194. Billcliff, P.G. and M. Lowe, *Inositol lipid phosphatases in membrane trafficking and human disease.* Biochemical Journal, 2014. 461: p. 159-175.
195. Raucher, D., et al., *Phosphatidylinositol 4,5-bisphoshate functions as a second messenger that regulates cytoskeleton-plasma membrane adhesion.* Cell, 2000. 100(2): p. 221-228.
196. Huang, C.L., S.Y. Feng, and D.W. Hilgemann, *Direct activation of inward rectifier potassium channels by PIP2 and its stabilization by G beta gamma.* Nature, 1998. 391(6669): p. 803-806.
197. Liang, T., et al., *Phosphatidylinositol 4,5-Biphosphate (PIP2) Modulates Interaction of Syntaxin-1A with Sulfonylurea Receptor 1 to Regulate Pancreatic beta-Cell ATP-sensitive Potassium Channels.* Journal of Biological Chemistry, 2014. 289(9): p. 6028-6040.
198. Perez, T.D., et al., *E-cadherin tethered to micropatterned supported lipid bilayers as a model for cell adhesion.* Langmuir, 2005. 21(25): p. 11963-11968.
199. Britten, C.D., *Targeting ErbB receptor signaling: A pan-ErbB approach to cancer.* Molecular Cancer Therapeutics, 2004. 3(10): p. 1335-1342.
200. Nam, J.M., et al., *A fluid membrane-based soluble ligand-display system for live-cell assays.* Chembiochem, 2006. 7(3): p. 436-440.
201. Korner, A., et al., *Cell Differentiation of Pluripotent Tissue Sheets Immobilized on Supported Membranes Displaying Cadherin-11.* Plos One, 2013. 8(2): p. 10.
202. Andreasson-Ochsner, M., et al., *Single cell 3-D platform to study ligand mobility in cell-cell contact.* Lab on a Chip, 2011. 11(17): p. 2876-2883.
203. Svedhem, S., et al., *In Situ Peptide-Modified Supported Lipid Bilayers for Controlled Cell Attachment.* Langmuir, 2003. 19(17): p. 6730-6736.
204. Huang, C.-J., P.-Y. Tseng, and Y.-C. Chang, *Effects of extracellular matrix protein functionalized fluid membrane on cell adhesion and matrix remodeling.* Biomaterials, 2010. 31(27): p. 7183-7195.
205. Bouter, A., et al., *Annexin-A5 assembled into two-dimensional arrays promotes cell membrane repair.* Nat Commun, 2011. 2: p. 270.
206. Kim, S.H., J. Turnbull, and S. Guimond, *Extracellular matrix and cell signalling: the dynamic cooperation of integrin, proteoglycan and growth factor receptor.* Journal of Endocrinology, 2011. 209(2): p. 139-151.
207. Balla, T., T. Bondeva, and P. Varnai, *How accurately can we image inositol lipids in living cells?* Trends in Pharmacological Sciences, 2000. 21(7): p. 238-241.
208. Botelho, R.J., et al., *Localized biphasic changes in phosphatidylinositol-4,5-bisphosphate at sites of phagocytosis.* Journal of Cell Biology, 2000. 151(7): p. 1353-1367.
209. Levental, I., et al., *Cholesterol-dependent phase separation in cell-derived giant plasma-membrane vesicles.* Biochemical Journal, 2009. 424: p. 163-167.
210. Dietrich, U., et al., *Interaction of the MARCKS peptide with PIP2 in phospholipid monolayers.* Biochimica Et Biophysica Acta-Biomembranes, 2009. 1788(7): p. 1474-1481.
211. Ellenbroek, W.G., et al., *Divalent Cation-Dependent Formation of Electrostatic PIP2 Clusters in Lipid Monolayers.* Biophysical Journal, 2011. 101(9): p. 2178-2184.

212. Wang, Y.H., et al., *Divalent Cation-Induced Cluster Formation by Polyphosphoinositides in Model Membranes.* Journal of the American Chemical Society, 2012. 134(7): p. 3387-3395.
213. Sarmento, M.J., et al., *Ca2+ induces PI(4,5)P-2 clusters on lipid bilayers at physiological PI(4,5)P-2 and Ca2+ concentrations.* Biochimica Et Biophysica Acta-Biomembranes, 2014. 1838(3): p. 822-830.
214. Clapham, D.E., *Calcium signaling.* Cell, 2007. 131(6): p. 1047-1058.
215. Long, S.B., E.B. Campbell, and R. MacKinnon, *Voltage sensor of kv1.2: Structural basis of electromechanical coupling.* Science, 2005. 309(5736): p. 903-908.
216. Guatimosim, S., et al., *Local Ca2+ signaling and EC coupling in heart: Ca2+ sparks and the regulation of The Ca2+ (i) transient.* Journal of Molecular and Cellular Cardiology, 2002. 34(8): p. 941-950.
217. Sabatini, B.L., T.G. Oertner, and K. Svoboda, *The life cycle of Ca2+ ions in dendritic spines.* Neuron, 2002. 33(3): p. 439-452.
218. Sergeev, I.N., *Calcium as a mediator of 1,25-dihydroxyvitamin D-3-induced apoptosis.* Journal of Steroid Biochemistry and Molecular Biology, 2004. 89-90(1-5): p. 419-425.
219. Gopich, I.V. and A. Szabo, *Photon counting histograms for diffusing fluorophores.* Journal of Physical Chemistry B, 2005. 109(37): p. 17683-17688.
220. Anikovsky, M., et al., *Photon Counting Histogram Analysis for Two-Dimensional Systems.* Chemphyschem, 2011. 12(13): p. 2438-2447.
221. Terada, N., et al., *Size distribution of linear and helical polymers in actin solution analyzed by photon counting histogram.* Biophysical Journal, 2007. 92(6): p. 2162-2171.
222. McGuigan, J.A.S., D. Luthi, and A. Buri, *Calcium Buffer Solutions and How to Make Them – A Do it Yourself Guide.* Canadian Journal of Physiology and Pharmacology, 1991. 69(11): p. 1733-1749.
223. Wang, T., et al., *Single Lipid Bilayers Constructed on Polymer Cushion Studied by Sum Frequency Generation Vibrational Spectroscopy.* Journal of Physical Chemistry C, 2011. 115(15): p. 7613-7620.
224. Benda, A., et al., *How to determine diffusion coefficients in planar phospholipid systems by confocal fluorescence correlation spectroscopy.* Langmuir, 2003. 19(10): p. 4120-4126.
225. Widengren, J., U. Mets, and R. Rigler, *Fluorescence Correlation Spectroscopy of Triplet-States in Solution - a Theoretical and Experimental-Study.* Journal of Physical Chemistry, 1995. 99(36): p. 13368-13379.
226. Culbertson, C.T., S.C. Jacobson, and J.M. Ramsey, *Diffusion coefficient measurements in microfluidic devices.* Talanta, 2002. 56(2): p. 365-373.
227. Digman, M.A., et al., *Mapping the number of molecules and brightness in the laser scanning microscope.* Biophysical Journal, 2008. 94(6): p. 2320-2332.
228. Thompson, N.L., *Fluorescence Correlation Spectroscopy*. Topics in Fluorescence Spectroscopy. Vol. 1. 1991, New York: Plenum Press. 41.
229. McCabe, I.P. and M.B. Forstner, *Polymer Supported Lipid Bilayers.* Open Journal of Biophysics, 2013. Vol.03No.01: p. 11.
230. Lupyan, D., et al., *A Molecular Dynamics Investigation of Lipid Bilayer Perturbation by PIP2.* Biophysical Journal, 2010. 98(2): p. 240-247.

231. Schwille, P., F.J. MeyerAlmes, and R. Rigler, *Dual-color fluorescence cross-correlation spectroscopy for multicomponent diffusional analysis in solution.* Biophysical Journal, 1997. 72(4): p. 1878-1886.
232. Gerold, P., V. Eckert, and R.T. Schwarz, *GPI-anchors: An overview.* Trends in Glycoscience and Glycotechnology, 1996. 8(42): p. 265-277.
233. Fein, M., et al., *Lateral mobility of lipid analogs and GPI-anchored proteins in supported bilayers determined by fluorescent bead tracking.* Journal of Membrane Biology, 1993. 135(1): p. 83-92.
234. Garner, A.E., D.A. Smith, and N.M. Hooper, *Sphingomyelin chain length influences the distribution of GPI-anchored proteins in rafts in supported lipid bilayers.* Molecular Membrane Biology, 2007. 24(3): p. 233-242.
235. Trippier, P.C., *Synthetic Strategies for the Biotinylation of Bioactive Small Molecules.* Chemmedchem, 2013. 8(2): p. 190-203.
236. Liu, Z., et al., *Specific bindig of avidin to biotin-containing lipid lamella surfaces studied with monolayers and liposomes.* European Biophysics Journal, 1995. 24(1): p. 31-38.
237. Qin, H., Z. Liu, and S.F. Sui, *2-dimensional crystallization of avidin on biotinylated lipid monolayers.* Biophysical Journal, 1995. 68(6): p. 2493-2496.
238. Carrico, I.S., B.L. Carlson, and C.R. Bertozzi, *Introducing genetically encoded aldehydes into proteins.* Nature Chemical Biology, 2007. 3(6): p. 321-322.
239. Wu, P., et al., *Site-specific chemical modification of recombinant proteins produced in mammalian cells by using the genetically encoded aldehyde tag.* Proceedings of the National Academy of Sciences of the United States of America, 2009. 106(9): p. 3000-3005.
240. Wang, A.M., et al., *Convenient one-step purification and immobilization of lipase using a genetically encoded aldehyde tag.* Biochemical Engineering Journal, 2013. 73: p. 86-92.
241. Rabuka, D., et al., *Site-specific chemical protein conjugation using genetically encoded aldehyde tags.* Nature Protocols, 2012. 7(6): p. 1052-1067.
242. Zhang, G.H., V. Gurtu, and S.R. Kain, *An enhanced green fluorescent protein allows sensitive detection of gene transfer in mammalian cells.* Biochemical and Biophysical Research Communications, 1996. 227(3): p. 707-711.
243. Cormack, B.P., R.H. Valdivia, and S. Falkow, *FACS-optimized mutants of the green fluorescent protein (GFP).* Gene, 1996. 173(1): p. 33-38.
244. Sun, W.C., K.R. Gee, and R.P. Haugland, *Synthesis of novel fluorinated coumarins: Excellent UV-light excitable fluorescent dyes.* Bioorganic & Medicinal Chemistry Letters, 1998. 8(22): p. 3107-3110.
245. Nair, P.M., et al., *Using patterned supported lipid membranes to investigate the role of receptor organization in intercellular signaling.* Nature Protocols, 2011. 6(4): p. 523-539.
246. Crisalli, P. and E.T. Kool, *Water-Soluble Organocatalysts for Hydrazone and Oxime Formation.* Journal of Organic Chemistry, 2013. 78(3): p. 1184-1189.
247. Sterling, S.M., et al., *Phospholipid Diffusion Coefficients of Cushioned Model Membranes Determined via Z-Scan Fluorescence Correlation Spectroscopy.* Langmuir, 2013. 29(25): p. 7966-7974.
248. Leonenko, Z.V., et al., *Investigation of temperature-induced phase transitions in DOPC and DPPC phospholipid bilayers using temperature-controlled scanning force microscopy.* Biophysical Journal, 2004. 86(6): p. 3783-3793.

249. Hink, M.A., et al., *Structural dynamics of green fluorescent protein alone and fused with a single chain Fv protein.* Journal of Biological Chemistry, 2000. 275(23): p. 17556-17560.
250. Setaka, M., et al., *A Stable Planer Bilayer Membrane of Phospholipid Supported Cellulose Sheets.* Journal of Biochemistry, 1982. 91(1): p. 79-85.
251. Darszon, A., *Strategies in the reassembly of membrane-proteins into lipid bilayer systems and their functional assay.* Journal of Bioenergetics and Biomembranes, 1983. 15(6): p. 321-334.
252. Mirzabekov, T.A., A.Y. Silberstein, and B.L. Kagan, *Use of planar lipid bilayer membranes for rapid screening of membrane active compounds.* Methods in enzymology, 1999. 294: p. 661-74.
253. Fauvel, J., et al., *Biochemical characterization of plasma membranes and intrecellular mambranes isolates from human platelets using percoll gradients.* Biochimica Et Biophysica Acta, 1986. 856(1): p. 155-164.
254. Zhao, Y.X., et al., *Proteomic analysis of integral plasma membrane proteins.* Analytical Chemistry, 2004. 76(7): p. 1817-1823.
255. Fleschner, C.R. and R.J. Cenedella, *Lipid-composition of lens plasma-membrane fractions enriched in fiber junctions.* Journal of Lipid Research, 1991. 32(1): p. 45-53.
256. Vanhoeve.Rp and P. Emmelot, *Studies of plasma-membranes . 18. Lipid class composition of plasma-membranes isolated from rat and mouse liver and hepatomas.* Journal of Membrane Biology, 1972. 9(2): p. 105-&.
257. Raguz, M., et al., *Lipid protein interactions in plasma membranes of fiber cells isolated from the human eye lens.* Experimental Eye Research, 2014. 120: p. 138-151.
258. Tang, D.X., et al., *The influence of membrane lipid structure on plasma membrane Ca2+-ATPase activity.* Cell Calcium, 2006. 39(3): p. 209-216.
259. Robenek, H., et al., *Lipid droplets gain PAT family proteins by interaction with specialized plasma membrane domains.* Journal of Biological Chemistry, 2005. 280(28): p. 26330-26338.
260. Loew, S., A. Hinderliter, and S. May, *Stability of protein-decorated mixed lipid membranes: The interplay of lipid-lipid, lipid-protein, and protein-protein interactions.* Journal of Chemical Physics, 2009. 130(4): p. 8.
261. Tocanne, J.F., et al., *Lipid domains and lipid protein interactions in biological membranes.* Chemistry and Physics of Lipids, 1994. 73(1-2): p. 139-158.
262. Vogler, O., et al., *Membrane interactions of G proteins and other related proteins.* Biochimica Et Biophysica Acta-Biomembranes, 2008. 1778(7-8): p. 1640-1652.
263. Marsh, D., *Electron spin resonance in membrane research: protein-lipid interactions from challenging beginnings to state of the art.* European Biophysics Journal with Biophysics Letters, 2010. 39(4): p. 513-525.
264. Eisenberg, S. and Y.I. Henis, *Interactions of Ras proteins with the plasma membrane and their roles in signaling.* Cellular Signalling, 2008. 20(1): p. 31-39.
265. Galdiero, S., M. Galdiero, and C. Pedone, *beta-barrel membrane bacterial proteins: Structure, function, assembly and interaction with lipids.* Current Protein & Peptide Science, 2007. 8(1): p. 63-82.
266. Vereb, G., et al., *Dynamic, yet structured: The cell membrane three decades after the Singer-Nicolson model.* Proceedings of the National Academy of Sciences of the United States of America, 2003. 100(14): p. 8053-8058.

267. Kam, L. and S.G. Boxer, *Cell adhesion to protein-micropatterned-supported lipid bilayer membranes.* Journal of Biomedical Materials Research, 2001. 55(4): p. 487-495.
268. Groves, J.T., L.K. Mahal, and C.R. Bertozzi, *Control of cell adhesion and growth with micropatterned supported lipid membranes.* Langmuir, 2001. 17(17): p. 5129-5133.
269. Korner, A., et al., *Cell Differentiation of Pluripotent Tissue Sheets Immobilized on Supported Membranes Displaying Cadherin-11*. 2013, Figshare.
270. Torres, A.J., et al., *Functional single-cell analysis of T-cell activation by supported lipid bilayer-tethered ligands on arrays of nanowells.* Lab on a Chip, 2013. 13(1): p. 90-99.
271. Harder, T., *The T Cell Plasma Membrane Lipid Bilayer Stages TCR-proximal Signaling Events.* Frontiers in immunology, 2012. 3: p. 50.
272. Sudimack, J. and R.J. Lee, *Targeted drug delivery via the folate receptor.* Advanced Drug Delivery Reviews, 2000. 41(2): p. 147-162.
273. Allen, T.M. and P.R. Cullis, *Drug delivery systems: Entering the mainstream.* Science, 2004. 303(5665): p. 1818-1822.
274. Moghimi, S.M., A.C. Hunter, and J.C. Murray, *Nanomedicine: current status and future prospects.* Faseb Journal, 2005. 19(3): p. 311-330.
275. Torchilin, V.P., *Recent advances with liposomes as pharmaceutical carriers.* Nature Reviews Drug Discovery, 2005. 4(2): p. 145-160.
276. Zimmermann, T.S., et al., *RNAi-mediated gene silencing in non-human primates.* Nature, 2006. 441(7089): p. 111-114.
277. Anand, P., et al., *Bioavailability of curcumin: Problems and promises.* Molecular Pharmaceutics, 2007. 4(6): p. 807-818.
278. Peer, D., et al., *Nanocarriers as an emerging platform for cancer therapy.* Nature Nanotechnology, 2007. 2(12): p. 751-760.
279. Davis, M.E., Z. Chen, and D.M. Shin, *Nanoparticle therapeutics: an emerging treatment modality for cancer.* Nature Reviews Drug Discovery, 2008. 7(9): p. 771-782.
280. Gabizon, A., et al., *Long-circulating liposomes for drug delivery in cancer therapy: A review of biodistribution studies in tumor-bearing animals.* Advanced Drug Delivery Reviews, 1997. 24(2-3): p. 337-344.
281. Webb, M.S., et al., *Comparison of different hydrophobic anchors conjugated to poly(ethylene glycol): Effects on the pharmacokinetics of liposomal vincristine.* Biochimica Et Biophysica Acta-Biomembranes, 1998. 1372(2): p. 272-282.
282. Allen, C., et al., *Controlling the physical behavior and biological performance of liposome formulations through use of surface grafted poly(ethylene glycol).* Bioscience Reports, 2002. 22(2): p. 225-250.
283. Szebeni, J. and S.M. Moghimi, *Liposome triggering of innate immune responses: a perspective on benefits and adverse reactions.* Journal of liposome research, 2009. 19(2): p. 85-90.
284. Abu Lila, A.S., et al., *Application of Polyglycerol Coating to Plasmid DNA Lipoplex for the Evasion of the Accelerated Blood Clearance Phenomenon in Nucleic Acid Delivery.* Journal of Pharmaceutical Sciences, 2014. 103(2): p. 557-566.
285. Farhood, H., N. Serbina, and L. Huang, *The role of dioleoyl phosphatidylethanolamins in cationic liposome-mediates gene transfer.* Biochimica Et Biophysica Acta-Biomembranes, 1995. 1235(2): p. 289-295.
286. Gao, X. and L. Huang, *Cationic liposome-mediated gene transfer.* Gene Therapy, 1995. 2(10): p. 710-722.

287. Xu, Y.H. and F.C. Szoka, *Mechanism of DNA release from cationic liposome/DNA complexes used in cell transfection.* Biochemistry, 1996. 35(18): p. 5616-5623.
288. Qian, Z.M., et al., *Targeted drug delivery via the transferrin receptor-mediated endocytosis pathway.* Pharmacological Reviews, 2002. 54(4): p. 561-587.
289. Afanasenkau, D. and A. Offenhausser, *Positively Charged Supported Lipid Bilayers as a Biomimetic Platform for Neuronal Cell Culture.* Langmuir, 2012. 28(37): p. 13387-13394.
290. Andersson, A.S., et al., *Cell adhesion on supported lipid bilayers.* Journal of Biomedical Materials Research Part A, 2003. 64A(4): p. 622-629.
291. Parthasarathy, R., P.A. Cripe, and J.T. Groves, *Electrostatically driven spatial patterns in lipid membrane composition.* Physical Review Letters, 2005. 95(4): p. 4.
292. Felice, D.L., J. Sun, and R.H. Liu, *A modified methylene blue assay for accurate cell counting.* Journal of Functional Foods, 2009. 1(1): p. 109-118.
293. Hassan, U. and R. Bashir, *Electrical cell counting process characterization in a microfluidic impedance cytometer.* Biomedical Microdevices, 2014. 16(5): p. 697-704.
294. Kohler, A. and W. Loos, *The phased contrast procedure and its application in the microscopy.* Naturwissenschaften, 1941. 29: p. 49-61.
295. McLaughlin, A., et al., *Dimethonium , a divalent-cation that exerts only a screening effect on the electrostatic potential adjacent to negatively charged phospholipid-bilayer membranes.* Journal of Membrane Biology, 1983. 76(2): p. 183-193.
296. Shinoda, W., M. Shimizu, and S. Okazaki, *Molecular dynamics study on electrostatic properties of a lipid bilayer: Polarization, electrostatic potential, and the effects on structure and dynamics of water near the interface.* Journal of Physical Chemistry B, 1998. 102(34): p. 6647-6654.
297. Saito, H., et al., *Molecular Dynamics Study of Electrostatic Potential along Lipid Bilayer with Gramicidin A.* 4th International Symposium on Slow Dynamics in Complex Systems: Keep Going Tohoku, 2013. 1518: p. 633-636.
298. Mikucki, M. and Y.C. Zhou, *Electrostatic forces on charged surfaces of bilayer lipid membranes.* Siam Journal on Applied Mathematics, 2014. 74(1): p. 1-21.
299. Dunlevy, J.R. and J.R. Couchman, *Controlled induction of focal adhesion disassembly and migration in primary fibroblasts.* Journal of Cell Science, 1993. 105: p. 489-500.
300. Crowley, E. and A.F. Horwitz, *Tyrosine phosphorylation and sytoskeletal tension regulate the release of fibroblast adhesions.* Journal of Cell Biology, 1995. 131(2): p. 525-537.
301. Schneider, G.B., et al., *Microinjection of protein tyrosine phosphatases into fibroblasts disrupts focal adhesions and stress fibers.* Cell Adhesion and Communication, 1998. 5(3): p. 207-219.
302. Herrera Abreu, M.T., et al., *Tyrosine phosphatase SHP-2 regulates IL-1 signaling in fibroblasts through focal adhesions.* Journal of cellular physiology, 2006. 207(1): p. 132-43.
303. Tamariz, E. and F. Grinnell, *Modulation of fibroblast morphology and adhesion during collagen matrix remodeling.* Molecular Biology of the Cell, 2002. 13(11): p. 3915-3929.
304. Baxter, L.C., et al., *Fibroblast and osteoblast adhesion and morphology on calcium phosphate surfaces.* European cells & materials, 2002. 4: p. 1-17.
305. Singhvi, R., G. Stephanopoulos, and D.I.C. Wang, *Effects of substratum morphology on cell physiology - Review.* Biotechnology and Bioengineering, 1994. 43(8): p. 764-771.

306. Cukierman, E., *A visual-quantitative analysis of fibroblastic stromagenesis in breast cancer progression.* Journal of Mammary Gland Biology and Neoplasia, 2004. 9(4): p. 311-324.
307. Schindler, A.E., *Gonadotropin-releasing hormone agonists for prevention of postoperative adhesions: an overview.* Gynecological Endocrinology, 2004. 19(1): p. 51-55.
308. Rid, R., et al., *The last but not the least: The origin and significance of trailing adhesions in fibroblastic cells.* Cell Motility and the Cytoskeleton, 2005. 61(3): p. 161-171.
309. Al Mustafa, M., et al., *In vitro adhesion of fibroblastic cells to titanium alloy discs treated with sodium hydroxide.* Clinical Oral Implants Research, 2015. 26(1): p. 15-19.
310. Wells, A., et al., *Shaping up for shipping out: PLC gamma signaling of morphology changes in EGF-stimulated fibroblast migration.* Cell Motility and the Cytoskeleton, 1999. 44(4): p. 227-233.
311. Velasco-Velazquez, M.A., et al., *4-Hydroxycoumarin disorganizes the actin cytoskeleton in B16-F10 melanoma cells but not in B82 fibroblasts, decreasing their adhesion to extracellular matrix proteins and motility.* Cancer Letters, 2003. 198(2): p. 179-186.
312. Tsirimonaki, E., et al., *Similarities and differences between the E5 oncoproteins of bovine papillomaviruses type 1 and type 4: Cytoskeleton, motility and invasiveness in E5-transformed bovine and mouse cells.* Virus Research, 2006. 115(2): p. 158-168.
313. Sheu, C.W., F.M. Moreland, and V.C. Dunkel, *The effects of cell passage on the susceptibility of BALB/3T3 clone A3-1-1-1 cells to 3-methylcholanthrene-induced morphological transformation.* Environmental Mutagenesis, 1987. 9(1): p. 59-67.
314. van der Heiden, A.P., et al., *Adsorption of proteins onto poly(ether urethane) with a phosphorylcholine moiety and influence of preadsorbed phospholipid.* Journal of Biomedical Materials Research, 1998. 40(2): p. 195-203.
315. Alberts, B., J. Wilson, and T. Hunt, *Molecular biology of the cell*. 2008, New York: Garland Science.
316. Lv, H., et al., *Toxicity of cationic lipids and cationic polymers in gene delivery.* Journal of Controlled Release, 2006. 114(1): p. 100-109.
317. Wegener, J., C.R. Keese, and I. Giaever, *Electric cell-substrate impedance sensing (ECIS) as a noninvasive means to monitor the kinetics of cell spreading to artificial surfaces.* Experimental Cell Research, 2000. 259(1): p. 158-166.
318. De Rosa, M., et al., *Cationic polyelectrolyte hydrogel fosters fibroblast spreading, proliferation, and extracellular matrix production: Implications for tissue engineering.* Journal of Cellular Physiology, 2004. 198(1): p. 133-143.
319. Webb, K., V. Hlady, and P.A. Tresco, *Relative importance of surface wettability and charged functional groups on NIH 3T3 fibroblast attachment, spreading, and cytoskeletal organization.* Journal of Biomedical Materials Research, 1998. 41(3): p. 422-430.
320. Qiu, Q., et al., *Attachment, morphology, and protein expression of rat marrow stromal cells cultured on charged substrate surfaces.* Journal of Biomedical Materials Research, 1998. 42(1): p. 117-127.
321. Rando, R.R., *Regulation of protein kinase-c activity by lipids.* Faseb Journal, 1988. 2(8): p. 2348-2355.
322. Zuris, J.A., et al., *Cationic lipid-mediated delivery of proteins enables efficient protein-based genome editing in vitro and in vivo.* Nature Biotechnology, 2015. 33(1): p. 73-80.

323. Konig, K., *Multiphoton microscopy in life sciences.* Journal of Microscopy, 2000. 200: p. 83-104.
324. McDonald, D.M. and P.L. Choyke, *Imaging of angiogenesis: from microscope to clinic.* Nature Medicine, 2003. 9(6): p. 713-725.
325. Sokolov, K., et al., *Real-time vital optical imaging of precancer using anti-epidermal growth factor receptor antibodies conjugated to gold nanoparticles.* Cancer Research, 2003. 63(9): p. 1999-2004.
326. Gao, X.H., et al., *In vivo molecular and cellular imaging with quantum dots.* Current Opinion in Biotechnology, 2005. 16(1): p. 63-72.
327. Helmchen, F. and W. Denk, *Deep tissue two-photon microscopy.* Nature Methods, 2005. 2(12): p. 932-940.
328. Ohki, K., et al., *Functional imaging with cellular resolution reveals precise micro-architecture in visual cortex.* Nature, 2005. 433(7026): p. 597-603.
329. Rappaz, B., et al., *Measurement of the integral refractive index and dynamic cell morphometry of living cells with digital holographic microscopy.* Optics Express, 2005. 13(23): p. 9361-9373.
330. Ntziachristos, V., *Going deeper than microscopy: the optical imaging frontier in biology.* Nature Methods, 2010. 7(8): p. 603-614.
331. Bennett, V. and A.J. Baines, *Spectrin and ankyrin-based pathways: Metazoan inventions for integrating cells into tissues.* Physiological Reviews, 2001. 81(3): p. 1353-1392.
332. Tyler, J.M., B.N. Reinhardt, and D. Branton, *Associations of Erythrocyte-Membrane Proteins - Binding of Purified Bands 2.1 and 4.1 to Spectrin.* Journal of Biological Chemistry, 1980. 255(14): p. 7034-7039.
333. Chang, T.L., et al., *Ankyrin is a target of spectrin's E2/E3 ubiquitin-conjugating/ligating activity.* Cellular and Molecular Biology, 2004. 50(1): p. 59-66.
334. Hsu, Y.J., W.E. Zimmer, and S.R. Goodman, *Erythrocyte spectrin's chimeric E2/E3 ubiquitin conjugating/ligating activity.* Cellular and Molecular Biology, 2005. 51(2): p. 187-193.
335. Hsu, Y.J. and S.R. Goodman, *Spectrin and ubiquitination: A review.* Cellular and Molecular Biology, 2005. 51: p. Ol801-Ol807.
336. Mishra, R. and S.R. Goodman, *Ubiquitination of erythrocyte spectrin regulates the dissociation of the spectrin-adducin-F-actin ternary complex in vitro.* Cellular and Molecular Biology, 2004. 50(1): p. 75-80.
337. Sangerman, J., et al., *Spectrin ubiquitination and oxidative stress: Potential roles in blood and neurological disorders.* Cellular & Molecular Biology Letters, 2001. 6(3): p. 607-636.
338. Frappier, T., J. Derancourt, and L.A. Pradel, *Actin and Neurofilament Binding Domain of Brain Spectrin Beta Subunit.* European Journal of Biochemistry, 1992. 205(1): p. 85-91.
339. Bok, E., et al., *Lipid-binding role of beta II-spectrin ankyrin-binding domain.* Cell Biology International, 2007. 31(12): p. 1482-1494.
340. Grzybek, M., et al., *Spectrin-phospholipid interactions - Existence of multiple kinds of binding sites?* Chemistry and Physics of Lipids, 2006. 141(1-2): p. 133-141.
341. Chorzalska, A., et al., *The effect of the lipid-binding site of the ankyrin-binding domain of erythroid beta-spectrin on the properties of natural membranes and skeletal structures.* Cellular & Molecular Biology Letters, 2010. 15(3): p. 406-423.

342. Ziemnicka-Kotula, D., et al., *Identification of a candidate human spectrin Src homology 3 domain-binding protein suggests a general mechanism of association of tyrosine kinases with the spectrin-based membrane skeleton.* Journal of Biological Chemistry, 1998. 273(22): p. 13681-13692.
343. Srinivasan, Y., et al., *Ankyrin and Spectrin Associate with Voltage-Dependent Sodium-Channels in Brain.* Nature, 1988. 333(6169): p. 177-180.
344. Rotter, B., et al., *alpha II-Spectrin interacts with Tes and EVL, two actin-binding proteins located at cell contacts.* Biochemical Journal, 2005. 388: p. 631-638.
345. Desilva, T.M., et al., *Analysis of human red cell spectrin tetramer (head-to-head) assembly using complementary univalent peptides.* Biochemistry, 1992. 31(44): p. 10872-10878.
346. Bignone, P.A., et al., *Phosphorylation of a threonine unique to the short C-terminal isoform of beta II-spectrin links regulation of alpha-beta spectrin interaction to neuritogenesis.* Journal of Biological Chemistry, 2007. 282(2): p. 888-896.
347. Morris, C.E., *Mechanoprotection of the plasma membrane in neurons and other non-erythroid cells by the spectrin-based membrane skeleton.* Cellular & Molecular Biology Letters, 2001. 6(3): p. 703-720.
348. Pinder, J.C. and A.J. Baines, *A protein accumulator.* Nature, 2000. 406(6793): p. 253-254.
349. Dubreuil, R.R., *Functional links between membrane transport and the spectrin cytoskeleton.* Journal of Membrane Biology, 2006. 211(3): p. 151-161.
350. Melkerson-Watson, L.J., et al., *Development of Na+/K+-ATPase polarity in the rat kidney proximal tubule: Regulation of the cytoskeletal elements, ankyrin and spectrin, during the redistribution Na+/K+-ATPase in the proximal tubule prior to birth.* Pediatric Research, 2000. 47(4): p. 449a-449a.
351. Collec, E., et al., *Novel role for the Lu/BCAM-spectrin interaction in actin cytoskeleton reorganization.* Biochemical Journal, 2011. 436: p. 699-708.
352. Mills, J.W. and L.J. Mandel, *Cytoskeletal Regulation of Membrane-Transport Events.* Faseb Journal, 1994. 8(14): p. 1161-1165.
353. Norman, K.R. and D.G. Moerman, *Alpha spectrin is essential for morphogenesis and body wall muscle formation in Caenorhabditis elegans.* Journal of Cell Biology, 2002. 157(4): p. 665-677.
354. Lee, J.K., et al., *Cell shape and interaction defects in α-spectrin mutants of Drosophila Melanogaster.* Journal of Cell Biology, 1993. 123(6): p. 1797-1809.
355. McMahon, L.W., et al., *Knockdown of alpha II spectrin in normal human cells by siRNA leads to chromosomal instability and decreased DNA interstrand cross-link repair.* Biochemical and Biophysical Research Communications, 2009. 381(2): p. 288-293.
356. Bennett, V. and J. Healy, *Organizing the diseases fluid membrane bilayer: diseases linked to spectrin and ankyrin.* Trends in Molecular Medicine, 2008. 14(1): p. 28-36.
357. van de Linde, S., et al., *Direct stochastic optical reconstruction microscopy with standard fluorescent probes.* Nature Protocols, 2011. 6(7): p. 991-1009.
358. Wolter, S., *rapidSTORM*. http://www.super-resolution.biozentrum.uni-wuerzburg.de/research_topics/rapidstorm/.
359. Stellwagen, N.C., *Apparent pore size of polyacrylamide gels: Comparison of gels cast and run in Tris-acetate-EDTA and Tris-borate-EDTA buffers.* Electrophoresis, 1998. 19(10): p. 1542-1547.

360. Hansen, S.B., *Lipid agonism: The PIP2 paradigm of ligand-gated ion channels.* Biochimica Et Biophysica Acta-Molecular and Cell Biology of Lipids, 2015. 1851(5): p. 620-628.
361. Rocha-Perugini, V., M. Gordon-Alonso, and F. Sanchez-Madrid, *PIP2: choreographer of actin-adaptor proteins in the HIV-1 dance.* Trends in Microbiology, 2014. 22(7): p. 379-388.
362. Zaydman, M.A. and J.M. Cui, *PIP2 regulation of KCNQ channels: biophysical and molecular mechanisms for lipid modulation of voltage-dependent gating.* Frontiers in Physiology, 2014. 5: p. 11.
363. Kettling, U., et al., *Real-time enzyme kinetics monitored by dual-color fluorescence cross-correlation spectroscopy.* Proceedings of the National Academy of Sciences of the United States of America, 1998. 95(4): p. 1416-1420.
364. Bacia, K., S.A. Kim, and P. Schwille, *Fluorescence cross-correlation spectroscopy in living cells.* Nature Methods, 2006. 3(2): p. 83-89.
365. van Rheenen, J., et al., *PIP2 signaling in lipid domains: a critical re-evaluation.* Embo Journal, 2005. 24(9): p. 1664-1673.
366. Levental, I., et al., *Calcium-Dependent Lateral Organization in Phosphatidylinositol 4,5-Bisphosphate (PIP2)- and Cholesterol-Containing Monolayers.* Biochemistry, 2009. 48(34): p. 8241-8248.
367. van den Bogaart, G., et al., *Membrane protein sequestering by ionic protein-lipid interactions.* Nature, 2011. 479(7374): p. 552-555.

Vita

Ian P. McCabe

Syracuse University
Department of Biomedical and Chemical Engineering
E-mail: imccabe@syr.edu
Phone: (518) 926 0027

Employment

Graduate Research Assistant **2008-present**
Department of Physics
Syracuse University, Syracuse, NY 13244
Supervisor: Prof. Martin B. Forstner

Education

Ph.D., Biomedical Engineering
Dept. of Biomedical and Chemical Engineering **2011-August 2015**
Syracuse University, Syracuse, NY 13244
Dissertation Title: "Observing, Understanding, and Manipulating Biological Membranes"
Thesis Advisors: Prof. Martin B. Forstner

M.Sc., Physics **2008-2011**
Syracuse University, Syracuse, NY, USA
Thesis Title: "Design and construction of an integrated FCS/TIRF microscopy platform for the study of membrane dynamics"
Thesis Advisor*:* Prof. Martin B. Forstner

Research Interests

Development of polymer supported lipid bilayer systems capable of dynamic tissue control. Utilizing advanced bio-photonic techniques to characterize and exploit membrane mediated cellular signaling behaviors.

Research Experience

Graduate Research

Fluorescence Correlation Spectroscopy (FCS) studies of ion induced lipid aggregation in polymer supported lipid bilayer systems under physiological conditions. Determining the role Ca^{2+} plays in the dynamic reorganization of PIP_2 phospholipids.

Study of the role bilayer surface charge plays in the adhesion and proliferation rate of fibroblast cells incubated directly on the lipid surface. Showing that cationic lipids inhibit the growth of adherent cells.

Development of a novel aldehyde based lipid-protein anchoring system. Incorporating green fluorescent proteins onto a fluid lipid bilayer via a genetically encoded aldehyde on the protein and an aminooxy group on the lipid.

A super-resolution microscopy study of the structural organization of Spectrin proteins in nonerytheroid cells. dSTORM superresolution was directed at fibroblast and cardiomyocyte cells to show the distribution and organization

Design and realization of a combined microscopy platform for dual color single molecule total internal reflection (TIRF) microscopy and dual color fluorescence correlation spectroscopy.

TEACHING EXPERIENCE

Supervision of undergraduate student research . **2011-present**
Direct supervision of training and education for multiple undergraduate student projects.

Teaching assistant for Introduction to Physics 1 & 2. **2008-2009**
Lead discussion sections that combined supplementary lectures and solving of example problems in collaboration with the students to assist their understanding of the course material. Supervise laboratory sections reinforcing lecture and Discussion materials. Provided individual problem solving sessions.

PROFESSIONAL ASSOCIATIONS

Biophysical Society **2009-present**
American Physical Society **2009-present**

PRESENTATIONS

Mc Cabe, I. P. Forstner, M. B. "Dynamics of PIP_2-Ca^{2+} Structures in Lipid Bilayers" *Poster*, 57th Annual Meeting of the Biophysical Society, Philadelphia PA, **2013**

Mc Cabe, I. P. Forstner, M. B. "Dynamics of PIP_2-Ca^{2+} Structures in Lipid Bilayers" *Poster*, Stevenson Biomaterials Symposium, Syracuse NY, **2013**

Mc Cabe, I. P. Forstner, M. B. "Dynamics of PIP_2-Ca^{2+} Structures in Lipid Bilayers" *Talk*, 56th Annual Meeting of the Biophysical Society, San Diego CA, **2012**

McCabe, I. P. Forstner, M. B." PIP_2/ Ca^{2+} Interactions on Supported Lipid Bilayers.", *Talk*, Syracuse IGERT Symposium, Syracuse NY, **2012**

McCabe, I. P. Forstner, M. B." PIP_2/ Ca^{2+} Interactions on Supported Lipid Bilayers", *Poster*, 55th Annual Meeting of the Biophysical Society, Baltimore MD, **2011**

PUBLICATIONS

McCabe, I. P. & Forstner, M. B., "Polymer Supported Lipid Bilayers." Open Journal of Biophysics, 2013, 3(1A), pp. 59-69

McCabe, I. P. & Forstner, M. B., "The Effects of Ca^{2+} on the dynamics of PIP_2 Containing Lipid Bilayer" *Submitted*.

McCabe, I. P., Wolfe, A., Movileanu, L., & Forstner, M. B., "The Effect of Bilayer Charge on the Adhesion and Proliferation of Adherent Cells " *in preparation*

McCabe, I. P. & Forstner, M. B., "A super resolution investigation into the distribution and organization of Spectrin in the membrane skeletons of non-erytheroid cells" *in preparation*

McCabe, I. P., Rabuka, D., Bader, R., & Forstner, M. B., "A modular, biosynthetic membrane-anchor/protein system based on a genetically encoded 'aldehyde tag'" *in preparation*